Investigating the emergence of neural circuits for navigation in developing rats using wireless technology

Tara O'Driscoll

A dissertation submitted in partial fulfillment of the requirements for the degree of

Doctor of Philosophy

of

University College London.

Department of Neuroscience, Physiology and Pharmacology
University College London

I, Tara O'Driscoll, confirm that the work presented in this thesis is my own. Where information has been derived from other sources, I confirm that this has been indicated in the work.

Abstract

The neural representation of space is encoded by spatially-modulated neurons including head direction cells (HD cells), place cells, and grid cells. Previous work has shown that these cell types emerge sequentially in rat postnatal development. Typically, spatial cognition experiments using *in vivo* electrophysiology are made as a single animal forages in an openfield environment while tethered to an acquisition system. In developmental studies, this requires the removal of the rat pup from its homecage, mother and littermates. Wireless technology is emerging as a promising alternative: neural data loggers permit the recording of single-unit neuronal activity in an animal's homecage, thereby tracking spatial cell development while minimising disruption of early sensory experiences.

Wireless recordings of spatial cells have not previously been conducted in the developing rat. The first experiment presented in this thesis was therefore a feasibility study demonstrating that wireless recordings of spatial cells in rat pups are comparable to standard techniques, focusing on HD cells in the anterodorsal thalamic nucleus (ADN), and place cells in the CA1 region of the hippocampus.

The second experiment of this thesis employed wireless homecage recordings to investigate whether the activity patterns of HD cells during development differed from those observed in traditional open-field recordings. To address the research question, HD cell ensembles in the ADN were wirelessly recorded in the homecage from postnatal day (P)12 to P16. The directional modulation of HD cells was analysed by calculat-

Abstract 4

ing both the mean resultant vector length (RV length) and directional information. Whilst RV length reflects the unidirectional tuning preference of individual HD cells, directional information quantifies any directional modulation of a cell, whether unidirectional or multidirectional. The results revealed that HD cells in the homecage exhibited lower RV lengths compared to those in the open field, indicating poorer unidirectional tuning. However, this difference was not reflected in the directional information of recorded cells, which remained consistent between environments until P16. This suggests that while heading direction in the open field is primarily encoded in a unidirectional manner, in the homecage it may be encoded through multiple preferred firing directions within a trial, indicating frequent resetting of HD cells. This phenomenon had the effect of equalising the directional information of cells between the two environments.

The temporal and spatial coupling of recorded cells was also investigated on short-timescales. Strikingly, in contrast to previous reports (Bassett et al., 2018), the temporal and spatial synchronisation of HD cell ensemble firing did not precede the establishment of stable unidirectional tuning in the homecage. The internal spatial organisation of the network did also not appear to be maintained between recording environments, which may be as a result of differing movement statistics between environments. This finding suggests that the attractor network properties of HD cells in developing rats may be contingent on the context in which they are studied.

Acknowledgements

I would like to thank the Wills/Cacucci lab members for their encouragement through what has been a very turbulent few years. Thanks to my supervisor, Tom Wills: I sincerely appreciate all of your guidance throughout this journey, and I am very much looking forward to seeing your research group thrive. My particular thanks go to Laurenz Muessig for his unwavering support regarding all things technical, troubleshooting and thesis-related. Also Joshua Bassett, whose extraordinary scientific knowledge paired with his gift for teaching have been invaluable in my learning and training in this research field. You have all helped me grow as a curious and industrious scientist.

I am eternally grateful to the women of science in my life, Megan Powell and Isabella Varsavsky, who have encouraged my resilience and inspired me to be the best that I can be. Also my BoobyBiome co-founders, Lydia Mapstone and Sioned Jones. The journey we have taken together has not been easy, but I am so proud of our achievements as a team and I cannot wait to continue our efforts in the coming years.

Thanks to all of my family, particularly Mum, Emer and Nana Mary. Your words of comfort and motivation are endlessly appreciated and I'm so looking forward to making up for lost time with you. Thanks also to my friends, who have been a constant source of joy and amazing chaotic energy throughout this PhD. Finally, I'd like to thank Craig Murray. Your friendship and compassion are more than I could have hoped for in a partner. I am so grateful for your constant support (and limitless patience) whilst I drove myself to madness.

Impact Statement

Navigation is a fundamental part of life for animals, enabling access to critical resources such as food, shelter and mates. In understanding the localisation, emergence and functional properties of cell types encoding various aspects of the neural map of space, investigators hope to elucidate the ways in which the brain orchestrates the ability to efficiently navigate. Furthermore, the collapse of navigational abilities and spatial awareness have been heavily implicated in degenerative brain diseases such as Alzheimer's.

Ontogenetic studies, in informing us of the building blocks of spatial cognition and memory, therefore afford a unique window to observe both healthy and pathological ageing. A key component of the neural map of space is direction, encoded by a network of head direction cells distributed throughout both cortical and subcortical brain regions. Head direction cells are the first spatial cell type to emerge in postnatal development in rats, prior to the earliest periods of spontaneous exploration. From a developmental perspective, the period of time immediately following head direction cell emergence is intriguing as it may shed light on the extent to which neural networks for navigation are either hardwired or learned through sensory experience. Likewise, understanding the constituent role of head direction cells in spatial cognition will furthermore inform us of the subsequent maturation trajectory of the collective ensemble of spatial cell types.

Ontogenetic studies of spatial cells are traditionally conducted in sim-

ple laboratory environments with controlled cues available to the animal, typically a pre-weanling rodent model. Yet in nature an animal's environment is complex, cue-rich, and dynamic. Recent advances in wireless technology for electrophysiological recordings presents an opportunity for studying spatial cell development while minimising disruption of early sensory experiences. To this end, the experiments presented in this thesis firstly demonstrate a novel method for conducting wireless recordings in developing rats with effective reproducibility of neuronal data compared to a standard, tethered data acquisition system. Secondly, this method was exploited for use in the study of postnatal head direction cell activity in a highly familiar and naturalistic environment for a laboratory rat: their homecage. The use of wireless technology for the *in vivo* recording of spatial cells set forth in this thesis expands on current techniques and best-practices in the challenging domain of ontogenetic studies in awake, behaving animals.

List of Abbreviations

ADN Anterodorsal thalamic nucleu	1DN	Anterodorsal	thalamic	nucleu
----------------------------------	-----	--------------	----------	--------

AHV Angular head velocity

ATI Anticipatory time interval

ATN Anterior thalamic nuclei

AVN Anteroventral thalamic nucleus

BVC..... Boundary vector cell

CW..... Clockwise

CCW Counter-clockwise

DTN Dorsal tegmental nucleus of Gudden

HD Head direction

LDN Laterodorsal thalamic nucleus

LFP Local field potential

LMN Lateral mammillary nuclei

MEC..... Medial entorhinal cortex

MVN Medial vestibular nuclei

nPH Nucleus prepositus hypoglossi

PFD Preferred firing direction

PoS......Postsubiculum

RSC.... Retrosplenial cortex

SGN Supragenual nucleus

TPD Theta-modulated place-by-direction

TWC......Time-windowed spatial cross-correlogram

VN Vestibular nuclei

Contents

1	Gen	eral in	troduction to rodent navigation	18
	1.1	The C	ognitive Map theory for navigation	18
	1.2	The h	ippocampus as a cognitive map	21
	1.3	Spatia	ılly-modulated cell types	26
		1.3.1	Place cells	26
		1.3.2	Head direction cells	31
		1.3.3	Grid cells	32
		1.3.4	Boundary cells	35
		1.3.5	Interactions between spatial cell types	35
		1.3.6	Studies of spatial cells in complex and naturalistic	
			scenes	38
	1.4	Sumn	nary	40
2	The	head d	lirection cell circuit	41
	2.1	Head	Direction Cell Properties	45
		2.1.1	Cue control of head direction cells	45
		2.1.2	Attractor network properties	53
	2.2	Variat	ions of canonical head direction cells	55
		2.2.1	Angular head velocity cells	55
		2.2.2	Conjunctive cells	57
		2.2.3	Theta-modulated head direction cells	57
		2.2.4	Head direction cells non-compliant with attractor	
			dynamics	58

Contents	10
----------	----

		2.2.5	Bi-lobed head direction cells	59
	2.3	Anato	my of the head direction cell network	59
		2.3.1	Dorsal tegmental nucleus	60
		2.3.2	Lateral mammillary nuclei	61
		2.3.3	Anterodorsal thalamic nucleus	64
		2.3.4	Laterodorsal thalamic nucleus	66
		2.3.5	Postsubiculum	66
		2.3.6	Retrosplenial cortex	68
		2.3.7	Medial entorhinal cortex	70
		2.3.8	Hippocampus	71
	2.4	Head	direction cells and behaviour	74
	2.5	Sumn	nary	77
•	ъ.	,	. 1 1 1	=0
3		•	tal development	79
	3.1		s a model for spatial cognition	80
	3.2		rimotor development	81
		3.2.1	Vestibular	81
		3.2.2	Olfactory	82
		3.2.3	Somatosensory	
		3.2.4	Auditory	
		3.2.5	Visual	84
		3.2.6	Motor	86
	3.3	Cogni	tive and behavioural development	87
		3.3.1	Activity in the nest	87
		3.3.2	Homing	88
		3.3.3	Exploration and nest egression	89
		3.3.4	Hippocampal-dependent learning and memory	89
		3.3.5	Maternal impact on cognitive development	91
	3.4	Spatia	ıl cell development	92
		3.4.1	Development of head direction cells	92
		3.4.2	Development of place cells	95

Contents 11

		3.4.3	Development of boundary-responsive cells and grid
			cells
	3.5	Sumn	nary and rationale for experiments
		3.5.1	Experiment 1 (Chapter 5)
		3.5.2	Experiment 2 (Chapter 6)
4	Gen	eral M	ethods 101
	4.1	Anima	al subjects and husbandry
	4.2	Micro	drive preparation
	4.3	Surgio	cal procedure for pre-weanling rat pups 104
		4.3.1	The effect of isoflurane in development 106
	4.4	Data a	acquisition
		4.4.1	General recording procedures 107
		4.4.2	Single-unit electrophysiological recordings 108
	4.5	Histol	ogy and Electrode Localisation
	4.6	Data a	analysis
		4.6.1	Processing of raw logger neural data 113
		4.6.2	Spike sorting and cluster separation 117
		4.6.3	Processing position data
		4.6.4	Construction of firing rate maps
		4.6.5	Quantitative analysis of spatial firing 119
		4.6.6	Statistics
5	Wir	eless re	ecordings of spatial cells in developing rats 122
	5.1	Backg	round and rationale
		5.1.1	Chronic <i>in vivo</i> electrode recordings 122
	5.2	Exper	imental aim
	5.3	Metho	ods
		5.3.1	Animal subjects
		5.3.2	Surgery
		5.3.3	Neural data logger assembly

Comtonto	17
Contents	12

		5.3.4	Behavioural paradigm	31
		5.3.5	Data analysis	33
	5.4	Result	ts	37
		5.4.1	Behavioural profile of animals in tethered and wire-	
			less recording trials	37
		5.4.2	Comparison of neuronal data from wireless and teth-	
			ered systems	49
		5.4.3	Head direction cell properties are similar between	
			recording systems	53
		5.4.4	Head direction cells are reliably recorded in the	
			homecage environment	61
		5.4.5	Place cell properties are similar between recording	
			systems	63
		5.4.6	Histology	71
	5.5	Chapt	ter discussion	73
6	Inve	estigati	ng the postnatal stabilisation of head direction cells in	
		Ü	tic environment	78
	6.1		round and rationale	78
		6.1.1	Prior work	
		6.1.2	Experimental aim	
	6.2		ods	
		6.2.1	Animal subjects	
		6.2.2	Surgery	
		6.2.3	Neural data logger assembly	
		6.2.4	Single-unit recording	
		6.2.5	Classification of head direction cells	
		6.2.6	Analysis of directional and spatial sampling 19	
		6.2.7	Analysis of epochs between passive movement 19	
		6.2.8	Random resampling of active movement epochs in	
			open field trials	95

Contents 13

		6.2.9	Quantification of temporal and spatial coupling of	
			cell pairs on short-timescales	. 195
		6.2.10	Statistics	. 197
	6.3	Result	S	. 198
		6.3.1	Behavioural profile of animals in different environ-	
			mental contexts	. 198
		6.3.2	Head direction cell firing differs between the homecag	je
			and open field	207
		6.3.3	Investigation of head direction cell activity during	
			active movement epochs	219
		6.3.4	Temporal and spatial coupling of recorded cells on	
			short-timescales	230
		6.3.5	Histology	241
	6.4	Chapt	er discussion	245
7	Gen	eral Di	scussion	254
	7.1	Summ	nary of findings	254
	7.2	Discus	ssion and future work	256
	7.3	Concl	uding Remarks	. 264
8	Refe	erences		266

List of Figures

1.1	Maze apparatus employed in Tolman's studies of latent	
	learning and a cognitive map in rats	21
1.2	Anatomical organisation of the rodent spatial processing	
	circuit	25
1.3	Schematic of theta sequences and phase precession	31
2.1	Example head direction cell	42
2.2	Simplified schematic of the relative connectivity of brain re-	
	gions containing head direction cells, grid cells and place	
	cells	44
2.3	Continuous ring attractor network model for head direction	
	cell activity	54
2.4	Representative angular head velocity cells recorded from the	
	dorsal tegmental nucleus	56
3.1	Summary timeline of rat postnatal development	82
4.1	Microdrive assembly for in vivo extracellular neuronal	
	recordings in rat pups.	103
4.2	Axona electrophysiology set-up	109
4.3	Neural data logger recording pipeline	111
4.4	Bonsai workflow for neural data logger recordings	112
4.5	Data synchronisation of logger neural data recordings	115
4.6	Example cluster separation and spike sorting on one tetrode.	117

5.1	Wireless neural data logger Deuteron MouseLog-16B 130
5.2	Behavioural paradigm for Chapter 5 experiment
5.3	Schematic of the laboratory set-up for Chapter 5 experiment. 133
5.4	Velocity of rats in wireless and tethered recordings 140
5.5	Spatial sampling of rats in wireless and tethered recordings 143
5.6	Example behavioural data from individual trials 148
5.7	Comparison of cluster isolation metrics in extracellular
	recordings
5.8	Comparison of cluster offset and cell waveform between
	Logger and DACQ trials
5.9	Representative HD cells (A-F) recorded from DACQ and the
	Logger within the same recording session
5.10	Burst index of recorded head direction cells
5.11	Spatial modulation metrics across head direction cell
	recording trials
5.12	Comparison of HD cell firing rates between Logger and
	DACQ recording trials
5.13	Representative HD cells (A-C) recorded in the homecage us-
	ing the neural data logger
5.14	Representative place cells (A-F) recorded by DACQ and the
	logger within the same recording session 166
5.15	Spatial modulation metrics across place cell recording trials. 169
5.16	Comparison of place cell firing rates between Logger and
	DACQ recording trials
5.17	Histology for Chapter 5 electrophysiology animal subjects 172
6.1	Wireless neural data logger Deuteron MouseLog-16C 185
6.2	Experimental set-up for Chapter 6 experiment 190
6.3	Behavioural paradigm Chapter 6 experiments 192
6.4	Directional sampling of animals
6.5	

	List of Figures	16
6.6	Movement velocity of animals	206
6.7	General properties of recorded cells	209
6.8	Representative head direction cells	211
6.9	Directional modulation metrics of recorded cells	214
6.10	Stability of cell firing within and between recording trials	218
6.11	Passive movement of animals during recording trials	221
6.12	Probability distribution of active movement epoch duration	
	in the homecage. \hdots	222
6.13	Analysis of HD cell activity during active movement epochs	
	after resampling from Open Field and Small Box trials	224
6.14	Representative HD cells before and after a period of passive	
	movement	228
6.15	Representative HD cells across consecutive epochs within a	
	trial	229
6.16	Spatial and temporal coupling between representative head	
	direction cells	234
6.17	Spatial cross-correlogram of head direction cells in the Open	
	Field and Homecage	235
6.18	Temporal cross-correlogram of head direction cells in the	
	Open Field and Homecage	237
6.19	Summary properties of time-windowed spatial cross-	

correlograms of head direction cells in the Open Field and

 $6.20\,$ Histology for Chapter $6\,$ electrophysiology animal subjects. . $244\,$

List of Tables

4.1	File formats of Axona DACQ files which were replicated for
	data recorded using the neural data logger
5.1	Summary of experimental subjects for Chapter 5 experiments.129
5.2	Electrode implant coordinates
6.1	Summary of experimental subjects for Chapter 6 experiments, 184

Chapter 1

General introduction to rodent navigation

1.1 The Cognitive Map theory for navigation

Navigation is a fundamental part of life for many animals, enabling access to food, shelter and reproductive mates. Further to this, humans and animals are inquisitive beings with an instinctive drive to explore their surroundings even without explicit danger or immediate reward. Mammalian nervous systems, as well as other vertebrate nervous systems, have therefore evolved over time to accommodate the task of navigation.

Early behaviourist theories for the cognitive basis of navigation posited that navigation was achieved by simple, stimulus-response learning. That is, route navigation was based on learning that required either reward or reinforcement (Watson, 1919; Hull, 1950). The pioneering work of Edward Tolman in the 1930s and 1940s has led to several proposed theories for the cognitive basis of navigation which contrast with early behaviourist views. Building on the work of his predecessor (Blodgett, 1929), Tolman conducted a series of behavioural experiments in rats which provided evidence that animals instead engage in latent learning. That is, learning may occur when an animal explores its environment through innate curiosity and in the absence of any intrinsic motivation. One par-

ticular study involved three groups of rats which were trained to navigate a maze which contained a food box at the end (Figure 1.1A; Tolman and Honzik, 1930). The first group received a reward each time they reached a certain point in the maze, the second group received no reward, and the third group were a combination of these two conditions: they received no reward until the eleventh day of training, at which point they began to be rewarded. Differences between groups in the number of errors (wrong turns) made while navigating the maze was striking. The first cohort of rats initially made errors, but quick improvement was made in their performance as the learning was reinforced via food reward. The second cohort made no decrease in errors with time, appearing to wander without aim throughout the maze. The third cohort initially made errors, similar to the second cohort. Then, upon receiving the reward, they rapidly began performing better in the maze task than the first group. Tolman extrapolated that the final cohort of rats were still learning when not being rewarded, but had no reason to demonstrate this learning until the motivation for reward was introduced. From this study, Tolman concluded that animals engage in latent learning (learning that is not immediately apparent or expressed until there is sufficient motivation) when exploring their environment. An internal representation of the environment is formed with experience, which can be flexibly used for spatial memory and navigation. This form of learning is created during exploration without explicit motivation, is rapidly acquired (Wilson and McNaughton, 1993) and can manifest later under the right conditions, such as in aversive or rewarding tasks (Thistlethwaite, 1951). Motivation such as these are useful for demonstrating the learning of an environment, but the learning will occur regardless.

A subsequent theory for how the brain performs navigation was that the brain contains an internal model of allocentric (world-centred, or external) space, termed a 'cognitive map'. It was first posited by Tolman following another of his seminal behavioural studies in rats using a sunburst maze (Tolman et al., 1946). In this study, Tolman trained a number of rats to retrieve a food reward at the end of a fixed maze (Figure 1.1B). Subsequent to training, the maze was altered such that the old route was blocked and replaced with multiple corridors branching off in different directions from the start location. The food reward remained in the same direction relative to the rat's starting point. Surprisingly, the rats still chose the most direct route to the food reward via the correct corridor. Tolman thus demonstrated that rats could pursue a different route than before using a previously unavailable shortcut to reach the food reward, by having a notion of the global location of the reward in relation to their starting point. In performing this task, rats demonstrated their ability to flexibly navigate the maze using what Tolman termed a 'cognitive map'. Tolman proposed that the rat's ability to do this was due to an internal representation of their external space being learned through exploration and sampling of their environment, which could then be used to guide their navigation-based behaviour: "In the course of learning, something like a field map of the environment gets established in the rat's brain" (Tolman, 1948). Therein, the cognitive map constitutes a global understanding of location, not just a reinforcement of actual routes or behaviour.

The findings from Tolman's work were corroborated via the development of an open-field water maze task (termed a Morris water maze; Morris, 1981; Morris et al., 1982) which probed whether rats had the ability to navigate to a goal object without having reference to local cues revealing the goal location (such as a light beacon, sound or smell). The absence of these cues removed the ability of the rats to use a simple, stimulus-response strategy for navigation. Rats were trained to escape from a pool of opaque water onto a hidden platform with a fixed location. Spatial learning was successfully demonstrated in these rats when they were required to begin their approach to the platform from a new starting location. This

task provided further evidence that rats hold a map-like representation which was flexibly used to navigate to the goal location (Morris, 1981; Morris et al., 1982). Rats were actively processing the location information of the platform, as opposed to learning solely as a stimulus-response.

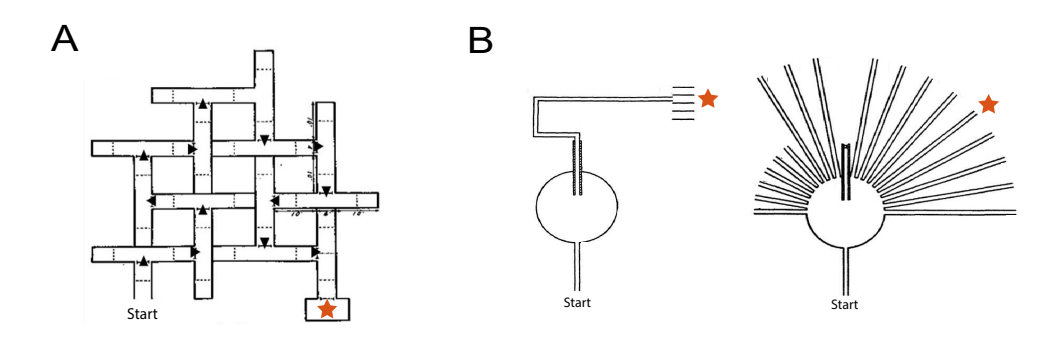


Figure 1.1: Maze apparatus employed in Tolman's studies of (A) latent learning and (B) an internal cognitive map in rats. (A) Latent learning experiment. Rats were trained on a 14-unit T-maze with a goal (food box) at the end (marked with an orange star) to study the effect of learning without reinforcement in rats. A subset of animals received a food reward each time they completed the maze, another subset did not receive a food reward, and a final group received a food reward upon completion of the maze only after 11 days of training. The group of animals which began receiving the reward at day 11 exhibited a rapid decrease in the number of errors on the maze and ultimately outperformed the group which received a food reward throughout the entire experimental period (demonstrating latent learning). Adapted from Tolman and Honzik, 1930. (B) Cognitive map experiment. Rats were trained to run for a food reward (goal location denoted by orange star) at the end of a fixed maze via an indirect route (left). Rats were subsequently tested in a sunburst maze in which the training route was blocked (right). A significant number of rats chose the most direct arm of the maze to reach the learned goal location. Adapted from Tolman et al., 1946.

1.2 The hippocampus as a cognitive map

The discovery of place cells in the hippocampus (O'Keefe and Dostrovsky, 1971) several decades after Tolman's seminal work lent credence to his cognitive map theory. The hippocampus has been a long-established point of interest in cognitive neuroscience given its association with memory consolidation in humans, stemming from patient HM (Scoville and Milner, 1957). HM underwent a bilateral removal of large portions of the medial temporal lobes (including the hippocampus) for the purpose of treating

his epileptic seizures. Following this surgical intervention, HM could no longer form new episodic memories (memory of events and experiences), termed anterograde amnesia. HM also suffered a loss of memories for some time preceding his surgery (indicative of partial retrograde amnesia), leading to the hypothesis that the hippocampus may be involved in generating new memories and consolidating them long-term (Scoville and Milner, 1957). In addition to the hippocampus, surrounding structures such as the entorhinal cortex and perirhinal cortex were also damaged. These areas are intimately connected to the hippocampus and play essential roles in memory processing.

Subsequent to this discovery, and using recently developed *in vivo* electrophysiology recording techniques, O'Keefe and colleagues implanted electrodes in the dorsal hippocampus of freely moving rats (O'Keefe and Dostrovsky, 1971). In doing so, they noticed that a certain population of pyramidal neurons in the hippocampus proper would preferentially fire when an animal was in a certain location within an environment, which they termed 'place cells'. Each place cell exhibited its own location-specific firing in two-dimensional space which was referred to as the cell's 'place field'.

Based on these findings, O'Keefe and Nadel proposed that the hippocampus was a likely candidate for the neural substrate or 'hub' of the cognitive map in their influential work *The Hippocampus as A Cognitive Map* (O'Keefe and Nadel, 1978). Some predictions posited by the authors were firstly that a cognitive map requires not only location information (provided by place cells), but also direction and distance information. Secondly, initial exploration of an environment would construct the cognitive map, and further exploration would inform the map in the instance when there are alterations or additions to an environment (driven by a so-called 'misplace detector'). Thirdly, the cognitive map would allow for flexible behaviour and permit predictions about a given environment. Building

the cognitive map would therefore require exploration and sampling of an environment, such that idiothetic information (from internally generated self-motion and proprioceptive cues; Whishaw and Brooks, 1999) be integrated with, and in reference to, allothetic cues (external environmental cues including landmarks; Whishaw and Brooks, 1999). The hippocampus was thus posited as the centre of a brain system which constructs, stores and flexibly utilises a cognitive map (or locale system) of allocentric space. This spatial system would be one of several, supporting various behavioural strategies.

O'Keefe and Nadel furthermore surmised that there are two forms, or strategies, for navigation: Navigation using the place method (cognitive map-based), or navigation using the taxon (response, or route-based) method (O'Keefe and Nadel, 1978). The taxon method is described as a route-based strategy which is the concatenation of familiar, stimulusresponse reflexes resulting in behaviour. For instance, in moving from one location to another the body makes a series of specific turns along the body axis (such as turning left along one path, followed by right along the subsequent path) which is informed by idiothetic inputs. This strategy follows a series of precise, somewhat inflexible series of behaviours and so in isolation is more likely to lead to disorientation or becoming lost. For instance, in unfamiliar territory or when the animal is moving in the reverse direction. The second method (place method) uses a map-like mental representation of an area and its geography, which caters to the previously described route-based navigation but permits additional flexibility. The place method of navigation is information-rich with respect to the spatial relationships of various locations and thus provides multiple alternative strategies for navigating from one place to another. This provides the means by which to navigate when alterations are made to an environment, for instance using detours or short-cuts.

These forms of navigation are vastly different and thus depend on dif-

ferent brain systems with different properties, working in synchrony depending on the cognitive and behavioural demands of the animal. A series of experiments by Packard and colleagues, among others, provided evidence for the differential roles of the hippocampus and striatum in these navigational strategies: The effect of both reversible (Packard and Mc-Gaugh, 1996) and irreversible (Packard et al., 1989; Packard and McGaugh, 1992) lesions to the hippocampus are an impairment in performance in a radial arm maze task and the ability to navigate to a hidden platform in the Morris water maze task, respectively (both tasks requiring place navigation). Post-training intrahippocampal injection of the NMDA antagonist AP5 produced similar impairments (Packard and Teather, 1997). Selective enhancement of hippocampal neurons via posttraining dopamine agonist injections resulted in improved performance in the radial arm maze task (Packard and White, 1991). Conversely, lesions to the caudate nucleus of the striatum (Packard et al., 1989; Packard and McGaugh, 1992) impaired the ability of rats to navigate to a visible platform in the Morris water maze as well as performance in a radial arm maze with a light beacon present at the baited arm (both being cued tasks requiring taxon navigation). Intracaudate injections of AP5 produced similar results (Packard and Teather, 1997). Post-training intracaudate injections of a dopamine agonist furthermore selectively enhanced performance in the radial arm maze task (Packard and White, 1991). Taken together, these results present dissociable roles of the hippocampus and striatum in place and response learning: While the hippocampus supports navigation requiring flexible, goal or reward-based strategy, the caudate nucleus of the striatum mediates stimulus-response navigation (Packard and McGaugh, 1996). Further experimental evidence suggests the amygdala plays a role in the modulation of both these memory systems (Packard et al., 1994).

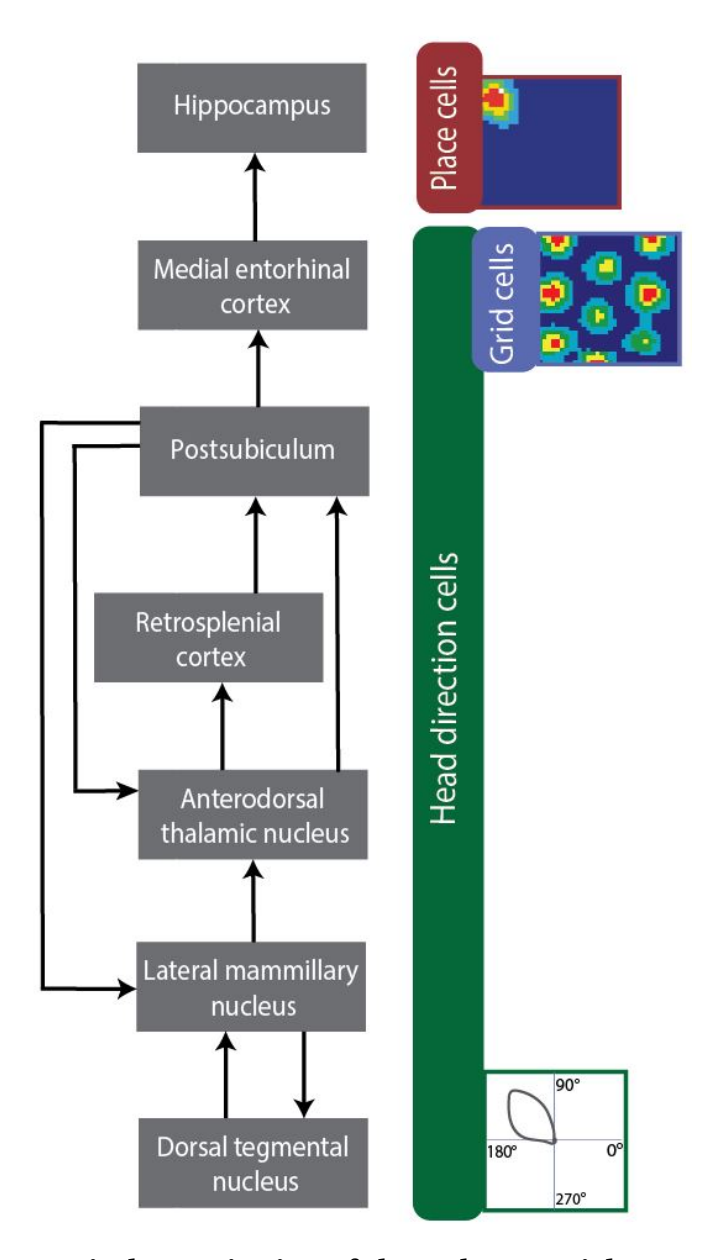


Figure 1.2: Anatomical organisation of the rodent spatial processing circuit, including the respective locations of head direction cells, grid cells and place cells within this circuitry. Arrows indicate the direction of signalling. Note that the subicular complex may be subdivided into pre-subiculum and parasubiculum (where grid cells are found), and the dorsal presubiculum (postsubiculum), where head direction cells are found. Top right: Place cell firing rate map. Falsecolour rate map showing firing rates of a cell within an environment, viewed from above (red = high firing, blue = low firing). The area of high firing indicates the cell's place field. The example place cell pictured has a place field in the northwest corner of the environment. Middle right: Grid cell rate map. False-colour rate map showing the firing rate distribution of a grid cell (red= high firing, blue= low firing). The periodic, hexagonal firing pattern seen here is typical of grid cell spatial firing fields. Bottom right: Head direction cell polar plot. The polar plot depicts the direction of maximal firing of the cell (preferred firing direction) with respect to the animal's heading direction. The example HD cell pictured has a preferred heading direction of approximately 135°.

1.3 Spatially-modulated cell types

The discovery of place cells opened up a new field of research which sought to further investigate the neural components of the cognitive map. This led to the discovery of other spatially modulated cell types throughout the medial temporal lobe and limbic system of rodents: Head direction (HD) cells, discovered in the postsubiculum (dorsal presubiculum), preferentially fire when an animal's head is pointing in a certain direction (Ranck, 1984). Grid cells, discovered in the medial entorhinal cortex (MEC), have a number of periodic, hexagonally-spaced firing fields which tessellate an environment and may function as a distance metric (Hafting et al., 2005). Border cells in the entorhinal cortex (Solstad et al., 2008), and boundary vector cells in the subiculum (Barry et al., 2006; Lever et al., 2009), are active in response to proximity of environmental boundaries. The finding that all of these cell types are modulated by an animal's location, position and orientation in space suggests that they work in synchrony to provide the building blocks of the cognitive map.

1.3.1 Place cells

Place cells are a population of pyramidal neurons located in the CA1 (O'Keefe and Dostrovsky, 1971) and CA3 (Olton et al., 1978) regions of the hippocampus. Each place cell preferentially fires in one location in an environment (termed the cell's 'place field'; Figure 1.2). Place cells active within an environment will have overlapping place fields with firing rates of Gaussian distributions, forming a distributed representation of the environment. Hippocampal CA1 place cell representations of an environment (the place code) appear to be rapidly acquired (Wilson and McNaughton, 1993) and persist over the timescale of days (Muller et al., 1987; Lever et al., 2002) or weeks (although over longer timescales place field positions can remain stable, their firing rates may fluctuate, meaning that the overall place code for an environment may change substantially; Ziv et al., 2013).

In an open field, their firing rates tend to be invariant to an animal's orientation or direction of movement, while cell firing tends to occur in a unidirectional manner on a linear track (Muller et al., 1994). Subsequent to their discovery in rodents, place-encoding cells have been identified in other mammals including bats (Ulanovsky and Moss, 2007), monkeys (Cahusac et al., 1989) and humans (Ekstrom et al., 2003).

One way in which place cells encode location is by a rate code (O'Keefe and Dostrovsky 1971). A given cell's firing rate changes as a function of the animal's location, preferentially firing when the rodent is in a specific location within a given environment (the place field; Figure 1.3). Location is also encoded by a temporal (phase) code in which cells fire at a specific phase of the theta rhythm, depending on the progression of the animal through the place field. The theta rhythm is a prominent 4-11 Hz oscillation in the local field potential (LFP) of the rodent hippocampus (Figure 1.3). It is characteristically observed during periods of locomotion and exploration (Vanderwolf et al., 1969), as well as during rapid eye-movement (REM) sleep (Winson, 1972). Theta rhythm in the hippocampus arises in the medial septum (Green and Arduini, 1954; Petsche et al., 1962). Phase coding has been studied in two different ways: phase precession which occurs at the level of single cells, and theta sequences which occur at the level of cell populations.

Phase precession is the process by which the spiking of a given neuron occurs at progressively earlier stages of successive theta cycles as an animal passes through the place field of that cell (Figure 1.3; O'Keefe and Recce, 1993). As the animal enters the place field, the cell will generally fire at the peak of the theta cycle. Spikes will fire at earlier phases of consecutive theta cycles ('precess'), firing at an early theta phase as the animal exits the place field. One possible function of phase precession is as a distance metric of the animal's position relative to the beginning of the place field (Huxter et al., 2003).

The firing of place cells in an organised manner with respect to the theta phase allows for coherent ensemble-level firing of cells throughout the theta cycle. This phenomenon is referred to as a theta sequence. Theta sequences are compressed events consisting of the sequential activation of place cells during each theta cycle (Figure 1.3; Skaggs et al., 1996; Dragoi and Buzsaki, 2006). The sequences correspond to an animal's trajectory within an environment, and occur in the order of place cells active from behind the animal's position to those encoding locations ahead of the animal. Place cells with fields behind the current position of the animal are active early in the theta cycle, while those ahead of the animal are active late in the cycle. This creates a forward sweep of position across each cycle.

Theta sequences are thought to be integral to the encoding of location sequences within experience, such as the path to a goal (Wilkenheiser and Redish, 2015). Memory encoding refers to the initial transformation of sensory input into a neural code, whereas memory consolidation involves the subsequent stabilisation and integration of this information into long-term memory. The reason theta sequences are thought to play a role in memory encoding is because they occur at a timescale permissive for spike-time dependent plasticity (Melamed et al., 2004). In this way, they facilitate the encoding spatial and contextual details of memories when an individual is actively exploring or learning. Theta sequences are not an epiphenomenon of phase precession, as studies have shown that phase precession can occur without theta sequences (Feng et al., 2015). Therefore, theta sequences are thought to encode pertinent information and construct representations of new experiences. Subsequently, this freshly encoded data undergoes stabilisation via memory consolidation.

Systems-level consolidation describes the mechanism wherein the hippocampus orchestrates the restructuring of neocortical information, ultimately enabling it to store memories independently of the hippocampus (Squire et al., 2015). This process facilitates the long-term storage of

memories within the brain (Squire et al., 1984; Squire and Alvarez, 1995; Dudai and Morris, 2000), such that temporary memories are consolidated into stable, enduring memories. Subsequent replay of place cell firing sequences in animals occurring during wake and sleep (Skaggs and McNaughton, 1996; Foster and Wilson, 2006; Diba and Buzsaki, 2007; Karlsson and Frank, 2009), as well as reactivation of recently active place cell ensembles in sleep (Wilson and McNaughton, 1994), are proposed mechanisms for achieving this. The extended communication between the hippocampus and the cortex, facilitated by replay, selectively strengthens its memory traces (Marr,1971) and is believed to gradually transition the memory into a form that is represented in the neocortex and becomes distinct from the hippocampus. In support of this, replay and reactivation have been shown to predict spatial memory performance (Dupret et al., 2010; Xu et al., 2019), as well as memory consolidation and retrieval (Girardeau et al., 2009; Jadhav et al., 2012).

Not only do place cells fire in response to an animal's location in the ways described, but place cell firing dynamics can also alter in response to spatial learning tasks and goal locations (Markus et al., 1995; Hollup et al., 2001; Hok et al., 2007). This in turn can infer behavioural choices in a spatial memory task (O'Keefe and Speakman, 1987) and predict performance in those tasks (Dupret et al., 2010). Evidence for encoding of non-spatial environmental features has also been demonstrated, with place cell firing reported in response to odour (Wood et al., 1999), tactile (Gener et al., 2013), and auditory stimuli (Aronov et al., 2017).

Vestibular input appears to be key to place cell activity, given that vestibular inactivation disrupts location-specific firing in place cells (Stackman et al., 2002). Despite the strong influence exerted by landmarks over place cell activity, place cell firing is not disrupted in the absence of visual inputs (Quirk et al., 1990; Save et al., 1998). Unlike other spatially-modulated cell types, which will fire in any given environment, place cells

can often remap from one context to the next: In one environment a given place cell may be active, and in another it may have a different place field or remain silent (termed global remapping; Muller and Kubie, 1987; Bostock et al., 1991). This remapping may also manifest as a change in firing rate (rate remapping; Bostock et al., 1991; Leutgeb et al., 2005) in a familiar environment with local changes introduced, such as a change in wall colour. Evidence furthermore suggests that place cell ensembles exhibit firing modulation in a context-dependent manner (Anderson and Jeffery, 2003). For instance, when animals in either a circular or square environment are exposed to an intermediate environment (made of a different material, then different shape), place cell ensembles rapidly remap in an all-or-none fashion (Wills et al., 2005). This is consistent with there being an attractor representation for each shape (or context) with no incremental change in firing. In this way, CA1 place cell ensembles tend to form unique maps of different environments with only a subset of place cells (Guzowski et al., 2006) active in a given environment, depending on the region and size of the environment (Alme et al., 2014).

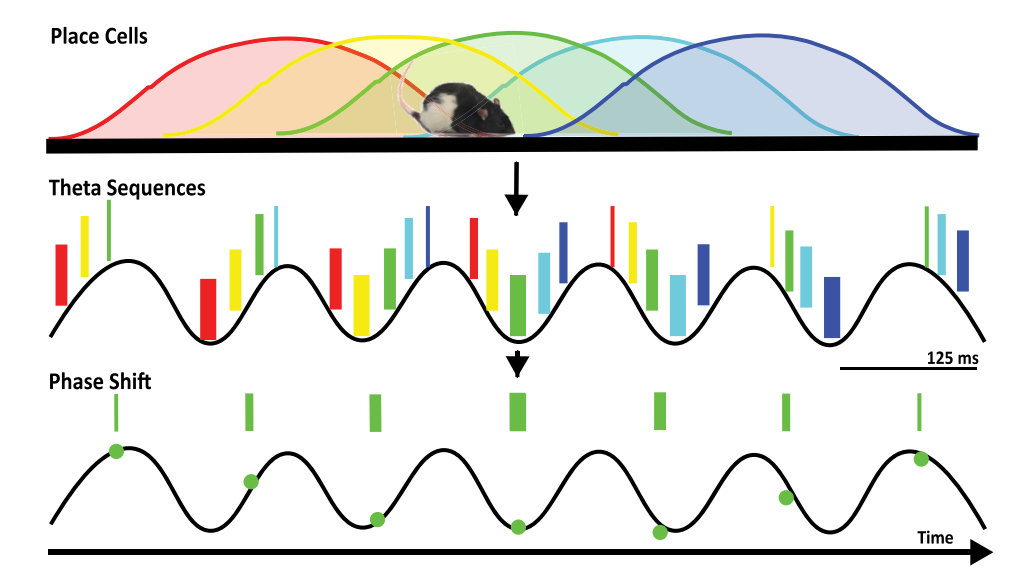


Figure 1.3: Schematic of theta sequences and phase precession. Top row: Place cells are represented by a different colour red, yellow, green, light blue and dark blue. Each tuning curve reflects the place field of the cell. **Middle row:** Theta sequences are the compressed firing of place cells representing the trajectory of an animal, sweeping from behind the animal to in front of it (from the red-coloured cell to the dark blue-coloured cell). A theta sequence occurs during each theta cycle. The firing of the cell within the theta sequences shown here can be seen in relation to the phase precession of spiking with successive theta cycles. **Bottom row:** Phase precession occurs at the level of individual cells. Phase precession of one place cell (green colour) is depicted here. The animal is currently located at the centre of this cell's place field. The sinusoidal wave depicts 6 successive theta cycles. The firing of the cell progressively fires at earlier stages of theta as the animal runs through the place field. Image courtesy of Isabella Varsavsky.

1.3.2 Head direction cells

HD cells were first observed in the postsubiculum (PoS) of rats, one of the input structures to the hippocampus (Ranck, 1984). These cells were seen to preferentially fire when the animal's head was facing in a given direction on the azimuth (horizontal) plane, irrespective of the animal's location (Figure 1.2). Head direction cells have since been identified in the anterodorsal thalamic nucleus (ADN; Taube, 1995), lateral mammillary nuclei (LMN; Stackman and Taube, 1998), dorsal tegmental nucleus (DTN; Sharp et al 2001b), retrosplenial cortex (RSC; Chen et al 1994), and MEC (Sargolini et al 2006), among other brain areas (Figure 1.2). Given that HD cells are the focus of this thesis, the reader is directed to Chapter 2 which

outlines in extensive detail the characteristic properties of HD cells and their underlying network structure.

1.3.3 Grid cells

Grid cells fire at multiple, discrete locations within an environment to form periodic firing fields which tessellate the environment in a hexagonal-like grid (Figure 1.2). Grid cells are localised in the MEC (Hafting et al., 2005), the presubiculum and parasubiculum (Boccara et al., 2010). They are characterised by three main properties: orientation (the rotation of the grid pattern), wavelength (the distance, or spacing, between firing fields), and phase (the location of the firing fields within an environment; Hafting et al., 2005). The relative offset of neighbouring cells occurs in such a manner that an entire environment is represented by a sufficiently large ensemble of grid cells (Hafting et al., 2005). Notably, grid cells throughout the MEC are discretised into independent modules, or subpopulations, which vary in terms of grid orientation and wavelength (unlike the smooth topographic representations of the sensory cortex; Stensola et al., 2012). Grid cells also exhibit a characteristic topography along the dorsoventral axis of the MEC, with grid cells of the ventral MEC having larger firing fields and wider spacing between fields than those of the dorsal MEC (Hafting et al., 2005). First identified in rats, they have also been found in mice (Fyhn et al., 2008), bats (Yartsev et al., 2011) and humans (Jacobs et al., 2013).

Grid cells are in some cases modulated by heading direction and speed (Sargolini et al., 2006; Hinman et al., 2016), and in deeper layers of the MEC grid cells are co-localised with cells which conjunctively encode grid and heading direction (Sargolini et al., 2006). Similarly to place cells, phase precession occurs in grid cells (layer II MEC) but this is independent of the hippocampus (Hafting et al., 2008). Theta band oscillations furthermore appear to be necessary for the spatial periodicity of grid cells in the MEC of rodents (Brandon et al., 2011; Koenig et al., 2011). Computationally, grid cell firing is often modelled via the integration of movement dis-

tance and direction information (Burgess et al., 2007; McNaughton et al., 2006). The regularity of grid cell firing fields has led to conjecture about whether grid cells may act as a path integrator (tracking self-motion cues over time to maintain an internal estimate of the animal's movement from an arbitrary starting location; McNaughton et al., 2006), or as a spatial metric for vector-based or goal-based navigation calculation (forward, direct trajectory planning; Bush et al., 2015; Erdem and Hasselmo, 2012; Kubie and Fenton, 2012).

Grid cells are believed to support vector-based navigation by the ensemble firing of grid cells at different scales and phases within an environment, which can provide information about an animal's distance and direction from a goal location (Bush et al., 2015). Evidence which suggests such a role for grid cells are the discretisation of the grid cell network (Hafting et al., 2005; Stensola et al., 2012) along with the co-localisation of object-vector coding cells, border cells and head direction cells in the MEC (Hoydal et al. 2019, Solstad et al., 2008; Sargolini et al., 2006). Grid cell maps can furthermore restructure or distort in response to environmental manipulations (Barry et al., 2007; Krupic et al., 2015) or reward locations (Boccara et al., 2019).

Evidence to support the theory that MEC grid cells are important for path integration includes impairments in path integration observed in MEC-lesioned animals (Allen et al., 2014) or when disruption to grid cell firing is brought on in NMDA knock-out mice (Gil et al., 2017). The integration of self-motion cues via path integration is prone to the accumulation of error without a correction mechanism. In order to maintain an accurate estimation of position, external landmarks are used to correct for accumulating error. This has been demonstrated via cue control experiments showing that when a polarising visual cue in an environment is rotated there is an equivalent shift in the orientation of grid cell firing (Hafting et al., 2005). Encounters with environmental boundaries have also

been shown to offset error accumulation in the grid cell network (Hard-castle et al., 2015). Changing the shape of an environment (deformation) by compressing the walls of the environment to change the size and shape tends to compress the grid by a corresponding amount (Barry et al., 2007). Evidence indicates that the ensemble grid symmetry is deformed in polarised environments: grid cell firing fields either orient towards the walls (in square environments, for example) or become more elliptical in trapezoid, or other highly-polarised, environments (Krupic et al., 2015).

Path integration has been revealed as a significant factor in shaping the spatial periodicity of grid cells, especially in one-dimensional circular environments (Jacob et al., 2019). Some studies have indicated that grid cell activity persists in darkness, albeit with reduced spatial precision and stability (Allen et al., 2014; Dannenberg et al., 2020). However, contrary evidence in mice suggests that grid cell spatial patterns are disrupted in complete darkness (Chen et al., 2016; Perez-Escobar et al., 2016), challenging the idea that grid cells rely solely on self-motion information for position estimation and implying a dependence on external visual cues.

Furthermore, Chen et al. (2016) demonstrated alterations in the relationship between running speed and theta frequency, as well as the firing rate of speed-modulated grid cells, in mice navigating familiar environments in the dark. This suggests that optic flow might be a crucial factor in calculating running speed, highlighting the insufficiency of vestibular and proprioceptive information alone in providing an accurate estimate of linear speed or spatial displacement in mice. Collectively, these findings emphasise the critical role of visual input in maintaining grid cell periodicity and stability in mice.

In summary, although grid cells are undoubtedly involved in path integration in rodents, the presence of visual cues, landmarks, and environmental boundaries remains essential for error correction and the preservation of the grid cell metric.

1.3.4 Boundary cells

The finding that place cell firing is partly defined by the geometric boundaries in an environment (Burgess and O'Keefe, 1996) led to the introduction of the boundary vector cell (BVC) model of place cell firing (Burgess et al., 1997; Hartley et al., 2000). The BVC model proposed a hypothetical cell as input to place cells that respond to barriers in an environment, which would project this information to place cells in the hippocampus.

Subsequent to this hypothesis, two types of boundary-responsive cells were identified, including border cells in the MEC (Solstad et al., 2008) and BVCs in the dorsal subiculum (Barry et al., 2006; Lever et al., 2009). Boundary cells are not sensory-bound but will respond to any barrier to movement in an environment, such as walls, ridges or objects (Stewart et al., 2013). While border cells tend to have location-specific firing adjacent to an environmental boundary, BVCs fire preferentially when the animal is at a certain distance and direction from a given boundary. A similar type of cell, termed a vector trace cell, has recently been described in the subiculum (Poulter et al., 2021). Vector trace cells generate new firing fields in response to an environmental boundary or an object inserted into the environment when encountered at a particular distance, which persists in the absence or removal of that object on the timescale of several hours (thereby generating a memory trace of the cue; Poulter et al., 2021). In this way, they are distinct from non-trace cells including boundary vector cells.

1.3.5 Interactions between spatial cell types

In order for place navigation to occur effectively, a cognitive map requires not only location information, but also direction and distance information (O'Keefe and Nadel, 1978). As discussed in the previous section, this information is provided by the combined inputs of a number of spatially-modulated cell types. The information ultimately coalesces in the hippocampus: Substantial evidence of place cell activity supports

the view that firing is influenced by inputs concerning environmental geometry (O'Keefe and Burgess, 1996; Lever et al., 2002), orientation (Fuhs et al., 2005) and path integration (Gothard et al., 1996). Place cell firing fields close to environmental boundaries are likely influenced by inputs from boundary-sensitive neurons, as suggested by developmental studies showing that the first place fields in postnatal development are most stable close to environmental boundaries (Muessig et al., 2015).

Orientation information, encoded by HD cells originating in subcortical regions, is necessary for normal functioning of higher cortical spatial cells. HD cell information reaches the MEC through ascending pathways arising from the subcortical brain areas of the DTN and LMN. The integration of HD cell information appears to be critical for spatial modulation of grid cell activity, given that disruption to HD cell firing disrupts the spatial periodicity of grid cells (Winter et al., 2015). Further evidence to support this was a recent study demonstrating that canonical grid cells are modulated by head direction in a multi-directional manner distinct from conjunctive grid-by-direction cells which are co-localised in the MEC (Gerlei et al., 2020).

The subsequent integration of orientation information in the hippocampus is consistent with findings that place cells and HD cells are strongly coupled in response to environmental cues (Knierim et al., 1995), and that place cell activity is modulated by heading direction relative to reference points (Jercog et al., 2019). A number of theoretical models have posited that the directional signal is integrated by place cells to establish and maintain location-specific firing (McNaughton et al., 1996; Touretzky and Redish, 1996), or possibly as a means to orient to a particular viewpoint for retrieval of spatial (or episodic) episodes via the conversion of inputs between egocentric and allocentric representations (Burgess, 2002). Although cue control of visual landmarks is disrupted in PoS-lesioned animals (Calton et al., 2003), place cell firing is preserved following lesions to

the HD cell network (Calton et al., 2003; Sharp and Koester, 2008).

Populations of cells containing directional heading, boundary and path integration information co-localise in the entorhinal cortex (EC; Sargolini et al., 2006). The EC, in turn, is the largest source of input to the hippocampus proper (Ramon y Cajal, 1902; Witter et al., 1989; Burwell, 2000), and consequently place cell firing (Brun et al., 2002; Brun et al., 2008). In this way, one may speculate that grid cells interact with place cells of the hippocampus through the encoding of idiothetic information. Conversely, grid cells in the MEC also require excitatory input from the hippocampus (Bonnevie et al., 2013). Specifically, inactivation of the hippocampus abolishes the grid cell firing pattern (Bonnevie et al., 2013), suggesting that excitation from hippocampal place cell projections provide allothetic information which enables the anchoring of grid cell firing fields to an external reference frame (Moser and Moser, 2008). Border cells in the MEC are furthermore thought to act as an error correction mechanism for grid cells (Hardcastle et al., 2015).

Ensemble grid cell activity in MEC appears to be predictive of the remapping of place cells in the hippocampus (Fyhn et al., 2007). In the instance where rate remapping of place cells occurs, for instance by changing the colours of the wall in an environment, grid cell firing fields remain stable. Conversely, when global remapping is induced either by changing the shape of an enclosure or moving between two different rooms, grid cell ensembles exhibit a shift in the firing vertices, while the network's relative phase structure remains stable (Fyhn et al., 2007). This may contribute to the associative memory network in the hippocampus as a means to distinguish overlapping, or similar, information. However, removing grid cell input to the hippocampus does not disrupt place field firing but instead results in a reduction in the spatial information of cells as well as a broadening of firing fields (Schlesiger et al., 2015). Furthermore, grid cell inputs are not required for place codes to emerge in a novel environment (Brandon

et al., 2014). However, phase precession is abolished upon lesioning of the MEC, suggesting that grid cell inputs to the hippocampus may be driving the temporal organisation (phase coding) of place cell firing (Schlesiger et al., 2015).

Studying the ontogeny of these cell types has helped experimenters to identify the relative dependencies and transmission of information between HD cells, grid cells, boundary-responsive cells and place cells. The respective roles for spatially-modulated cell types described here are thus reflected in their developmental timeline in rats (Wills et al., 2010; Langston et al., 2010; Bjerknes et al., 2015; Muessig et al., 2015), which are discussed in detail in Chapter 3. Briefly, head direction cells are the first to emerge (Wills et al., 2010; Langston et al., 2010), followed by border cells (Bjerknes et al., 2014) and place cells (Wills et al., 2010). Grid cells, in turn, emerge last (Wills et al., 2012).

1.3.6 Studies of spatial cells in complex and naturalistic scenes

A limitation which applies to all of the research mentioned thus far is that the study of spatial cells is traditionally conducted in simple environments, with controlled cues available to the animal. These cues are often restricted to being the boundaries of the recording enclosure and a single, polarising visual cue. In the wild, however, an animal's environment is far less abstract or static. Their environment is complex, cue-rich, and dynamic. Few studies have investigated the behaviour of spatial cells in complex or naturalistic environments, and none as yet have assessed the effect of complex environments on the developmental trajectory of spatial cells in postnatal rats.

Of those which have sought to probe this: One study, which exploited the use of wireless technology, recorded HD and grid cells in the MEC and parasubiculum of adult rats as they explored their homecage (Sanguinetti-Scheck and Brecht, 2020). The authors sought to investigate whether

the embedding of the homecage within the environment evoked an egocentric, home-bearing signal in the population of recorded HD and grid cells. The homecage in this case was embedded within a larger, square environment with multiple polarising cues available. The homecage had two doors present which allowed the animal to freely enter and exit the homecage to explore the outside environment, and the animal was habituated to this enclosure over a period of two weeks before recording began. Throughout a given trial, the homecage was periodically moved to different positions around the arena. The authors found that HD cell activity did not alter either in the presence of the homecage or following translation of the homecage to another section of the environment. Meanwhile, although grid cells did not globally remap, the authors remarked that there was a local shift in single firing fields towards the embedded homecage.

Regarding the activity of spatial cells as a function of the complexity of an animal's rearing environment, some studies have demonstrated improved performance in spatial memory tasks such as the Morris water maze in animals exposed to complex environments compared to those reared in isolated environments (Tees, 1999). One particular study assessing the relative impact of exposure to a complex environment on the activity of hippocampal place cells (Bilkey et al., 2017) reported that ultimately the population encoding of novel environments by CA1 place cells was sparser than control groups, but did not affect the fundamental spatial firing properties of recorded cells. Conversely, rats raised in bare cages which lack enrichment have demonstrated spatial learning deficits (Schrijver et al., 2004). It should be noted that any atypical rearing conditions can impact the development of hippocampal learning. This includes, for example, poor or deprived maternal care (Liu et al., 2000). A caveat of the finding that rearing in bare enclosures results in spatial learning impairments may therefore be a consequence of an animal's stress response, rather than merely a lack of exposure to complex stimuli.

A limitation of the lack of experimental evidence for spatial cell behaviour in complex or naturalistic environments, at least from a developmental perspective, is that the ability of the animals to use landmark cues is not possible until eye-opening (which in rats occurs around postnatal day (P) 15). Findings such as those discussed here therefore beg the question: Are the behaviour of spatial cell types such as HD cells being effectively studied in development when the probe environment is unlike anything found in nature? This will be discussed in detail in the remaining chapters of this thesis, exploiting recent advances in wireless technology.

1.4 Summary

In understanding the localisation, emergence and functional properties of the cell types described, investigators hope to elucidate the ways in which the brain orchestrates the ability to efficiently navigate. Furthermore, the collapse of navigational abilities and spatial awareness have been heavily implicated in Alzheimer's disease (Salmon and Bondi, 2009) and schizophrenia (Park and Holzman, 1992; Salgado-Pineda et al., 2016). It is therefore important to understand the building blocks of spatial cognition and memory to understand how these systems may deteriorate with disease. Studying the components of the hippocampal formation and its constituent role in spatial memory therefore affords a unique window into both healthy and pathological ageing (Wolbers et al., 2014).

Chapter 2

The head direction cell circuit

Head direction (HD) cells are important components in the neural representation of space, unexpectedly discovered by James B. Ranck Jr. (1984) when he happened to implant electrodes in the postsubiculum (PoS; also termed dorsal presubiculum) of the rat brain. He identified a population of cells which preferentially fired when the rat's head was facing a certain direction on the horizontal (azimuth) plane (Figure 2.1).

Subsequent work by Jeffrey Taube and colleagues led to more detailed characterisation of the characteristic properties of HD cells in the PoS (Taube et al., 1990a; Taube et al., 1990b). HD cells were found to fire independently of location and with each direction equally represented across the population of recorded HD cells. The average directional range of firing for a given HD cell was 84°, and the entire 360° directional range was represented when all cells' preferred firing directions (PFD) were pooled together. The activity of the cells was monitored when the animal was placed into a novel environment or an environment of differing shape (for instance, moved from a cylinder to a rectangular environment), at which time the HD cells would maintain their characteristic firing properties but the cells' PFD would often shift to a new direction. When returned to the original environment, the cells would shift to their former PFD for that context (Taube et al., 1990a). In the same vein, landmark control of HD cells was investigated. The introduction of a salient, polarising landmark

into the environment reliably introduced a shift in the cells' PFDs such that they became anchored to the landmark.

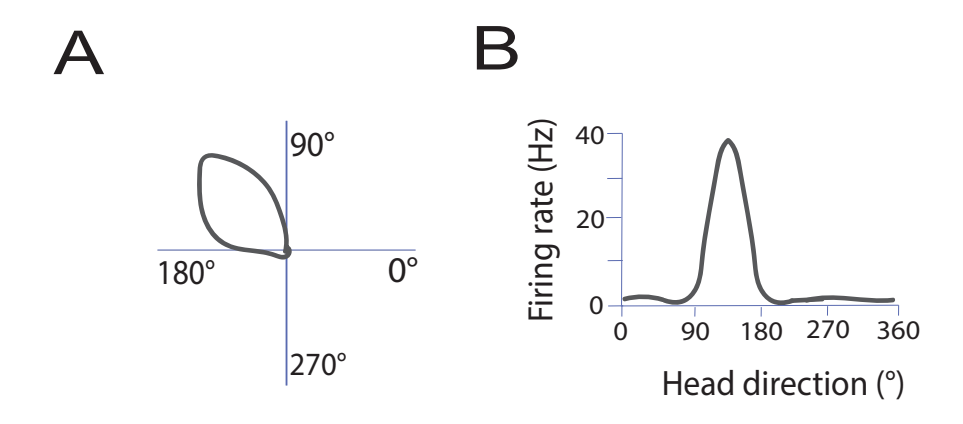


Figure 2.1: Example head direction cell with preferred firing direction of approximately 130°. (A) Polar plot of cell firing. Firing rate (in arbitrary units) is depicted as a function of head direction, within the absolute reference frame of the recorded room. (B) Linear plot of cell firing. The firing rate of the cell versus head direction is shown. HD cells typically form a Gaussian tuning curve, with maximal firing in the cell's preferred firing direction, and minimal firing (close to zero) outside of this range.

Since these first notable experiments were conducted in the PoS, HD cells have been identified in a distributed network of cortical and subcortical brain areas. The core HD cell circuit includes the dorsal tegmental nucleus (DTN; Sharp et al., 2001a), lateral mammillary nuclei (LMN; Stackman and Taube, 1998), anterodorsal thalamic nucleus (ADN; Taube, 1995), retrosplenial cortex (RSC; Cho and Sharp, 2001), PoS (Ranck, 1984; Taube et al., 1990a) and the MEC (Sargolini et al., 2006). HD cells have also been identified in the laterodorsal thalamic nucleus (LDN; Mizumori and Williams, 1993) and striatum (Wiener, 1993). In this way, the HD cell system forms an extended network between the brainstem and neocortex, with many recurrent connections. In addition to rats, HD cells have also been identified in mice (Yoder and Taube, 2009), non-human primates (Robertson et al., 1999; Laurens et al., 2016), bats (Finkelstein et al., 2015), chinchillas (Muir et al., 2009), birds (Ben-Yishay et al., 2021), and indirectly in humans (Shine et al., 2016).

Alongside those properties already outlined, experiments have revealed further detail on typical HD cell properties. It is notable that HD cells fire purely as a result of head direction with respect to the static surroundings, and not by the relative position of the head to the body (Blair and Sharp, 1995) or the direction of gaze (Robertson et al., 1999). HD cells also exhibit anticipatory firing (Blair and Sharp, 1995), wherein the cells will fire in advance of the rat facing their PFD. In this way, the cells appear to be optimised for firing before the animal's head reaches the predicted future heading direction. The interval in which the cell begins to fire before reaching the PFD is termed the anticipatory time interval (ATI; Blair and Sharp, 1995). The ATI differs in respective brain regions, with the LMN having the longest interval (ranging from 40 ms to 75 ms; Blair and Sharp, 1998; Stackman and Taube, 1998). The ADN and RSC have comparable ATIs, at approximately 25ms (Blair and Sharp, 1995; Cho and Sharp, 2001), while the ATI of PoS-located HD cells is 0ms such that these cells fire when the animal's head is directly in the PFD (Blair and Sharp, 1995). In this way, the ATI of HD cells decreases as you ascend from the respective 'vestibular' component regions of the HD network to the 'landmark' component, cortical regions of the HD circuit.

The HD network is generally considered to be hierarchical in structure (Figure 2.2), discussed in detail in Section 2.3. Briefly, the principal circuit arises in the DTN and LMN, where vestibular signals (such as angular head velocity; AHV) are integrated for use in path integration (Stackman and Taube, 1998; Bassett and Taube, 2001). The HD signal is projected to the PoS via the ADN (Goodridge and Taube, 1997). From the ADN, the HD signal is conveyed to the RSC and PoS, which in turn projects to the MEC (Mehlman and Taube, 2018).

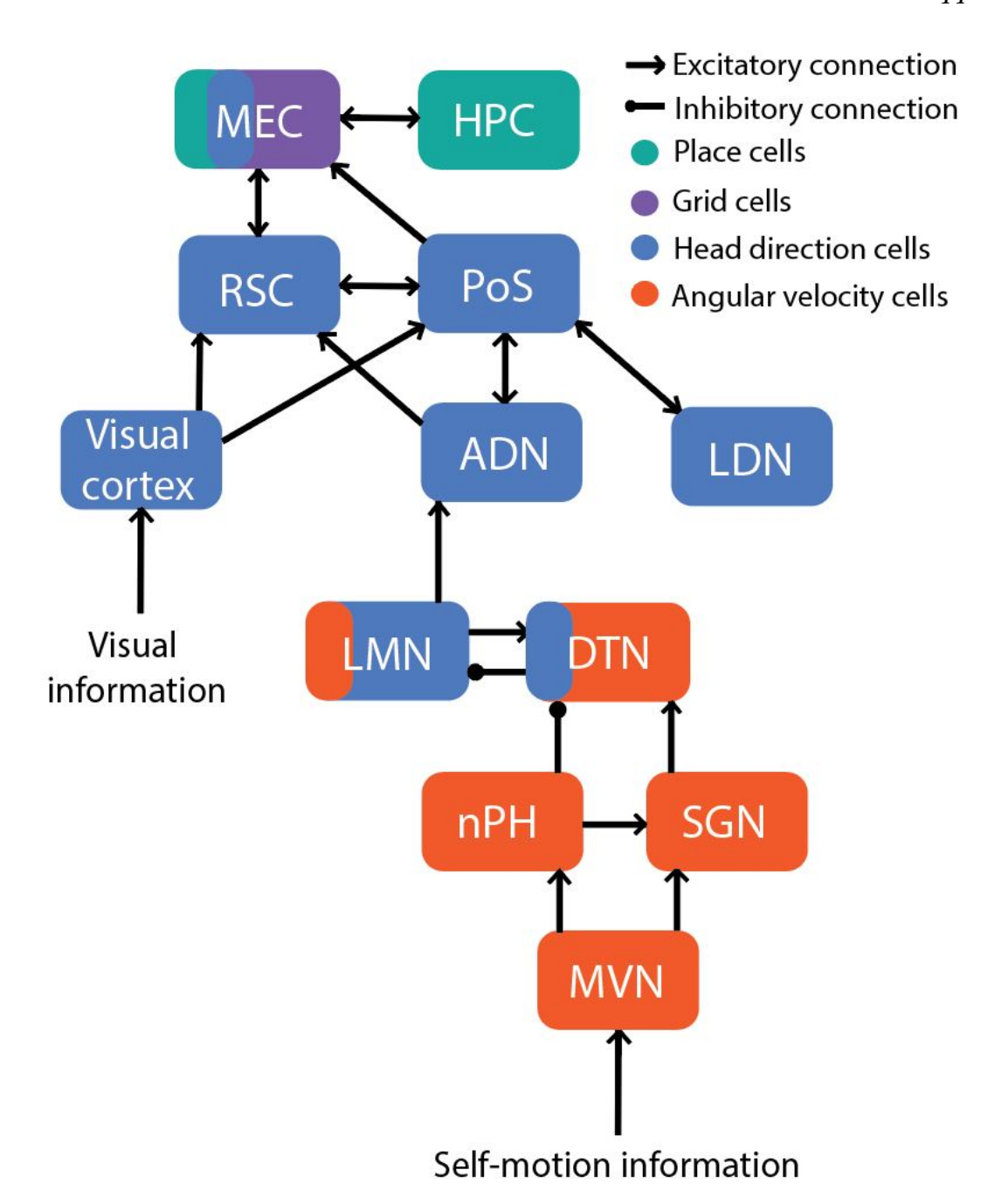


Figure 2.2: Simplified schematic of the relative connectivity of brain regions containing head direction cells, grid cells, place cells and angular head velocity cells. Arrows indicate the direction of signalling. MVN, medial vestibular nuclei; nPH, nucleus prepositus hypoglossi; SGN, supragenual nucleus; DTN, dorsal tegmental nucleus; LMN, lateral mammillary nuclei; ADN, anterodorsal thalamic nucleus; LDN, laterodorsal thalamic nucleus; RSC, retrosplenial cortex; PoS, post-subiculum; MEC, medial entorhinal cortex; HPC, hippocampus.

2.1 Head Direction Cell Properties

Generation of the HD cell signal principally occurs by the integration of vestibular (idiothetic) cues. HD cells can maintain their PFDs for short periods in different rooms, in novel environments, and in the dark (Taube and Burton, 1995; Goodridge et al., 1998). HD cells are thus able to maintain an estimate of direction without reference to landmark cues through integration of self-motion information, although this is prone to error without a reset mechanism due to incorrect directional signals accumulating over time. External cues are assessed in order to correct the HD estimate and maintain a stable HD signal with respect to the environment, and familiar visual landmarks have generally been shown to exert stronger control over HD cell firing than path integration when both are available (Goodridge and Taube, 1995). The PoS is a key component of the HD cell network in this respect, integrating information about visual landmarks which enables resetting of the HD signal (Figure 2.2; Goodridge and Taube, 1995). Experimental findings which support these properties of the HD cell network are discussed below.

2.1.1 Cue control of head direction cells

2.1.1.1 Allothetic cue control: Visual landmarks

As mentioned, when landmark control of HD cells was tested by Taube and colleagues (Taube et al, 1990a; Taube et al, 1990b), it was found that the PFDs of HD cells became anchored to a salient visual cue (a white cue card) in the environment. If the landmark was subsequently moved or shifted, all cells shifted their PFDs coherently in accordance with the degree of movement of the cue. A subsequent study sought to ascertain the relative contribution of external versus internal sensory inputs to the activity of HD cells (Goodridge and Taube, 1995). A rat was introduced to an environment with a salient visual cue in a cylindrical environment, at which point the cue was removed and the HD cells remained stable (there

was no drift in PFD). Upon moving the cue to a different part of the environment, the PFD of the HD cells shifted to anchor to the new cue location. This demonstrated that sensory inputs in the form of salient, visual landmarks are capable of overriding idiothetic information provided by vestibular, proprioceptive or motor efference copy cues (Goodridge and Taube, 1995). Futher experiments demonstrated that exposure to a new landmark introduced into an environment (in this case a white cue card) for just 8 minutes was sufficient for the novel cue to exert control over the cells' PFD (Goodridge et al., 1998). Exposure times of 1 and 3 minutes were also tested, however this resulted in cue control of cells in only half of those trials (Goodridge et al., 1998).

When both distal (background) and proximal (foreground) visual cues were tested for their relative impact on cue control, it was found that distal but not proximal cues are used as the primary reference for HD cells (Zugaro et al., 2001). When distal and proximal cues are in conflict, coherence is maintained between HD cells such that they will rotate as an ensemble in line with the distal cue (Yoganarasimha et al., 2006). CA1 place cells, by contrast, will exhibit split representations of the environment such that some place fields will change to reflect rotation of the proximal cue, while others will reflect the rotation of the distal cue (Yoganarasimha et al., 2006).

Another study, conducted on place cells in the CA3 region of the hip-pocampus (Lee et al., 2004), yielded contrasting results compared to CA1 place cells. Specifically, CA3 exhibited a more consistent representation because its place fields tended to (in most cases) rotate in the same direction. Therefore, in an environment where familiar landmarks were dynamically shifted relative to each other, the CA3 population's representation of the environment remained more cohesive compared to CA1. CA3 is distinct in the hippocampus due to its recurrent collateral circuitry, allowing its pyramidal cells to establish excitatory synaptic connections with each

other (Lorente de Nó, 1934; Ishizuka et al., 1990). In contrast, CA1 pyramidal cells lack extensive interconnections (Amaral and Witter, 1995). These findings highlight a functional disparity between the place cells of CA3 and CA1 at the level of neural population representations. The hippocampus is often conceptualized as an autoassociative memory network capable of retrieving the originally stored representation even in the presence of incomplete, corrupted, or noisy inputs, a process referred to as "pattern completion" (Marr, 1971; McNaughton and Morris, 1987). Through its recurrent collateral circuitry, the CA3 region is believed to perform such autoassociative functions (Treves and Rolls, 1994; Hasselmo et al., 1995). The findings of Lee et al. (2004) are consistent with this theory, and implies that the internal attractor dynamics governing head direction cells more closely resemble those of CA3 than CA1.

Cue control of non-visual cues in the form of tactile, olfactory and auditory stimuli have also been investigated (Goodridge et al., 1998). A consistent finding is that while auditory cues do not tend to have an effect on the firing of HD cells, in some instances tactile and olfactory cues exert control such as when rotations of the environment apparatus occur (Goodridge et al., 1998). Nonetheless, the prevalent view is that the relative effect of non-visual allothetic cues on the activity of adult HD cells is usually minimal.

Researchers have deduced from these experiments that external cues are assessed in order to correct the HD estimate and maintain a stable HD signal with respect to the environment. The PoS is an important convergence point in the HD cell network for the integration of visual landmarks, which enables resetting of the head direction signal (Goodridge and Taube, 1995). This is supported by studies in which lesions to the PoS result in disruption of cue control (the ability of visual cues or landmarks to exert a change in the PFD of cells) in HD cells of the ADN (Goodridge and Taube, 1997) and the LMN (Yoder et al., 2015). Through the integration

of idiothetic (AHV) and allothetic (visual landmark) information, HD cells are able to maintain a constant internal estimate of direction which is coherent across the cell population.

2.1.1.2 Allothetic cue control : Response to geometric cues

Interest has also been placed on the relative importance of geometric cues in providing a directional reference frame for HD cells, with a particular focus on environmental boundaries and wall geometry. Studies have shown that if an adult rat is disoriented, it is geometric cues which are primarily used for reorientation rather than feature information cues such as odour or colour (Cheng, 1986). One such study involved a number of rats being trained to forage for a food reward in one corner of a rectangular environment. It was found that rats consistently searched for the reward in the diagonally opposite corner to the actual location of the reward, despite the presence of salient, non-geometric cues in the correct location which could serve as a means to disambiguate the two opposite corners (such as distinct odours, patterned or coloured walls). The proportion of times the rat searched in the correct corner compared to the diagonally opposite corner was about 50% (Cheng, 1986).

More recent studies have explored this phenomenon in tandem with electrophysiological recordings of HD cell units. In one such study (Knight et al., 2011), rats explored three environments with distinct geometry (trapezoid, teardrop-shaped, and isosceles triangle-shaped) which each had a salient, distal landmark in the form of a white cue card within the curtained arena. In non-disoriented animals a shift in relative PFD of the recorded HD cells to align with the distal visual cue was observed when the environment was rotated. When the animals were first disoriented before recording onset, the HD cells shifted to align with the geometry of the environment when the environment was rotated. If the salience of the visual cue was diminished (with the use of a grey cue card, instead of white), the cue did not reliably induce a corresponding shift in cell PFD when it

was rotated. The authors concluded that the use of external cues may be salience-driven, wherein highly salient visual cues override the use of geometric cues (Knight et al., 2011; Clark et al., 2012a). In this case, geometric cues only weakly influence HD cell firing in non-disoriented rats. This finding complements studies showing that when a rat is trained to forage for food in a cylindrical environment, and then the shape of the environment is changed to a rectangle, there is a distinct shift in the directional firing of recorded HD cells despite the presence of a proximal landmark (white cue card) (Taube et al., 1990b; Golob et al., 2001).

The effect of disorientation has been shown to result in unstable HD cells which are limited in the extent to which they become associated with visual cues in the environment. This was ascertained in a study by Knierim and colleagues (1995), in which they performed single-unit recording of both thalamic HD cells and hippocampal place cells. Rats were trained to forage for food pellets in a cylindrical environment with a white card placed inside the cylinder wall acting as a salient visual cue. A subset of the rats were disoriented prior to recording while the other subset were not. It was found that despite all HD cells and place cells remaining strongly coupled across all recording trials, the visual cue was much less likely to exert control over the PFD of the cells recorded in disoriented animals. The authors inferred that the ability of a salient cue to control the activity of the cells depended on the rat's learned associations between the cues and their internal direction sense. In the case of disorientation, the rat was unable to form an association between its directional sense and the stability of the visual cue.

Another study produced conflicting results (Dudchenko et al. 1997). Rats were trained to perform a similar task, with the addition of an 8-arm radial maze to the standard cylinder environment used by Knierim and colleagues. Animals were disoriented both before and after each trial. The cue control of the landmarks in both environments was assessed by ro-

tating the landmark and observing the subsequent shift in PFD of the HD cells. Surprisingly, the rotation of the cue resulted in a corresponding shift in the PFD of the cells. This suggests that the relative salience of a visual cue may be increased when in environments with more complex geometry, such as the radial arm maze used in this study, and consequently will continue to exert cue control over HD cells in disoriented rats.

It should be noted that such studies have not been conducted in rats before eye-opening, wherein geometric cues are likely the most salient cues available in an environment. The relative dependence on geometric and feature cues also appears to vary with age, such that young animals and children may rely more heavily on geometric cues than feature cues for reorientation (Hermer and Spelke, 1994; Twyman et al., 2013).

2.1.1.3 Idiothetic cue control

The HD cell system, in receiving input from subcortical regions containing vestibular and angular velocity information, maintains a stable directional orientation based on idiothetic cues which provide an internal sense of movement (Yoder and Taube, 2014). The relative use of idiothetic and allothetic cues in the encoding of head direction was assessed by Blair and Sharp (1996). HD cells in the anterior thalamus were recorded while an animal explored a rotatable cylindrical environment that had no salient visual cue but rather had alternating black and white stripes on the walls, angled at 45°. In rotating the environment, the rat was provided with both visual motion and angular motion (vestibular) cues. When a rotation of 90° occurred at a speed slow enough that the rats did not notice, all HD cells shifted by a corresponding 90°. However, if the environment was rotated at a speed noticeable to the rats then the cells did not shift their PFD. The authors concluded that both visual motion cues and angular motion cues interact to determine the animal's directional reference frame.

When cue control of external spatial cues is put in conflict with internally-derived, idiothetic cues, the behaviour of the HD cell firing de-

pends on the extent of the mismatch in cues (Knierim et al., 1998). For instance, when there is a small mismatch (approximately 45°) between the landmarks in the environment and the rat's internal HD representation then the HD cells are more likely to shift to comply with the visual cue. However, if the mismatch is large, the HD cells will likely not reorient towards the landmarks (Knierim et al., 1998). In this study, it was the rat's idiothetic cues that exerted control over HD cell firing. In some instances, the landmark cue caused a shift in the PFD of cells to reflect the degree of cue rotation, but this occurred with a time delay. Consistent with Goodridge et al. (1998), HD cell firing was largely stable when the animal was recorded in the dark, but drift in the HD cell PFD could be induced by slowly rotating the platform. Upon turning the lights on after a large drift in cell PFD, then the cells tended to maintain their firing. However, if there was a minor amount of drift before the lights came on, the cells would revert back to their initial PFDs before the dark trial (Knierim et al., 1998).

Cell ensembles have also been concurrently recorded in the ADN, MEC, parasubiculum and CA1 of the hippocampus (Hargreaves et al., 2007) to investigate coherent activity of their respective cell types in response to internal cues conflicting with external landmark cues. This experiment consisted of the rat being placed in a covered bucket while a visual cue was counter-rotated. Similar to Knierim et al. (1998), it was observed that in a subset of trials the cells shifted their response (place fields or HD cell tuning curves) to comply with the magnitude of the bucket rotation, or maintained their firing with respect to the landmark cue. While most recorded brain regions exhibited a uniform response, place cell ensembles responded with a greater degree of heterogeneity. These studies support the idea that HD cells may be controlled by the integration of self-movement (idiothetic) cues when it comes in conflict with the external framework. This defines the directional reference frame while maintain-

ing intrinsic network coherence.

2.1.1.4 Passive transport

Studies of the dynamics of HD cell firing during passive transport have been used to assess the importance of voluntary movement cues (motor commands and optic flow, as well as efference copy and proprioceptive inputs) in driving HD cell responses. In some of the preliminary studies on HD cells in the PoS, passive transport of the rat resulted in either a decline (to approximately 50%) of the peak firing rates observed in freely-moving trials, or complete cessation of firing (Taube et al., 1990b). In this instance, the means of restraint was via an experimenter loosely holding the rat in a towel (Taube et al., 1990b). Similar results have also been observed in the ADN (Taube, 1995; Knierim et al., 1995) and the RSC (Chen et al., 1994b). Other studies have reported increased modulation of HD cell firing rates by AHV during passive transport, resulting in an overall decrease in peak firing rates of slow passive motion versus active motion at matched speed (Zugaro et al., 2002).

Furthermore, when an animal is moving from a familiar environment to a novel one via passive transport of the experimenter (either in the dark or in the light), there is a much more significant shift in the PFD of recorded HD cells than when the animal actively moves from one location to the other (Stackman et al., 2003). These findings suggest that optic flow and vestibular input are not the only idiothetic inputs which are required for an accurate directional representation, but that motor efference copy and proprioceptive inputs are also essential for accurate encoding of heading direction (Stackman et al., 2003; Yoder et al., 2011). This is supported by the fact that results in these paradigms tend to differ by the method of passive transport (the extent to which the animals are restrained). The decrease in HD cell firing rates observed in studies where the animal was tightly restrained (Taube, 1995) was more pronounced than in studies where the animal was immobile and unrestrained (Zugaro

et al., 2002).

2.1.2 Attractor network properties

A consistent observation in studying the effect of allothetic cue control on HD cells is that all cells shift their PFDs coherently to maintain their relative directional offset (Taube et al., 1990b). This network-level coherence is consistent with dynamics of a one-dimensional continuous ring attractor neural network (Skaggs et al., 1995; Redish et al., 1996; Zhang, 1996). This network model describes how those HD cells with similar PFDs (<60° offset; Peyrache et al., 2015) recurrently excite each other, while those with largely differing PFDs (>60° offset; Peyrache et al., 2015) suppress activity via lateral inhibition.

The attractor is conceptualised as a network of cells arranged in a circle, or ring, representing all PFDs (Figure 2.3). Through mutual excitation, a subset of HD cells (the 'activity packet' or 'hill of activity') fire when an animal's head is pointing in a certain direction. The state space (representation of head direction) is continuous, given that neighbouring nodes (HD cells) in the network have overlapping receptive fields (tuning curves; Figure 2.3). An estimate of the current HD is achieved by vector summation of previous HD and angular displacement to the current heading (McNaughton et al., 1991). The activity packet thus indicates the current heading direction of the animal, and the position of the activity hill moves along a circular state path in line with corresponding rotations of the head (Figure 2.3). Movement around the ring attractor shifts in line with the angular velocity of head turns (Bassett and Taube, 2001). Within this model, all cells maintain their relative PFDs (Figure 2.3).

As mentioned, this is supported by experimental evidence of a coherent shift in PFDs of cells in response to landmark control (Taube et al, 1990a; Taube et al, 1990b). The attractor dynamics of HD cells are also present in the ADN and PoS during sleep, observed by continued temporal coordination across brain states (Peyrache et al., 2015; Chaudhuri et

al., 2019). In these studies, the order of firing of HD cells reflected the same PFD offsets observed during exploration (inferring that the neural state space is the same in sleep and wake brain states). This is consistent with the HD system having an internally-organised mechanism for directional encoding (Peyrache et al., 2015). As may be expected, the temporal coordination of HD cells in regions which primarily integrate idiothetic cues (such as the ADN) had significantly more preserved temporal coordination than those regions which are influenced by allocentric cue integration (such as the PoS; Peyrache et al., 2015).

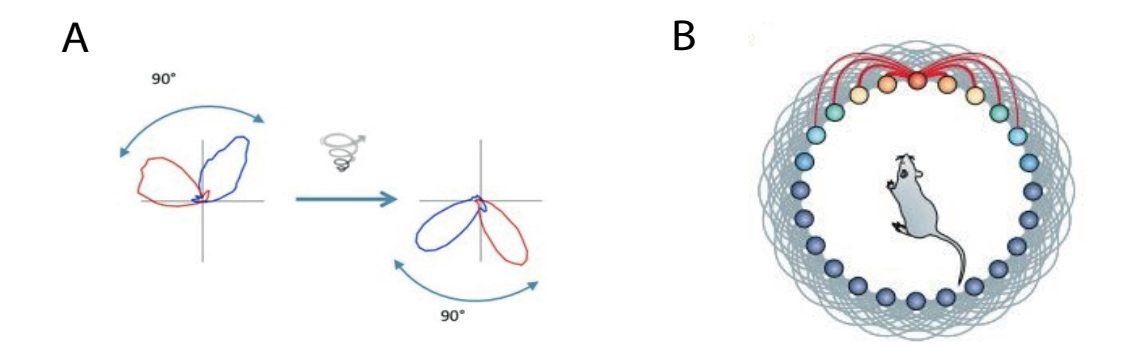


Figure 2.3: Continuous ring attractor network model for head direction cell activity. (A) The preferred firing directions of HD cells are coupled such that when there is a change in firing direction of cells, there is a coherent shift in the preferred firing directions of cells such that the relative offset in preferred direction is maintained. **(B)** The neuronal 'activity packet' corresponding to the direction of an animal's head in the yaw plane moves in line with corresponding rotations of the head. This activity packet arises from recurrent excitation of cells with similar preferred firing directions and is driven by angular head velocity signals from the DTN and LMN. Adapted from McNaughton et al., 2006.

Recurrent connectivity between the LMN and DTN is considered to be the source of this attractor network within the HD cell system (Sharp et al., 2001b) via the integration of vestibular inputs (AHV encoding the direction and speed of head rotations; Bassett and Taube, 2001) with the current directional heading. The confluence of these inputs in the DTN gives rise to a subset of cells which conjunctively encode AHV and head direction (Bassett et al., 2001; Sharp et al., 2001b). This network connectivity is then inherited in upstream components of the HD cell network including the

ADN, PoS and RSC (Chen et al., 1994b; Peyrache et al., 2015).

The intrinsic state transition dynamics which determine the manner in which a population of HD cells will reorient towards a landmark is of interest in understanding the continuous attractor network properties of the HD cell circuit. Zugaro and colleagues (2003) observed that spatial reorientation of HD cells in the ADN occurred rapidly after rotations of surrounding landmarks, in approximately 80ms for a 90° rotation. They claim that the short latency observed in this study may indicate that the firing activity of HD cells does not gradually traverse the entire population of cells with PFDs between the two orientations, but rather the network activity can abruptly jump from cells with the original preferred orientation to cells with the distal PFD, bypassing the cells between. The authors speculate that the short latency observed here may be a consequence of the degree of rotation, but also the salience of the cue; suggesting that in more complex visual scenes the latency may be longer. In isolation, this finding is not clear evidence for or against the mechanisms underlying the attractor network properties of HD cells.

Interestingly, a HD-encoding network has also been identified in the *Drosophila melanogaster* central complex which is akin to the mammalian HD system (Seelig and Jayaraman, 2015). Here, the anatomically circular arrangement of neurons encoding heading direction are indicative of the hypothesised ring attractor dynamics in the mammalian HD cell circuit.

2.2 Variations of canonical head direction cells

2.2.1 Angular head velocity cells

A subset of cells in the HD cell network, within the LMN (Blair et al., 1998; Stackman and Taube, 1998) and DTN (Bassett and Taube, 2001; Sharp et al., 2001a), encode AHV. Among recorded DTN cells, the vast majority encode AHV (approximately 75%), supporting the role of the DTN in idiothetic cue integration of head movement.

Symmetric cells have also been recorded which increase their firing rate proportionally in either direction, clockwise (CW) or counterclockwise (CCW; Figure 2.4A), accounting for 25% of AHV cells in the DTN (Bassett and Taube, 2001). Within the LMN, a small yet significant subset of neurons encode AHV (43% neurons), and these appear to be only of the symmetric classification (Stackman and Taube, 1998).

Within the population of AHV-encoding cells, there is a subset of AHV cells which have skewed firing responses to head turns (asymmetric AHV cells; 75% AHV cells in the DTN). One form of asymmetric AHV cells increase their firing rate in one direction (either CW or CCW), and decrease their firing rate when the animal moves its head in the other direction (Figure 2.4B). Some lateralisation is observed in these cells, wherein asymmetric AHV cells are often localised in the contralateral hemisphere to the preferred head turn direction. Other types of asymmetric AHV cells alter their firing in response to head movements in only one direction, responding with either an increase or a decrease in firing when the head moves in the preferred direction and does not alter its firing rate in response to head turns in the other direction (Figure 2.4C).

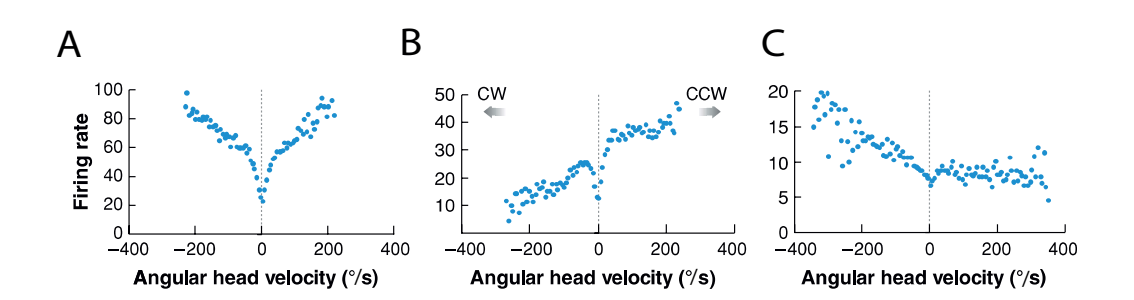


Figure 2.4: Representative angular head velocity (AHV) cells recorded from the dorsal tegmental nucleus. (A) Symmetric AHV cell which increases its firing rate in response to head turns in both the clockwise (CW) and counterclockwise (CCW) direction. (B) Asymmetric AHV cell which increases its firing rate in response to head turns in the CCW direction and decreases its firing rate in response to head turns. (C) Asymmetric AHV cell which increases its firing rate in response to head turns in the CW direction and does not alter its firing rate in response to CCW head turns. Adapted from Bassett and Taube, 2001.

2.2.2 Conjunctive cells

A small proportion of cells conjunctively encode AHV and HD, also identified in the DTN. Their abundance ranges in reports from 11% (Bassett and Taube, 2001) to 13% (Sharp et al., 2001a) of DTN neurons. The encoding of HD in these cells is broader than classic HD cells. Nevertheless, these cells are of particular interest to the HD cell network as they satisfy the criterion posited by theoretical models: a cell type which drives the activity hill of the continuous attractor network of head direction, in one direction or another (Sharp et al., 2001b).

Further conjunctive neurons are found in the MEC, where a subset of cells conjunctively encode head direction and grid signals (Sargolini et al., 2006; Brandon et al., 2011). These cells display spatial periodicity which is typical of grid cells, with an additional directional bias that confers a firing preference for a particular location and orientation.

Similarly, theta-modulated place-by-direction (TPD) cells have been identified in the PoS and parasubiculum (Cacucci et al., 2004) which conjunctively encode location and orientation. The directional firing of these cells is invariant to different environments, but the locational firing of these cells is dependent on the environment.

It is possible that the purpose of conjunctive theta-modulated cells is to transform the HD signal from 'pure' HD cells into a theta-modulated signal for use in allocentric navigation in the hippocampal formation (Cacucci et al., 2004). Interestingly, when theta rhythmicity is abolished via medial septum inactivation the spatial periodicity of MEC conjunctive grid-by-head-direction cells is lost, but TPD cells (as well as pure HD cells) retain their directional selectivity (Brandon et al., 2011).

2.2.3 Theta-modulated head direction cells

Theta-modulated cells comprise 75% of neurons in the anteroventral thalamic nucleus (AVN; Vertes et al., 2001). Within this, there is a population

of theta-modulated HD cells (Tsanov et al., 2011). This is interesting considering the AVN does not receive direct input from the LMN but instead from the medial mammillary bodies (Shibata, 1992). In this way, there appear to be two ascending pathways through the anterior thalamus: one pertaining to the head direction signal (through the ADN), and the other subserving thalamocortical theta projections through the AVN to the RSC (Lomi et al., 2021). There is speculation as to whether there exists a feedback loop which may account for an HD signal in the AVN, wherein the ADN projects the HD signal to the RSC and PoS, which then provide descending input to the AVN (Clark and Taube, 2012).

2.2.4 Head direction cells non-compliant with attractor dynamics

A subset of non-theta-rhythmic HD cells in the MEC and parasubiculum exhibit directional tuning but are not constrained by attractor dynamics (Kornienko et al., 2018). These cells are more strongly controlled by visual landmarks than co-recorded theta-rhythmic HD cells of the same region, therein conjunctively encoding heading direction and visual landmarks. In one study, when changes in non-rhythmic cell PFD occurred as a result of manipulation to a salient visual cue, the changes were often incoherent (the cells did not maintain the relative offset in PFD after shifting to anchor to the cue; Kornienko et al., 2018). This differed from the co-localised theta-rhythmic cells, which shifted coherently in accordance with continuous attractor dynamics of traditional HD cells. One function of these non-rhythmic cells may be to integrate information about the current directional heading with visual landmarks, whereas their theta-rhythmic counterparts likely support the integration of the HD signal by grid cells (Kornienko et al., 2018).

2.2.5 Bi-lobed head direction cells

The dysgranular region of the RSC comprises a population of cells which independently encode a landmark-dominated HD signal (Jacob et al., 2017). These cells express bidirectional firing patterns in environments which are bidirectionally symmetrical. These cells contrast with traditional HD cells which exhibit a unidirectional firing preference (which are also present in the dysgranular RSC and are presumably driven primarily by canonical HD cells in the PoS).

The presence of these cells was determined in the following context: An animal foraged for food in an environmental apparatus consisting of two chambers connected by a doorway, with identical visual cues placed on the opposing end walls. Despite the animal actively traversing between the chambers (therefore maintaining a global HD signal), a subset of recorded cells fired in polar opposite directions in one room versus the other. These findings suggest that landmark cues exert the strongest control over directional firing of these dysgranular RSC cells even when in conflict with a coherent directional signal (Jacob et al., 2017).

2.3 Anatomy of the head direction cell network

The HD cell network forms part of the Papez circuit, which is associated with the encoding of emotion and memory processes within the limbic system. This circuit consists of the hippocampal formation, mammillary bodies, anterior thalamus, cingulate cortex and parahippocampal gyrus (Papez, 1937). Each anatomical component of the principal HD cell network will be described in detail here, with emphasis on the connectivity and functionality within each respective region. In this way, the reader will begin to understand how the constituent components of the network give rise to the canonical HD cell behaviour thus far described.

2.3.1 Dorsal tegmental nucleus

The dorsal tegmental nucleus of Gudden (DTN) is considered to be an initial source of the head direction signal (and thus the source of HD attractor network properties), given the presence of both classic HD cells and AHV cells.

The DTN receives inputs from the nucleus prepositus hypoglossi (nPH; Liu et al., 1984) and supragenual nucleus (SGN; Biazoli et al., 2006), both of which are interconnected with the medial vestibular nuclei (MVN) and likely convey AHV information to the DTN. The DTN also sends projections to the interpeduncular nucleus both directly and indirectly via the habenular nuclei (Groenewegen and van Dijk, 1984). Within these connections, there is some subdivision wherein the ventral DTN (pars centralis) connects primarily to the LMN and the dorsal DTN (pars pericentralis) connects primarily to the interpeduncular nucleus (Hayakawa and Zyo, 1990). The DTN also has connections with the lateral habenula (which contains AHV neurons; Liu et al., 1984) and so may also be involved in the integration of non-vestibular, motor processing information given the presence of velocity-modulated neurons (Sharp et al., 2006).

In this subcortical brain area, between 12.5% to 14% are classic HD cells (Bassett et al., 2001; Sharp et al., 2001a). A large proportion of DTN cells encode AHV (75%; Bassett and Taube, 2001), while a smaller portion of cells are found to conjunctively encode both AHV and coarse HD (11%-13%; Bassett and Taube, 2001; Sharp et al., 2001a). This is in agreement with predictions made by theoretical models of HD continuous attractor network properties (Redish et al., 1996; Zhang et al., 1996). These conjunctive cells are classified as either symmetric (about 50% of total DTN neurons), or asymmetric (about 25% total DTN cells; Bassett and Taube, 2001). Only asymmetric cells have been identified in some studies, of which a higher abundance was reported (83%; Sharp et al., 2001a).

As well as being modulated by AHV, some cells in the DTN are modu-

lated by linear velocity (approximately 40% of AHV neurons) or head pitch (15.9%; Bassett and Taube, 2001). Symmetric AHV neurons whose firing rates are negatively correlated with both head directions and which have been observed in other brain areas (most notably the LMN), have not been observed in the DTN (Bassett and Taube, 2003). It should be noted that the cells of the DTN have a higher propensity towards conjunctive encoding of multi-modal cues such as AVH and HD or AHV and pitch (Bassett and Taube 2001; Sharp et al., 2001) than cells in the LMN (Stackman and Taube, 1998).

The proposal for the hierarchical nature of the HD cell circuit arises in part from lesioning studies which demonstrate a disruption to the HD signal in brain regions downstream from the lesioned structure. For instance, lesions of the DTN tend to abolish the directional signal in the ADN (Bassett et al., 2007). Behaviourally, lesions to the DTN also impair the ability to successfully navigate in a homing task after foraging for food but the performance of animals is still above chance levels (Frohardt et al., 2006). This suggests that there is little redundancy in HD signalling at the level of the DTN, but tasks which may be solved with dependence on allothetic inputs such as external landmarks may depend less on the DTN.

2.3.2 Lateral mammillary nuclei

The mammillary bodies are situated at the caudal-ventral border of the hypothalamus, and are subdivided into the lateral mammillary nuclei (LMN) and medial mammillary nuclei. The LMN is noted to harbour the largest cells in the mammillary bodies, is spherical in shape and has no further subdivisions or anatomical evidence for the presence of interneurons (Guillery, 1955).

There are two parallel circuits of the mammillary bodies to the anterior thalamus, both of which are unidirectional. The circuit relevant to the HD network is conveyed from the LMN to the ADN (Guillery, 1955). The other pathway is from the medial mammillary nucleus (MMN) to the an-

teromedial thalamus (AMN) and the AVN (Vann et al., 2007). This circuit exhibits a high abundance of theta-modulated neurons (Kocsis and Vertes, 1994), consistent with theta-modulated cells comprising 75% of AVN cells (Vertes et al., 2001).

The LMN is an interesting point of convergence in the HD cell network, as it receives input from both cortical and subcortical regions of the circuit, is bilaterally connected and has many reciprocal and topographical connections as discussed below. There appears to be a level of lateralisation of the LMN such that LMN HD cells tend to have narrower tuning curves when the animal's head is turning in the ipsilateral direction versus the contralateral direction (Blair et al., 1998). There are predicted to be about 4000-5000 cells in the LMN (Bassett and Taube, 2003), of which about 25% are classic HD cells (Stackman and Taube, 1998). HD cells in the LMN have a longer ATI than other brain areas of the HD cell circuit, ranging somewhere between 40ms (Blair et al., 1998) and 70ms (Stackman and Taube, 1998). This may reflect the proximity of the LMN to the source of the HD signal in subcortical brain regions.

About 44% of cells in the LMN are AHV cells (Stackman and Taube, 1998), although there is some debate about whether these cells are symmetric AHV cells or asymmetric AHV cells (Blair et al., 1998; Stackman and Taube, 1998). This may be a consequence of differences in recording sites within the LMN. Both fast (52.5% AHV cells) and slow AHV neurons (47.5% AHV cells) have been observed in the LMN (Stackman and Taube, 1998). These cells are named as such based on whether they increase (fast) or decrease (slow) their firing rate as a function of AHV. A further cell type which encodes the pitch orientation of the animal's head (head pitch cell) in the vertical plane (Stackman and Taube, 1998) is present in the LMN. These cells fire maximally when the animal's head is pointing directly upwards (pitch angle of 90° from the horizontal, or azimuth, plane) and linearly decreases to minimum firing rates at a head pitch angle in line with earth

horizontal (0° pitch angle).

A major input source to the LMN is the DTN via the mammillary peduncle (Groenewegen and van Dijk, 1984; Shibata, 1987; Hayakawa and Zyo, 1989). This input is inhibitory, given the predominance of GABAergic projections (Gonzalo-Ruiz et al., 1993; Wirtshafter and Stratford, 1993), and likely modulates ascending LMN projections. Tuning curves of HD cells in the DTN are wider than those in the LMN (Sharp and Cho, 2001), suggesting that neural activity in the DTN serves to sharpen the tuning of LMN HD cells, and that the activity in these two areas serves as a path integration mechanism for the HD cell circuit (Sharp and Cho, 2001). This, in combination with the presence of AHV-modulated HD cells in the LMN and DTN, lead many to think that the LMN-DTN connectivity gives rise to the continuous attractor network properties of the HD circuit (Redish et al., 1996; Zhang et al., 1996).

The LMN are similarly important to the DTN in the generation of the HD cell signal. Early studies seeking to investigate the role of the LMN in encoding of HD showed that bilateral lesions of the LMN abolished the HD cell signal in the ADN in rats. For instance, Blair and Sharp (1998) lesioned the LMN and performed single-unit electrophysiology in the ADN in parallel. The HD signal was eradicated in the ADN following LMN-lesioning, and was never recovered. The LMN HD signal also precedes that in the ADN by about 15-20 ms (Blair and Sharp, 1998) supporting the evidence for a hierarchical connection between the two brain regions. A follow-up study showed that it is only bilateral, not unilateral, lesions of the LMN which will permanently abolish the ADN HD cell signal (Blair and Sharp, 1999; Bassett et al., 2007). They further characterised the activity of HD cells in the ADN following lesions to the LMN: HD cells exhibited rhythmic oscillations and spike activity which was uncorrelated from HD (Blair and Sharp, 1999). With respect to unilateral lesions, LMN neurons in the intact LMN hemisphere remain HD cell-like.

The LMN projects to the ADN in a unidirectional manner (Hayakawa and Zyo, 1989). Interestingly, the LMN also receives projections from the PoS (Shibata, 1989), suggesting that landmarks exert control over the HD cell signal first at the LMN within the HD circuit hierarchy. Experimental support for this was demonstrated when landmark control of HD cells in the LMN was disrupted subsequent to bilateral lesions of the PoS in rats (Yoder et al., 2015).

2.3.3 Anterodorsal thalamic nucleus

Broadly, the thalamus comprises most of the diencephalon and is a bilateral structure which functions in part as a sensory relay system to the cerebral cortex. It is divided into a number of nuclei based on their location and function (anterior, ventral, medial and lateral). The anterior thalamic nuclei (ATN) include the ADN, AVN and AMN. The thalamic reticular nucleus (TRN) has inhibitory connections to the thalamus (Gonzalo-Ruiz et al., 1997), thereby moderating thalamocortical activity. Of particular interest to the HD cell network is the ADN. This has the highest proportion of HD cells in the HD network (60%, Taube 1995), the highest signal-to-noise ratio, and is a major convergence point in the circuit (Bassett and Taube, 2003). For these reasons, the ADN was chosen for all HD cell recordings conducted in this thesis.

The ADN, unlike the LDN, receives strong input from the LMN (Hayakawa and Zyo, 1989; Shibata, 1992). In comparison to the LMN, HD cells here have narrower tuning curves (Bassett and Taube, 2003). The ADN also receives inputs from the anterior cingulate cortex and the caudal dorsal reticular nucleus. In turn, the ADN projects to the entorhinal cortex, RSC, presubiculum, parasubiculum, and PoS (Shibata, 1993; Blair and Sharp, 1995). During cue control there is a very short latency for HD cells in the ADN to orient themselves to the visual cue (about 80ms; Zugaro, 2003), supporting evidence for direct projections from the retina to the ADN (Conrad and Stumpf, 1975) as well as indirect visual input via the

RSC and PoS (Shibata, 1998; Lomi et al., 2021).

There is a positive correlation of HD cells in the ADN with linear velocity and AHV (Taube, 1995) and the firing rate is increased when the animal's head passes through the preferred direction of angular head movement (Taube and Muller, 1998). As mentioned, the presence of an ATI has been demonstrated in the ADN, wherein cells will fire in advance of their preferred firing direction (Blair and Sharp, 1995). In the ADN, cells fire approximately 25ms before the head is facing the cell's preferred direction and will shift the preferred firing direction as a function of the AHV of the animal (Blair and Sharp, 1995). This will tend to happen to the left during CW head movements and to the right during CCW head turns.

The HD cell signal here is vulnerable to damage in upstream subcortical areas, supporting the hierarchical structure of the circuit. Lesions to the SGN impair the HD signal in the ADN (Clark et al., 2012b) via a reduction in the stability and numbers of characteristic HD neurons. Likewise, damage to the nPH also leads to a loss of direction-specific firing which is highly unstable in the dark, and induces bursty spiking uncorrelated with the animal's directional heading in line with loss of accurate vestibular input (Butler and Taube, 2015). Lesions to the vestibular nuclei impair the directional signal in the ADN (Stackman and Taube, 1997) by disrupting the firing rate of HD cells and their directional stability. For instance, in one study a number of ADN neurons in lesioned animals displayed burst firing that was uncorrelated from head direction (approx 20-40 spikes bursting approx 2-5 times/minute; Stackman and Taube, 1997). As mentioned, bilateral lesions to the LMN remove the HD signal (Blair and Sharp, 1999), as do lesions to the DTN (Bassett et al., 2007).

Downstream lesions to the hippocampus have little to no effect on HD cell activity in the ADN (Golob and Taube, 1997). HD cells in the ADN are also spared when lesions are made to the RSC (Clark et al., 2010). Conversely, lesions to the ADN disrupt HD cell activity in the PoS (Goodridge

and Taube, 1997). Poor cue control is observed in ADN HD cells when the PoS is lesioned (Goodridge and Taube, 1997): the shift in PFDs of HD cells does correspond to movement of a visual cue, but is accompanied by wider tuning curves and intra-session drift.

2.3.4 Laterodorsal thalamic nucleus

Within the diencephalon, HD cells have also been identified in the LDN (Mizumori and Williams, 1993). Anatomically, the LDN receives extensive input from the RSC and PoS (van Groen and Wyss, 1990; Shibata, 2000) but interestingly does not receive input from the ADN or LMN (Thompson and Robertson, 1987). Unlike the ADN, lesions to the LDN do not disrupt HD firing in the PoS (Golob et al., 1998).

An interesting observation was made by Mizumori and Williams (1993) concerning the dynamics of HD cell firing in the LDN, wherein the cells exhibited no directional firing when an animal was first placed in the recording environment in the dark and only began to become directionally tuned once the lights were turned on. This firing then persisted when the animal was once again in the dark, except for a slow and systematic rotation of the PFD of the cells. This suggests some fundamental differences in the properties of LDN HD cells to other cells in the HD circuit, which is compounded by the absence of direct projections from the LMN to the LDN (unlike the anterior thalamus).

2.3.5 Postsubiculum

The PoS forms part of the wider subicular complex comprising the subiculum proper, parasubiculum and the presubiculum (with the PoS often referred to as the dorsal extension of the presubiculum). Anatomically the PoS comprises 6 layers, which may be subdivided into external and internal laminae based on their characteristic Nissl-staining properties (cells in the external laminae form clusters and those in the internal laminae form parallel rows of cells; van Groen and Wyss, 1990). The characteristic his-

tology of this region, paired with the presence of HD cells, distinguishes the PoS from the remaining presubiculum. HD cells were first discovered here (Ranck, 1984) and the basic characteristics of PoS HD cells were established in subsequent studies (Taube et al., 1990a; Taube and Ranck, 1990b). About 25% of neurons in the PoS are HD cells (Taube et al., 1990a).

The PoS is another convergence point in the HD cell circuit, with extensive connections to both subcortical and cortical regions containing HD cells. The PoS receives major projections from the subiculum (this is the primary output target of the hippocampus, and also contains place cells; van Groen and Wyss, 1990). The PoS has reciprocal connections with the ADN (Blair and Sharp, 1995) and RSC (van Groen and Wyss, 1990) as well as the LDN (van Groen and Wyss, 1990). The PoS also receives direct input from the visual cortex (specifically areas 17/18b; Vogt and Miller, 1983), indicating its importance in the integration of visual inputs into the wider head direction system. The PoS projects to the superficial layers of the EC (van Groen and Wyss, 1990; Caballero-Bleda and Witter, 1993) which then projects to the hippocampus. This allows for visual inputs to bypass the usual route through the parietal cortex (i.e. the dorsal visual stream). The PoS also projects back to a subcortical component of the HD cell network, the LMN (Allen and Hopkins, 1989; van Groen and Wyss, 1990).

HD cells here have narrower tuning curves than the LMN and ADN (Bassett and Taube, 2003). Cells in the PoS do not tend to have an ATI and will instead fire when the animal's head is in the exact, momentary PFD (Blair and Sharp, 1995). HD cells here fire at their preferred direction irrespective of any AHV modulation (Blair and Sharp, 1995), in contrast to the ADN. In addition to the presence of HD cells, the PoS also contains a subset of cells which are moderated by other spatial correlates, including angular head velocity (10% PoS cells), linear velocity and location (Sharp, 1996).

Functionally speaking, given the direct visual inputs to the PoS, it is the brain area in which HD cells may correct for drift by integrating information provided by allothetic inputs and anchoring the HD cell preferred firing direction to these cues (Goodridge and Taube, 1995). In line with this, lesions to the PoS have a detrimental impact on landmark control of HD cell tuning in the ADN and LMN (Goodridge and Taube, 1997; Yoder et al., 2015) and cue control of place cells in the hippocampus (Calton et al., 2003). Lesions of the PoS do not eradicate the directional signal, however, in subcortical structures (Goodridge and Taube, 1997). Recent work has begun to deconstruct the role of the PoS in the integration of sensory cues with HD activity at the cortical level: The PoS conveys border-modulated HD activity via the integration of egocentric and allocentric information (40% PoS cells, both HD and non-HD cells, responded to borders) more predominantly than the ADN (only 10% exhibiting border-modulated activity; Peyrache et al., 2017). In contrast, lesions to upstream subcortical structures affect the directional signal in the PoS, in accordance with the hierarchical nature of the HD cell circuit. For instance, lesions to the LMN and DTN both abolish the directional signal in the PoS (Sharp and Koester, 2008), as well as lesions to the ADN (Goodridge and Taube, 1997).

2.3.6 Retrosplenial cortex

The RSC is a cortical component of the HD cell network (situated in the posterior cingulate cortex), with around 10% of neurons here being classic HD cells (Chen et al., 1994a; Cho and Sharp, 2001). The RSC comprises granular and dysgranular regions, of which the granular region is further subdivided into granular a and granular b (Wyss and Sripanid-kulchai, 1984). HD cells are evenly distributed across both the granular and dysgranular regions (Cho and Sharp, 2001). Both the dysgranular and granular regions of the RSC project reciprocally to the PoS, the ADN, and LDN (van Groen and Wyss, 1992; Shibata, 1998; Shibata, 2000; van Groen and Wyss, 2003). Interestingly, HD cells in the RSC have in some instances

been shown to have two PFDs, termed bidirectionality (as described in Section 2.2.5; Jacob et al., 2017). A number of non-HD RSC neurons are positively correlated with running speed, and AHV (Cho and Sharp, 2001; Keshavarzi et al., 2021).

Similarly to the PoS, the RSC is an important nodal point in the HD cell circuit for the integration of internal and external reference frames for the directional signal (reviewed in Stacho and Manahan-Vaughan, 2022). The RSC processes information of spatial landmarks by the integration of visual cues. This is due to the fact that the RSC receives direct inputs from the same regions of the visual cortex to the PoS, namely areas 17/18b (van Groen and Wyss, 1992).

Lesions to the RSC appear to disrupt the use of allothetic cues in spatial tasks. From an electrophysiological perspective, RSC lesions result in HD cells within the ADN having an unstable PFD which drifts with time when a stable landmark is available, but idiothetic cue processing remains intact (Clark et al., 2010). The spatial tuning of place cells in the hippocampus is also affected by transient inactivation of the RSC, causing remapping of place cells (Cooper and Mizumori, 2001). RSC lesions in rats result in a decreased performance in a radial-arm maze task when the maze is rotated mid-trial (Vann and Aggleton, 2004; Pothuizen et al., 2008), suggesting that the rats ability to use available distal cues for selecting the correct maze arm is impeded.

Of importance to the interpretation of these results is the apparent distinction between the granular and dysgranular regions of the RSC in processing idiothetic and allothetic inputs. Systematic differences in the expression of immediate early-gene activity was observed during a radial-arm maze task, such that expression of these genes (c-fos and zif268) increased in the granular RSC region regardless of whether the rat was conducting the task in the light or dark; whereas expression only increased during the light condition in the dysgranular RSC region (Pothuizen et al.,

2009). This study suggests that dysgranular RSC may be specialised for visual landmark processing, while the granular RSC may unify both visual and non-visual cues. This is further supported by selective lesions of the dysgranular RSC disrupting the use of allothetic cues in a radial-arm maze task (Vann and Aggleton, 2005).

Studies in humans have shown that damage to the RSC can impair the ability to utilise familiar landmarks in navigation via the onset of topographic disorientation or topographic amnesia (Takahashi et al., 1997). Functional imaging studies have provided further clinical evidence for a role of the RSC in navigation and memory, with increased activation of the RSC in neuroimaging studies of event recall and virtual reality (VR) tasks involving large-scale navigation (Maguire, 2001; Burgess, 2002).

2.3.7 Medial entorhinal cortex

The MEC is a brain region heavily connected with both the hippocampus and aforementioned HD cell-containing brain regions. It receives input from the hippocampus proper (Ramon y Cajal, 1902), postrhinal cortex (Koganezawa et al., 2015), pre- and parasubiculum (Caballero-Bleda and Witter, 1993), RSC (Czajkowski et al., 2013), ATN (Winter et al., 2015), and PoS (van Groen and Wyss, 1990).

Superficial layers of the MEC contain a number of co-localised cell types, including grid cells (Hafting et al., 2005), HD cells (Sargolini et al., 2006), as well as conjunctive grid-by-HD cells (Burgalossi et al., 2011; Hardcastle et al., 2017). HD cells found in the MEC are less directionally-selective than 'classic' HD cells due to their lower peak firing rates and broader tuning curves. Topographical organisation of HD cells in the MEC is also exhibited: HD cells have narrower tuning curves in the dorsal MEC, compared to broader tuning curves in the ventral MEC (Giocomo et al., 2014). This mirrors the increase in grid cell scale observed along the dorsal-ventral axis of the MEC (Hafting et al., 2005). Recurrent subcircuits of HD cell firing have also been identified in MEC superficial layers (Zut-

shi et al., 2018), which may allow for the local processing of afferent HD signals and precise firing of grid cells. These recurrent networks could also ensure persistence of the HD signal in the absence or disruption of grid cell firing (Bonnevie et al., 2013; Brandon et al., 2011; Miao et al., 2017).

Local head direction modulation of pure grid cells has also been demonstrated, distinct from that observed in conjunctive cells of the MEC (Gerlei et al., 2020). The difference in directional modulation here is that pure grid cells may exhibit multidirectional modulation arising from local circuits, whereas conjunctive cells typically have unidirectional firing with strongly correlated fields (indicating global circuitry; Gerlei et al., 2020). This directional modulation of pure grid cells, which is observable at the level of individual firing fields, is speculated to emerge as an assimilation of directional inputs from conjunctive cells with differing fields for the purpose of providing place cells with information specific to local viewpoints (Gerlei et al., 2020).

The HD cell network is necessary for normal function of grid cells in the MEC and parahippocampal network (Winter et al., 2015). This was demonstrated by either inactivation or lesioning of the anterior thalamus and recording grid cells in the MEC and parasubiculum. While theta rhythmicity was spared, the grid cell and HD cell signalling in these regions was disrupted. For grid cells, this occurred via a reduction in spatial periodicity and grid-like firing patterns, or a significant reduction in the number of recorded grid cells. HD cell signalling in the MEC is furthermore impaired by anterior thalamic inactivation, resulting in a broadening of directional tuning and reduction in HD cell numbers (Winter et al., 2005). The effect of manipulations to the MEC and input HD signal suggests a dependency on directional inputs for grid cell computations.

2.3.8 Hippocampus

The hippocampus is considered the central node of the spatial navigation network, with vast input and output projections to cortical and subcortical

brain regions. It receives projections primarily from the MEC (Ramon y Cajal, 1902) and lateral entorhinal cortex (LEC), but also from the ADN (Wyss et al., 1979), PoS (Amaral and Witter, 1995), and RSC (Wyss and van Groen, 1992).

The HD signal projects via the PoS, through the MEC, to the hippocampus (Amaral and Witter, 1995). In this way, HD information is integrated into the hippocampus for encoding of information about an animal's location. The hippocampus is therefore likely a source for mnemonic information with respect to the HD signal, by detecting changes to spatial contexts using directional information. This is supported by studies which have shown that place cells display identical firing fields in visually identical mazes arranged in parallel (Spiers et al., 2015), but this place field repetition is not observed when the maze compartments face in different directions (Fuhs et al., 2005; Grieves et al., 2016). The contribution of the hippocampus in disambiguating spatial contexts based on HD cell inputs was further demonstrated by comparing the activity of place cells while animals which had either lesioned or intact LMN explored a multi-compartment maze (Harland et al., 2017). In animals without lesions, place cells had distinct firing patterns in each maze compartment. In lesioned animals, place cells had near identical firing patterns in each compartment, suggesting impairments to the ascending directional signal in these animals impeded the ability of the hippocampus to discern the relative direction of external landmarks and thus differentiate two spatial contexts.

Hippocampal lesions, conversely, do not disrupt the directional signal in upstream brain regions like the PoS and ADN (Golob and Taube, 1997). Specifically, the PFD of recorded HD cells in lesioned animals remained stable over a period of days in a novel environment. This effect was observed even in disoriented animals, supporting the role of extra-hippocampal signalling in the generation and maintenance of the

HD signal. Unlike lesions to the PoS and RSC, hippocampal lesions do not have an impact on landmark control of HD cells (Golob and Taube, 1999). Instead, the hippocampus may be enabling the continuation of HD cell PFD between connected environments which have only proximal orientation cues, using path integration measures. This was tested first in hippocampal-lesioned animals which explored a novel environment. HD cells recorded in the PoS and ADN were unable to maintain a stable PFD when moving from a familiar to a novel environment, unlike control animals. A landmark cue exerted control over the HD cells in both cohorts of animals, but there was significant drift in the PFD of cells when the animals were recorded in the dark (Golob and Taube, 1999). Taken in concert, this suggests a role of the hippocampus in path integration mechanisms for upkeep of an accurate directional signal.

In terms of the effect of damage to the HD cell system on hippocampal place cell firing: Lesions to the PoS alter place cells of the hippocampus such that their place field enlarges with poorer in-field firing, resulting in reduced spatial information (Calton et al., 2003). Reduced landmark control of hippocampal place cells was evident in PoS-lesioned animals, which was present but noticeably less pronounced in ADN-lesioned animals. Removal of the visual cue also led to instability of place fields in animals with PoS lesions, which was not the case in animals with ADN lesions (Calton et al., 2003). A similar disruption of place cell firing has also been reported in LDN-lesioned animals (Mizumori et al., 1994), but not LMN-lesioned animals (Sharp and Koester, 2008). These results suggest a hierarchy of directional input to the hippocampal function, with directional afferents from regions most heavily influenced by landmark cues (PoS, RSC and to some extent the ADN) having the largest impact on place cell firing.

2.4 Head direction cells and behaviour

Given the importance of the directional signal within the broader neural networks for navigation, a number of electrophysiological studies have attempted to find a correlation between HD cell activity and behaviour. For example, an increase in directionality of LMN HD cells have been shown to occur concurrently to a decrease in errors made on a radial-arm maze task (Mizumori and Williams, 1993). Consequently, lesions to the LMN result in impaired direction discrimination in a four-way odour-location discrimination task and a T-maze task (Smith et al., 2019).

Behaviourally, lesions to the LMN show little to no impairment in performance on an alternating T-maze task (Vann, 2005; Vann, 2011), in comparison to lesions of the anterior thalamus (Aggleton et al., 1995). This may reflect the ability of the animal to integrate non-directional cues in the performance of the task when lacking a stable directional framework from the LMN. This is strengthened by the finding that even when any mismatch between allocentric and egocentric cues are removed, for instance by recording in the dark, LMN-lesioned animals performed to the same level as control animals (Vann, 2011). LMN lesions likewise appear to render only temporary impairments in performance of a water maze (Vann, 2005; Harland et al., 2015), perhaps suggesting a more critical importance for the LMN HD signal in the rapid encoding of spatial information which may be compensated for with learning. This is supported by findings that lesions to the LMN disrupt the cortical HD cell signal while the place cell signal is preserved (Sharp and Koester, 2008).

Behaviourally, lesions of the ADN have shown mixed results. In some instances, there are impairments of performance in T-maze and Morris water maze tasks which can be improved with training (Aggleton et al., 1996; van Groen et al., 2002b). In contrast, another study showed that a decrease in performance in a radial arm maze task upon damage to the ADN (Beracochea et al., 1989) was only observed when the inter-trial in-

terval was lengthened from 15s to 45s. Further evidence for the use of ADN-located HD cells as a framework for spatial behaviour was observed by Dudchenko and Taube (1997). In this experiment, rats were trained to retrieve a food reward from an arm on an elevated plus maze with a distal visual cue available. When the cue was rotated around the maze there was a corresponding shift in the arm chosen by the rat relative to the cue, which correlated with the shift in direction of firing of the recorded cells (Dudchenko and Taube, 1997). Impairments in a path integration task have similarly been observed (Peckford et al., 2014) but this effect was less pronounced than those seen in animals with DTN lesions (Frohardt et al., 2006). Further evidence that path integration is impaired via ADN lesioning was demonstrated in a food carrying task (Frohardt et al., 2001). This all suggests that animals are worse at homing tasks following lesions to the HD cell network when compared to discrete choice tasks. Both permanent and reversible ADN lesions have also been shown to cease spatial firing in the subiculum, impairing performance on both spatial alternation and object recognition tasks (Frost et al., 2021). More broadly, evidence for the role of the anterior thalamus in episodic and spatial memory has been demonstrated when pharmacological inhibition of the ADN led to impairments in event recall for recent, but not remote, fear memory (Lopez et al., 2017; Vetere et al., 2021).

It appears that the LDN is also important for spatial learning tasks, given damage to the LDN results in detriments of performance in the water-maze task (van Groen et al., 2002a) and radial-arm maze (Mizumori et al., 1994), which may be due to disruption of place cell activity (Mizumori et al., 1994). Impairments are particularly pronounced when damage extends to both the LDN and the ADN (Wilton et al., 2001; van Groen et al., 2002a), resulting in severe impairments to performance in T-maze alternation and water maze tasks. This suggests a lack of redundancy between the LDN and ADN. Conversely, improvements in performance of a radial-arm

maze task correlate with increases in the directional tuning of LDN HD cells (Mizumori and Williams, 1993).

The role of the PoS in spatial reference and spatial working memory tasks is more difficult to distinguish than other regions of the HD circuit given its anatomical location deep within the hippocampal formation. Nonetheless, lesions to the PoS have been shown to impede performance in radial arm maze and also Morris water maze tasks, but interestingly this effect was transient as performance improved with learning (Taube et al., 1992). Bilateral neurotoxic lesions of the PoS impair performance in a homing task in both light and dark conditions (Yoder et al., 2019). In contrast to control animals, PoS-lesioned animals were unable to use visual or idiothetic cues to make a direct return to the nest after retrieval of a food pellet. A similar homing experiment was conducted which involved the rats retrieving a food reward at the centre of a platform, which was then rotated before the rat returned to the nest (Van der Meer et al., 2010). The authors reported a consistent association between a shift in the rats' choice of nest location in response to the rotation of the platform and the directional shift in firing of recorded HD cells (Van der Meer et al., 2010). Blindfolded rats were trained to perform a similar homing task, which had similar findings (Valerio and Taube, 2012): A clear correlation between shift in firing direction of cells and the rat's heading error was observed. Two correction processes were identified as strategies for reorientation to reduce subsequent heading errors. The first was a total resetting of the cell PFD upon return to the nest, which occurred as a consequence of small heading errors. When large heading errors were observed, the HD cells remapped to a new reference frame irrespective of the nest (either a tactile or geometric environmental feature) which was found to improve performance in the subsequent trial (Valerio and Taube, 2012). These findings highlight the importance of an accurate directional frame of reference for successful path integration, and potential reorientation measures taken by the HD cell system to mitigate future errors.

Correlation between the shift of cell PFD and the behavioural choice of the rat is not always observed. Another task involved training rats to run for a reward in one corner of a box (square, and then rectangle) which had a proximal cue along one wall (Golob et al., 2001). In both environments, shifts in the chosen corner by the rat were not consistent with shifts in the directional firing of the HD cells (Golob et al., 2001). A blend of these results was observed in a third study (Weiss et al., 2017), when HD cells (and grid cells) were recorded in the MEC while rats performed a reorientation task in a rectangular arena (as in Cheng, 1986). While the HD signal remained stable across trials, this was not indicative of the choice of corner by the rat, which varied. Despite this, there was an increase in performance which linearly correlated with the number of consecutive trials in which HD firing remained stable (Weiss et al., 2017). This suggests that the use of directional heading for choice in a navigational task may be contingent on the stability of the signal. Additionally, the HD signal is better primed for tasks dependent on path integration versus discrete choice tasks.

2.5 Summary

Directional information is a key component of the neural basis for the cognitive map, encoded by a network of HD cells distributed throughout both cortical and subcortical brain regions. The integration of multi-modal information within these component structures enables the ability to perform flexible, place navigation within the wider context of other spatially-modulated cell types. The distributed nature of HD cells within the brain enables some redundancy (with the exception of the ADN) which indicates how paramount the heading direction signal is to effective navigation in the neural representation of space. An intriguing finding since the discovery of HD cells is that they are the first spatial cell type to emerge in post-

natal development in rats, prior to the onset of spontaneous exploration. This provides a unique opportunity for experimenters to investigate the constituent role of HD cells in spatial navigation, and how this may feed into the subsequent maturation of the collective ensemble of spatial cell types. This will be discussed in detail in the following chapter.

Chapter 3

Rat postnatal development

A key question which arises in discussing the neural basis for spatial cognition and navigation is to what extent does sensory experience contribute to the generation and coherence of this neural representation of space? In reference to the work of Immanuel Kant, *The Hippocampus as a Cognitive Map* (O'Keefe and Nadel, 1978) proposed that the brain holds an a priori view of the world. In his original work, Kant postulated that rather than space being an empirical construct which is the product of experience (*a posteriori*), spatial knowledge is instead something we are born with (*a priori*; Kant, 1781). Namely, allocentric (world-centred rather than observer-centred) pre-existing network representations may exist prior to external sensory input. These pre-configured networks may act as the scaffold for subsequent sensory experience (O'Keefe and Nadel, 1978).

One way to address this theory is to study the development of spatial representations in young animals. By assessing how these representations are generated, we may understand the extent to which these networks are pre-configured and to what extent they are shaped by sensory experience during early development. Work from this lab and others have provided strong evidence supporting the hypothesis that allocentric spatial representations develop before the contribution of spatial experience: Spatial cells encoding heading direction (Wills et al., 2010; Langston et al., 2010) are already present when rodents first leave the nest around postnatal day

16 (P16; Alberts and Leimbach, 1980). The networks underlying such spatial representations rapidly mature and stabilise with early sensory experience, enabling the subsequent emergence of adult-like hippocampal-dependent spatial memory.

3.1 Rats as a model for spatial cognition

The Norwegian laboratory rat (*Rattus norvegicus*) is a common animal model in the study of spatial and episodic memory, in which the constituent spatial cells of the cognitive map have been most extensively studied. There are abundant similarities in cellular architecture, physiology and circuit-level dynamics in the hippocampus of rodents and humans. Learning and memory in rats is therefore studied in order to better understand these processes in the healthy human brain (Squire, 1992). The study of rat behaviour and neuronal network activity in spatial memory tasks, taken as a proxy for human episodic memory, has enabled experimenters to better understand the neural basis for higher cognitive function.

Rats are also an ideal animal model for studying the development of the cognitive map because their postnatal development is analogous to human development in several ways. Similar to humans, rats are altricial animals. This means that they are helpless at birth: deaf, blind, and incapable of full mobility (Rosenblatt, 1976). Their sensorimotor, cognitive and behavioural development to adult-like maturity occurs over a protracted time period of several weeks. Hippocampal-dependent learning and memory also emerge late: While in humans, the ability to recall hippocampal-dependent episodic memories emerges around 3 years of age (Alberini and Travaglia, 2017), rats exhibit similar memory capabilities from approximately 6 weeks (Schenk, 1985).

This thesis sought to probe further the early dynamics of spatial cell types (HD cells in particular), and ways in which to improve laboratory

techniques for ontogenetic studies of spatial cells in rodents. Given the focus on the postnatal emergence of neural circuits for navigation in rats, it is important to understand the sensorimotor, cognitive and behavioural development of these animals. The focus of this chapter is therefore to guide the reader through key developmental milestones in rat pups, beginning with sensorimotor development, followed by cognitive, behavioural, and spatial cell development.

3.2 Sensorimotor development

As rats are altricial animals, their sensorimotor repertoire is extremely limited at birth. There is rapid maturation of the sensorimotor capabilities within the first two weeks of life, a major factor in the onset of both spatial cell development and subsequent hippocampal-dependent learning capabilities of the animal (Figure 3.1). Vestibular and olfactory sensory functions are present in rudimentary form from birth, closely followed by tactile, auditory and visual capabilities. These sensory functions all undergo pronounced functional changes over the first two weeks of life (Figure 3.1). Much of the initial sensory stimulation comes from the rat's mother. Therefore, the infant-mother relationship is a complex and critical component to the postnatal rearing of rat pups.

3.2.1 Vestibular

The vestibular apparatus in vertebrates comprises three semicircular canals (whose placement is orthogonal to receive information for all three axes of movement) which sense rotational movement, and two otolith organs (named the saccule and the utricle) which encode linear accelerations. The semicircular canals encode angular velocity via the movement of endolymph fluid associated with head movements. Vestibular-dependent structures in the rat are considered to be morphologically developed at birth (Sudarshan and Altman, 1975; Figure 3.1).

The righting reflex (rotating forward onto the feet, or belly, when

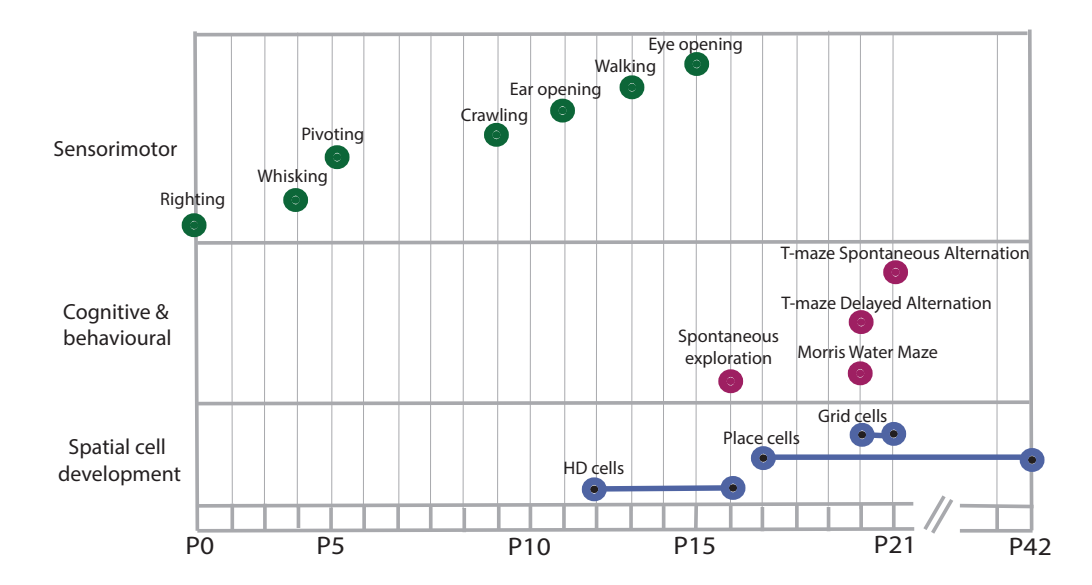


Figure 3.1: Summary timeline of rat postnatal development. Key milestones in the sensorimotor (green), cognitive & behavioural (purple), and spatial cell development (blue) of rat pups are shown from birth (postnatal day P0) to weaning (P21) and adulthood (P42).

placed on the back) associated with the vestibular system is the first observation made in pups at P0 (Altman and Sudarshan, 1975). This coincides with the pups' ability to orient themselves to their mother's nipple for feeding. Further maturation of the vestibular system occurs rapidly from P0. Horizontal semicircular canal primary neuronal firing reaches adult-like sensitivity to angular acceleration by P4 (Curthoys, 1979a). This is closely followed by the onset of central and peripheral vestibular neural responses within the first week of life by P6 (Lannou et al., 1979). The secondary vestibular nuclei mature throughout the first two weeks (Curthoys, 1979b), and primary vestibular nuclei appear matured by P22 (Lannou et al., 1979). Furthermore, growth occurs in both the utricle and saccule until P32 (Dechesne et al., 1986), at which point the vestibular system may be considered fully matured.

3.2.2 Olfactory

Olfaction is the next sensory modality to emerge (Figure 3.1), with odourguided behaviour being observed in pups as young as P4. At this age, rats exhibit a preference for their own nest shavings over other unfamiliar scents (Cornwell-Jones and Sobrian, 1977). In a similar vein, pups display an odour preference for their mother from as early as P2-P4 (Polan and Hofer, 1998) which directs suckling behaviour. Sustained nipple attachment resulting from an olfactory conditioning paradigm is possible within hours of birth (Cheslock et al., 2000), which can be disrupted experimentally by the use of an organic solvent on the nipple (Teicher and Blass, 1977). Pups are also capable of associative learning for odour-aversion as early as P2 (Rudy and Cheatle, 1977). This is indicated by the observation that when nausea is induced in P2 pups using lithium-chloride, discrimination of the aversive odour, as well as odour avoidance, is exhibited at P8. The olfactory senses are then considered fully mature in the rat by age P15, at which point rats will exhibit adult-like sniffing behaviour (Altman and Sudarshan, 1975).

3.2.3 Somatosensory

Somatosensory feedback including pain and skin contact are important for awareness of the animal to external threat and thermoregulation (Alberts, 1978a). Whisking is another important part of the rodent tactile experience, which involves the rapid and repetitive movement of whiskers (6-9 Hz) to scan the environment (active vibrissae movements). This enables suckling and huddling (Sullivan et al., 2003) as well as later behaviours including communication with their conspecifics and nocturnal exploration (Mitchinson et al., 2007; Hartman, 2011). Rats have whiskers from birth, but initially only receive sensory information from the whiskers via passive touch which enables communication with the mother and littermates (Fox, 1992; Sullivan et al., 2003). Rhythmic movement of the whiskers emerges between P10-P13 (concurrent with sniffing behaviour; Grant et al., 2012). There is then a steady increase in the frequency and amplitude of whisking movements until P21 (Figure 3.1; Welker, 1964), corresponding to experience-dependent plasticity in trigeminal nerve afferents (Landers and Zeigler, 2006). Within this time, from P11 to P17,

contact-dependent whisking also develops (Grant et al., 2012). By P21, the somatosensory capabilities of the rat are considered adult-like (Welker, 1964).

3.2.4 Auditory

Audition is one of the last sensory modalities to develop, due in part to the rat's ear canal remaining closed until P12-P13 (Brunjes and Alberts, 1981). Prior to ear opening, the first observable activity of the auditory system in pups are cochlear potentials reflecting stimulation of the inner ear hair cells at P8-P9 (Uziel et al., 1981). Pups subsequently begin to evoke reflex (startle) response to an auditory stimulus between P10-P12 (Hyson and Rudy, 1984) prior to the ear canal becoming unplugged between P12 and P13 (Figure 3.1; Brunjes and Alberts, 1981). Rats then begin to display learned responses to auditory stimuli one to two days after ear opening (Brunjes and Alberts, 1981; Hyson and Rudy, 1984). Sound-evoked neural responses have been recorded in the auditory cortex as early as P13 (Zhang et al., 2001), with responses to high frequency sounds preceding the maturation of neural responses to low frequency sounds (Zhang et al., 2001). Behaviourally, from P14 rats are capable of sound discrimination and associative learning of a sound stimulus with a food reward (Rudy and Hyson, 1984), reminiscent of adult behaviour.

3.2.5 Visual

Vision is the last sensory modality to emerge in rats, with the eyelids becoming unfused over a period of one to two days between P14 to P16 (Figure 3.1; Gandhi et al., 2005). Responses to visual stimuli have nonetheless been reported before eye opening. For instance, negative phototaxis (movement away from a light stimulus) has been observed in animals as young as P6 (Routtenberg et al., 1978). This behaviour has been shown to be dependent on an intact superior colliculus (Routtenberg et al., 1978). Primitive responses to visual stimuli in the form of short bursting periods

have also been reported in the visual cortex before eye-opening (from P8 to P11) in rats (Colonnese et al., 2010). This bursting activity is interspersed with prolonged periods of network silence, which is thought to reflect the maturation of retinal processing and thalamocortical network properties (Colonnese et al., 2010). If a rat's eyes are surgically opened well in advance of the natural course of eye opening, between P6 to P8, certain exploratory behaviours such as rearing and open-field sampling increase compared to controls (Foreman and Altaha, 1991). These animals also perform better than controls at the T-maze alternation task, suggesting that the onset of vision enables rapid development of these behaviours in rats (even when this is artificially induced; Foreman and Altaha, 1991).

In any case, rats have the ability to recognise a visual landmark within 24 hours of eye opening. This is indicated in spatial navigation experiments in which HD cells in the ADN become anchored to a polarising, distal visual cue as in adults (Tan et al., 2015). Studies of P15 rats have also demonstrated their ability to detect a flashing light (Moye and Rudy, 1985). Capability for associative learning of a visual cue paired with an aversive stimulus is not reached until approximately P17 (Moye and Rudy, 1985).

Adult-like neural responses in the primary visual cortex have in some cases been observed as rapidly as two days after eye-opening in response to patterned vision (Prevost et al., 2010). In other reports, there is a protracted timescale for responses in the primary visual cortex, such that functional properties of visual cortical neurons do not reach adult levels until P45 (Fagiolini et al., 1994). Specifically, the visual responses to bars and gratings of primary visual cortical neurons subsequent to eye-opening are immature between P17 and P19 (Fagiolini et al., 1994). This is inferred by the larger receptive fields of neurons, and a lack of discrimination to either the movement direction or orientation of bars and gratings. Visual acuity (ability to distinguish the details of objects, including their shape) is also immature at this age (Fagiolini et al., 1994). Visual acuity may be

delayed if the animal is either reared in the dark or undergoes monocular deprivation (Fagiolini et al., 1994). According to Vrolyk et al. (2018), the rat eye reaches histomorphological maturity at P21. Adult-like visual responses of orientation selectivity, specifically neurons which preferentially fire in response to stimuli at certain angles, are seen at P30 (Fagiolini et al., 1994).

3.2.6 Motor

The first locomotor experience of the pup tends to be through transportation from the mother by way of loose skin on the back of the pup's neck (Altman and Sudarshan, 1975). Independent movement of the pup is observed as early as P0, though the range of movement is limited to moving along the mother's stomach to reach a nipple for nursing (Eilam and Smotherman, 1998). Then, in rapid succession: pivoting (circular motion, or rotation, of the forelimbs; Altman and Sudarshan, 1975) occurs between P3 to P9, crawling is seen from P9 to P14, and quadrupedal walking from P11 to P13 (Altman and Sudarshan, 1975; Figure 3.1). All of these voluntary motor skills emerge with development of postural control (Geisler et al., 1993). Finally, additional motor acts such as self-grooming and the ability to rear on their hind legs occur from around P13 (Geisler et al., 1993). It is between P12-P16 that the uncoordinated movements of juvenile rats transition to fluid, adult-like motor patterns (Geisler et al., 1993). This is in line with studies that found the largest increase in neuronal connectivity in the motor cortex occurs between P12 and P20 (Hicks and D'Amato, 1975). Maturation of Purkinje cell firing in the cerebellum also occurs at this same time (Altman, 1982), contributing to fine motor skills and motor guidance in navigation (Rondi-Reig et al., 2002).

3.3 Cognitive and behavioural development

3.3.1 Activity in the nest

Before any spontaneous exploration occurs in the rat, the majority of their time is spent laying with their littermates in a pile termed the huddle (Alberts, 1978a). Pups will spend extended time in the huddle with repeated attempts to move to the centre (Alberts, 1978a). Given the relative inability of pups to thermoregulate, heat is one of the primary cues which elicits huddling in young rats (termed 'physiological huddling'; Alberts 1978b; Sokoloff and Blumberg, 2001). Odour cues elicited by littermates also become a salient cue for huddling after about 2 weeks (termed 'filial huddling'; Alberts, 2007). The pups will remain huddled together in the natal nest for about 2 weeks (Alberts, 1978a), during which point the mother remains with the litter almost constantly (Grota and Ader, 1969; Leon et al., 1978).

Normally mothers will nurse for about 1 hour, then may briefly leave the nest to rest or eat (Koolhaas, 2010). If any pups escape from the nest, the mother will retrieve it and this is aided by ultrasonic vocalisations emitted by a pup (Koolhaas, 2010). They will reliably return to the huddle when sleeping throughout postnatal development (Alberts and Leimbach 1980; Thiels et al. 1990). Standard weaning age in the lab is 21 days, but studies have shown that rats will wean much later in the wild (Calhoun, 1963). In the wild pups will nurse until P35, and solid food intake begins at P18 (Thiels et al., 1990). Between weaning and about 60 days old, there is a period where pups will play and fight intensely with each other, which is important for the development of social skills for adulthood (Pellis and Pellis, 1998). The pups will remain in close proximity with their mother for as long as 2 months (Calhoun, 1963).

Studies examining the habitats of rats in the wild inform us that they will build and reside in subterranean burrows with many interconnected

tunnels (Pisano and Storer, 1948). The tunnels then terminate in chambers which are primarily used for nesting, food storage, and mating (Calhoun, 1963). Additionally, the burrow provides a means of protection against predators and harsh weather conditions (Steiniger, 1950). When the size of these burrows systems have been measured, they tend to occupy between 2-4m², with tunnels ranging in diameter of 5-7 cm and length 0.25-1.5m (in this case in a poultry yard; Pisano and Storer, 1948). Furthermore, the burrows of both wild and domesticated rats living in an enclosure are nearly identical (Flannelly and Lore, 1977; Boice, 1977).

In nature, mother rats will birth their young in the burrow within the confines of a secure, underground chamber (Davis, 1953). When the behaviour of a captive colony of wild rats was investigated in an enclosed outdoor pen, mother rats were seen to also birth and rear their young in 'harbourage boxes' which were placed by the experimenters at the surface of the burrow (Calhoun, 1963). Commonalities in the rearing habitat of rats in the wild therefore tends to be defined by a private chamber (nest) which connects to an outdoor space via a tunnel.

3.3.2 Homing

One of the initial behaviours of relevance to spatial behaviour in rats includes their ability to navigate back to the nest if removed by an experimenter (termed homing). Rats tend to orient their bodies towards the nest from P3 and first exhibit the ability to home back to the nest from P8 (Altman and Sudarshan, 1975). One of the first studies exploring this tested the ability of rats to return to their home nest within a certain amount of time (3 minutes), when moved 20cm away: no pups were able to achieve this at P7, but performance steadily improved until P13 when all pups successfully homed to the nest with adult-like performance (Altman and Sudarshan, 1975). Comparable findings have been presented in a similar paradigm involving position and tactile discrimination (Bulut and Altman, 1974).

3.3.3 Exploration and nest egression

It is around eye-opening (P15-P16) in the rat pup when nest egression generally first occurs (Figure 3.1), although this is dependent on environmental temperature (warmer temperatures tend to induce an earlier onset of spontaneous nest egression, but no earlier than P14; Gerrish et al., 1996). In the outdoors, rats spontaneously leave the nest much later (around P23-P40; Calhoun, 1963), although this may be a consequence of the cooler temperatures than those observed in a laboratory environment. There is also a clear dissociation between the onset of the repertoire of motor behaviours in pups and the onset of spontaneous and active exploration (Nadel et al., 1992). While the development of motor activity in rats occurs in a gradual manner, the occurrence of nest egression and exploration in pups appears to happen abruptly (Nadel et al., 1992).

From P16 onwards, the ability of the rats to path integrate is observed by shorter and more direct routes taken by the pups on return to the nest, versus the longer, more circuitous outward journeys (Loewen et al., 2005). Activity increases rapidly thereafter from around P18 to weaning age (Altman and Sudarashan, 1975; Loewen et al., 2005). The rats will tend to stray further from the huddle with each consecutive nest egression, as well as make more frequent trips away from the huddle (Ruppert et al., 1985; Loewen et al., 2005).

3.3.4 Hippocampal-dependent learning and memory

An array of studies have sought to investigate the emergence of hippocampal-dependent learning and memory in rats (Brown and Whishaw, 2000; Loewen et al., 2005; Akers et al., 2007; Schenk, 1985). The predominant findings discussed below are that adult-like spatial navigation dependent on the hippocampus (allocentric spatial tasks) is observed from laboratory weaning age onwards (P21), with a steady increase in performance on spatial navigation tasks until six to eight weeks postnatally (Figure 3.1).

Spatial navigation behaviour is evident in rats from P17 when they first begin to successfully locate the platform in a Morris water maze task if the platform is visible (i.e. cued platform). At this age, rats will use proximal cues for navigating to the platform, instead of distal visual cues (Rudy et al., 1987). Subsequent place learning and hippocampal-dependent spatial memory first begin to emerge at approximately P20 (Schenk, 1985), demonstrated by a reduced latency to locate the platform in a Morris water maze when the platform is hidden (Brown and Whishaw, 2000). Fully adult-like spatial learning is observed between P32 and P42, indicated by direct path-taking to the hidden platform in a Morris water maze task (Schenk, 1985).

Similar observations have been made in rats performing a T-maze delayed alternation task (Green and Stanton, 1989; Bronstein and Spear, 1972), in which rats must choose alternating arms for reward in successive trials. Rats aged from P15 to P27 are all capable of performing this task (Green and Stanton, 1989). A similar paradigm is the forced alternation task, which involves a forced run where the animal must go down one arm of the maze, followed by a choice run (Green and Stanton, 1989). Performance is assessed based on how often the pup runs down the alternate arm to the forced arm in the choice run. When this paradigm is tested P15 pups are unable to perform the task, but pups older than P21 perform well (Green and Stanton, 1989). An additional place learning task is the radial arm maze, in which performance is based on the rat's ability to retrieve a food reward at the end of each arm of the eight-arm maze without returning to previously visited arms (Rauch and Raskin, 1984). Similar to findings regarding performance in the aforementioned tasks, rats were found to successfully perform in the radial-arm maze task from P21 onwards (Rauch and Raskin, 1984). These studies, when taken together, suggest that an animal's ability to complete tasks dependent on the hippocampus arise from around three weeks of age approximately coincident with the weaning period. The full repertoire of hippocampal-dependent learning and memory behaviours does not then reach adult-like abilities until around six to eight weeks postnatally.

3.3.5 Maternal impact on cognitive development

Of interest to the performance in these studies, pups who have an attentive mother who licks and grooms them often have been shown to develop better spatial navigation abilities and improved memory, as well as reduced stress levels (Champagne and Curley, 2009; Liu et al., 2000; Weaver et al., 2004; Zhang et al., 2010). To this end, a number of studies in rodents have furthermore suggested that early-life stress may have a longstanding impact on spatial learning and memory abilities. Maternal deprivation of infant rats has pronounced effects during development, including on spatial learning and memory (Oitzl et al., 2001). For instance, in one study, 24 hours of maternal deprivation in postnatal rats (in this case P3) resulted in significantly reduced levels of cell proliferation, neuronal differentiation and hippocampal neurogenesis (Oomen et al., 2010). There is conjecture over the extent to which these morphological observations impact adult hippocampal function and spatial learning, as some reports suggest that early-life stress does not affect performance in spatial learning tasks but instead primes an animal for optimal performance in high-stress situations as an adult (Oomen et al., 2010). Other studies conflict with this finding and instead show that early-life stress can chronically impair cognitive function (Naninck et a., 2014). In any case, this emphasises the importance of mother-pup interactions for normal cognitive development.

Postnatal *in vivo* electrophysiology experiments studying the ontogenesis of spatial cells, as outlined in this thesis, require shorter periods of isolation and the ages of animal subjects tend to be older (no younger than P9 or P10) than the classic early-life stress studies described here. Although developing rats in spatial navigation studies are not raised in social isolation or barren homecages, the effect of maternal separation or

exploration of cue-deprived, unfamiliar open field arenas (however brief) may have a discernible impact on the trajectory of spatial cell stabilisation. Although great care is taken when conducting chronic electrophysiology experiments in developing rats (as a matter of procedure: faster surgeries, reduced screening and recording time, minimal necessary disruption to feeding schedules are all observed), it is difficult to discount that there may be knock-on effects regarding the ontogenesis of spatial-mapping cells such as head direction cells.

3.4 Spatial cell development

An integrated understanding of the postnatal emergence of spatial cells is fundamental to our understanding of the development of hippocampal formation-dependent learning and behaviours. We know from previous studies in rats that spatial cell types emerge and mature sequentially, parallel to major developmental milestones such as eye-opening and spontaneous exploration (Figure 3.1). Briefly, the HD circuit is the first of the known spatially-modulated neural networks to emerge and stabilise during postnatal development (Langston al 2010; Wills et al, 2010), from approximately P12. Place cells first emerge from P16 to P17 onwards, with a more protracted trajectory to adult-like stability (Martin and Berthoz, 2002; Scott et al., 2011). Studies of grid cells suggest the emergence of stable grid cells occurs at P20 and they rapidly reach adult-like stability within one to two days (Wills et al, 2010).

3.4.1 Development of head direction cells

A rudimentary head direction signal, with above chance directional tuning, is present several days before eye-opening in rats from P12 in the ADN and PoS (with eye-opening occurring, on average, between P14-P16), albeit containing low directional information and having poor stability compared to adult rats (Tan et al., 2015; Bjerknes et al., 2015). In the period of time between HD cells first emerging and eye-opening, stability of HD

cells may be observed at P13-P14 in a small environment (such as 20 x 20cm, Bassett et al., 2018). HD cells can thus anchor to non-visual cues (corners) in the environment (Bassett et al., 2018). Immature encoding of AHV appears to be the source of the instability in HD signalling observed in larger arenas (such as the $62.5 \times 62.5 \text{cm}$ arena employed in Bassett et al., 2018).

HD cells in the open field exhibit adult-like stability early in development at P16 (Langston et al., 2010; Wills et al., 2010), coinciding with eyeopening and the first periods of pup nest egression (Gerrish and Alberts, 1996). The emergence of HD cells is therefore not dependent on active exploratory experience (Wills et al., 2010). Within 24 hours of eye-opening, a prominent visual cue has the ability to control HD cell responses (showing the rapid integration of visual inputs) and stability of cell firing also rapidly increases (Tan et al., 2015). This work, along with the ability for HD cells to exhibit adult-like maturity before P15 (Bassett et al., 2018), provides strong evidence towards the theory that allocentric spatial representations develop before the contribution of spatial experience, given that HD cells are present before the onset of active exploration. Given that HD cells are the subset of spatial cells which are the first to exhibit adult-like stability in preweanling rats, this may also reflect the HD signal as being the principal driving signal for subsequent spatial neuron development (Langston et al., 2010; Wills et al., 2010).

3.4.1.1 Self-organising attractor dynamics in the head direction circuit

Despite the instability of HD cell directional preference before eyeopening, the relative PFDs of cells remain coherent (exhibiting fixed spatial and temporal offsets) over both short (10 seconds) and long (several minutes) timescales (Bjerknes et al., 2015; Bassett et al., 2018). The HD cell network therefore exhibits properties characteristic of an attractor network without reference to an external landmark. This reinforces the idea that continuous attractor network activity of HD cells is self-organising and occurs prior to HD cell PFDs reaching adult-like stability.

A handful of studies have attempted to computationally model the self-organisation of these attractor dynamics in the developing HD cell network (Stringer et al., 2002; Hahnloser, 2003; Stringer and Rolls, 2006; Stratton et al., 2010; Page et al., 2018a; Smithe and Stringer, 2022). These models often train the network using both self-motion and visual inputs, with the network self-organising via a combination of Hebbian-like associative and competitive learning rules.

The Stringer model (Stringer et al., 2002) was the first to model the self-organisation of HD cells. The network architecture consists of a layer of rotation cells encoding head turns in both directions, which project their inputs to a population of HD cells. By a process of associative learning based on a stable distal visual cue, continuous attractor neural network properties are generated. The HD cells described have a PFD relative to allothetic inputs at the onset of training, with no indication of how visual landmarks gain control over the HD cell circuit nor how this may self-organise with respect to vestibular or self-motion inputs.

Stringer and Rolls (2006) subsequently built on this model architecture with the addition of a layer of combination cells encoding both head direction and AHV. Each cell becomes tuned to a specific combination of these variables by a process of competitive learning with a temporal trace rule: Presynaptic firing associated with a certain combination of head direction and AHV is coupled with postsynaptic firing associated with the upcoming head direction.

The Hahnloser model (Hahnloser, 2003) is similar to the Stringer model (Stringer et al., 2002) in that visual input calibrates the HD cell circuit. Vestibular input is also entrained in the network prior to learning. The network architecture implemented by Hahnloser is that of two rings of HD cells which receive both visual and vestibular inputs. Each ring of

HD cells receives information about head rotation from AHV cells with asymmetric tuning. After learning, the network is capable of sustaining an activity packet during immobility as well as in line with rotational head movements.

The Stratton model in turn begins with a rudimentary circular attractor topology which is refined with vestibular input (Stratton et al., 2010). The model proposed here incorporates both symmetric and asymmetric AHV cells in the network. Each HD cell receives input from two layers of asymmetric AHV cells (corresponding to both direction of head turns), as well as input from a layer of symmetric AHV cells. In this model the cell connectivity is pre-defined, which the authors propose may be as a consequence of chemical gradients during neurogenesis.

A caveat of these models is that no theory is presented as to how the visual inputs become entrained in the network processing, nor how the attractor dynamics internally organise before visual inputs are available (i.e. before eye-opening). There is speculation around whether the entrainment of HD attractor network dynamics occurs via integration of purely intrinsic cues (vestibular input), or whether this occurs via the confluence of additional early sensory cues which precede vision, such as odour or environmental boundaries (Tan et al., 2017). This remains to be investigated in future theoretical models, with the addition of new experimental findings such as those presented in this thesis.

3.4.2 Development of place cells

Place cells first emerge from P16 to P17 onwards, with an extended timescale of maturation trajectory to adult-like stability at approximately P45-P50 (Martin and Berthoz, 2002; Scott et al., 2011). Place cells appear to develop on a cellular rather than network level (unlike HD cells and grid cells), wherein at early recording timepoints (P16-P17) there is a small subset of hippocampal pyramidal neurons exhibiting adult-like place cell properties (particularly with respect to spatial information and stability;

Langston et al., 2010; Wills et al., 2010). The majority of recorded place cells at P16-P17 still exhibit properties of immature place cells, including poorly defined place fields and low stability across trials. The proportion of place cells in the hippocampus steadily increases over the course of several weeks, until reaching adult-like proportions around P28-P35. There continues to be a steady increase in the spatial information and stability of place cells until P40-P50 (Martin and Berthoz, 2002; Scott et al., 2011). This is a timescale consistent with the findings described regarding hippocampal-dependent spatial learning, that rats' use of allocentric cues for navigation remain immature until several weeks postnatally (Schenk, 1985).

Before the emergence of grid cells, place cell firing is maximally accurate close to environmental boundaries (Muessig et al., 2015), denoted by more numerous and more stable firing fields. There is subsequently a switch in the stability and spatial information content of place cell firing which coincides with the emergence of grid cells, suggesting that the onset of grid cell firing at weaning age stabilises place fields further from environmental boundaries where landmarks are less available (Muessig et al., 2015). The heterogeneity of place cells early in development, wherein a subset of cells exhibit adult-like properties from the earliest recorded ages, is indicative that grid cell input is not necessary for stable place cell firing (similar to findings in adults; Koenig et al., 2011; Zhang et al., 2013).

As discussed in detail in Section 1.3.1, theta band oscillations in the hippocampal LFP of adult rats are an important contributor to the phase coding aspects of place cell function. In development, theta oscillations are present in the pup hippocampus from P8 and gradually increase in frequency with age (Leblanc and Bland, 1979; Mohns and Blumberg, 2008). The first observations of theta from P8 until P11-P12 are coincident with myoclonic twitches in active sleep (Mohns and Blumberg, 2008). At these early ages, theta power is low and behavioural correlates are not well de-

fined (Leblanc and Bland, 1979). Nevertheless, a small proportion of hippocampal cells already exhibit a theta phase preference at P8 (Mohns and Blumberg, 2008). By approximately P15, theta is reliably recorded during voluntary movement at approximately 5 Hz (Leblanc and Bland, 1979), with higher adult-like frequencies of 7-12 Hz present from P23 onwards (Leblanc and Bland, 1979).

3.4.3 Development of boundary-responsive cells and grid cells

The postnatal emergence of boundary-responsive cells in the MEC at approximately P17 precedes the onset of grid cell activity (Bjerknes et al., 2014). Boundary-responsive cells at this age exhibit adult-like proportions and cell firing fields when recorded in an open-field environment. This coincides with the onset of mature HD cell activity in the rat, suggesting that these two cell types may act as the building blocks for subsequent maturation of the spatial code, in line with the boundary vector cell model of place cell formation (Hartley et al., 2000). This is reinforced by findings that the geometry of an environment is influential in the calibration of grid cell and place cell firing patterns (O'Keefe and Burgess, 1996; Barry et al., 2007; Krupic et al., 2015).

The discovery that boundary responses in these cells develop early in postnatal development (Cacucci et al., 2013; Bjerknes et al., 2014) and that place cells are more stable close to boundaries before grid cells develop (Muessig et al., 2015), suggests that boundary cells may provide the input that drives and stabilises early place fields.

Ontogenetic studies of grid cells suggest that the earliest age at which stable, adult-like grid cells are reliably recorded is at P20-P21 (Wills et al, 2010; Wills et al., 2012). This coincides with the period of active exploration in rat pups as well as when hippocampal-dependent learning and memory first begin to emerge. The rapid switch in grid cell firing from immature to adult-like maturity reflects a network-level coherence in grid

cell maturation. This network connectivity is reflected by co-recorded grid cells at P21 sharing the same wavelength and relative spatial phases (Wills et al., 2010), consistent with mature grid cells (Hafting et al., 2005; Barry et al., 2007). The relatively late onset of grid cell activity is furthermore consistent with computational models which predict that the onset of grid cell firing is brought about in part by HD cell firing, which is then stabilised by boundary-responsive cell firing (Burgess et al., 2007).

3.5 Summary and rationale for experiments

Current understanding of the ontogeny of neural circuits for navigation outside the scope of the laboratory environment is fragmentary. Nearly all existing knowledge of spatial neuron development is based on highly controlled, simple behavioural paradigms involving a single rat pup exploring an open field environment. This is suitable in instances where the behaviour of the animal and its access to cues must be strictly controlled. However, a paradigm such as that is entirely dissimilar to the natural rearing environment of the animal. Evidence that early-life stress can result in poor performance in spatial memory tasks lends support to efforts to minimise these disruptions when studying the ontogeny of spatial learning and memory, therein removing these confounding factors from experiments. There is a compelling need to investigate neural circuits in more naturalistic settings, thereby enabling us to integrate the findings discussed in detail here with the complexities of development outside of the lab.

The comparatively short timescale over which rodent spatial circuits develop and stabilise are extremely useful for developmental studies. The emergence of new technologies such as wireless recording devices will allow us to investigate whether the developmental timescales which have been investigated are reflective of what happens in the animal's natural environment. In this way, the work presented in this thesis may serve as a

framework for incorporation into future experimental work.

3.5.1 Experiment 1 (Chapter 5)

Wireless recordings have not previously been conducted in the developing rat. Therefore, the primary aim of Experiment 1 (Chapter 5) was the piloting of chronic *in vivo* electrophysiology in developing rats using a commercially available neural data logger. One way to validate wireless recordings in rat pups was to directly compare neuronal data acquired with a neural data logger to that of a tethered system that is well-established in this lab (DACQ, Axona Ltd., UK). Both systems record in vivo neural activity by the same physical input (omnetics connectors attached to implanted tetrodes). This makes serial recordings of both systems within an experimental session possible, in order to directly compare neural data. Wirelessly recorded data was subsequently processed in such a way as to be compatible with the proprietary clustering and data visualisation software of Axona to directly compare the same cells in *post hoc* analysis. Two spatial cell types whose postnatal emergence have been extensively studied were chosen for recording, including HD cells of the ADN and place cells of hippocampal area CA1.

3.5.2 Experiment 2 (Chapter 6)

As mentioned, current electrophysiology techniques employed in the domain of rodent developmental research have been limited in the extent to which the early sensory experiences of a pup may be studied. The early life of a rat is, for the most part, spent feeding or huddling with littermates (Alberts, 1978). Immersing a young pup into a laboratory environment to study the emergence of spatial representations may not be a true reflection of the early organisation of these networks in the developing rodent brain.

The aim of Experiment 2 (Chapter 6) was therefore to record the early responses of putative HD cells in a more naturalistic environment

than previous experiments, to discover which sensory cues may support stable directional signalling before eye-opening. To address this, I recorded responses of HD cells in the ADN while the rat pup remained in the homecage with its mother and littermates. Ensembles of HD cells were recorded to investigate whether they are stable at P12 in a familiar, cue-complex environment, earlier than previously reported in standard recordings (P16; Wills et al., 2010; Langston et al., 2010). Experiment 2 therein investigated whether the presence of attractor network connectivity without a stable HD cell signal typically observed in pre eye-opening pups holds in different environmental contexts to previous experiments (Bjerknes et al., 2015; Bassett et al., 2018).

Chapter 4

General Methods

4.1 Animal subjects and husbandry

All animal subjects in this thesis were Lister-hooded rats (Charles River, UK) which were bred in-house. Female rats (prospective dams) were group housed with other females until the point at which they were suitable for mating (typically when greater than 300g in weight). The female rat was then co-housed with a male rat (stud) for 10 days to maximise the chances for reproductive success. The dam was subsequently individually-housed with abundant bedding and tissue for nest preparation. The dam was checked regularly for signs of pregnancy. Prior to birth of the pups, the dam was handled extensively to familiarise her with the experimenter and reduce maternal stress. The breeding cage was cleaned weekly until the point at which the dam was heavily pregnant, after which point the cage was cleaned subsequent to experiment end. Pregnant dams were checked daily, and the day of the litter birth was marked as P0. At P4, litters were culled to 8 pups per dam to minimise inter-litter variability. Home cages were 42 x 32 x 21cm in size, and maintained on a 12:12 hour light:dark schedule (lights off at 10.00 am) with food available ad libitum. Rooms were regulated for temperature and humidity on a daily basis (temperature range: 20°C to 24°C; humidity range: 45% to 60%). In the week preceding experimental onset, the pups were handled daily (between P4 and

P9). Handling consisted of picking up, weighing, holding and replacing each pup into the huddle. Animals were given 24 hours post-operative recovery before the general recording procedure began. Implanted pups remained co-housed with their dam and littermates throughout the experimental period until weaning at P21. At weaning, implanted pups and the remaining litter were housed separately to the mother. All procedures were conducted in accordance with the UK Animals Scientific Procedures Act (1986).

4.2 Microdrive preparation

Tetrodes were prepared as previously described (O'Keefe and Recce, 1993). Microdrives were loaded with 8 tetrodes (composed of four HML-coated 90% platinum-10% iridium 17µm diameter insulated microwires twisted together, California Fine Wire). A central cannula (stainless steel 26G x 15mm, Coopers Needle Works Ltd., UK) was secured between two Omnetics connectors (Figure 4.1; A79010-001, Omnetics Connector Corporation, USA) with the aid of heat shrink tubing (Farnell, UK) and superglue (Loctite, Germany). A protective sleeve (stainless steel 21G x 4mm, Coopers Needle Works Ltd., UK) was inserted over the cannula. The sleeve serves as an attachment point to the skull during implantation (Figure 4.1), to allow travel of the cannula through the sleeve. Tetrodes are fed through this cannula (Figure 4.1). Silver conductive paint (Electrolube Ltd., UK) was applied over the Omnetics contact pins and un-insulated tetrode microwires, to improve electrical conductivity.

The presence of conspecifics in homecage recordings necessitated the internal (rather than external) grounding of microdrives. This was achieved by soldering a fine copper hook-up wire (36 AWG, Alpha Wire, USA) between the cannula and the ground pin on the Omnetics plug of the microdrive. The microdrive assembly is protected with a liberal amount of dental cement (Figure 4.1; Simplex Rapid, Kemdent, UK).

Tetrodes are then cut to a uniform length using surgical-precision scissors (Fine Science Tools, Germany). The microwires were electroplated with an input frequency of 1kHz (Ferguson et al., 2009) with 1:9 0.5% gelatine:Kohlrausch platinum solution (NanoZ, Neuralinx, USA), within 48 hours before surgical implantation. This serves to reduce the electrical impedance of the wires to approximately 200 k Ω (at the input frequency, 1kHz) and improve the signal-to-noise ratio of recorded neuronal potentials (Ferguson et al., 2009).

The principle of the microdrive is based on a central, captive screw within a microdrive mechanism (Figure 4.1; stainless steel, purpose built in-house) consisting of two outer posts which are secured to the microdrive with dental cement (Simplex Rapid, Kemdent, UK). Once implanted, the tetrode array is advanced ventrally by turns of the captive screw (1 turn corresponds to 250 µm tetrode travel).

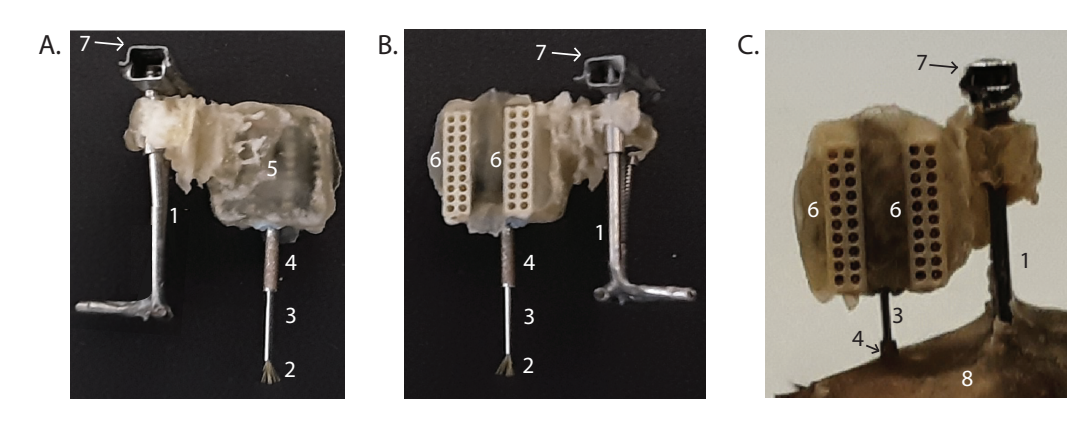


Figure 4.1: Photo of pup microdrive assembly for implantation in the ADN before (A,B) and after (C) surgical implantation. Tetrode arrays are implanted in the brain area of interest via a central cannula. A drive mechanism is cemented to the skull by the mechanism 'feet', which stabilises the drive mechanism on the skull and advances the tetrode area by means of a captive screw which pushes the cannula downwards through the protective sleeve. The microdrive array is protected by a layer of dental cement. A male connector is then plugged into the corresponding female Omnetics connector on the rat for *in vivo* electrophysiology recordings. 1: Drive mechanism; 2: tetrode array; 3: cannula; 4: protective sleeve; 5: dental cement encasing; 6: female Omnetics connector; 7: captive screw; 8: skull surface.

Standard rat pup microdrive implants have capacity for 8 tetrodes (i.e. two Omnetics connectors), however the neural data logger used in this

thesis had capacity for 4 tetrodes (i.e. one Omnetics connector). To account for the polarisation of the neural data logger Omnetics plug, a dual 16-channel mouse headstage with attached Litz wire (both left pegs) was therefore purpose-made for neural data logger experiments (Axona Ltd., St Albans, UK). A jumper wire was added to the headstage between the top and bottom guide pins on the Omnetics connectors such that both guide pins were grounded. This was to ensure compatibility of grounding between the neural data logger and Axona configurations.

4.3 Surgical procedure for pre-weanling rat pups

On the day preceding surgeries, a 'dummy' drive was placed into the nest to habituate the dam and pups to the smell of the microdrive and its component materials. On the day of surgery the heaviest pup was chosen. Aseptic technique was adhered to via the following procedure: Surgery tools were autoclaved and surfaces including the surgical table, microscope and stereotaxic apparatus (Kopff Model 963 Ultra Precise Small Animal Stereotaxic Instrument) were thoroughly cleaned using a 70% ethanol spray.

Rats pups were anaesthetised with 3% isoflurane and received a subcutaneous injection of $0.15 \, \text{mg/kg}$ body weight buprenorphine (Vetergesic, Ceva) before being placed back in the home cage for 30-40 minutes to allow for onset of analgesia. After this time elapsed, the rat was retrieved from the homecage before being re-anaesthetised with 1-3% isoflurane. The pup's head was shaved before the pup was placed on the stereotaxic apparatus with a heat pad maintained at 37°C. The rat's head was stabilised via positioning of the bite bar and either zygomatic arch clamps (pups aged < P13) or ear bars (pups aged > P13).

When the pup was well anaesthetised, Betadine antiseptic and 70% ethanol were applied to the shaved area of the pup's head. An incision

was made along the anteroposterior axis of the head along the midline with a feather-edged scalpel blade (#15 surgical scalpel blade, Swann Morton, UK). Connective tissue on the skull surface was removed, and sterile saline was used to clean the skull surface. Using a sterile needle mounted on the stereotaxic arm, bregma and lambda were identified on the skull and, if necessary, the pup's head tilt was adjusted such that bregma and lambda were less than or equal to 0.05 mm apart on the dorsoventral axis. The anteroposterior and mediolateral stereotaxic coordinates for the microdrive implant site were marked on the pup's skull. Holes for support screws (to stabilise the microdrive implant) were drilled around the skull using a burr drill, avoiding the implant site. The screws were inserted, before glue (Krazy Glue, USA) was applied to the base of each screw as well as to the interface of the skull and skin, around the perimeter of the incision site. A trephine hole was then drilled at the implant site and the bone disk removed. The dura was excised using a sterile needle. The pup was chronically implanted with the microdrive to the desired dorsoventral coordinate for the brain region of interest. Using a fine needle, sterile vaseline was applied onto the craniotomy around the cannula of the microdrive. The protective outer sleeve was lowered until it sat on the sterile vaseline at the surface of the skull. Dental cement (Super-Bond, Sun Medical Co. Ltd, Japan) was prepared and applied to exposed areas of the skull around the base of the drive mechanism and around the protective sleeve (Figure 4.1C), until the microdrive assembly was stable and well adhered to the pup's head.

Once the cement was dry, the anaesthetic equipment was disconnected and the pup removed from the stereotaxic apparatus via loosening of the nose clamp and zygomatic cups (or ear bars). Post-operative care included cleaning the area around the rat's head wound thoroughly with a saline-moistened cotton bud. The pup was placed on a heat pad in a recovery chamber in the surgery ante-room. The pup was monitored until it

woke, demonstrating a righting reflex and started walking when touched or moved. The pup was placed back in its homecage and the maternal response observed for at least 15 minutes. The pup was re-checked intermittently between 30 minutes and several hours post-surgery.

4.3.1 The effect of isoflurane in development

Isoflurane is a commonly used inhalant anaesthesia in rodents. The benefits of inhalation anaesthetics for neonates include their low solubility in the bloodstream (resulting in swift anaesthesia onset and wake-up) and precise management of anaesthetic depth (Huss et al., 2016) in comparison to other methods of anaesthesia such as hypothermia.

However, the effect of isoflurane on development is not yet fully understood. Previous research has shown that isoflurane exposure in newborn rodents can lead to acute neuronal death and persistent cognitive dysfunction (Jevtovic-Todorovic et al., 2003; Stratmann et al., 2009a; Stratmann et al., 2009b). It has also been shown that repeated neonatal exposure to anaesthesia in rats leads to more significant long-term cognitive impairments compared to a single exposure (Murphy and Baxter, 2013), aligning with human studies reporting similar effects of multiple versus single early-life anaesthetics on long-term cognitive function (Flick et al., 2011). Similarly, Lee et al. (2014) found that exposure to isoflurane increased neuronal death in the thalamus and hippocampus with no difference between male and female subjects. However, when it came to behavioural outcomes, only males showed impairments in tasks related to recognizing objects in different locations and contexts, as well as deficient social memory. This suggests that males are more susceptible to long-term cognitive effects from isoflurane exposure, and these effects may not be solely due to neuronal death.

It's important to note that neonates, including rodents, are more vulnerable to anaesthesia-related complications due to physiological differences compared to adults, such as less efficient drug metabolism (Clowry and Flecknell, 2000) and differences in blood-brain barrier permeability, body-water content, hepatic enzyme systems, and albumin concentrations (Flecknell et al., 2007). Therefore, the potential long-term effects of the usage of isoflurane as a gas anaesthetic for these studies, and the duration of such effects, should be considered.

4.4 Data acquisition

4.4.1 General recording procedures

Rats were given 24 hours for postoperative recovery, after which point the data acquisition process began. If the pups were feeding at the time recording was to commence, the experimenter refrained from removing the pup from the homecage for at least 20 minutes. Prior to each experimental recording, a screening procedure was conducted in a small, rectangular enclosure to functionally identify single-unit putative cells in the brain region of interest (in all cases using the Axona data acquisition system; Axona Ltd, UK). A rotating table (Lazy Susan, Amazon) placed in the environment aided in the detection of single-unit HD cells. If single-unit activity was confirmed then the experimental procedure for electrophysiological recordings was followed. If no cells were present, the tetrodes were advanced between 62.5 µm to 250 µm deeper in the brain to maximise the success for isolation of single-unit activity in the subsequent screening session. The pup was then placed back in the homecage. At least three hours were left between screening sessions to ensure the brain tissue had settled following tetrode movement, and to offset intra-experimental tetrode drift. Screening procedures were conducted in pups approximately three times per day throughout the experimental timeframe, until cells were no longer observed or it was judged that the electrodes had been advanced beyond the dorsoventral depth of the brain region of interest.

4.4.2 Single-unit electrophysiological recordings

All experiments were conducted under dim lighting in rooms containing anti-static linoleum flooring. The environmental apparatus, presence of distal cues, and duration of recording sessions differed depending on experimental procedure (detailed in Chapters 5 and 6), and were not cleaned between recordings. The rats were not habituated to the environment before recording. During recordings, the experimenter monitored the behaviour of the rat and encouraged uniform sampling of the environment by dispensing drops of soya-based formula milk on the floor of the arena in various locations.

As mentioned, the neural data logger has capacity for 16 channel recordings. The subsequent cell yield was therefore maximised by identifying the Omnetics plug from which the most single-unit activity was confirmed, and then recording from this plug in the subsequent neural data logger experiment. If single-unit activity was present on both plugs, then the option for running an experiment in series was possible with the inclusion of a suitable inter-trial interval.

4.4.2.1 Axona tethered recordings

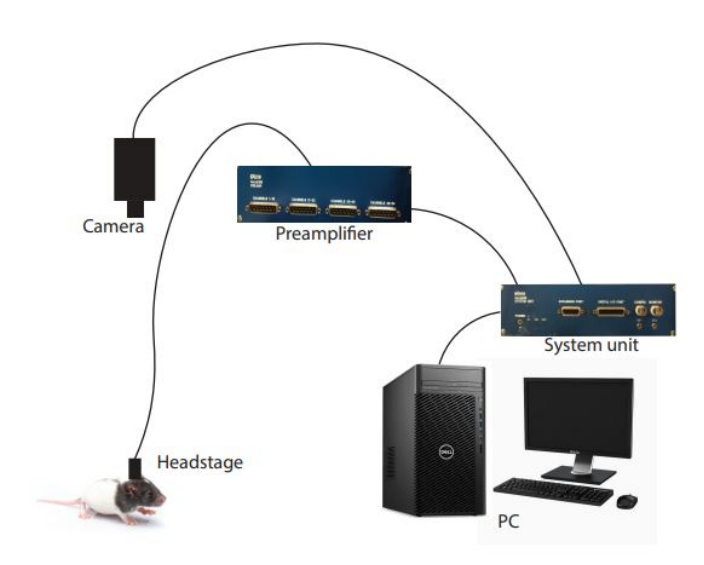


Figure 4.2: Standard electrophysiology set-up for Axona tethered recordings. Animals are plugged into a headstage which is connected to a data acquisition system via a tethered cable. An LED 'boom' is attached to the headstage of the animal which enables automated video tracking. Note that the LEDs on the headstage are spaced 6 cm apart.

Standard extracellular recording with tethered data acquisition systems were performed using Axona Ltd.'s DacqUSB system (hereafter termed DACQ). The DACQ set-up functions as follows. An acausal band-pass filter was applied to remove low-frequency activity less than 300 Hz and remove high-frequency noise greater than 7 kHz. Spikes were detected online via an amplitude threshold. Automated video tracking occurred at 50 Hz, by the detection of two LEDs (spaced 6 cm apart) attached to a boom on the headstage. In the system unit, digital signal processor (DSP) modules combine the amplified, digitised neural signal with the video tracker position in a time-synchronised manner. This is then transferred via USB cable to the PC for storage and post-processing (Figure 4.2). The output file formats are described in detail in Table 4.1.

4.4.2.2 Neural data logger recordings

Batteries were charged before recording sessions to maximise recording time. The neural data logger (MouseLog16; Deuteron Technologies Ltd., Israel) was plugged into the microdrive on the animal. When the set-up was ready, neural data recording was started via the MouseLog16 command programme (LoggerCommand3, Deuteron Technologies Ltd., Israel). This communicates with the wireless logger device via a transceiver (Step 1, Figure 4.3). Position recording is subsequently started in Bonsai (Bonsai v2.4; Lopes et al., 2015) via a keyboard press (Step 2, Figure 4.3). The Bonsai programme instructs an Arduino-UNO (Step 3, Figure 4.3) to transmit 50 Hz transistor-transistor logic (TTL) pulses to the camera (Point Grey Chameleon3 USB 3.0, FLIR) to begin video recording (Step 4, Figure 4.3). The framerate for position sampling was 50 Hz. The Arduino-UNO simultaneously sends 1 Hz TTL pulses to the logger device via the transceiver, which are stored on the logger for downstream synchronisation of neural and position data. When the recording session has reached the desired trial duration, recording is stopped first on Bonsai (again by a keyboard press) and then stopped on the neural data logger via the LoggerCommand3 programme. Trial metadata (date, trial name, neural data logger number, rat number, trial environment and duration, recorded tetrodes) are then manually input on a master spreadsheet by the experimenter for downstream processing. If a trial needs to be restarted, this procedure is repeated and the erroneous trial is noted in the master spreadsheet so as to be ignored in downstream processing.

The Bonsai pipeline for video tracking is as follows (Figure 4.4): The video stream is fed to Bonsai, cropped to the size of the environmental boundaries, then split into its RGB components. As the LEDs utilised by the logger are green and red, the image was split into its green and red constituent parts. Each image was then thresholded to discount any spurious light sources not emanating from the LEDs. The centroid of each LED is dilated using a morphological operator to enlarge the region of interest for more successful frame-to-frame tracking. Binary region analysis was then conducted on the image to extract the largest binary region. The

centroid of the largest binary region was computed, corresponding to the x- and y-coordinates for each LED at each sampled time (50 Hz). Bonsai also enables the experimenter to monitor the animal's movements and spatial sampling in real-time via a thresholding module which produces a histogram of visited bins. At the end of the experiment (signalled by a keyboard press from the experimenter), the data is merged and written to CSV and AVI files for downstream processing (Figure 4.4). Following a recording session, logger neural data files were copied from the micro-SD memory card to the host computer.

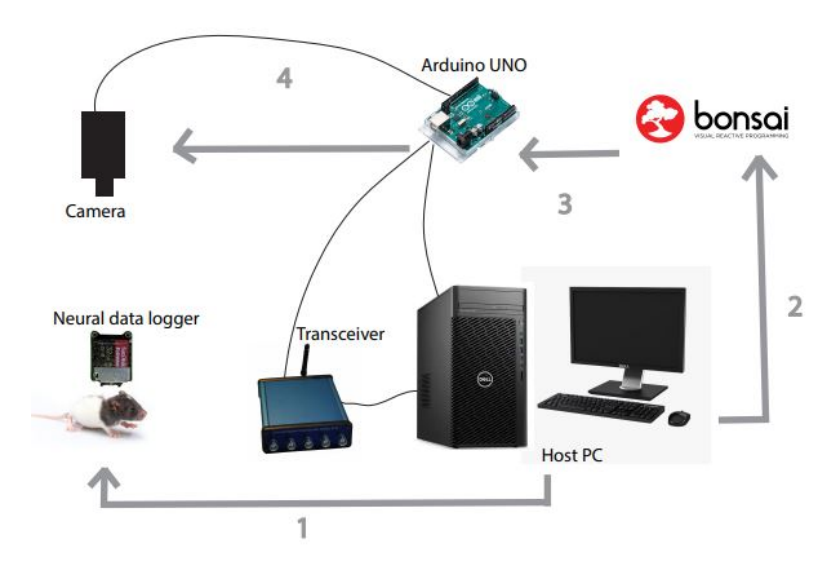


Figure 4.3: Procedure for neural data logger recording. (1) The logger is instructed to begin recording by the experimenter on the PC, which communicates with the logger device via a transceiver. (2,3) Video tracking is conducted using a specialised Bonsai pipeline, in which Arduino UNO-triggered video sampling occurs. (4) TTL pulses from the Arduino UNO are also sent to the logger for subsequent synchronisation with neural data.

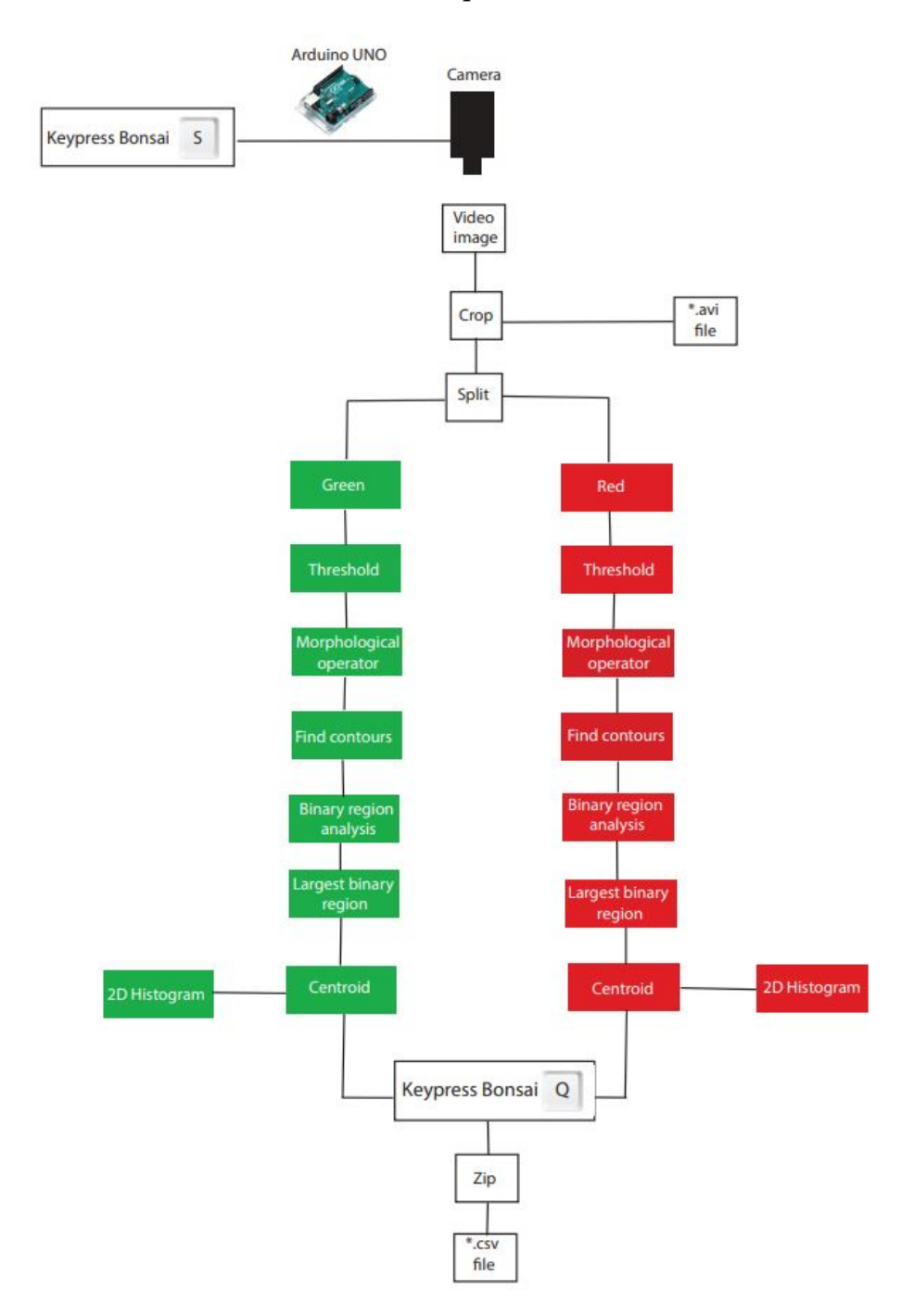


Figure 4.4: Bonsai dataflow processing of the input video image during recording trials. Beginning corresponds to the top of the figure. The pipeline start is triggered by a keyboard press from the experimenter. Each node in this pipeline performs a specialised task in sequence. The input image from the camera is split into its RGB components (red and green) to specifically process the logger-mounted LEDs for tracking of the animal's position during the experiment. Termination of the pipeline at the end of recording is instructed via a keyboard press from the experimenter. At the end of recording, position data is saved as a comma-separated file (CSV) for downstream analysis. A video file (AVI) is also saved which allows for post-hoc optimisation of tracking offline, as well as any additional video processing.

4.5 Histology and Electrode Localisation

At the end of the experimental period, rats were anaesthetised with 3% isoflurane before being administered an overdose of sodium pentobarbital (Euthatal, Merial). Upon cessation of breathing and pinch reflex, rats were then transcardially perfused with phosphate buffered saline (PBS) followed by 4% paraformaldehyde in PBS. The brain was then extracted and fixed in 10% neutral buffered formalin for several days, before transferring the brain to a formalin(10%)-sucrose(30%) solution for cryoprotection. Brains were sliced into 30µm coronal sections using a cryostat and were stored in PBS before being wet-mounted onto gelatin-subbed slides. Nissl staining (Nissl, 1894) was conducted and brain slices were then imaged using a Leica microscope to confirm tetrode localisation (Leica, Germany).

4.6 Data analysis

4.6.1 Processing of raw logger neural data

In order to compare the neural data logger (Deuteron Technologies Ltd., Israel) directly with DACQ data (Axona Ltd., UK) the raw logger data was processed such that it would be compatible with TINT Cluster Cutting and Analysis Software (Axona Ltd, UK), the proprietary software for examining DACQ single-unit data. Neural data storage fundamentally differs between DACQ and logger systems: DACQ data is recorded at a sampling rate of 48kHz. The data is stored as a series of thresholded spikes, wherein a spike event is detected and data from all channels on a tetrode is stored over a 1ms spike window. DACQ data is amplified with variable gain (with a dynamic range between $\pm 150 \mu V$), which is set by the user prior to commencing a recording session. The data is subsequently digitised and stored in 8-bit precision. By contrast, logger data is stored as continuous neural data at a sampling rate of 31.25kHz without detected spike events. All signals

are measured relative to ground and a lowpass filter of 300 Hz applied. The data in each file is stored as an array of 16-bit unsigned integers, structured in the same order as the data is recorded. The logger data is recorded with fixed gain (with a range ±6.8 mV). The data sequentially fills 16MB data files, each corresponding to approximately 17 seconds of data. The end of each neural data file is contiguous with the beginning of the subsequent data file. Spike extraction from the logger data was conducted *post hoc* by applying parameters for spike threshold and gain extracted from the corresponding DACQ trial.

All data processing was conducted in MATLAB (Mathworks). Neural data files were opened and processed in sequence, then written to TINT-formatted tetrode files (the file format of TINT files is described in Table 4.1). Data processing and spike extraction consisted of a number of procedures: The neural data was converted from unsigned 16-bit values to voltage data (μV) by the following equation:

$$Volts = Resolution * (uint 16_{value} - 2048)$$
 (4.1)

where the bit resolution is 3.3µV per level. The signal was interpolated such that the sampling rate of logger unit data matched that of DACQ (48 kHz). The data was highpass filtered at 7 kHz. To correct for any direct current (DC) offset in the data, the median signal was subtracted from each channel. Tetrode data was then separated and mapped such that they matched the equivalent tetrodes in DACQ.

Spikes were extracted on a tetrode-by-tetrode basis according to Axona spike detection parameters: Inflections in the signal which surpassed the spike threshold from the corresponding DACQ trial (generally maintained at $70\mu V$) on any channel was considered a spike. 1ms for each spike was extracted from the data across all 4 channels on that tetrode (equivalent to 200 μ s before the threshold crossing, and 800 μ s after the threshold event), as well as the corresponding spike timestamp. An artefact rejec-

tion criteria was used to ensure that only 'true' spikes were stored and erroneous results discarded. This criteria ensured spikes consisted of a positive peak in the first half of the spike window, followed by an after-hyperpolarisation and a return to baseline in the second half of the spike sampling window.

Position samples and corresponding timestamps were extracted from the Bonsai-output comma-delimited file. A binary file (Eventlog) is stored on the micro-SD card of the logger, which is converted to a commadelimited file for data extraction. This maintains a log of all events, in this case neural data filenames, timestamps (1µs resolution) and TTL pulses corresponding to video tracking framecounts at 50 Hz sampling rate (Figure 4.5). To synchronise neural data with position data, the timestamp of the first received TTL pulse from Bonsai is extracted here and the number of logger pulses at the beginning of the trial to be removed are computed (Figure 4.5).

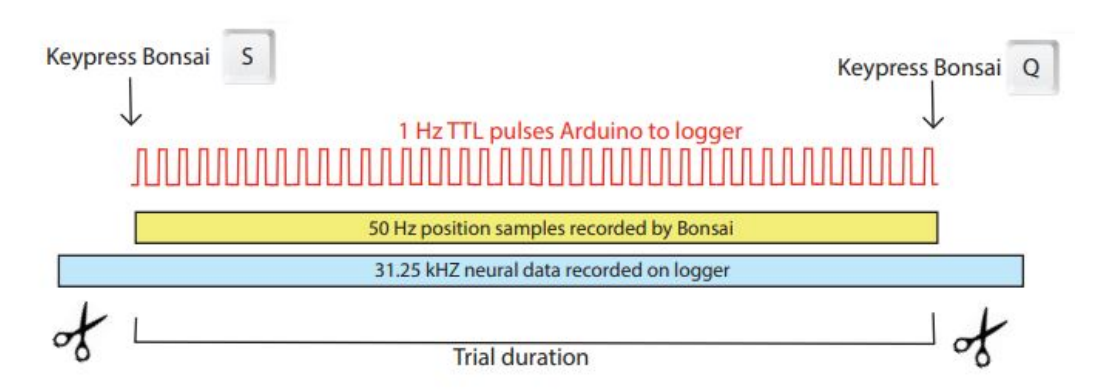


Figure 4.5: Data synchronisation of logger neural data recordings. Logger neural data recording begins prior to Bonsai position tracking (which begins with a keyboard press by the experimenter). When Bonsai is running, it records position samples of LEDs at a sampling rate of 50 Hz. At the same time, 1 Hz TTL pulses are sent from Bonsai (via an Arduino) to the logger which are stored for offline processing. Neural data is synchronised with position data by comparison of TTL-pulse timestamps stored in the logger and the Bonsai-output file.

File type	File extension	File format
System setup	*.set	The system setup file is an ASCII text file which contains trial metadata including hardware settings, gain and referencing configurations, filter settings, video tracking information such as number of LEDs (in this case, two) and their relative offset, experimenter ID, trial name, trial date, and trial time.
Position file	*.pos	The position file begins with an ASCII header containing video tracking information such as the tracking boundaries of the environment, the pixels per metre for the environment, distance between LEDs (in pixels). This file contains all of the position samples for the trial, sampled at 50Hz. Each sample is 20 bytes, including a 4-byte framecount, eight 2-byte words which allow for up to tracking of 4 LEDs simultaneously. Two LEDs were used in these experiments, therefore the words describe the x- and y-coordinates for each LED as well as their respective number of pixels, the total number of tracked pixels and the corresponding position for each. For samples in which the LED was not tracked (for instance, due to occlusion of the LED), an empty place marker is included.
Spike data (unit data)	*.1 to *.8	Spike data files begin with an ASCII header which contains information such as the number of recorded spikes, sampling rate, the timebase of the timestamps, trial date, trial time and experimenter. Each file corresponds to a given tetrode, denoted by the number in the file extension. Each spike recorded on this tetrode is stored for every channel (four channels per tetrode). Spikes are thresholded events (threshold decided by the experimenter). Data is stored in 1ms segments, with 200µs preceding the threshold event and 800µs following the threshold event. Spikes are structured as 216 bytes (54 bytes per channel), with a 4 byte timestamp corresponding to the time of the spike event, and 50 byte spike data samples.

Table 4.1: File formats of Axona DACQ files which were replicated for data recorded using the neural data logger. All data in these files are of big-endian format (most significant byte first).

4.6.2 Spike sorting and cluster separation

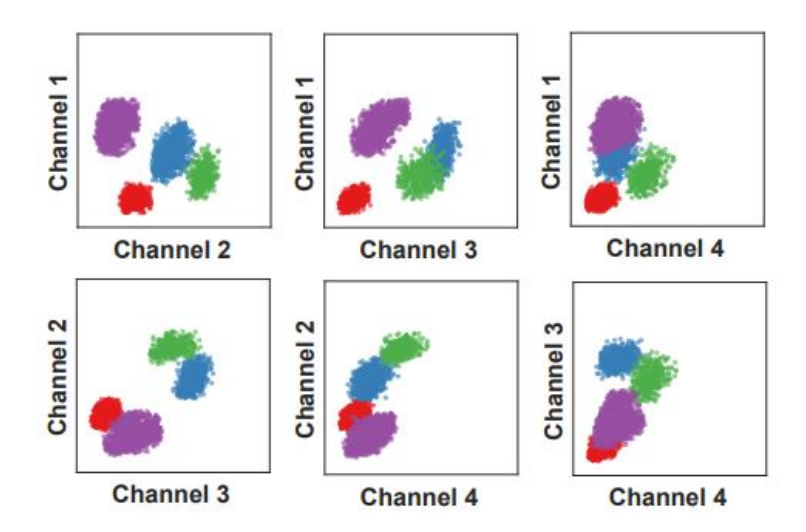


Figure 4.6: Example cluster separation and spike sorting on one tetrode. Spikes recorded on a given tetrode are distinguished based on amplitude differences across recording electrodes (Channels 1-4). Spikes are assigned to a cluster using KlustaKwik, corresponding to a putative neuron. Each cluster here is represented by a different colour. Clusters are then manually curated to remove spurious or outlying spikes.

Spike sorting and cluster separation was conducted offline using TINT (Axona Ltd, UK). Spike sorting is the process by which single-unit activity is segregated from noisy, time series neural data such that action potentials of recorded neurons are isolated. Recordings using tetrodes enables spike isolation because of the differences in spike amplitude recorded on each neighbouring electrode. Spikes recorded further from a given electrode will have an attenuated action potential, while electrodes in closer proximity to the neuron will record higher-amplitude potentials. This spatial segregation of action potentials produces a unique profile which enables the allocation of each action potential trace to a given cell. By plotting the amplitude of a spike recorded on one electrode versus another electrode, a scatterplot is produced, and this is done for each combination of electrode (or channel, such as shown in Figure 4.6).

Cluster separation was then conducted using automated clustering software KlustaKwik (Harris et al., 2000; Kadir et al., 2014). This process

groups spikes according to their principal components (including spike amplitude, spike width, waveform peak-to-trough amplitude difference) into clusters corresponding to individual neurons. Manual curation of clusters was conducted by a process termed cluster cutting, using the software package TINT (Axona Ltd, UK). This involves visualising scatter plots showing the amplitudes of recorded action potentials relative to each pair of electrodes on a tetrode (Figure 4.6). Spikes (action potentials) which assemble into a cluster are presumed to originate from the same cell. Manual curation involves qualitatively assessing each cluster and removing spikes which appear spurious or incorrectly assigned to a given cluster.

4.6.3 Processing position data

Missing video frames were linearly interpolated. Position data was then smoothed with a 400ms boxcar filter kernel (moving average filter). The position data was filtered such that speed samples greater than 100 cm/s were removed (samples in excess of this were presumed to be tracking errors). Instantaneous linear velocity was calculated by the distance/time between successive position samples. The momentary directional heading of the animal was computed by the inverse tangent of the position of the two LEDs on the animal's head. The instantaneous angular head velocity was calculated as the difference in head direction angle between successive position samples.

4.6.3.1 Quantitative analysis of the thigmotactic response

To quantify the amount of time animals spent near the boundaries of the recording environment, the enclosure was divided into a boundary region (wall zone; outer 15% edge of the environment floor) and an inner floor region (central zone; 70% total floor length and width). The thigmotactic response was therefore quantified as the proportion of total time spent by the animal in the outer, boundary region of the environment in a given trial.

4.6.4 Construction of firing rate maps

All spike and positional data were filtered to remove periods of immobility (speed $< 2.5 \,\mathrm{cm/s}$). Positional data was then sorted into $2.5 \,\mathrm{x}\,2.5 \,\mathrm{cm}$ spatial bins. Following this, total positional dwell time and spike count for the whole trial was calculated for each spatial bin. Binned data was smoothed using adaptive smoothing (Skaggs et al., 1996): To calculate the firing rate for a given bin, a circle centred on the bin was expanded in radius r until

$$r \ge \frac{\alpha}{d\sqrt{s}} \tag{4.2}$$

where $\alpha = 200$, d is the dwell time(seconds) and s is the number of spikes within the circle. The firing rate assigned to the bin was then set equal to s/d. Firing rate polar plots for directional data were generated by sorting the data into 6° bins in the yaw plane. The total dwell time (d) and spike count (s) for the whole trial was calculated for each directional bin. Binned position dwell time and spike count maps were smoothed with a boxcar filter of 5 spatial bins. Firing rate for each directional bin was then defined as s/d.

4.6.5 Quantitative analysis of spatial firing

4.6.5.1 Spatial and directional information

Spatial information is an estimate of the mutual information (I(R|X)) between firing rate R and location X (Skaggs et al., 1993), given by the equation

$$I(R|X) \approx \sum_{i} p(\vec{x}_i) f(\vec{x}_i) log_2\left(\frac{f(\vec{x}_i)}{F}\right)$$
 (4.3)

where $p(\vec{x}_i)$ is the probability for the animal being at location \vec{x}_i , $f(\vec{x}_i)$ is the firing rate observed at \vec{x}_i , and F is the overall firing rate of the cell. Mutual information is divided by the overall mean firing rate of the cell in the trial, providing a bits/spike estimate of spatial information. Directional infor-

mation is the mutual information between firing rate and direction.

4.6.5.2 Unidirectional modulation of head direction cells

The Rayleigh vector (RV; mean resultant vector from the binned and smoothed directional rate map) was computed. The RV is a measure of unidirectional departure from uniformity of a circular distribution (unlike directional information, which detects any modulation of firing by head direction). The RV is bounded between 0 and 1: an RV of 0 indicates a cell has no unidirectional firing modulation, an RV of 1 demonstrates all firing is clustered in one direction only.

The Rayleigh vector length is computed by the following equation (Zar, 2010):

Rayleigh vector length =
$$\frac{\pi}{n \cdot \sin\left(\frac{\pi}{n}\right)} \sum_{j=1}^{n} r_{\phi_j} e^{-i\theta_j} / \sum_{j=1}^{n} r_{\theta_j}$$
 (4.4)

where n is the number of directional bins, θ_j is the angle (in radians) of the j-th bin, and r_{θ_j} is the average firing rate of the cell for that particular head direction.

4.6.5.3 Within- and across-trial stability

Across-trial stability was calculated as the Pearson pairwise correlation coefficient (r) between the corresponding spatial (or directional) bins from two consecutive trials. This excludes bins with a 0Hz firing rate in both trials. Within-trial stability was calculated as the Pearson pairwise correlation (r) between corresponding spatial or directional bins from the first and second half of a given trial.

4.6.6 Statistics

All statistical analysis was conducted with SPSS (IBM) and Matlab (Mathworks). The Shapiro Wilk's test was applied to all data to confirm whether the data was normally distributed (Matlab *swtest*), which then decided the subsequent statistical test to be performed on the data (either parametric

or non-parametric). p=0.05 is considered the threshold significance level in these statistical analyses. In all figures, p-value significance level is indicated by the following: * p< 0.05 significance, ** p< 0.01 significance, *** p< 0.001 significance.

If data met the assumption of normality, parametric statistical tests were performed. A paired t-test was used for statistical comparison of two groups (paired measurements), using Matlab *ttest* function. For parametric analysis of greater than two paired groups, a 1-way (within-subjects) repeated measures ANOVA was performed (SPSS). For analysis of within-subject and across-subject comparisons, a 2-way mixed ANOVA was performed (SPSS). Partial eta squared (η_p^2) was used as a measure of the effect size of either age, environment, or recording system on the dependent variable. $\eta_p^2 >= 0.14$ were considered large effects, $\eta_p^2 >= 0.06$ were considered moderate effects, and $\eta_p^2 >= 0.01$ were considered negligible effects (Cohen, 1988). A post-hoc comparison of group means was conducted using Tukey's Honest Significant Difference (HSD).

For non-normally distributed data, a non-parametric Wilcoxon signed-rank test was conducted. A Wilcoxon signed rank test was used for statistical comparison of two groups (paired measurements), using Matlab *signrank* function. For parametric analysis of more than two paired groups, a Friedman test was performed (Matlab *friedman* function) followed by multiple pairwise comparison of group ranks. A Bonferroni correction was applied for all post hoc statistical tests.

Comparing group means of circular data was conducted by a Watson-Williams test (Matlab $circ_wwtest$), which assumes that the data follows a Von Mises distribution with a resultant vector length > 0.7 and concentration parameter $\kappa > 1$ (tested using Matlab $circ_kappa$). If the assumption of the Watson-Williams test were not met, then a non-parametric multisample test for equal medians of circular data (a circular analog of the Kruskal-Wallis test) was conducted using Matlab $circ_cmtest$.

Chapter 5

Wireless recordings of spatial cells in developing rats

5.1 Background and rationale

5.1.1 Chronic *in vivo* electrode recordings

Extracellular electrophysiology techniques are commonly used in the field of spatial navigation research. Chronic in vivo extracellular recordings using microwire electrodes provide high temporal resolution of neural activity in one or several brain regions, which can be conducted as an animal freely behaves in a given environment. The advantage of this is that the neural correlates of functional behaviours such as exploration, homing, working memory tasks or sleep may be extrapolated during these recordings. The progression from single electrodes (Hubel, 1957; used in the first study identifying place cells, O'Keefe and Dostrovsky, 1971) to stereotrodes (comprised of two electrodes; McNaughton et al., 1983a), to tetrodes (O'Keefe and Recce, 1993; Wilson and McNaughton, 1993) has incrementally improved the ability to discriminate single-unit activity. Bundles of microwires, such as tetrodes, enable more precise discrimination of individual neurons within an area of brain tissue through the relative waveform amplitude of different neurons in three-dimensional extracellular space. Tetrodes are particularly useful when recording neurons which are densely packed, as is the case in the thalamic nuclei and the pyramidal cell layer of the hippocampus.

The number of implanted tetrodes can vary, with consideration being taken for the tissue damage or gliosis caused by larger tetrode arrays, as well as the weight of the miniaturised microdrive on the animal's head, both of which are particularly pertinent to developmental studies. Currently, the favoured technique for investigating the activity of spatial cells in developing rats are tetrode recordings using miniaturised microdrives. Microdrive implants may be adapted so that they are durable against typical grooming and maternal behaviours exhibited by the dam during this period, as well as the huddling behaviour with littermates in the days preceding weaning. Microdrives also enable the advancing of tetrodes ventrally through the brain tissue subsequent to implantation, which is invaluable for chronic single-neuron recording in the developing brain given the rapid growth in brain size over a short time period.

5.1.1.1 Tethered electrode recordings

Typically, spatial cognition experiments using tetrode recordings are conducted as a single animal forages in an open-field environment while tethered to a data acquisition system. A typical recording set-up such as Axona (Axona Ltd., UK) involves the *in vivo* implantation of a microdrive, which is plugged to a headstage experimental trials.

Until recently, most systems followed a common design: The animal is plugged into the acquisition system by a headstage amplifier, placed as close to the recording electrodes as possible (on the head of the animal, by connecting to the microdrive). In most cases the headstage amplifiers are unity gain, meaning that neuronal signals are transmitted at the same amplitude as they are detected. The headstage conducts signal buffering to prevent noise pickup during transmission of the neural signal through the low-impedance wires to the preamplifier. The headstage then passes the signal via a long, tethered cable to a preamplifier where the neural signal is

amplified. The preamplifier then connects to the data acquisition system (system unit) via a multiplanar cable (or an overhead commutator in some cases; Mehlman and Taube, 2018), in which further amplification occurs and an analog-to-digital converter (ADC) digitises the neural signal. Such designs are limited to having one wire per microelectrode which connects the animal to the acquisition system via the tether, but are advantageous as the headstages tend to be lighter without the need for an ADC.

In some cases such as Intan (Intan Technologies, USA), amplification and ADC occurs on the headstage. Digitising the neural signal on the headstage limits the susceptibility of the signal to noise en route to the data acquisition system. This design furthermore permits the multiplexing of signals so that the neural signals corresponding to multiple microelectrodes may be carried along one wire to the data acquisition system. This in turn reduces the cable requirements for such a system. In most cases, video tracking of the animal's movements is typically conducted via an automated system which detects headstage-mounted LEDs to infer the animal's location and directional heading in the environment.

There are several limitations for this technique from the outlook of developmental research. In circumstances where recordings in more complex environments are sought such as in the presence of conspecifics or environments with overhanging features, the cables involved in these recordings are vulnerable to damage and the range of motion of the animal is limited. Tethered headstages can also be a heavy weight on the heads of small animals such as pre-weanling rat pups. Tethered recordings therefore require the removal of the rat pup from its homecage, mother and littermates. This is a stressful experience for a young animal, and limits the duration of recording sessions. It's unclear whether this recording environment may have consequences in terms of the stability of spatial cells when compared to naturalistic environments such as its homecage.

5.1.1.2 Wireless electrode recordings

Wireless technology is emerging as a promising alternative (Fan et al., 2011; Hasegawa et al., 2015), presenting the opportunity of conducting experiments in complex or naturalistic environments where tethered recordings are not suitable. These devices are typically categorised as either neural data loggers (neural data stored locally on the device), or telemetry devices (which transmit the neural data wirelessly in real-time).

Neural data loggers (hereafter termed 'loggers') store the neural data locally on a memory card in a digitised, unprocessed format which is transferred to a computer after recording (Jeffery et al., 2018). Recordings are controlled by a host computer, which synchronises with the logger via a radio transceiver. As the logger is switched on by a magnetic switch and controlled remotely, once the animal is plugged in minimal contact is required throughout a recording session. One limiting feature of these wireless devices is the need for a power source, necessitating the use of a battery. The total wireless apparatus which is thus mounted on the animal's head includes the recording device with attached plug, battery, micro-SD card for data storage, antenna and protective casing. A disadvantage of this method is that online processing of data is not possible, as the data is stored on the animal until transferred to a PC post hoc for download and data processing. The distance over which these wireless recordings may be conducted is of note. Given that only a synchronisation signal, rather than the neural data itself, needs to be transmitted, recordings from distances of up to 20m in typical lab conditions can successfully be conducted. Devices capable of recording in environments up to a staggering 700m in size are currently in development by some researchers (Marx, 2021).

Specifications of neural data loggers can vary substantially. Those implemented in this thesis (MouseLog16B and MouseLog16C, Deuteron Technologies Ltd., Israel) have several specifications which are of interest to spatial navigation and ontogenetic studies in neuroscience. These de-

vices are miniaturised and lightweight (ranging from 2.8g to 3.5g, including the battery; Deuteron Technologies, Israel), which are important for the ability of young rats to locomote freely. These loggers have additional optionality for recording the wideband neuronal signal. In this way, both the low-amplitude neuronal signal (the LFP) and high-frequency single-unit neuronal activity may be extracted from the data (as do some tethered systems, such as Axona). Newer versions of these devices (MouseLog16C, Deuteron Technologies Ltd., Israel) also enables simultaneous recordings from multiple devices as well as the ability to record motion sensor data (accelerometer, gyroscope, magnetometer). This has many downstream applications including for the precise quantification of the neural correlates of social behaviours, as well as motion and orientation information.

Another format for wireless recording devices are implantable telemetry devices (Grieves et al., 2021) such as those designed by Data Sciences International (Harvard Bioscience, USA) wherein the preamplifier is plugged to the rodent's implant, and the neural signal is transmitted wirelessly to a receiver embedded in the data acquisition system via an antenna. This enables the real-time monitoring of neural activity as an animal performs a behavioural task because the data is transmitted immediately to the experimenter's PC in a thresholded, filtered manner. One limitation of telemetry devices is the possibility for electrical interference in the transmission of neural data which may not be remedied in the course of a recording trial. Furthermore, there are limitations placed on the number of channels which may simultaneously record neuronal data. For example, Bluetooth transmission of data has a bandwidth which permits the transmission of approximately one dozen channels simultaneously, whereas Wifi has the capacity for more channels but depletes the battery life of wireless devices significantly more (Marx, 2021). The additional hardware necessary for telemetry furthermore increases the weight of these devices, which may not be counterbalanced as in tethered recordings and so renders these devices ill-suited for developmental studies.

Previous uses of wireless devices include the study of place and grid cells in three-dimensional space in rodents (Grieves et al., 2020; Grieves et al., 2021) and bats (Ginosar et al., 2021), activity of grid and head direction cell activity in an adult rat's home environment (Sanguinetti-Scheck and Brecht, 2020), or neural spatial representation in the goldfish lateral pallium (a brain structure homologous to the mammalian hippocampus; Vinepinsky et al., 2017; Vinepinsky et al., 2020).

5.2 Experimental aim

There are many possible benefits to wireless recordings. In terms of development, the logger should allow us to track the emergence of spatial signals while minimising disruption of early sensory experiences. Current (wired) electrophysiology techniques employed in the field of rodent developmental research have been limited in the extent to which the early sensory experiences of a pup may be studied. The early life of a rat is, for the most part, spent feeding or huddling with littermates (Alberts, 1978). Immersing a young pup into a typical open-field testing environment, isolated from conspecifics, may not therefore produce data which is a true reflection of the early organisation of these networks in the developing rodent brain.

Wireless recordings have not previously been conducted in the developing rat. Therefore, an initial step in addressing this research question was the piloting of chronic *in vivo* electrophysiology in developing rats using a neural data logger. One way to do this was to compare logger recordings with those from a system that is well-established in the field of electrophysiology (DACQ, Axona Ltd., UK). Both systems record neural activity by the same physical input (omnetics connectors attached to implanted tetrodes). This makes serial recordings possible from the same implant. In order to directly compare neural data from the two systems, the same

neurons were recorded in rapid succession. Logger data was subsequently processed in such a way as to be compatible with the proprietary clustering and data visualisation software of Axona to directly compare the same cells in *post hoc* analysis.

The primary aim of the present study was to validate wireless neural recordings in investigating the emergence of spatial cells in rat postnatal development. We therefore chose to test the system recording HD cells in the ADN and place cells in hippocampal CA1, two cell types whose postnatal development using tethered recordings are well documented (Wills et al., 2010; Langston et al., 2010). Potential technical problems with wireless recordings include the stability of recordings made by the device, whether the animal has the ability to easily dislodge the device, the durability of the system to expected wear-and-tear when working with animals, as well as the resultant signal-to-noise ratio of these devices and how they compare to standard tethered recording devices. These experiments were therefore designed to test whether wirelessly acquired data was of an equivalent quality to data collected using tethered recordings.

5.3 Methods

5.3.1 Animal subjects

Experimental subjects were Lister Hooded rat pups (see summary of experimental subjects in Table 5.1). General methods for animal husbandry of pre-weanling rat pups are described in detail in Section 4.1. Those animals in which there was no yield of cells which passed the criteria for classification of head direction cell or place cell, respectively, were included in behavioural analysis and excluded from electrophysiological analysis (and thus histological analysis).

Rat ID	Brain area	Age at experiment end (Postnatal day)	Sex	Analysis	Number recorded cells	Days data con- tributed
r879	ADN	P19	M	Behaviour	n/a	P20
r887	CA1	P24	F	Behaviour	n/a	P24
r904	ADN	P25	M	Electrophysiology, behaviour	5	P24, P25
r905	CA1	P24	M	Electrophysiology, behaviour	6	P18, P23, P24
r924	ADN	P20	M	Electrophysiology, behaviour	2	P18, P19
r926	ADN	P20	F	Electrophysiology, behaviour	2	P19
r941	ADN	P17	M	Behaviour	n/a	P16
r942	ADN	P17	M	Behaviour	n/a	P15, P17

Table 5.1: Summary of experimental subjects for Chapter 5 experiments. Subjects with which the target brain region was not reached were included only in behavioural analysis, whilst those animals with putative head direction cells or place cells recorded were included in both electrophysiological and behavioural analysis.

5.3.2 Surgery

All animals were implanted as described in Section 4.3. Tetrode bundles (8 tetrodes) were aimed at the stereotaxic coordinates for either the ADN or hippocampal CA1, described in Table 5.2.

Brain area	AP axis	ML axis	DV axis
ADN	-1.72mm	-1.37mm	-4.2mm
CA1	-3mm	-2mm	-1.5mm

Table 5.2: Electrode implant coordinates. All coordinates shown are the distance from bregma. AP = anterior-posterior; ML = medial-lateral; DV = dorsal-ventral.

5.3.3 Neural data logger assembly

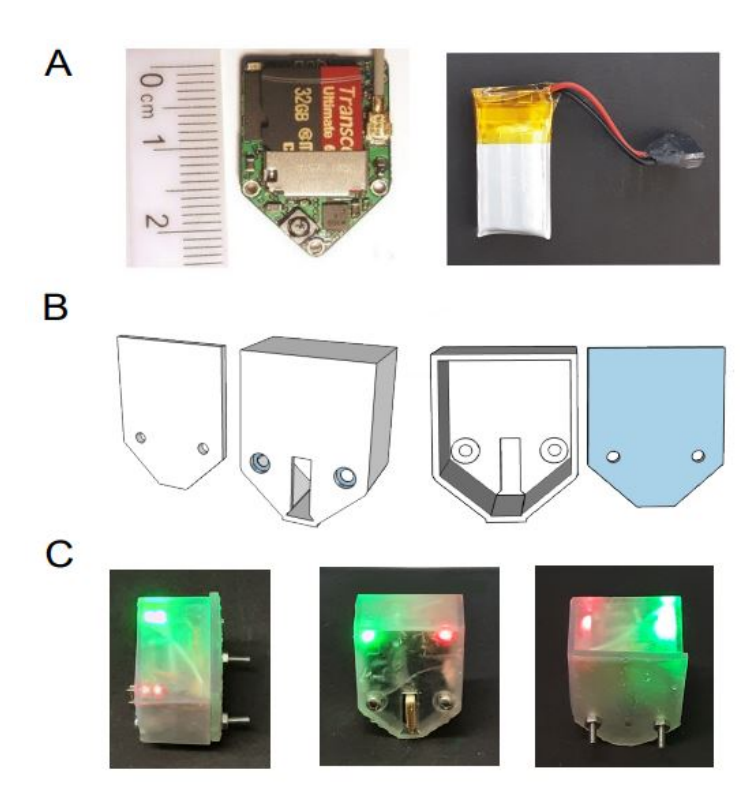


Figure 5.1: Wireless neural data logger Deuteron MouseLog-16B (Deuteron Technologies Ltd., Israel). (A) Animals are plugged into the logger and neural data is stored on a micro-SD memory card (left panel). The attached antenna allows for communication with a host computer. The logger is powered with a single cell lithium polymer battery (right panel). (B) 3D-printed case for protective housing of the logger. Clear resin is used to permit visibility of LEDs for tracking. The two sides of the case are held in place with screws (size M1.6 and corresponding-sized nuts). Left panel: front view; right panel: back view. (C) Neural data logger assembly used in recordings. Green and red LEDs in-built on the logger PCB, spaced 2cm apart, are visible through the transparent case, which are used for animal tracking. Left panel: side view; middle panel: front view showing the Omnetics plug, which plugged into the microdrive on the animal's head; right panel: back view.

Wireless single-unit data was acquired using the Deuteron MouseLog-16 logger (Deuteron Technologies Ltd, Israel). The logger component consisted of a printed circuit board (PCB) with micro-SD memory card (San-Disk, USA), and a single cell lithium polymer battery (Figure 5.1A). A built-in 2-light tracking system was used which included 2 LEDs spaced 2cm apart (Figure 5.1A and 5.1C). For mechanical support of the logger

and protection from damage, a purpose-built 3D-printed protective case (Form 3 Printer, Formlabs, USA) was used to house the logger (Figure 5.1B and 5.1C). Clear resin was used to maintain LED visibility for tracking (Formlabs, USA). The total weight of the neural data logger with attached antenna, battery and protective housing was 4.5g (by comparison, the weight of the Axona 32-channel headstage used for tethered recordings in this study was 5.66g). The logger has capacity for 4-tetrode recordings (equating to one Omnetics plug), thereby allowing the user to switch between banks of channels on each Omnetics plug. The plug corresponding to tetrodes with the most single-unit activity was chosen for logger recordings.

Note that the Axona tethered recordings were conducted following the procedures outlined in Section 4.4.2.1. It's important to highlight a distinction in the tracking methodology for animal movements between the Axona and Logger recordings. In the Logger recordings, tracking is achieved using two LEDs placed 2cm apart, whereas in the Axona recordings, two LEDs spaced 6cm apart are affixed to a headstage boom on the animal.

5.3.4 Behavioural paradigm

Behavioural trials took place in a recording arena (a square-walled grey box) which was 62.5 x 62.5 cm in size and 50 cm high, placed on a platform within the open laboratory. Each trial consisted of an open-field exploration. The open-field arena is one of the most commonly employed paradigms in behavioural neuroscience and spatial navigation research (Muller and Kubie, 1987). This is preferentially used in postnatal rats as it requires little or no explicit training for the animal to achieve relatively uniform spatial and directional sampling of the arena in order to assess spatial modulation of neural activity, and provides a rapid assessment of exploratory behaviours and their underlying neural correlates. Distal visual cues were available in the form of the fixed apparatus of the laboratory. The rat actively explored the arena and foraged for soya-based infant

formula milk (SMA, Nestle, Switzerland). Each recording session consisted of three trials (DACQ-A, Logger, DACQ-B; Figure 5.2). Trial duration was 10 minutes (ADN trials) or 15 minutes (CA1 trials), with a 10 or 15 minute inter-trial interval, respectively. The floor of the arena was not washed between trials.

A representative schematic of the laboratory set-up is depicted om Figure 5.3. Note that due to the position of the preamplifier, some tension may have been introduced to the tether in the areas of the environment furthest from the preamplifier (certain edges of the environment). This in turn may lead to a tendency of the animals to avoid the edges of the environment where the tension is at its greatest (such as the south-east corner of the open field).



Figure 5.2: Behavioural paradigm for open-field recordings comparing a well-established tethered recording system (DACQ) and wireless recordings (Logger) in developing rats. Trial duration was 10 minutes (ADN trials) or 15 minutes (CA1 trials), with a 10 or 15 minute inter-trial interval, respectively. The testing procedure involved placing the animal in the centre of the square-walled arena, and recording the animal's locomotion and neural activity for post hoc analysis.

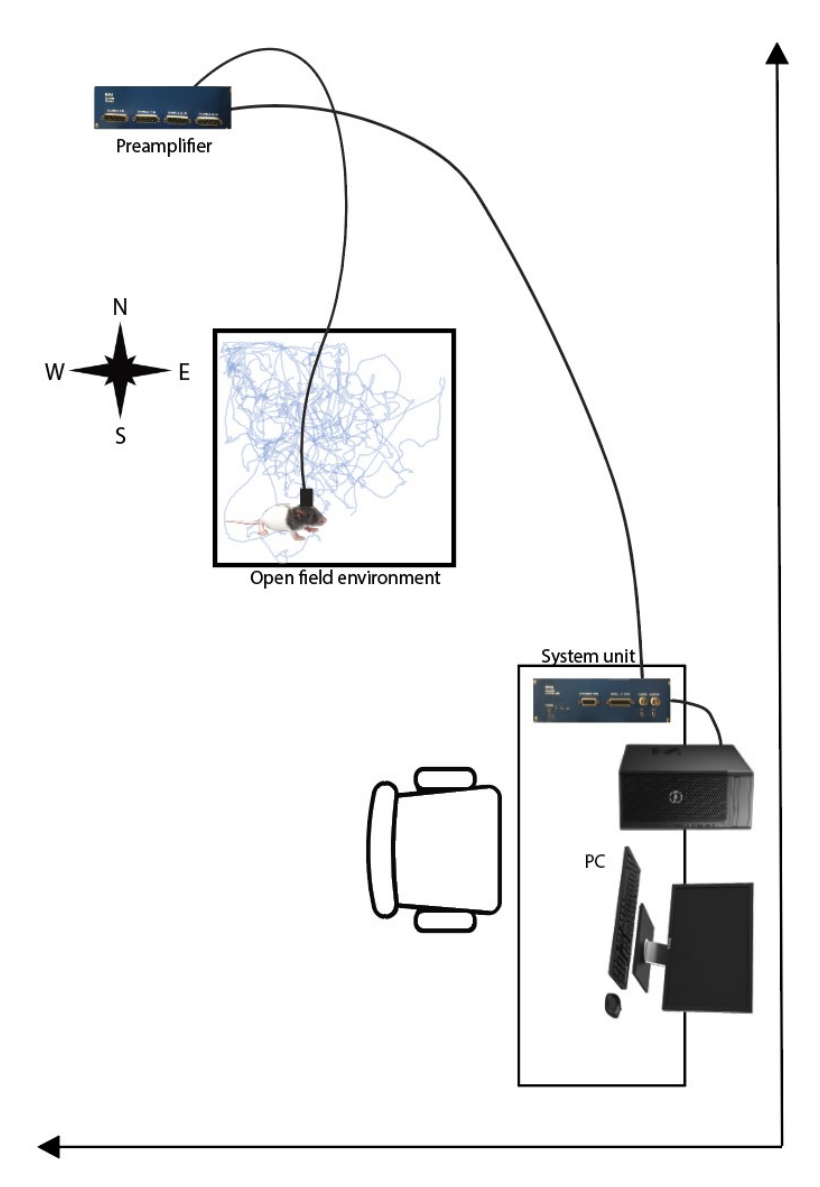


Figure 5.3: Schematic of the laboratory set-up for experiment. Shown here is the relative positioning of the equipment comprising the electrophysiology set-up for this experiment (not to scale). Lines at the right and bottom edges of the image denote the laboratory room walls. The laboratory extends beyond the area illustrated in the figure, denoted by arrows. The compass directions indicate the directional heading with respect to the camera which conducted video tracking of the animal's movements. The preamplifier was elevated to be approximately 1.5-2 metres above the open field environment employed in this paradigm. The blue trace depicted in the open field environment is a representative trajectory of an animal during a recording trial.

5.3.5 Data analysis

All data processing was conducted in MATLAB (Mathworks). Raw logger neural data was extracted and processed (described in detail in Section 4.6.1). Isolation of single-units was then performed manually on the basis of peak-to-trough amplitude and principal components using the software package TINT (Axona, UK) and KlustaKwik automated clustering software (Kadir et al., 2014) for both DACQ and logger data.

5.3.5.1 Quantifying the spatial sampling of animals

Position data was processed as described in Section 4.6.3. Briefly, position data was smoothed with a 400ms boxcar filter kernel (moving average filter) and tracking errors removed (speed samples greater than 100 cm/s).

Subsequently, the continuous position samples were binned into 2.5cm spatial bins, and the percentage was calculated representing the number of bins visited relative to the total number of spatial bins within the environment.

5.3.5.2 Classification of head direction cells

A single unit from the ADN was included in analysis if it fired more than 100 spikes per recording trial. Cells were classified as HD cells if they surpassed a previously reported threshold mean resultant vector length (RV length > 0.17), which was calculated based on the 95th percentile of RV lengths derived spatially shuffled, age-matched data (Wills et al., 2010).

5.3.5.3 Classification of place cells

Single units recorded in CA1 were included in analysis if they fired more than 75 spikes per recording session (Muessig et al., 2015). Units were characterised as complex spiking putative pyramidal neurons if they met the following criteria: a spike width (peak to trough) >= 0.3ms, having the first moment (mean) of the temporal auto-correlogram <= 25ms (within a 50 ms window), and a mean firing rate <= 5Hz (Csicsvari et al., 1999). A minimum spatial information (described in Section 4.6.5.1) threshold of 0.15 was also applied in order to limit the analysis to those cells which exhibited spatial tuning.

5.3.5.4 Construction of temporal auto-correlograms and quantification of bursting characteristics

Temporal auto-correlograms were generated from the auto-correlation of the spike train (constructed using the MATLAB *xcorr* function), bin size 0.01 seconds with a maximum time lag of 0.5 seconds (ADN HD cells), or bin size 0.00625 seconds with a maximum time lag of 0.125 seconds (hippocampal CA1 place cells).

A burst index was used to quantify the spiking properties of HD cells. Given that the bursting of HD cells is based on the animal's head direction and is therefore non-periodic, a burst index measure previously introduced by Yoder and Taube (2009) was used. Spike trains were binned into 1 second bins, and the burst index was calculated as follows:

Burst index =
$$\frac{(\#bins > 1.75FR) + (\#bins < 0.25FR)}{\#bins_{total}}$$
 (5.1)

where FR is the mean firing rate of the cell. This quantifies the bursting properties of a cell between a value of 0 (indicating a cell with a constant firing rate) and 1 (a 'bursting' cell).

5.3.5.5 Quantitative analysis of cluster isolation and drift

L-ratio and isolation distance measures for cluster isolation were computed as described previously (Schmitzer-Torbert et al., 2005). Briefly, the L-ratio indicates to what extent a cluster may be compromised by noise or other units by measuring the amount of noise within the vicinity of the cluster. The isolation distance (Mahalanobis distance) indicates the separation of the cluster spikes from other spikes on the same tetrode.

The mean absolute error (MAE) of spike waveforms across trials was defined as:

$$MAE = \frac{1}{n} \sum_{j=1}^{n} |y_j - \hat{y}_j|$$
 (5.2)

where each waveform consisted of 50 samples (n = 50), y_j represented the j-th actual (observed) value (i.e. the j-th waveform value (μ V) recorded by the Logger for a given spike), and \hat{y}_j represented the j-th predicted value (i.e. the j-th waveform value (μ V) recorded by DACQ for a given spike). This measure was used as an inference for the level of deviation of Logger-recorded spike waveforms from DACQ-recorded spike waveforms.

Relative cluster offset between cells across consecutive trials was calculated by finding the cluster centroid in both recordings and calculating the Euclidean distance between these clusters in four-dimensional amplitude space. That is, for a cell with centroid (a_1,b_1,c_1,d_1) in one trial and centroid (a_2,b_2,c_2,d_2) in the subsequent trial, the offset of the cluster (d) across trials in amplitude space was calculated as:

$$d = \sqrt{(a_2 - a_1)^2 + (b_2 - b_1)^2 + (c_2 - c_1)^2 + (d_2 - d_1)^2}$$
 (5.3)

5.3.5.6 Quantitative analysis of firing rate correlation with velocity

The correlation of firing rate with AHV and linear velocity was computed only for well sampled velocities (excluding velocity samples exceeding the 95th percentile velocity distribution). After discarding speed samples exceeding this threshold, speed samples were binned into 2.5cm/s bins (linear velocity) and 10°/s bins (AHV). Spike data was temporally binned to find the corresponding firing rate for each speed bin. Pearson's correlation coefficient (*r*) was then computed using Matlab *corr* function. To determine whether the correlation was significant, a two sample t-test was conducted to assess whether the observed correlation coefficient was significantly different from zero (no correlation).

5.4 Results

To validate the wireless system as a feasible technology for studying postnatal development of spatially-tuned neurons, we sought to directly compare the logger with an electrophysiology system currently well established in this lab (Axona Ltd., UK). Behaviour, ADN (14 HD cells) and CA1 (5 place cells) data from both systems was analysed and compared.

5.4.1 Behavioural profile of animals in tethered and wireless recording trials

Overall trends in behaviour with respect to velocity and spatial sampling were compared between systems, to assess whether the Logger notably changes the behavioural profile of the animals compared to tethered recordings.

The median AHV of the pups increased during Logger trials compared to both DACQ-A and DACQ-B trials (Figure 5.4A; 1-way repeated measures ANOVA: F(2,29) = 25.631, p<0.001). This suggests that faster head rotations are enabled with wireless recordings. A reason for this may be that the cable in tethered recordings exerts tension (or torque) on the animal's head which slows rotational head movements, while this is not the case with the Logger. When differences between groups were investigated at different ages (Figure 5.4B), there was no significant main effects of age on AHV overall (2-way mixed ANOVA: F(6,23)=2.136, p=0.088, η_p^2 =0.358), but there was a significant interaction between trial type and age (2-way mixed ANOVA: F(12,46) = 2.987, p=0.004, η_p^2 =0.438) on AHV. Specifically, in DACQ recordings there is more variability in the observed AHV of animals, with AHV decreasing with an increase in age (Figure 5.4B). When the distribution of AHV was compared between recording trials (Figure 5.4C), AHV is skewed towards higher values in Logger trials compared to DACQ trials. Additionally, two separate peaks in the AHV distribution in Logger trials are observable. A likely explanation for this is that one peak corresponds to periods of immobility, while the other corresponds to periods of movement (when animals do turn their heads, they turn faster). It's important to highlight a disparity in the LED distances between the two recording systems. On the neural data logger, LEDs are positioned 2cm apart, whereas on the Axona headstage boom, they are spaced 6cm apart. This difference in LED separation could potentially influence the precision of heading direction measurements. When LEDs are positioned closer together, it's likely that their positions may be less accurately detected due to the limited pixel resolution of the camera. Consequently, this could have an impact on the accuracy of angular velocity estimates and may, to some extent, contribute to the observed variations between the two systems.

The linear velocity of the animal was significantly higher in Logger trials compared to DACQ-B but not DACQ-A trials (Figure 5.4D; 1-way repeated measures ANOVA: F(2,29)=4.349, p=0.0174). An overall decrease in the speed of the animal in the second DACQ trial may be expected due to fatigue from the previous two trials (Figure 5.4D), although this is slightly negated by the fact that there was no significant difference between the first and second DACQ trials. When linear velocity of the animals was separated by age, there was no significant main effect of the recording trial on linear velocity (Figure 5.4E; 2-way mixed ANOVA: F(2,46) = 3.089, p=0.055, η_p^2 =0.118). There was, however, a significant effect of age (2-way mixed ANOVA: F(6,23) = 6.233, p<0.001), as well as an interaction between environment and age (2-way mixed ANOVA: F(12,46) = 2.378, p=0.018) on the linear velocities of animals. At younger ages there is minimal difference in linear velocity of animals between wireless and tethered recordings. There is then a discernible decrease in linear velocity with age in DACQ trials, while the linear velocity of animals remains relatively stable during Logger trials. This disparity increases with age until at P23 and P24 there is a significant difference between recording systems (Tukey's HSD; P24: Logger vs DACQ-B: p=0.003; P25: Logger vs DACQ-B: p=0.012), such that older animals have a higher linear velocity with the Logger. In accordance with these findings, the distribution of speeds across all trials is shown in Figure 5.4F, demonstrating a marginal skewness of the velocity of animals towards higher values in Logger trials and lower values in DACQ-A and DACQ-B trials. This suggests that either the tether most impedes movements of older animals, or a fear of potential predators arises in these animals which makes them afraid of the cable. However, a caveat of this is that typically such an instinct would manifest as thigmotactic behaviour (the animal would seek contact with the walls of the environment as a means to hide from predators). Another, more likely, reason is that the location of the tether with respect to the location of the open field in the lab (Figure 5.3) may also be increasing tension on the animal, thereby limiting the uniform freedom of movement around the environment.

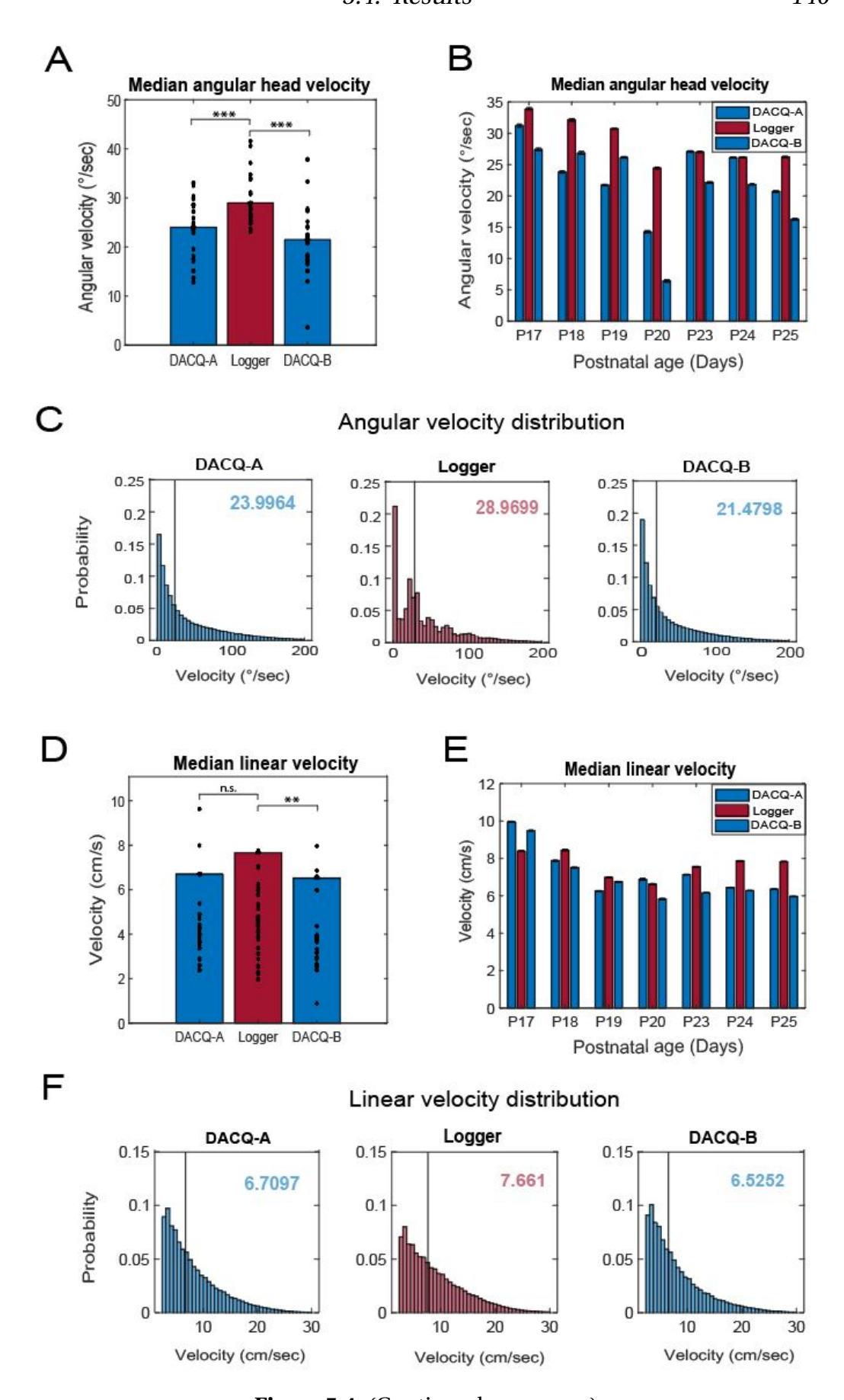


Figure 5.4: (Continued over page.)

Figure 5.4: Rats run significantly faster during logger trials than during DACQ (tethered) trials. (A) Median AHV across all trials (n=36 trials/group). AHV was significantly higher in Logger trials compared to DACQ trials. 1-way repeated measures ANOVA: F(2,29) = 25.631, p<0.001. Paired t-test: DACQ-A vs Logger: p<0.001; DACQ-A vs DACQ-B: p=0.1015; Logger vs DACQ-B: p<0.001. Bar charts show the mean (±SEM). Black dots indicate values for individual trials. (B) Median AHV split by age. There was a significant main effect of the trial type on AHV (2-way mixed ANOVA: F(2,46) = 30.87, p<0.001, η_p^2 =0.573). There was a significant interaction between trial type and age in terms of AHV (2-way mixed ANOVA: F(12,46) = 2.987, p=0.004, $\eta_p^2 = 0.438$). There was no significant main effect of age on AHV overall (2-way mixed ANOVA: F(6,23)=2.136, p=0.088, η_p^2 =0.358). Number of trials per age group: P17: n=6; P18: n=2; P19: n=7; P20: n=3; P23: n=3; P24: n=9; P25: n=5. (C) Angular velocity distributions across all trials (n= 36 trials/group). Vertical lines indicate the median speed (°/s). Logger trials are skewed to higher speeds than in DACQ trials. (D) Median linear velocity across trials (n = 36 trials/group). Linear velocity significantly increases during logger trials compared to DACQ-B trials but not DACQ-A trials. 1-way repeated measures ANOVA: F(2,29)=4.349, p=0.0174. Paired t-test: DACQ-A vs Logger: p=0.18; DACQ-A vs DACQ-B: p=0.12; Logger vs DACQ-B: p=0.0064. Bar charts show the mean (±SEM). Black dots indicate values for individual trials. (E) Median linear velocity split by age. There was no significant main effect of the environment on linear velocity (2-way mixed ANOVA: $F(2,46) = 3.089, p=0.055, \eta_p^2=0.118$). There was a significant interaction between environment and age in terms of linear velocity (2-way mixed ANOVA: F(12,46) = 2.378, p=0.018, $\eta_p^2 = 0.383$). There was a significant main effect of age on linear velocity overall (2-way mixed ANOVA: F(6,23) = 6.233, p<0.001, η_p^2 =0.619). Number of trials per age group: P17: n=6; P18: n=2; P19: n=7; P20: n=3; P23: n=3; P24: n=9; P25: n=5. (F) Linear velocity distributions across all **trials** (n=36 trials/group). Distribution shows velocity samples when the animal is mobile (speed > 2.5cm/sec). Vertical lines indicate the median speed (cm/s). Logger trials are skewed to higher speeds than in DACQ trials.

The animal's spatial sampling of the testing arena between recording systems was then compared (spatial bins were 2.5cm in size). It was found that rats travelled further during Logger trials compared to DACQ-B, but not DACQ-A trials (Figure 5.5A; Friedman test: $\chi^2(2)$ =6.67, p=0.0357; Wilcoxon signed rank: DACQ-A vs Logger: p=0.221; DACQ-A vs DACQ-B: p=0.1254; Logger vs DACQ-B: p=0.023). This aligns with the finding that animals run faster during Logger and DACQ-A trials. However, when position data was split by age there is no significant main effect of the recording system on path length (Figure 5.5B; 2-way mixed ANOVA: F(2,46) = 2.473, p=0.095, η_p^2 = 0.097). There was, however, a significant impact of age on the distance travelled (2-way mixed ANOVA: F(6,23) = 5.121, p=0.002,

 η_p^2 =0.572), wherein pups travelled furthest at the youngest ages (Tukey's HSD: P17-P19: p=0.004, P17-P20: p=0.002, P17-P23: p=0.025, P17-P24: p=0.002, P17-P25: p=0.004). The period of development from P18 onwards coincides with a stark increase in the amount of time an animal spends self-grooming and exhibiting adult-like exploratory behaviours (Thiels et al., 1990), therefore the shortened path length in animals observed from P19 may be a result of increased time spent grooming, rearing, or possibly sniffing.

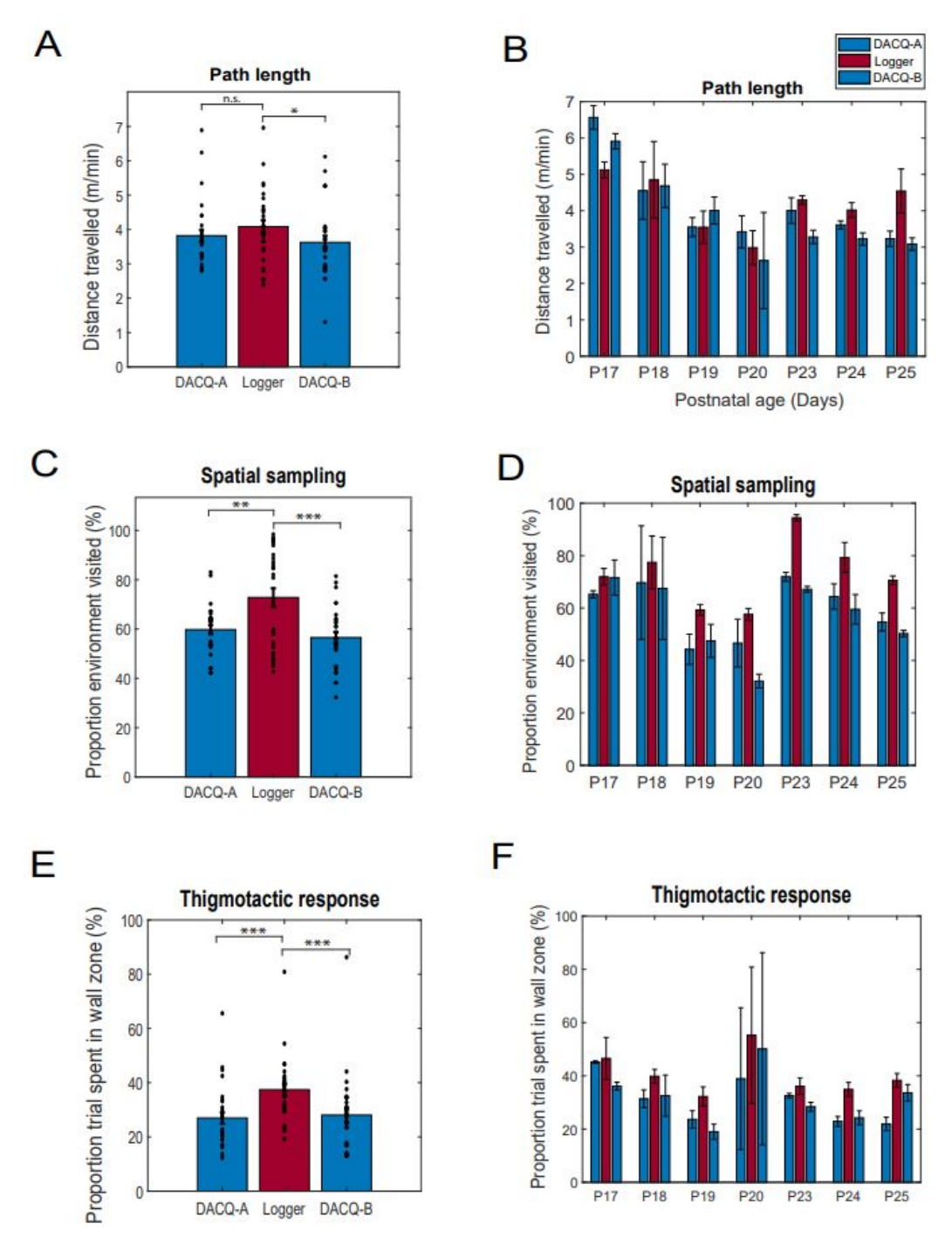


Figure 5.5: (Continued over page.)

Figure 5.5: Spatial sampling is improved in logger trials. (A) Path length (n=36 trials/group). Rats travelled further during logger trials than during DACQ-B trials but not DACQ-A trials. Bar graphs show mean ±SEM. Black dots indicate values for individual trials (n= 36 trials/group), Friedman test: $\chi^2(2)$ =6.67, p=0.0357. Wilcoxon signed rank test: DACQ-A vs Logger: p=0.221; DACQ-A vs DACQ-B: p=0.1254; Logger vs DACQ-B: p=0.023. (B) Path length split by age. There was no significant main effect of the recording system on path length (2-way mixed ANOVA: F(2,46) = 2.473, p=0.095, $\eta_p^2 = 0.097$). There was a significant interaction between trial and age in terms of path length (2-way mixed ANOVA: F(12,,46) = 2.934, p=0.004, η_p^2 = 0.434). There was a significant main effect of age on path length overall (2-way mixed ANOVA: F(6,23) = 5.121, p=0.002, $\eta_p^2 = 0.572$). Number of trials per age group: P17: n=6; P18: n=2; P19: n=7; P20: n=3; P23: n=3; P24: n=9; P25: n=5. **(C) Spatial sampling** (n=36 trials/group). Rats sampled significantly more of the environment during logger trials than DACQ trials (n = 36 trials/group; spatial bins: 2.5x2.5cm). Friedman test: $\chi^2(2) = 9.6$, p=0.0082. Wilcoxon signed rank test: DACQ-A vs Logger: p=0.0019; DACQ-A vs DACQ-B: p=0.2095; Logger vs DACQ-B: p<0.001. (D) Spatial sampling split by age. There was a significant main effect of the recording system on spatial sampling (2-way mixed ANOVA: F(2,46) = 19.655, p<0.001, η_p^2 = 0.461). There was a significant interaction between system and age in terms of spatial sampling (2-way mixed ANOVA: F(12,46) = 7.811, p<0.001, $\eta_p^2 = 0.671$). There was a significant main effect of age on spatial sampling overall (2-way mixed ANOVA: F(6,23) = 4.011, p=0.007, $\eta_p^2 = 0.511$). Spatial bins were 2.5x2.5 cm in size. Number of trials per age group: P17: n=6; P18: n=2; P19: n=7; P20: n=3; P23: n=3; P24: n=9; P25: n=5. **(E) Thigmotactic response** (n=36 trials/group). There was a significant increase in the thigmotactic response of animals during logger trials compared to DACQ trials, χ^2 (2) = 24.47, p<0.001. Wilcoxon signed rank test: DACQ-A vs Logger: p<0.001; DACQ-A vs DACQ-B: p = 0.3932; Logger vs DACQ-B: p < 0.001. (F) Thigmotactic response split by age. There was a significant main effect of the recording trial on observed thigmotactic response (2-way mixed ANOVA: F(2,12) = 14.562, p<0.001, $\eta_p^2 = 0.388$). There was no significant interaction between trial and age in terms of thigmotactic response (2-way mixed ANOVA: F(12,46) = 1.517, p=0.152, $\eta_p^2 = 0.284$). There was no significant main effect of age on the overall thigmotactic response (2-way mixed ANOVA: F(6,23) = 2.098, p=0.093, $\eta_p^2 = 0.354$). Number of trials per age group: P17: n=6; P18: n=2; P19: n=7; P20: n=3; P23: n=3; P24: n=9; P25: n=5.

There was furthermore a significant interaction between acquisition system and age on path length (2-way mixed ANOVA: F(12,46) = 2.934, p=0.004, $\eta_p^2=0.434$), wherein at younger ages the animals tend to travel further in tethered recordings. There is subsequently an increase in the difference of path length observed in wireless compared to tethered recording trials as the animal's age increases (Figure 5.5B). Whilst path length significantly decreases with age in tethered data, this is less apparent during

wireless trials.

Overall, spatial sampling of the environment was improved in wireless recordings. A greater proportion of the environment was visited by the animal during Logger trials compared to both DACQ-A and DACQ-B trials (Figure 5.5C; Friedman test: $\chi^2(2)$ = 9.6, p=0.0082. Wilcoxon signed rank test: DACQ-A vs Logger: p=0.0019; DACQ-A vs DACQ-B: p=0.2095; Logger vs DACQ-B: p<0.001). This is consistent with the finding that the acquisition system has a significant impact on the spatial sampling of animals when split by age (Figure 5.5D; 2-way mixed ANOVA: F(2,46) = 19.655, p<0.001, η_p^2 = 0.461). There was also an effect of age on environment sampling (2-way mixed ANOVA: F(6,23) = 4.011, p=0.007, η_p^2 =0.511), such that there is a large increase in spatial sampling in older animals during Logger trials (from P23). This is reflected in the distance travelled, given that at the oldest recorded ages animals tended to sample the environment to a greater extent in wireless than tethered recording trials (Tukey's HSD; P23: DACQ-A vs Logger: p<0.001, Logger vs DACQ-B: p<0.001; P24: DACQ-A vs Logger: p<0.001, Logger vs DACQ-B: p<0.001; P25: DACQ-A vs Logger p=0.018; Logger vs DACQ-B: p<0.001). A striking finding is that in some cases, the percentage dwell during Logger trials is close to 100%. This may be as a result of the data having been smoothed with a 400ms boxcar filter kernel, before binning the data (described in Section 5.3.5.1). Smoothing before binning can spread data across multiple bins, potentially leading to an inflated estimate of visited bins. Given that the same method was applied for all trials, the relative offset in the amount of the environment which was visited by the animal may still be observed.

Furthermore, the movement trajectories of the animals tended to follow previously reported findings of thigmotaxis-based navigation to optimise safety (Whishaw et al., 2006; Nemati et al., 2013), wherein animals tended to remain close to the walls of the environment (wall zone, see Section 4.6.3.1) compared to the central zone of the environment (Figure

5.5E). Interestingly, animals spent a greater proportion of time near the wall zone of the environment during wireless recordings (Friedman test: $\chi^2(2)=24.47$, p<0.001. Wilcoxon signed rank test: DACQ-A vs Logger: p<0.001; DACQ-A vs DACQ-B: p=0.3932; Logger vs DACQ-B: p <0.001). When investigated as a function of age (Figure 5.5F), there was a significant main effect of recording system on the thigmotactic response (2-way mixed ANOVA: F(2,12) = 14.562, p<0.001, $\eta_p^2 = 0.388$; Tukey's HSD: DACQ-A vs Logger: p<0.001, Logger vs DACQ-B: p=0.003), but no significant effect of age (2-way mixed ANOVA: F(6,23) = 2.098, p=0.093, η_p^2 = 0.354). This is a surprising result considering the animals more extensively sampled the environment during wireless recordings. Nevertheless, although the thigmotactic response is generally considered to be an indication of safetyseeking (Whishaw et al., 2006), in this case it is possible instead to look at the thigmotactic response as a proxy for the freedom of movement of the animal, considering the only difference between trials is the recording device on the animal's head. The increase in time spent close to the wall in wireless recordings may be a consequence of less impeded movement close to environmental borders than in corresponding tethered trials.

For illustration of the behavioural profile of animals during wireless compared to tethered recordings, example data from individual trials at each recorded age are shown in Figure 5.6. Consistent with the findings reported above, spatial sampling of the environment is consistently higher in wireless recordings (Friedman test: $\chi^2(2)$ = 9.6, p=0.0082). Angular head velocity is skewed to higher values in the overall distribution in Logger trials (1-way repeated measures ANOVA: F(2,29) = 25.631, p<0.001), but there is no overall significant effect of the recording system on linear velocity (2-way mixed ANOVA: F(2,46) = 3.089, p=0.055, η_p^2 =0.118). In some cases, such as Figure 5.6D, F and G, there appears to be some level of avoidance of the south-east corner of the environment. This may be due, at least in part, to the positioning of the tether cable with respect to the open field

(Figure 5.3) introducing a level of tension on the cable which impedes the animal's ability to easily explore this section of the environment.

In summary, the results here demonstrate that wireless recordings with the Logger do not impede behaviour of rat pups compared to standard, tethered recordings. Indeed, for some measures presented here (AHV, path length, spatial sampling), the Logger trials had significantly higher values than the corresponding DACQ trials. This suggests that wireless recordings may be conducive to more naturalistic behaviours than tethered recordings, and at the very least may improve the data yield for spatial navigation experiments. Given that the developing rodent's behaviour in entirely naturalistic contexts has not been characterised, further work would need to be conducted to explore this.

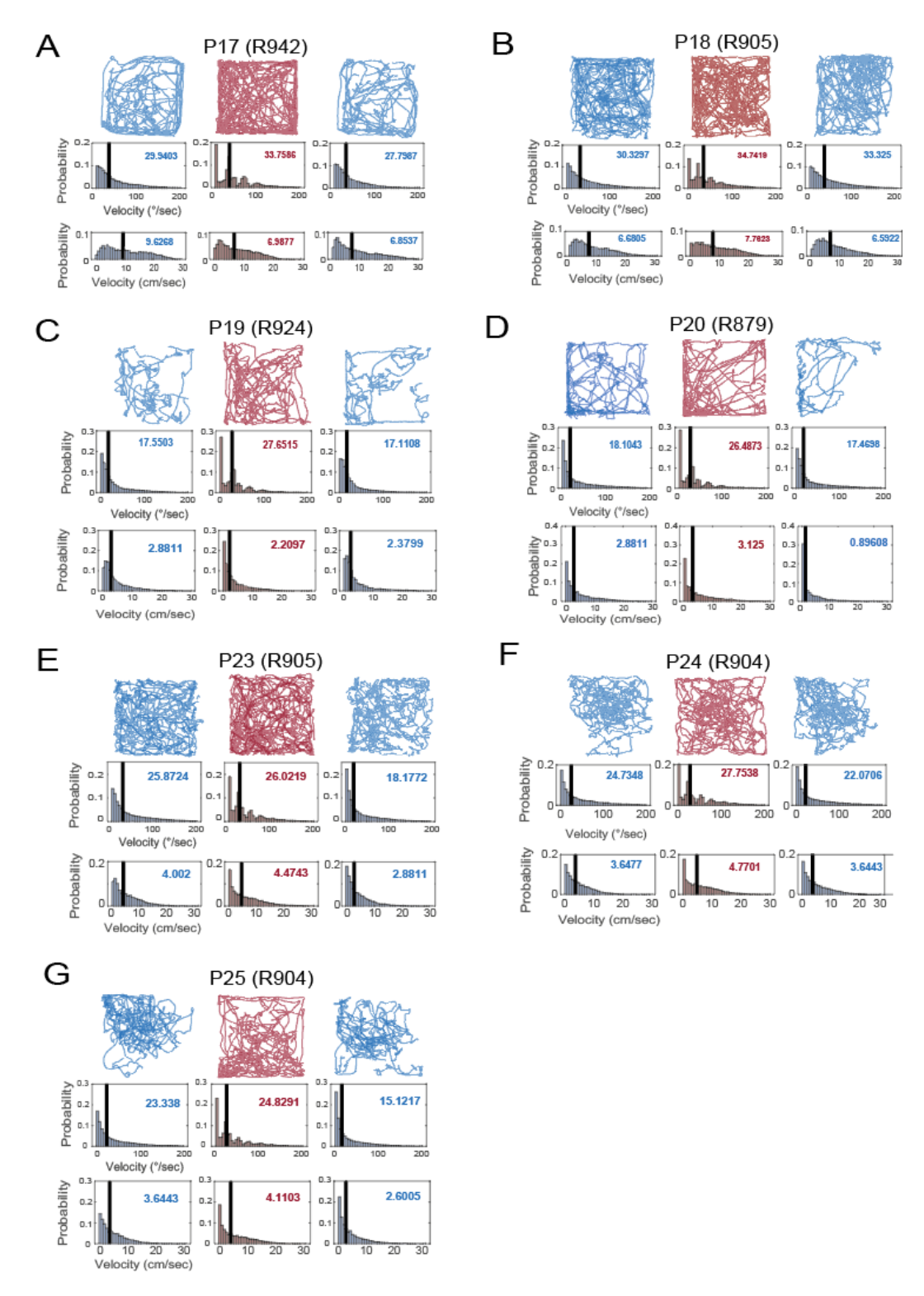
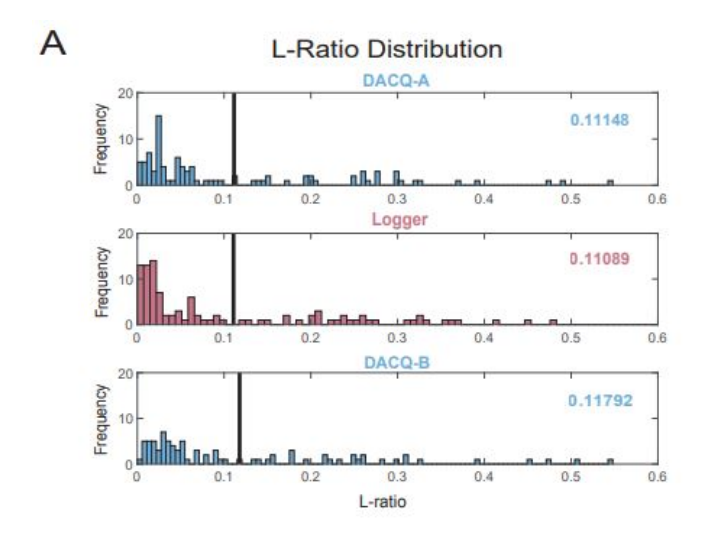


Figure 5.6: Example behavioural data from individual trials across postnatal day (A) P17 to (G) P25 in DACQ-A, Logger, and DACQ-B trials. From left to right: Data from DACQ-A, Logger, and DACQ-B trials are shown, respectively. From top to bottom: Trajectory of the animal during the trial, distribution of angular head velocity, and distribution of linear velocity are shown, respectively. The black vertical line and value shown in the top right corner of each histogram denote the median velocity for that trial.

5.4.2 Comparison of neuronal data from wireless and tethered systems

In tetrode recordings, spikes are simultaneously recorded on four electrodes. The amplitude of the spike on a given electrode will vary depending on its proximity to the neuron, giving rise to a profile of relative waveform shapes which are used to isolate neurons recorded on the same tetrode. By plotting the amplitude of a spike recorded on one electrode versus another electrode, a scatterplot is produced. Clusters of spikes in this feature space may then be isolated, which should correspond to one neuron. Tetrode instability with respect to adjacent brain tissue is a common occurrence which results in changes in waveform amplitude across trials ('drift'). This may occur through extended recording sessions and multiple connections and disconnections of the recording equipment from the head-mounted tetrodes on the animal. DACQ-A vs Logger differences were therefore compared to DACQ-A vs DACQ-B differences to indicate whether the Logger introduced more instability than that expected from the passage of time.

Firstly, the quality of cell cluster isolation and how this compared across systems was assessed using standard cluster isolation metrics: L-ratio and isolation distance (Schmitzer-Torbert et al., 2005). Isolation distance describes the distance in Mahalanobis space between spikes of different cell clusters. These provide an indication of how well separated the spikes in a given cluster are from noise and other spikes on the same tetrode. A small L-ratio and a large isolation distance indicates good cluster isolation (Schmitzer-Torbert et al., 2005). For example, a mean isolation distance of 15 \pm 3, and L-ratio of 0.15 \pm 0.02, has previously been reported in CA1 cells of age-matched animals (Wills et al., 2010). Previous reports of age-matched values for L-ratio and isolation distance measures in the ADN could not be found. A summary of these calculations is presented in Figure 5.7. Although the L-ratio distributions in this report are



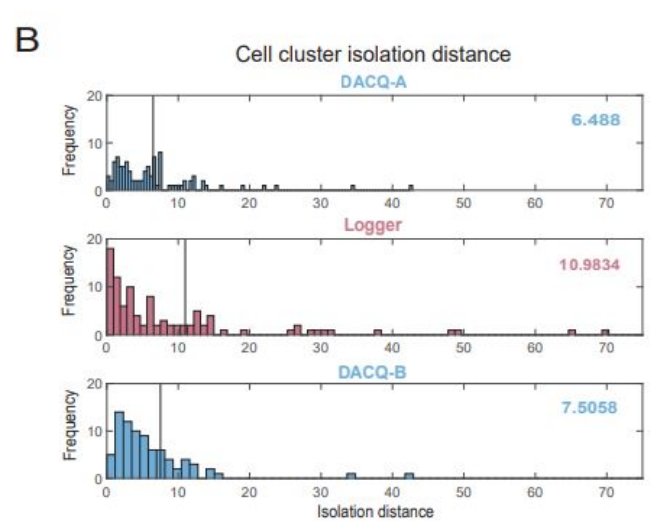


Figure 5.7: Comparison of cluster isolation metrics in extracellular recordings (n= 83 cell clusters/system). Black vertical lines indicate the mean value, which is denoted in the top-right corner of each histogram. **(A) Distribution of L-ratio values for all clusters in recording trials.** Cluster L-ratios were not significantly different in Logger trials than DACQ trials (Friedman test: $\chi^2(2) = 2.48$, p =0.2891. Shapiro-Wilk test for normality: p<0.001). **(B) Isolation distance of all clusters in recording trials.** The isolation distance of recorded cells was not significantly different between recording trials (Friedman test: $\chi^2(2) = 0.68$, p=0.7136. Shapiro-Wilk test for normality: p=0).

lower than previously reported data (Wills et al., 2010), there was no significant difference between groups (Figure 5.7A; Friedman test: $\chi^2(2) = 2.48$, p =0.2891). Cluster isolation distance was also not significantly different between groups (Figure 5.7B; Friedman test: $\chi^2(2) = 0.68$, p=0.7136), indicating similar cluster quality of the data from both acquisition systems.

Neural data from all trials (DACQ-A, Logger, and DACQ-B) was clustered together to identify spikes assuming to belong to the same neuron within an experimental session. Potential differences in the spikes recorded from a putative neuron were then quantitatively assessed on the basis of cluster drift and the offset in spike waveforms. Cluster offset between DACQ and Logger recordings was quantified as the relative offset in amplitude space between trials. This was achieved by computing the Euclidean distance between cluster centroids in DACQ-A vs Logger (DACQ-Logger) and DACQ-A vs DACQ-B (DACQ-DACQ) recording trials. There was an increase in the offset of clusters between the Logger and DACQ trials (Figure 5.8A, DACQ-Logger) compared to the DACQ-A and DACQ-B trials (Figure 5.8A; DACQ-DACQ) which was statistically significant (Wilcoxon signed rank test: p=0.0266). This may be due to minor differences in the hardware between systems introducing some cluster movement between Logger and DACQ recordings.

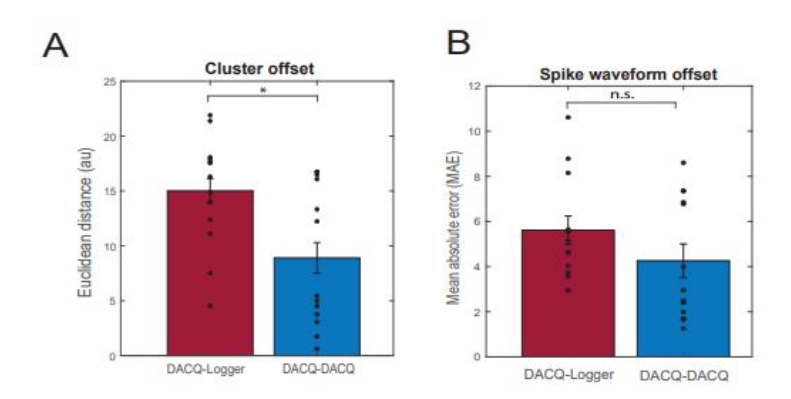


Figure 5.8: Comparison of cluster offset and cell waveform between logger and **DACQ trials** (n= 13 cells/group). Values indicate the mean \pm SEM. (A) Cluster offset. The offset (distance) between respective clusters in DACQ-A vs DACQ-B trials was significantly lower than DACQ vs Logger trials (Wilcoxon signed rank test: p=0.0266. Shapiro-Wilk test for normality: p=0.0317). (B) **Spike waveform offset.** Mean absolute error (MAE) in mean waveform of cells recorded in DACQ-A vs DACQ-B were also lower than DACQ-Logger, although this was not significant (Paired t-test: p=0.3822).

For each cell, similarity of the mean waveform shape on the channel with the highest amplitude was also compared across systems by evaluating the mean absolute error (MAE; Section 5.3.5.5). There was no signif-

icant difference in MAE between Logger-DACQ and DACQ-A vs DACQ-B waveform comparisons (Figure 5.8B; Paired t-test: p=0.3822), indicating that the spike data recorded on the Logger was the same as that recorded with the DACQ system. It is intriguing that quantification of the cluster offset is significantly different between systems, but the MAE of spike waveforms is not. One possible reason for this is that whilst the cluster position for a given cell is quantified by the centroid only (representing the peakto-trough distance for the neuron), the MAE measures the average across the whole spike waveform.

To summarise, the relative quality of extracellularly recorded data from the Logger is comparable to the DACQ (Axona) system when quantified by the L-ratio and isolation distance measures (Schmitzer-Torbert et al., 2005). This indicates there are no discernible differences in the relative separation of clusters between systems or the amount of electronic or mechanical noise pick-up, providing a positive evaluation of the reproducibility of extracellular recording data of the Logger in this study. Nonetheless, there was a statistically significant difference in the offset of clusters belonging to the same neuron in respective Logger trials compared to DACQ trials (Figure 5.8A; Wilcoxon signed rank test: p=0.0266). Minor hardware differences which are not possible to manually rectify may be introducing such discrepancies. Encouragingly, there was no significant difference in the offset of spike waveforms recorded with the Logger system compared to DACQ (Figure 5.8B; Paired t-test: p=0.3822). This indicates that although there is a difference in the relative location of cell clusters in amplitude space between systems, the Logger can reliably reproduce spike waveform data recorded in DACQ. Further comparisons between recording systems were made on the basis of cell type characteristics, including spatial correlate and temporal spiking properties. These will be discussed separately below for HD cells and place cells, respectively.

5.4.3 Head direction cell properties are similar between recording systems

The aim of the present study was to assess the viability of the neural data logger in recording spatially-modulated neurons in developing rat pups. To investigate the capacity of the Logger to record HD cells, tetrode bundles were implanted in the ADN. Presented in Figure 5.9 are representative examples of HD cells which were isolated and recorded using both DACQ and Logger acquisition systems, from the 9 total HD cells which were recorded. The spatial correlates (polar plot of firing rate versus head direction), temporal spiking patterns, cluster position in amplitude space and waveforms of these cells were comparable between systems. The PFDs of these cells and the strength of this preference was consistent across trials (Circular analog of Kruskal-Wallis test: p=0.4277), indicated by the polar plots and Rayleigh vector length (Figure 5.9, top-left panel; Friedman test: $\chi^2(2)=0.32$, p=0.8539). Spike bursting is visible in the corresponding auto-correlograms (Figure 5.9, top-right panel), characteristic of HD cell firing observed in the ADN (Stackman and Taube, 1997). The temporal spiking patterns of these cells were not significantly different between systems, indicated by the measured burst index which was notably high across all recorded cells (Figure 5.10; Yober and Taube, 2009). The burst index quantifies the extent to which a cell either fires in high-frequency bursts (values close to 1), or fires at a constant rate throughout a given trial (values close to zero). The position of the spike cluster in amplitude space (across the four tetrode channels) was similar in both systems (Figure 5.9, bottom panel), although some differences were expected given the finding that cluster offset was significantly different between recording systems. There is furthermore a strong overlap in the mean waveform of these cells on the tetrode channel with the highest spike amplitude (Figure 5.9, topmiddle panel), in agreement with the lack of statistically different offset in spike waveforms discussed above.

Logger **DACQ** 26.7Hz (\hat{\sqrt{1}}) epntildwe -50 **A** R924 0.93 48.1Hz 0.82 ونجو 0 00 8,0 0 40 40 Channel 1 Channel 1 Channel 2 Channel 3 Channel 4 Channel 2 Channel 3 Channel 4 Channel 3 Channel 2 Channel 3 Channel 4 Channel 4 Channel 4 Channel 3 Channel 4 **B** R924 | 13.1Hz 25.6Hz 0.67 amplitude (µV) 40 D'S 0 0; 20 25 40 0 Channel 1 Channel 1 Channel 1 Channel 1 Channel 1 Channel 2 Channel 3 Channel 4 Channel 2 Channel 3 Channel 2 Channel 3 Channel 2 Channel 3 Channel 2 Channel 3 Channel 4 Channel 4 Channel 4 Channel 3 Channel 4 C R904 0.94 22.0Hz منه 40 40 Channel 1 Channel 1 Channel 1 Channel 1 Channel 1 Channel 1 Channel 3 Channel 4 Channel 2 Channel 2 Channel 3 Channel 4 Channel 2 Channel 2 Channel 3 Channel 3 Channel 2 Channel 2 Channel 3 Channel 4 Channel 4 Channel 4 Channel 4 Channel 3

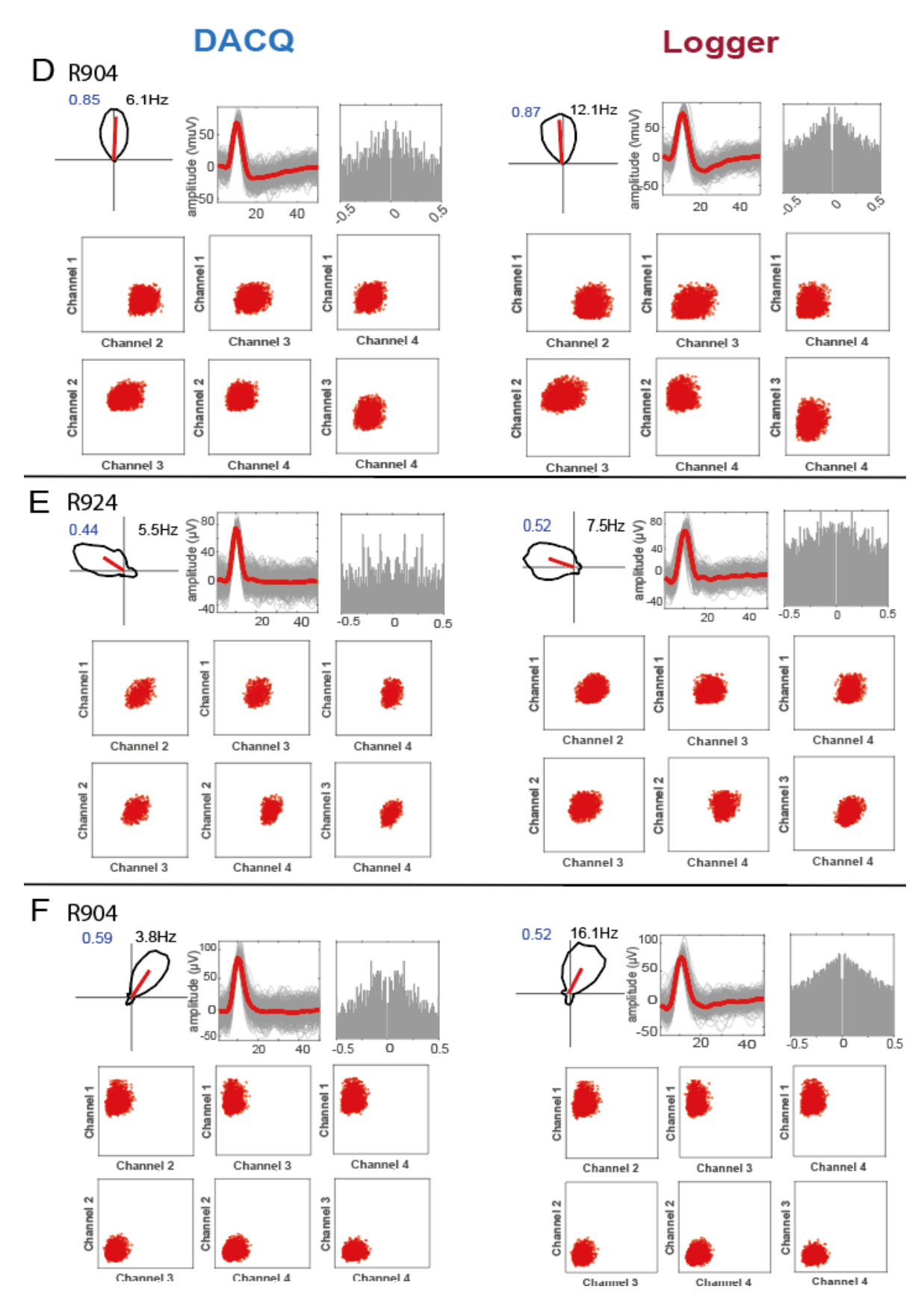


Figure 5.9: (Continued on following page.)

Figure 5.9: Representative HD cells (A-F) recorded from DACQ (left) and the Logger (right) within the same recording session. From left to right: Polar plot of cell firing rate versus head direction. The number in blue indicates the Rayleigh vector length, and the number in black indicates the peak firing rate (Hz); **Neuronal spike waveforms** from the cell on the channel with the highest amplitude. Shown are the mean waveform (red line) and all spike waveforms (shaded grey area); **Temporal autocorrelogram** (500ms time lag, bin size 10ms); **Position of spike clusters in waveform amplitude space** is shown using a 2x3 grid, with 2 tetrode channels (electrodes) represented in each grid. Each dot (red) within a grid denotes the relative spike amplitude between two channels.

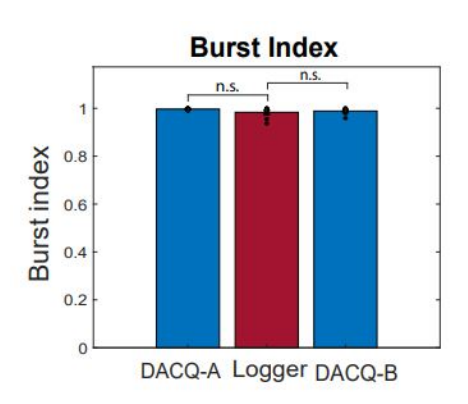


Figure 5.10: Burst index of recorded head direction cells (n = 9 cells/group). Burst index represents the proportion of time a neuron fires in high-frequency bursts during a given trial. The burst index of cells did not significantly differ between trials. Friedman test: $\chi^2(2)=3.31$, p=0.1911. Shapiro-Wilk test for normality: p<0.001.

The modulation of firing by head direction as recorded in the Logger and DACQ systems were compared in a number of ways, including the directional tuning, directional information and stability of recorded HD cells. Directional tuning of a cell is inferred by the length of the mean resultant vector (Rayleigh vector; RV), with a longer RV length indicative of strong unidirectional tuning. Conversely, RV length values close to zero indicate a lack of unidirectional bias of a HD cell. Directional tuning of HD cells recorded with DACQ and the Logger were not significantly different (Figure 5.11A; 1-way repeated measures ANOVA: F(2,20) = 0.527, p=0.5983), and were comparable to previous reports for RV lengths of agematched, ADN HD cells (0.6 \pm 0.05; Bassett et al., 2018). Another measure commonly used to infer the spatial modulation of HD cell signalling is directional information (Skaggs et al., 1993). Directional information is a measure of how well the spiking of a cell predicts the actual heading direction of the animal. There was no significant difference in directional information of HD cells recorded with DACO and the logger (Figure 5.11B;

Friedman test: $\chi^2(2) = 1.27$, p=0.5292). The stability of the spatial correlate (PFD) of HD cells was calculated both within and across trials. Stability is quantified as the Pearson correlation (r) between corresponding directional bins in the firing rate maps of cells. The across-trial stability of cells between DACQ and Logger recordings (Figure 5.11C) was consistent with a previously reported mean stability score for ADN head direction cells recorded at a similar age (0.8 ± 0.05; Tan et al., 2015) and did not significantly differ between groups (Friedman test: $\chi^2(1) = 0.82$, p=0.3657). There was furthermore no significant difference in the within-trial stability of cells in the Logger recordings compared to DACQ trials (Figure 5.11D; Friedman test: $\chi^2(2) = 3.2$, p=0.2019). Additionally, both Logger and DACQ within-trial stability values reported here fall within the range of values reported elsewhere (0.9 ± 0.05; Tan et al., 2015).

HD cells fire maximally at one head direction, termed the PFD (Taube et al., 1990), with background firing rates remaining close to zero when the animal's head is not facing within the range of the PFD. HD cell firing properties were compared to assess the reproducibility between recording systems. Although mean firing rates of recorded cells reported from Logger data were slightly higher (Figure 5.12A; 4.2 ± 1 Hz in the Logger compared to 2 ± 0.5 Hz in DACQ-A trials and 3.4 ± 0.8 Hz in DACQ-B trials), this difference was not statistically significant between systems (Friedman test: $\chi^2(2) = 1.56$, p=0.4594). Peak firing rates of cells also varied depending on the trial, with an increment in peak firing rates between DACQ-A to Logger and DACQ-B trials, respectively (Figure 5.12B). Again, this difference was notable but not statistically significant between Logger and DACQ recordings (1-way repeated measures ANOVA: F(2,10) = 1.732, p=0.2260).

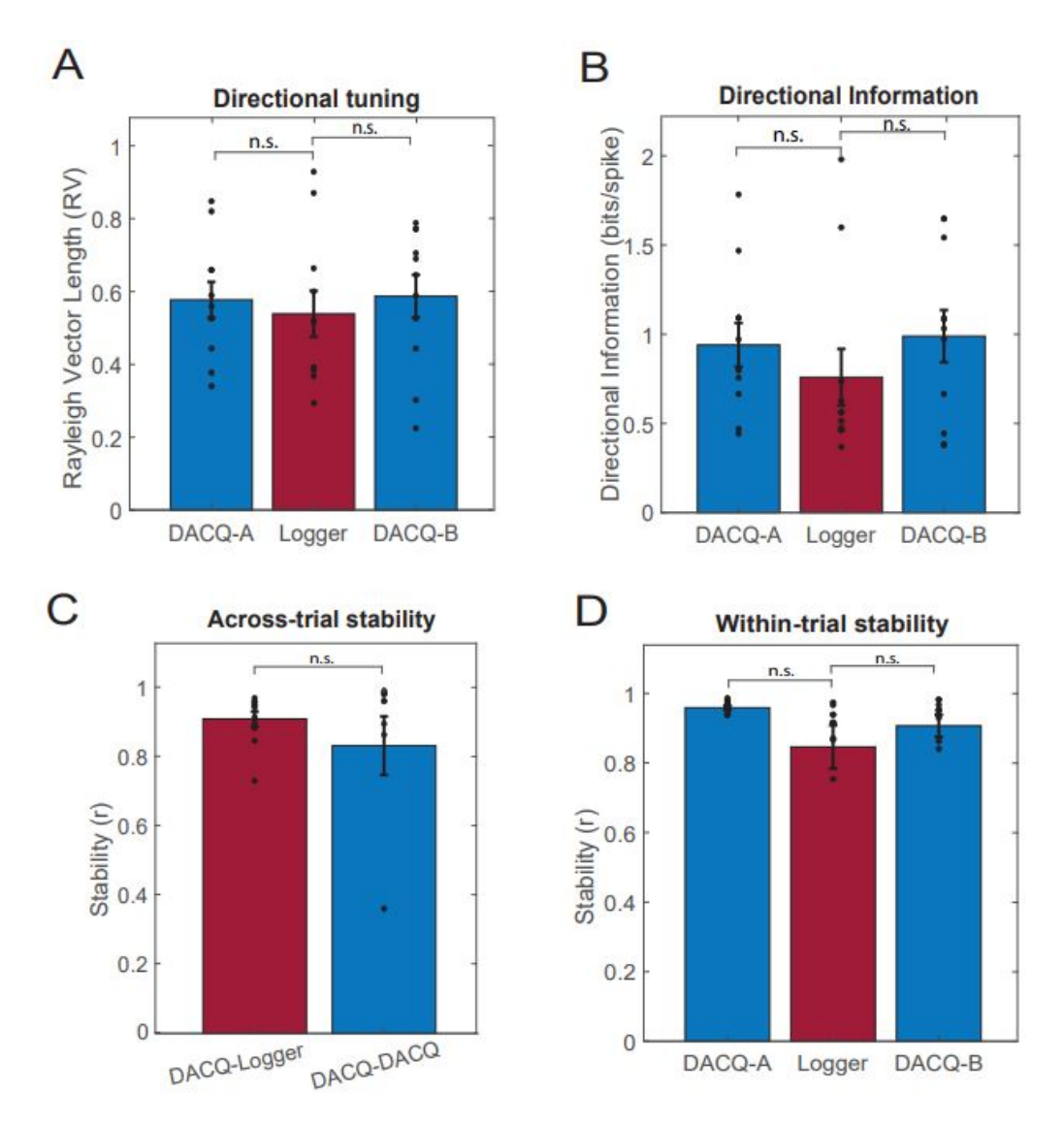


Figure 5.11: Spatial modulation metrics across head direction cell recording trials. Bar charts show the mean (± SEM). Black dots indicate values for individual cells. n = 9 cells/group. (A) Directional tuning. There was no significant difference in the quality of directional tuning of recorded HD cells across trials, measured by the Rayleigh vector (RV) length. 1-way repeated measures ANOVA: F(2,20) = 0.527, p=0.5983. (B) Directional information. There was no significant difference in the quality of directional information encoded by recorded HD cells across trials. Friedman test: $\chi^2(2) = 1.27$, p=0.5292. Shapiro-Wilk test for normality: p= 0.0024. (C) Across-trial stability. Head direction cells are stable across DACQ and Logger trials. DACQ-Logger indicates cell stability between DACQ-A and Logger trials, while DACQ-DACQ indicates cell stability between DACQ-A and DACQ-B trials. Friedman test: $\chi^2(2) = 0.82$, p=0.3657. Shapiro-Wilk test for normality: p<0.001. (D) Within-trial stability. Head direction cells are stable within a trial. There was no significant difference in within-trial stability between DACQ and Logger recordings. Friedman test: $\chi^2(2)=3.2$, p=0.2019. Shapiro-Wilk test for normality: p<0.001.

Given the dependence of vestibular input on HD cell firing (including the relay of the AHV signal), the correlation of firing rate with linear velocity and AHV was measured as described in Section 5.3.5.6. This was done in order to assess how well increases in firing rate were explained by speed. There was a positive correlation of AHV with HD cell firing rate, which was statistically significant (Figure 5.12C; r=0.5775 \pm 0.0512; Two sample t-test: p=0.008), similar to previous reports (Stackman and Taube, 1997). There was no significant difference between recording systems and the correlation of the AHV of the animal with cell firing rate (Friedman test: $\chi^2(2) = 5.17$, p=0.0755).

Conversely, there was no significant correlation between linear velocity and HD cell firing rate (Figure 5.12D; Two-sample t-test: p=0.1654). There was large variability between trials on the correlation of linear velocity with HD cell firing rate ($r=0.3075\pm0.1434$), however overall there was no significant difference between systems (1-way repeated measures ANOVA: F(2,8)=0.223, p=0.8047). The correlation of linear velocity with HD cell firing was most consistent with previous reports (r=0.515; Taube et al., 1995) in the Logger recording (r=0.52682) than in either DACQ-A (r=0.0379) or DACQ-B (r=0.35774) recordings.

In summary, key HD cell firing characteristics were reproduced in Logger recording data and did not significantly differ from DACQ recordings. The PFD of HD cells, their temporal firing properties and the neuronal spike waveforms were replicated across trials. Cell directional tuning, directional information, within-trial stability and across-trial stability were all consistent across recording systems. Larger variability was observed in HD cell mean and peak firing rates between systems, but this was not statistically significant.

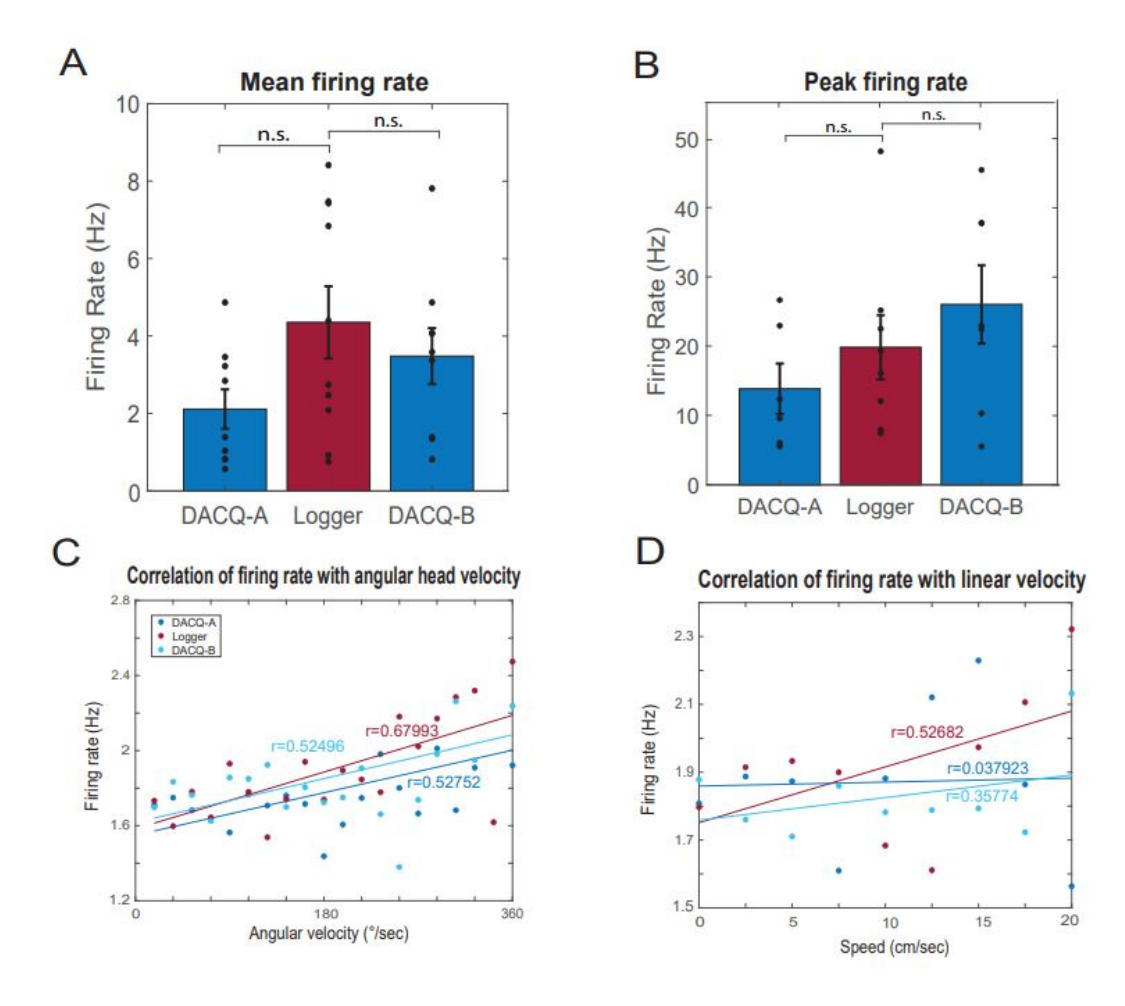


Figure 5.12: Comparison of HD cell firing rates between Logger and DACQ recording trials. Bar charts show the mean (± SEM). Black dots indicate values for individual cells. (A) Mean firing rate (n = 9 cells/group). The mean firing rate of head direction cells was not significantly different in Logger trials compared to DACQ trials. Friedman test: $\chi^2(2) = 1.56$, p=0.4594. Shapiro-Wilk test for normality: p = 0.0056. (B) Peak firing rate (n = 9 cells/group). The maximum firing rate of HD cells did not significantly differ between recording trials. 1-way repeated measures ANOVA: F(2,10) = 1.732, p=0.2260. (C) Correlation of HD cell firing rate with AHV in recording trials (n= 20 trials/group). There was a high correlation (r $= 0.5775 \pm 0.0512$) of HD cell firing rate with AHV, which was statistically significant (Two-sample t-test: p=0.007). There was no significant difference between trials (Friedman test: $\chi^2(2) = 5.17$, p=0.0755). Dots represent binned spike data. (D) Correlation of HD cell firing rate with linear velocity in recording trials (n= 20 trials/group). There was no significant correlation of linear velocity with HD cell firing rate ($r=0.3075 \pm 0.1434$; Two sample t-test: 0.1654). There was no significant difference between trials (1-way repeated measures ANOVA: F(2,8) = 0.223, p=0.8047). Dots represent binned spike data.

5.4.4 Head direction cells are reliably recorded in the homecage environment

The primary aim in piloting the recording of spatially modulated cell types in developing rats using wireless technology was for eventual recording of these cells in the animal's homecage. Therefore, a key aim for this study was to demonstrate that HD cells which may be recorded in a standard open field foraging task may also be recorded in the homecage. Therefore, in one instance in which HD cells in the open field were isolated, an additional Logger trial was conducted in the rat's homecage in the presence of littermates (2 additional pups). As before, DACQ-A and DACQ-B trials were conducted in the open field while the animal foraged alone. The intermediate trial was again conducted with the Logger system, but in this case the homecage was placed on top of the floor of the open field. In this way, HD cells (n=4) were wirelessly recorded while the animal explored a familiar setting and a direct comparison could be made to the activity of the cells in the open field. Cells recorded in the homecage environment were excluded from group comparisons of across-trial stability, within-trial stability and behaviour due to differences in recording environment between the Logger (homecage) and DACQ (standard open-field environment) trials.

Encouragingly, four HD cells recorded during the corresponding DACQ-A trial were replicated in the homecage by the Logger (Figure 5.13). This demonstrates a proof-of-principle that successful wireless recordings may be undertaken whilst the animal explores its homecage in the presence of conspecifics. The spatial correlates (Figure 5.13) remained the same between groups (Circular analog of Kruskal-Wallis test: p=0.4277). Rayleigh vector length was not significantly different between trials (1-way repeated measures ANOVA: F(2,4) = 0.322, p=0.7418), nor was directional information of recorded cells (1-way repeated measures ANOVA: F(2,4) = 1.884, p=0.2652). The temporal spiking patterns, cluster position in am-

plitude space and waveforms of these cells were also replicated (Figure 5.13).

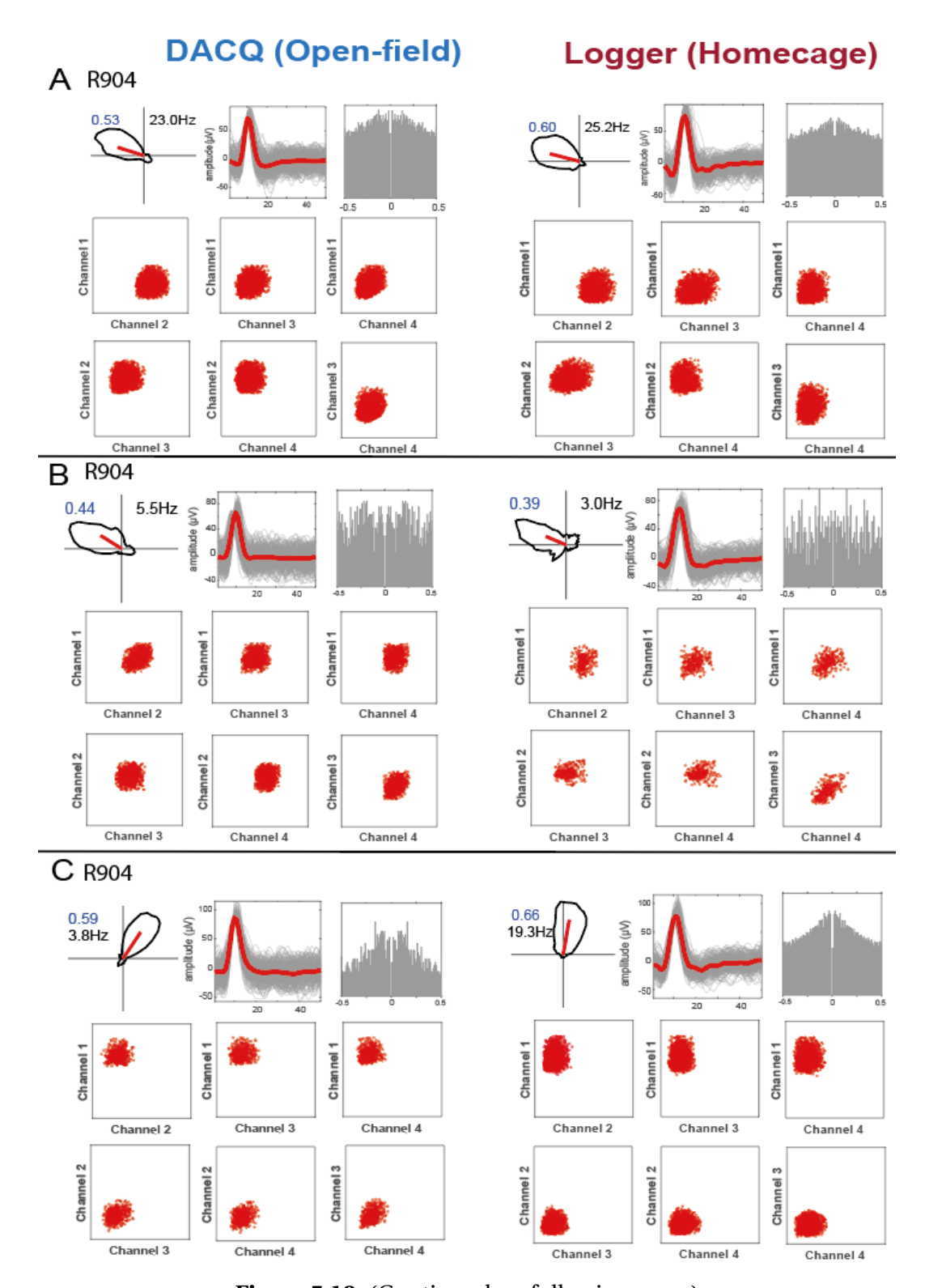


Figure 5.13: (Continued on following page.)

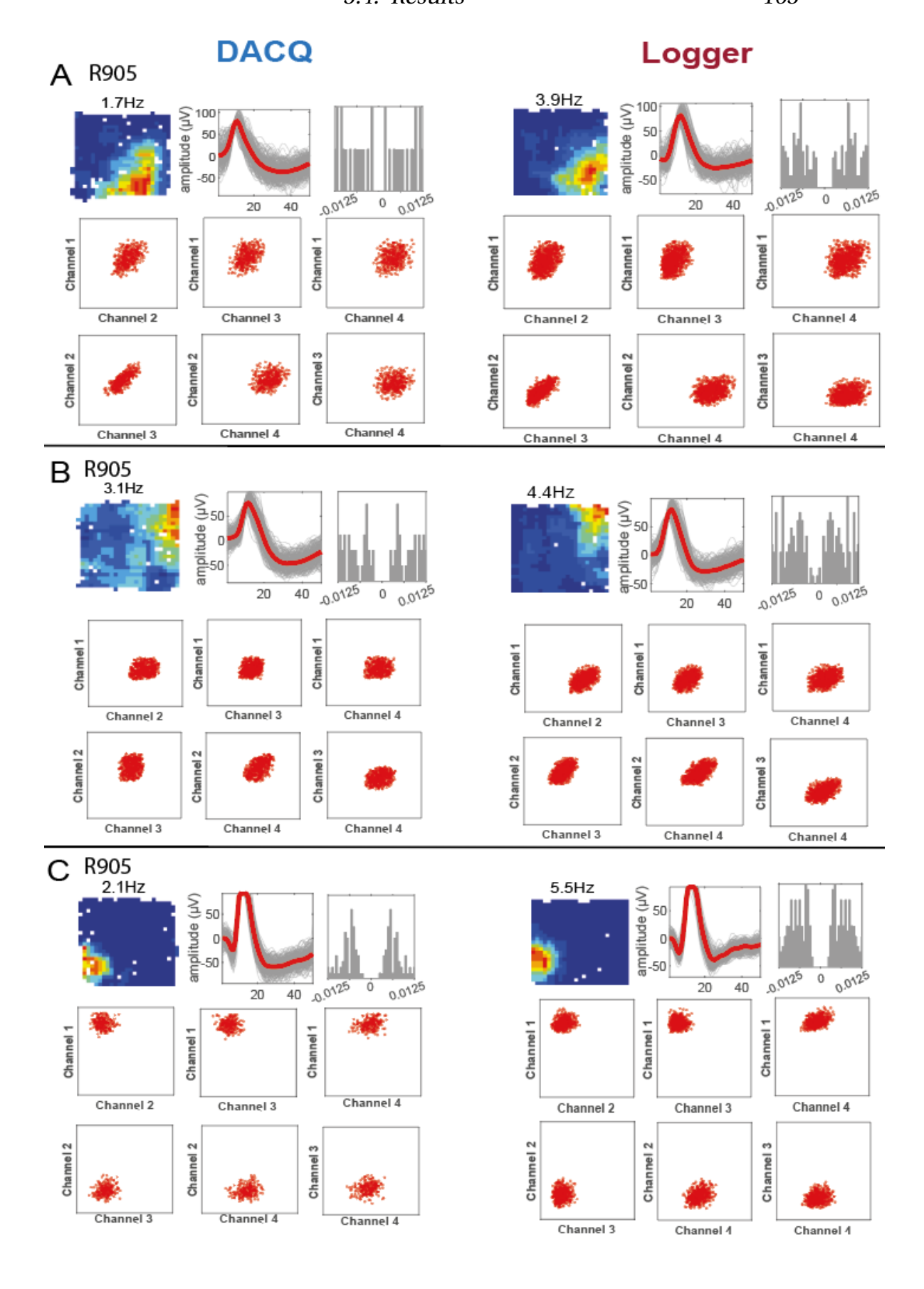
Figure 5.13: Representative HD cells (A-C) recorded in the homecage using the neural data logger (DACQ trials conducted as normal). Generated from data recorded in DACQ (left) and logger (right). From left to right: Polar plot of cell firing rate versus head direction generated from data recorded in DACQ (left) and logger (right). The number in blue indicates the Rayleigh vector length, and the number in black indicates the peak firing rate (Hz); Neuronal spike waveforms from the cell on the channel with the highest amplitude. Shown are the mean waveform (red line) and all spike waveforms (shaded grey area); Temporal autocorrelogram (500ms time lag) from DACQ (left) and logger (right) data; Position of spike clusters in waveform amplitude space is shown using a 2x3 grid, with 2 tetrode channels represented in each grid. Each dot (red) within a grid denotes the relative spike amplitude on two channels within the 4D amplitude space.

5.4.5 Place cell properties are similar between recording systems

Place cells are a well-defined, spatially-modulated hippocampal cell type which exhibit location-specific firing fields (O'Keefe and Dostrovsky, 1971). The activity of place cells in postnatal development has also been extensively documented (Langston et al., 2010; Wills et al., 2010; Muessig et al., 2015; Muessig et al., 2016; Muessig et al., 2019), making it a suitable cell choice for proof-of-concept wireless recordings in developing animals. The next aim of this study was therefore to demonstrate reproducible recording capabilities of place cells in the Logger when compared to standard DACQ recordings in rat pups.

In total, 7 place cells were recorded. Presented in Figure 5.14 are representative spatially-selective putative pyramidal neurons which were recorded in both DACQ and the Logger, at P23 and P24. The spatial correlate (firing rate map), temporal spiking activity and waveform of these cells are similar between the systems: The preferred firing locations (i.e. place field; Figure 5.14, top-left panel) of these cells was consistent across trials. The temporal spiking activity of these cells are also comparable: The characteristic complex-spike bursts (spikes occurring in rapid succession) of pyramidal cells was identified across both trials, indicated in the auto-correlogram by a short peak at 3-5ms followed by an immediate ex-

ponential decay (Figure 5.14, top-right panel; Csicsvari et al., 1999). The position of the spike cluster in amplitude space was similar across trials (Figure 5.14, bottom panel), with some small differences expected as a result of the change in recording system (as in Figure 5.10). There is also a strong overlap in the mean waveform of these cells on the tetrode channel with the highest amplitude (Figure 5.14, top-middle panel), consistent with results shown in Figure 5.8.



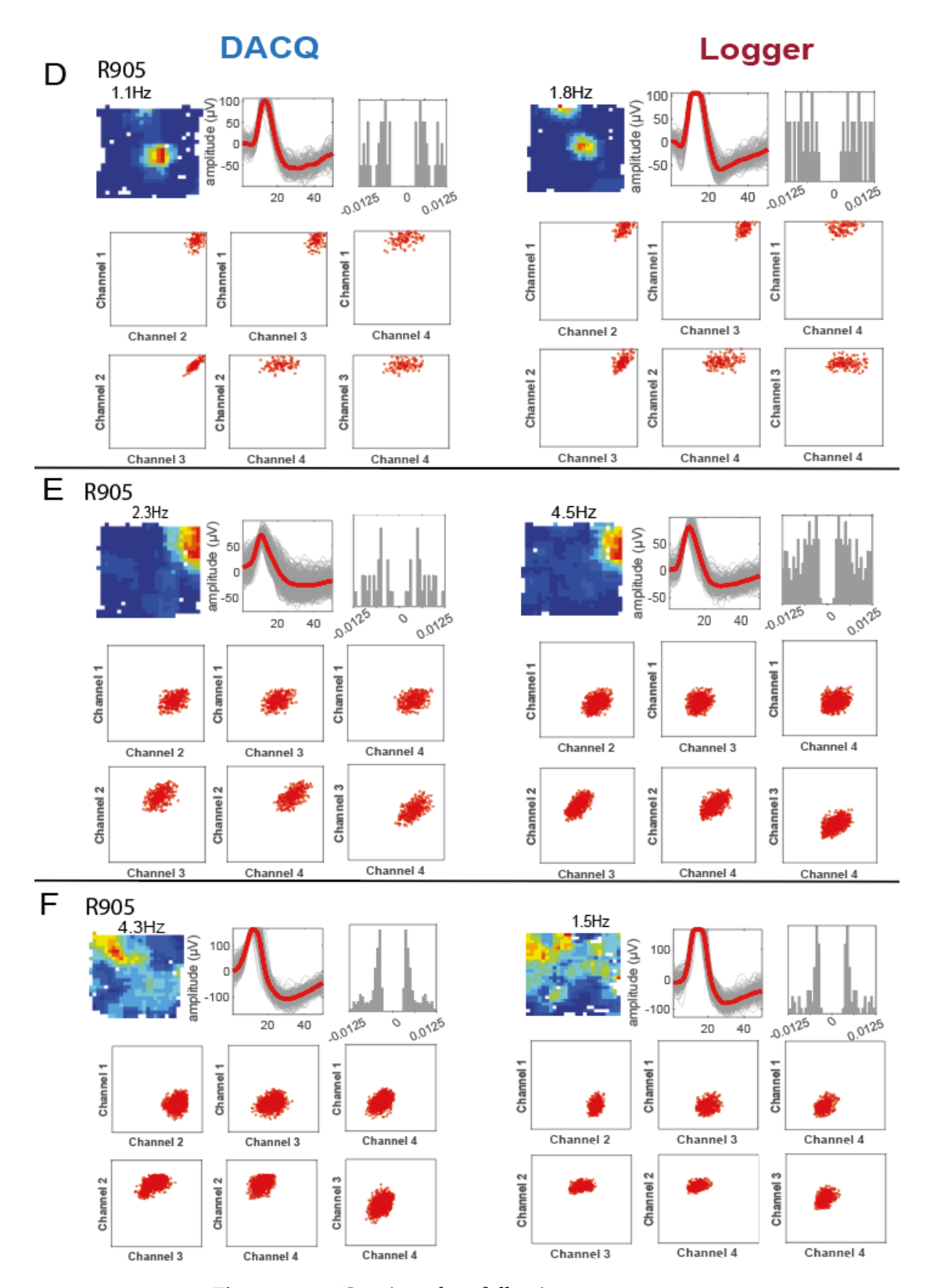


Figure 5.14: (Continued on following page.)

Figure 5.14: Representative place cells (A-F) recorded by DACQ and the logger within the same recording session. Generated from data recorded in DACQ (left) and logger (right). From left to right: False-colour firing rate map showing firing rates in different locations (red = high firing, blue = low firing). Number above the rat map indicates the peak firing rate (Hz); Neuronal spike waveforms from the cell on the channel with the highest amplitude. Shown are the mean waveform (red line) and all spike waveforms (shaded grey area); Temporal autocorrelogram (125ms time lag, bin size 62.5 ms) from DACQ (left) and logger (right) data; Position of spike clusters in waveform amplitude space is shown using a 2x3 grid, with 2 tetrode channels represented in each grid. Each dot (red) within a grid denotes the relative spike amplitude on two channels within the 4D amplitude space.

There was no significant difference in the spatial information of place cells recorded with DACQ and the logger (Figure 5.15A; Friedman test: $\chi^2(2)$ =2.8, p=0.2466). There was some variability in spatial information of recorded cells, but the mean spatial information of all cells fell within previously reported ranges for all recording systems (0.85 ± 0.1, Langston et al., 2010; Wills et al., 2010). Stability of the spatial correlate of cells was calculated both within and across trials. The across-trial stability of cells (Figure 5.15B) was maintained between Logger and DACQ recordings, indicated by the lack of significant difference between groups (Wilcoxon signed rank test: p=0.8413). This was consistent with previous reports in age-matched animals (0.58 ± 0.02; Wills et al., 2010). There was likewise no significant difference in within-trial stability across systems (Figure 5.15C; 1-way repeated measures ANOVA: F(2,10) = 0.015, p=0.9850), the values of which were slightly higher than a previously reported range (0.45 ± 0.8; Langston et al., 2010).

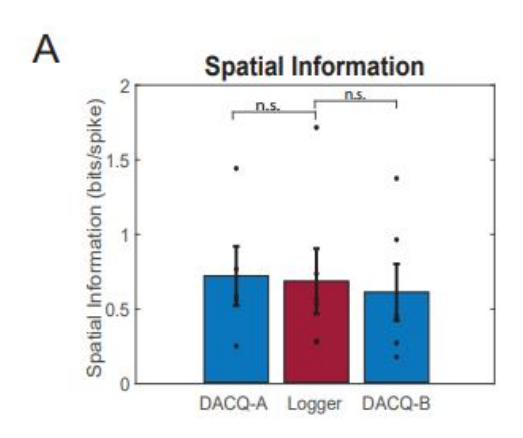
The firing properties of place cells were then investigated to assess the behaviour of cells when recorded with the Logger. The mean firing rate of place cells was comparable between systems (Figure 5.16A; 1-way repeated measures ANOVA: F(2,12)=1.365; p=0.2924), but there was a significant increase in peak firing rates of place cells during Logger trials than during DACQ trials (Figure 5.16B; 1-way repeated measures ANOVA: F(2,10)=11.151; p=0.0028).

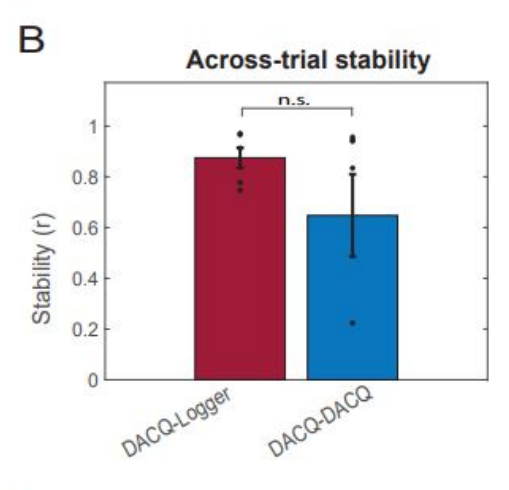
As with HD cells, modulation of cell firing as a function of velocity has

been demonstrated in place cells (McNaughton et al., 1983b). The interaction between firing rate and both AHV and linear velocity was therefore investigated, as outlined in Section 5.3.5.6. Increases in AHV were positively correlated with increases in cell firing (Figure 5.16C; $r=0.7299\pm0.0556$), which was statistically significant (Two sample t-test: p=0.006). There was no significant difference between trials (Friedman test: $\chi^2(2)=0.51$, p=0.7768). There was furthermore a strong correlation of linear velocity with firing rate in place cells (Figure 5.16D; $r=0.7839\pm0.0557$), which was also significant (Two sample t-test: p=0.007). Again, there was no difference observed in the correlation of linear velocity with firing rate between cells in Logger and DACQ trials (Friedman test: $\chi^2(2)=1.29$, p=0.5258). The strong correlation between velocity and firing rate reported here may shed light on the significantly higher peak firing rates observed in Logger trials, given the increased velocity of older animals (within the range of these recordings, P23 and P24) during wireless recordings.

Overall, these results demonstrate a proof-of-concept for the ability of the logger to reliably record place cells in hippocampal area CA1 in the developing rat. Key spatial modulation metrics were replicated between the Logger and DACQ systems, including cell place field, temporal firing and waveform characteristics. Logger data did not differ significantly from DACQ recording data in terms of spatial modulation of the recorded cells, including spatial information and stability. An interesting difference was observed between systems in terms of the peak firing rate, with place cells recorded during wireless trials exhibiting significantly higher rates than in the corresponding tethered trials. Given the strong correlation of velocity with place cell firing, consistent with previous reports (McNaughton et al., 1983b), the trend of animals to travel faster during wireless recordings may be one contributing factor to this occurrence. The data presented here is from just one animal, which was sufficient for demonstrating a proof-of-concept for wirelessly recording place cells in developing animals. More

data would need to be collected to make any further inferences about the activity of place cells during wireless versus tethered recordings, outside the scope of this thesis.





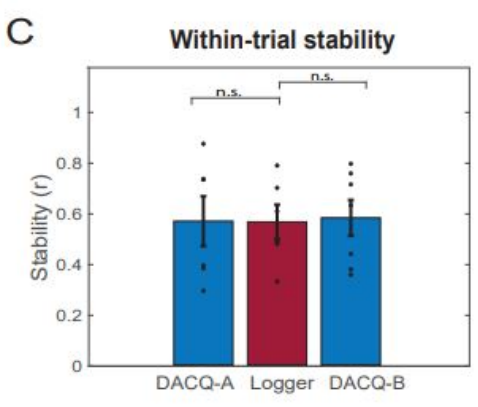


Figure 5.15: Spatial modulation metrics across place cell recording trials (n=7 cells/group). Bar charts show the mean (± SEM). Black dots indicate values for individual cells. (A) Spatial information. There was no significant difference in the quality of spatial information encoded by recorded place cells across trials (Friedman test: $\chi^2(2)=2.8$, p=0.2466). Shapiro-Wilk test for normality: p=0.0275. Across-trial stability. Place cells are stable across DACQ and logger trials. DACQ-Logger indicates cell stability between DACQ-A and Logger trials, while DACQ-DACQ indicates cell stability between DACQ-A and DACQ-B trials. There was no significant difference between groups (Wilcoxon signed rank test: p=0.8413. Shapiro-Wilk test for normality: p<0.001.) (**D**) Within-trial stability. Place cells are stable within a trial. There was no significant difference in within-trial stability between DACQ and Logger recordings. 1-way repeated measures ANOVA: F(2,10) = 0.015, p=0.9850.

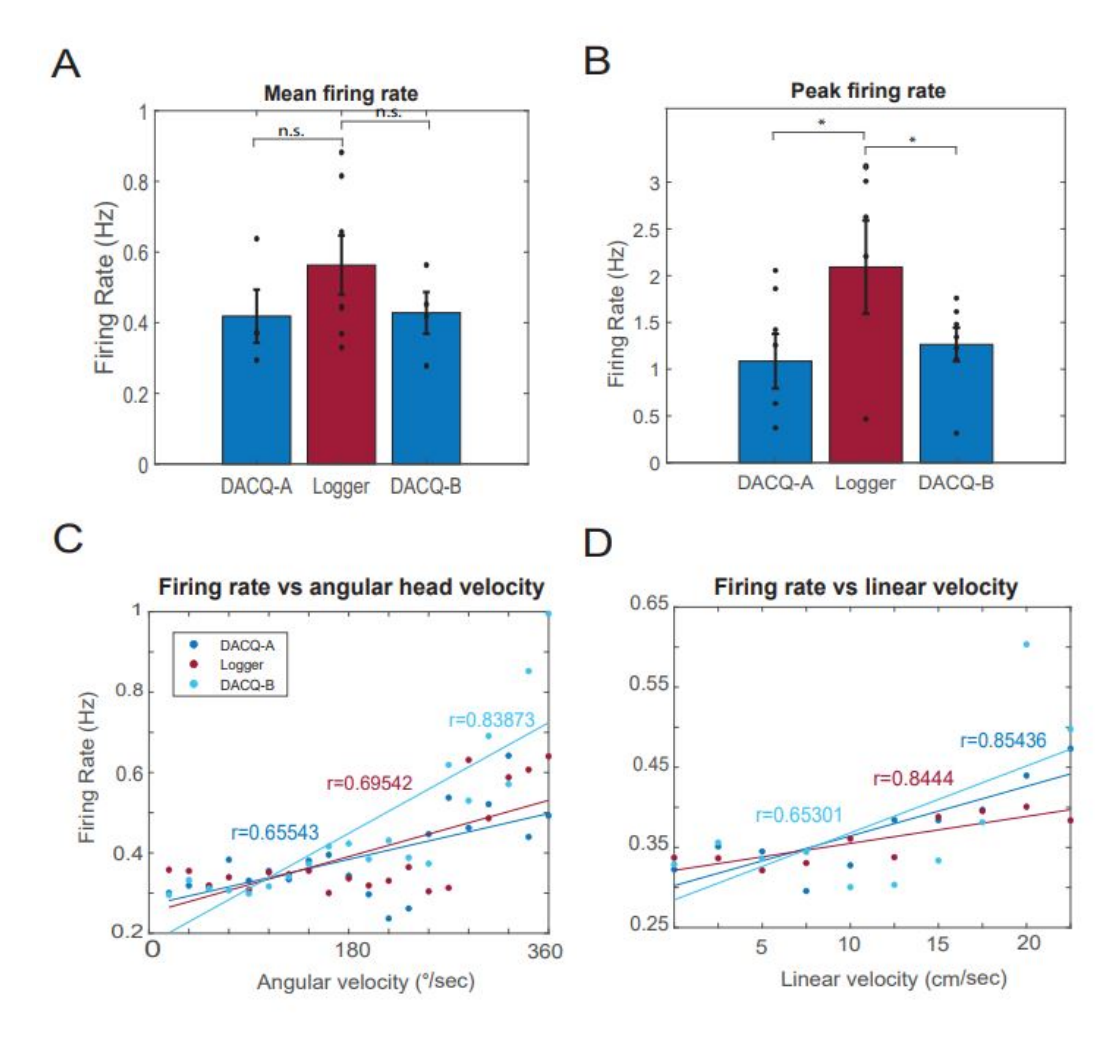


Figure 5.16: Comparison of place cell firing rates between Logger and DACQ recording trials. (A) Mean firing rate (n= 7 cells/group). The mean firing rate of place cells did not significantly differ between Logger trials and DACQ trials. 1-way repeated measures ANOVA: F(2,12)=1.365; p=0.2924. (B) Peak firing rate (n= 7 cells/group). The maximum firing rate of place cells significantly increased in Logger trials compared to DACQ trials. 1-way repeated measures ANOVA: F(2,10)=11.151; p=0.0028. Paired t-test to compare groups: DACQ-A vs Logger: p=0.0159; Logger vs DACQ-B: p=0.0089; DACQ-A vs DACQ-B: p=0.9261. (C) Correlation of place cell firing rate with AHV in recording trials (n = 7 trials/group). There was a significant positive correlation of place cell firing rate with AHV across trials (r = 0.7299 \pm 0.0556; p=0.006). There was no significant difference between groups (Friedman test: $\chi^2(2) = 0.51$, p=0.7768). Dots represent binned spike data. (D) Correlation of place cell firing rate with linear velocity in recording trials (n = 7 trials/group). There was a positive correlation (r=0.7299 ±0.0557) of HD cell firing rate with linear velocity across trials which was significant (Two sample t-test: p=0.007). There was no significant difference between trials (Friedman test: $\chi^2(2) = 1.29$, p=0.5258). Dots represent binned spike data.

5.4.6 Histology

Histology from animal subjects used in this experiment are presented in Figure 5.17. The anatomical localisation of recorded neurons presented in this Chapter were inferred both by the post mortem histological evidence of electrode tracks as well as tetrode-lowering records from experiments. This ensured that the data presented here was collected from the target brain region of interest, which was the pyramidal cell layer of hippocampal CA1 for animal r905 (Figure 5.17B), and the ADN for the remaining animals r904, r924, and r926 (Figure 5.17A, C and D). Note that the electrode tracts pass through the hippocampus in r905, corresponding to electrode movements made subsequent to the recording data presented in this Experiment.

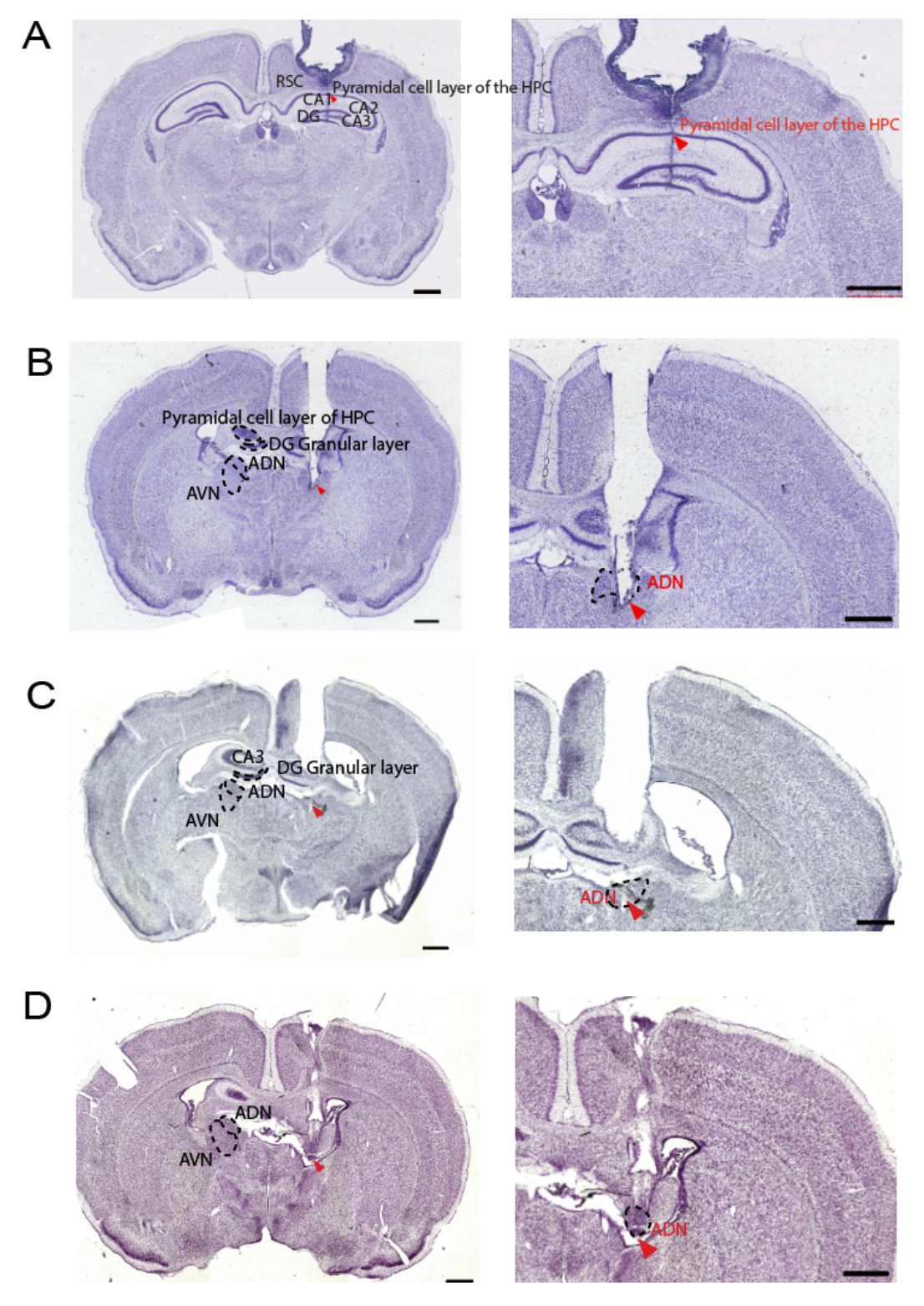


Figure 5.17: Histology of electrophysiology animal subjects. Red arrows point to the target brain region of interest (For animals A and C-D this is the ADN. For animal B, this is the pyramidal cell layer of CA1), where there are discernible electrode penetration marks. Black scale bars represent 1mm. ADN: Anterodorsal thalamic nucleus; AVN: Anteroventral thalamic nucleus; DG: Dentate gyrus; RSC: Retrosplenial cortex.

5.5 Chapter discussion

A proof-of-concept study was conducted in order to validate the use of wireless recordings in young animals. Some key findings were made in terms of animal behaviour during wireless and tethered recordings. Firstly, there was a significant increase in the AHV of Logger trials compared to DACQ trials. There tended to be two peaks in the distribution of AHV during Logger trials, one at very low values and the other peak at high values. This likely corresponds behaviourally to a tendency of the animals to either remain immobile, or rotate their heads at a high velocity. As mentioned in Section 5.4.1, it's worth noting a distinction in the separation between LEDs in the two recording systems. While the neural data logger LEDs are spaced 2cm apart, the LEDs on the Axona headstage boom are spaced 6cm apart. This dissimilarity in LED spacing may potentially influence the precision of heading direction measurements. When LEDs are closer together, it's possible that their positions might be detected with less accuracy due to the camera's limited pixel resolution. This could impact the reliability of angular velocity estimations and may, in part, contribute to the observed variations between the Logger and DACQ trials.

Overall linear velocity tended to be similar between Logger and DACQ-A trials, with a significant difference between these trials and the final DACQ trial. This may be as a consequence of tiredness of the animal or potential habituation to the environment. There was furthermore a significant interaction between recording environment and age on the linear velocity of animals, such that at older ages there was an increase in difference between the linear velocity of animals during wireless recordings compared to tethered recordings. One reason for this disparity in behaviour may possible tension being introduced on the tether on the basis of the equipment positioning within the room, which impedes the animal's ability to easily explore this section of the environment. Differences in the weight of the logger compared to a 32 channel Axona head-

stage (4.5g Logger assembly versus 5.66g Axona headstage) may also have impeded the locomotion of the animal.

In terms of spatial sampling, there were two key findings. Firstly, the path length and spatial sampling of animals tended to be either the same, or significantly improved (particularly with respect to DACQ-B) in wireless recordings. When the thigmotactic response was computed as a function of the amount of time spent by the animal in the wall zone, a surprising finding was that the animals spent more time in the wall zone during Logger recordings. This finding may in some respects infer an anxiety response of animals during wireless trials (Whishaw et al., 2006; Nemati et al., 2013). When taken in concert with a higher proportion of the environment being sampled, one might instead reason that the freedom of movement of the animal is improved in these trials close to environmental boundaries and corners. This is reflected in the trajectory of the animal in individual recording trials, where the proportion of the environment visited during wireless trials is not paralleled in the tethered recordings. Instead, during tethered recordings the animal exhibits less of a thigmotactic response indicative of the animal sampling less in close proximity to environment boundaries. An interpretation of this is that as the animal moves from the environment centre (where there is the least amount of tension on the tether) to the periphery there is an increase in cable tension, making it more difficult for the animal to move. This reflects one of the difficulties posed by tethered recordings, wherein tension placed on the tether during these recordings is difficult to keep stable over the whole environment: If it is correct in the centre of the environment then it will necessarily be taut at the environment edge. By comparison, during Logger trials such tension on the animal's head is absent. Overall, the behavioural data presented here may indicate that more natural behaviours are elicited by animals during logger recordings compared to standard recordings. Since the behavior of developing rodents in entirely naturalistic settings has not been thoroughly examined, a behavioural comparison with unimplanted animals in naturalistic contexts would need to be conducted in order to investigate this further.

Given the subsequent application of the Logger in this thesis for studying very young animals (from P10), a key query from this experiment was whether the Logger produces equal or better behaviour than for tethered recordings at the youngest recorded age. During DACQ recordings, the distribution of both the AHV and linear velocity of the animal tended to decrease with age whilst in the Logger these values tended to remain stable across age. This may reflect a more reliable read-out of animal behaviour using the Logger at younger ages. In terms of spatial sampling, there was a higher level of fluctuation in the path length, spatial sampling and thigmotactic responses of animals, but there was no significant differences at P17. Therefore, one can reasonably conclude from these results that behaviour of young animals (in this experiment the youngest recording age being P17) during wireless recordings trials was comparable, and in some cases (AHV, spatial sampling) improved, compared to tethered recordings.

A major determining factor in the feasibility of wireless recordings for the remainder of this PhD thesis was the reproducibility of neural data logger recordings with respect to a seasoned data acquisition system which is well established in *in vivo* recording labs. Two major spatial cell types were therefore recorded with wireless technology in rat pups, HD cells in the ADN and place cells in hippocampal area CA1. For a given cell recorded across both systems, the Logger replicated several key spatial coding metrics including directional (HD cells) and spatial (place cells) information with no statistically significant difference between recording systems. Cell stability within trials was not significantly different between the systems, and cell stability across trials was similar to previous reports of age-matched data (Tan et al., 2015; Muessig et al., 2015).

Although there was no difference in the mean firing rate of place cells

and HD cells recorded in this study, there was a significant increase in the peak firing rate of place cells in wireless recordings. One reason for this may be the increased velocity profile of this particular animal (r905) in wireless recordings (DACQ-A: 6.04 ± 0.01 cm/s; Logger: 6.77 ± 0.013 cm/s; DACQ-B: 5.3154 ± 0.009 cm/s), given the positive correlation of both linear and AHV with firing rate observed in this study. This correlation is in keeping with modulation of cell firing as a function of linear velocity having previously been reported in place cells (McNaughton et al., 1983b).

Quantitative measures which indicate the quality of extracellular recording data include L-ratio and isolation distance. There was no difference between wireless and tethered recordings in this respect. However, there was a significant difference between recording systems in terms of the relative cluster offset for corresponding neurons between trials. Therefore, data from this study shows that HD cells and place cells can be reliably recorded with the logger but the data is not identical to the Axona system. In practice this has implications only if attempting to corecord cells with both systems, but in every other respect the data was reproducible.

Whilst adult rats are generally amenable to testing in an open field environment, young pups may find these conditions stressful (due to separation from the mother and litter, as well as being placed in an unfamiliar enclosure). It is unclear whether this stress affects the activity of spatially-modulated cells. Wireless recordings offer a promising alternative to standard recordings in this respect. As a rat's homecage is entirely familiar, wireless recordings will permit the study of relatively 'normal' brain activity across a number of developmental ages (in other instances where strict control of local cues and animal behaviour are pertinent to the research question being asked, homecage recordings may be less suitable). A subset experiment was therefore conducted, in which HD direction cells were wirelessly recorded while the animal explored its homecage in the pres-

ence of conspecifics. This recording was flanked once again by tethered recordings in order to directly compare the data, with no significant differences observed between trials. This was an important milestone as it supports the reliability of findings in the subsequent experiment set forth in this thesis (Chapter 6), which investigated the postnatal emergence of HD cell stability in rat pups while they explored their homecage.

It should be noted that the weight of the model of neural data logger used in this study (MouseLog16B, Deuteron Technologies Ltd.) was the most lightweight commercially available logger at the time that this experiment was conducted. However, its suitability for animals less than P14 or P15 was debatable given the component weight and therefore recordings on younger animals were not conducted. A newer model was released subsequent to this which was smaller, more lightweight, and had additional specifications to improve the quality of recorded data (MouseLog16C, Deuteron Technologies Ltd.). Adjustments made to the recording pipeline which differ from those of this Experiment will be described in Chapter 6.

Chapter 6

Investigating the postnatal stabilisation of head direction cells in a naturalistic environment

6.1 Background and rationale

Head direction cells are a particularly interesting component of the neural representation of space. A rudimentary head direction signal is present before eye-opening in rats (Tan et al., 2015; Bjerknes et al., 2015), which then rapidly stabilises to adult-like firing within 24 hours of eye-opening around P16 (Wills et al., 2010; Langston et al., 2010). The period between which HD cells have first been identified (P11-P12) and when they demonstrate adult-like firing properties subsequent to eye-opening offers a unique window of opportunity for experimenters to investigate whether there are critical periods of plasticity in the HD cell network which precedes the integration of visual inputs.

During this period of development, rats tend to remain in the huddle and do not spontaneously explore their environment until after eyeopening (Gerrish and Alberts, 1996). Therefore, the finding that HD cells are present before this period of spatial experience in rats suggests that to some extent an animal's sense of direction is innate. Visual landmarks are known to exert strong control over the HD cells' PFD (Goodridge and Taube, 1995). However, the presence of HD cells before eye-opening (Tan et al., 2015; Bassett et al., 2018) in combination with findings that lesions to the vestibular system abolish directional firing in ADN HD cells (Stackman and Taube, 1997) and that stable HD cells are reported in blind animals (Asumbisa et al., 2022) demonstrate that vestibular and other nonvisual inputs guide the organisation of HD cell circuit assembly. HD cells are not stable at P12 over long periods of time (even in a small box), but do show attractor coupling. This appears to disprove previous models where a stable input trains the HD cell network to create a ring attractor (as they predict the attractor emerges simultaneously with HD cell tuning; Stringer et al., 2002; Hahnloser, 2003; Stratton et al., 2010). One counter-argument is that stable HD cells are indeed present earlier, simultaneously with attractor tuning, if animals are recorded in naturalistic environments. The reason for this is that the stimuli that would normally anchor HD cells at this age may only be present in the animal's nest environment, not in the open field. This is what this experiment aims to deduce.

6.1.1 Prior work

Several studies have shed light on the underlying dynamics of HD cells in the postnatal period, which are of particular relevance to this thesis. The main findings from Tan and colleagues (Tan et al., 2015) are that HD cells are present in the ADN and PoS from as early as P12 in rat pups, before the onset of exploration. Although at P12 there is a significant population of cells that show more than chance directional tuning, the specificity and stability of tuning are hugely reduced compared to adults. At this stage of postnatal development, eye opening has not yet occurred and pups display limited mobility. Across the experimental recording period P12 to P20 in this study, there was an increase in the directional tuning of cells with a rapid increase coinciding with the day of eye-opening, as well as the stability of cells within trials and across successive trials. Notably, visual

landmarks were able to establish significant control over recorded HD cell PFDs on the first day following eye-opening. A subset of cells responded to the presence of the visual cue on the day of eye-opening but this was not significant, suggesting that a period of time is necessary subsequent to eye-opening for the integration of visual information into the HD circuit at the population level. This makes sense when considering that the process of eye-opening in pups occurs gradually over the period of about 24 hours (Gandhi et al., 2005). A similar study was conducted in the PoS and MEC, which found that cells can also be found as early as P11-P12 in these areas (Bjerknes et al., 2015). The authors calculated the circular correlations between pairs of co-recorded cells and found that although the PFD of HD cells before eye-opening are prone to drift, the ensemble of HD cells tended to drift coherently in line with an attractor network.

Bassett and colleagues (2018) probed further the attractor dynamics of HD cells before eye-opening. They found that co-recorded ensembles of HD cells are temporally and spatially coupled on short timescales (10 seconds) even when no stable HD correlates are visible. The attractor structure is preserved when these cells drift. The finding that cell pair couplings exist at P12 (when the HD correlate is never stable) supports the notion that the intrinsic network structure of HD cell activity is present before the network is able to be calibrated with reference to visual input. This suggests that the self-organisation of HD cell attractor dynamics is not learned according to the Stringer and Hahnloser computational models described in Section 3.4.1.1 (Stringer et al., 2002; Hahnloser, 2003).

Another intriguing finding was that HD cells could become adult-like at P13 when the animal was placed in a small box (20cm x 20cm; Bassett et al., 2018), suggesting that the HD cells became anchored to the local, geometric cues (specifically corners) in the immediate environment. The finding that HD cells remain coupled in the standard box condition (dimensions 62.5 cm x 62.5 cm) even when their PFD drifts is also consistent

with self-organisation of the attractor: that is, the attractor could be learnt under conditions where it is stable (such as in the small box), but then come 'unanchored' from the external world in the larger box.

Bayesian decoding analysis performed by the authors suggest that the divergence of HD cell stability between the small box and standard box is due to an under-signalling of AHV in the standard box condition (Bassett et al., 2018). This under-signalling was not mitigated by the integration of alternative sensory cues such as the environmental boundaries (unlike in the small box where the incidence of boundary encounters is much higher). This study suggests that corners in particular may be useful for minimising path integration errors in young animals. Subsequent to eye-opening, ADN HD cells recorded in the small box and standard box have equal directional tuning and cell firing is comparatively stable (Bassett et al., 2018).

In summary, the current understanding of HD cell network activity in developing rats is that a rudimentary directional signal is present before eye-opening and precedes the onset of active exploration. Furthermore, despite marked instability of cells both within and between recording trials before eye-opening, HD cell ensembles drift in a coherent manner consistent with attractor network dynamics. This suggests that an integration of self-motion information is sufficient to provide instantaneous directional heading information. The stability of the directional signal, with respect to the external world, is dependent on access to geometric inputs, with environmental corners being particularly important for accurate signalling of angular velocity. The presence of attractor connectivity before stable HD cell firing occurring in any environment contradicts previous computational studies investigating the self-organisation of attractor dynamics (Stringer et al., 2002; Hahnloser, 2003). In these models, stable HD cell firing instead emerges simultaneously with attractor connectivity. The homecage is a sensible environment to test whether the above observation (attractor network connectivity without a stable HD cell signal) holds in different environmental contexts.

6.1.2 Experimental aim

Few studies have attempted to reconcile our current understanding of HD cell firing in pre eye-opening rats with what occurs in complex, or more naturalistic, environments than a standard laboratory open-field. This raises the possibility that studies of spatially-modulated cell types in developing rats are vulnerable to perturbations in both the rearing and immediate experimental conditions of the animal. There is therefore uncertainty concerning whether the manifestation of HD cell activity in early development is dependent on the context within which the animal is situated. In other words, does HD cell attractor network connectivity truly arise before stable directional firing or is this a symptom of the environment the animal is recorded in.

The experimental aim was therefore to investigate whether HD cells are stable in a familiar, naturalistic environment from the same age that attractor network connectivity is observed (P12; Bassett et al., 2018) and before HD cells are adult-like in typical recording environments (P16; Tan et al., 2015; Bassett et al., 2018). The hypothesis is that HD cells will show increased stability in a familiar, cue-rich environment than when recordings are made in a cue-deprived laboratory environment.

To investigate this, HD cells in the ADN were wirelessly recorded while the rat remained in the homecage with its littermates. Each homecage trial was followed by an open field arena trial in a conventional electrophysiology laboratory to make an empirical comparison of cell activity in a controlled versus naturalistic environment. Familiarity and cue complexity (regarding the presence of the mother and littermates) are the key distinguishing factors between the homecage and standard open-field recordings. In other words, although a standard lab cage may be considered less naturalistic compared to a simulation of rearing conditions in the wild, the

presence of the mother and littermates mean that the most important and salient cues of the animal's rearing environment are in place.

6.2 Methods

6.2.1 Animal subjects

The litter for this experiment was housed in a separate, secondary animal unit to the rest of the colony due to space requirements for electrophysiology recording equipment. The cage was moved from the primary animal unit to the experimental animal unit 1 week before surgeries to permit thorough habituation of the room. The cage was placed on a table beneath the neural data logger recording equipment (Figure 6.2). A makeshift enclosure was made to surround the cage, with cardboard walls around the outside to reduce maternal stress. The cage remained in this room until the end of the experiment, at which point the cage was moved back into the primary animal unit. Animals were kept on a 12:12 hour dark:light cycle. All animals used in this experiment are summarised in Table 6.1.

6.2.2 Surgery

All surgeries were performed as described in Section 4.3. All animals implanted for this experiment were implanted between P9 to P11 (summarised in Table 6.1). Tetrode bundles were aimed at the stereotaxic coordinates for the ADN corresponding to this developmental age range. The coordinates were 1.72mm posterior to bregma, 1.17 mm lateral to the midline, and 4.2mm ventral from bregma.

6.2.3 Neural data logger assembly

The MouseLog16C (Deuteron Technologies Ltd., Israel; Figure 6.1A) was implemented in this experiment, which is a more lightweight neural data logger than the legacy MouseLog16B implemented in Chapter 5. The total weight of the neural data logger with attached antenna, mounted battery and protective housing was 3.5g. As with the MouseLog16B, it has capacity

Rat ID	Age at time of surgery (Postnatal day)	Sex	Analysis	Number recorded cells	•
r982	P10	M	Electrophysiology, behaviour	2	P14
r983	P11	M	Electrophysiology, behaviour	3	P15, P16
r988	P10	F	Electrophysiology, behaviour	17	P12, P13, P14, P15
r989	P10	M	Electrophysiology, behaviour	82	P15, P16
r990	P11	M	Electrophysiology, behaviour	4	P16
r998	P11	M	Electrophysiology, behaviour	5	P14, P15
r1005	P10	M	Electrophysiology, behaviour	25	P13, P14, P15
r1006	P10	M	Behaviour	n/a	P13, P14
r1045	P9	M	Electrophysiology, behaviour	19	P12, P13, P15, P16
r1046	P10	M	Behaviour	n/a	P15, P16
r1062	P9	M	Electrophysiology, behaviour	14	P13, P14, P15, P16
r1096	P9	M	Electrophysiology, behaviour	10	P12, P13, P14, P15
r1108	P9	M	Electrophysiology, behaviour	6	P12, P13, P16
r1115	P9	M	Behaviour	n/a	P14
r1116	P10	M	Behaviour	n/a	P12, P13
r1125	P10	M	Behaviour	n/a	P12, P13
r1126	P10	F	Electrophysiology, behaviour	2	P14
r1127	P11	M	Behaviour	n/a	P14, P15
r1129	P10	F	Behaviour	n/a	P12, P13

Table 6.1: Summary of experimental subjects for Chapter 6 experiments Animals for which no HD cells were recorded have been excluded from neural data analysis but included in behavioural analysis. All other animals are included in both analyses, and the corresponding histology is shown in Section 6.3.5.

for 16 channels which are each sampled at 31.25 kHz. The MouseLog16C comes equipped with a plug-in battery module which consists of a printed

circuit board and small lithium-polymer battery (60 mAh). As the in-built LEDs of the logger were not visible from the range of view of the overhead camera, a green LED and red LED were mounted on the battery by the experimenter which enabled automated movement tracking in Bonsai (Figure 6.1C). A 3D-printed case was designed to fit the dimensions of the MouseLog16C assembly, with a slot-on back cover which removed the need for screws and nuts to hold the 3D case in place over the logger assembly (Figure 6.1B and C). This improvement to the protective housing, combined with the lack of battery wires and connectors, significantly reduced the overall weight on the animal's head compared to the legacy MouseLog16B neural data logger.

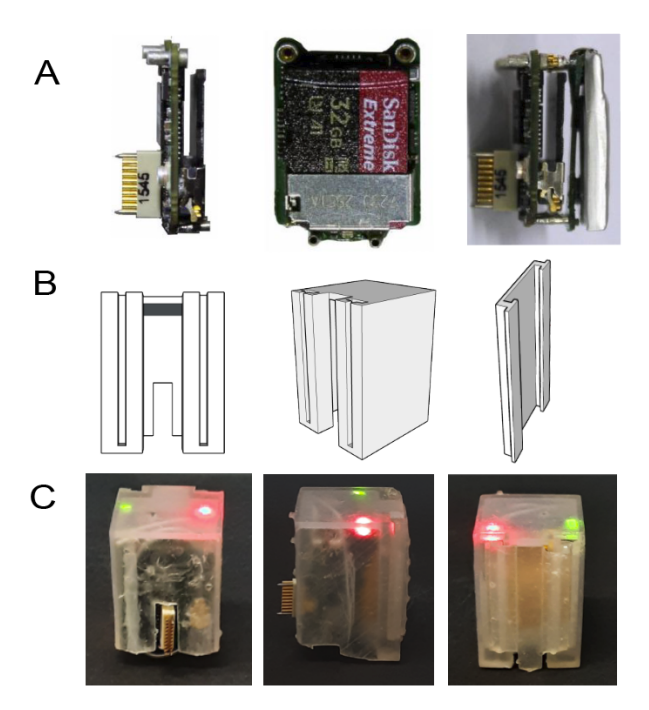


Figure 6.1: Wireless neural data logger Deuteron MouseLog-16C (Deuteron Technologies Ltd., Israel). (A) Animals are plugged into the logger and neural data is stored on a micro-SD memory card. An antenna is attached (not shown) which allows for communication with a host computer. The dimensions of the printed circuit board are 18x13mm. **(B)** 3D-printed case for protective housing of the logger. Clear resin is used to permit visibility of LEDs for tracking. Shown here are the back view, side view and lid, respectively. **(C)** Neural data logger assembly used in recordings. Green and red LEDs are mounted on the logger PCB such that they are visible through the transparent case from above and behind, which are then used for animal tracking.

6.2.4 Single-unit recording

Prior to recording, rat pups were screened in a cage directly adjacent to their homecage, which had a layer of bedding on the floor to replicate the homecage (Figure 6.2A). Screening was conducted using the Axona tethered data acquisition system. If the presence of single-unit activity was confirmed, then the experimental procedure began. Recording equipment was placed on a trolley for mobility (Figure 6.2B). This included equipment necessary for the neural data logger (PC, transceiver, Arduino UNO, cables for connection to the camera) as well as Axona DACQ (PC, pre-amplifier, system unit). Single-unit recordings were conducted as described in Chapter 4, following the behavioural paradigm described below (Section 6.2.4.1).

The reason DACQ recordings were used only for screening purposes and not for experimental recordings was firstly to reduce recording time. Secondly, according to the results presented in Chapter 5, DACQ and Logger data is not identical for various reasons (including cluster movements and rate changes), and so is not ideal for direct comparisons of cell activity. Therefore, it would not be an effective use of recording time, which is limited due to the young age of the pups.

The developing rat typically prefers to stay huddled together until it initiates active exploration around postnatal day 15 (P15; Gerrish and Alberts, 1996). To ensure meaningful results regarding the encoding of heading direction, it was essential to have a substantial amount of data from all heading directions. Consequently, to promote consistent and thorough data collection in the environment, the experimenter initiated each trial recording by dispersing the huddled pups and placing them pseudorandomly around the cage. This action encouraged the pups to explore the homecage.

If the implanted pup, equipped with the attached neural data logger, remained immobile for more than two minutes, the experimenter relocated it to another spot within the cage. This relocation served a dual purpose: by prompting a change in the animal's orientation, there was an increase in both the sampling of different directional bins and the length of the directional path during the trial.

Events when the pup was touched were logged by the experimenter on the neural data logger command programme (LoggerCommand3, Deuteron Technologies, Israel). In doing so, an event string was logged on the Logger so that those position samples, and therefore spike data, were ignored in downstream analysis. This was made possible with string logging fields in the Logger interface on the PC, which allow for variable inputs to be used to log occurrences of certain behaviours. When the button is pressed, a log of the event with a timestamp and in both the eventlog on the SD card of the Logger and on the local log on the host computer.

Additionally, apart from the experimenter's interventions, the mother rat displayed a tendency to reorganise the pups into a 'huddle' configuration within the cage. She would move the pups to different locations approximately two to three times during each trial. Her method involved picking up each pup in turn (by the scruff) and relocating them within the cage. Following this, the pups would either naturally return to a huddle arrangement or explore away from the point where the mother had placed them. Video recordings of the animals were obtained for each trial which may be used in future to quantify the passive movements made by the dam and the littermates outlined here, using tools such as DeepLab-Cut (Mathis et al., 2018; Lauer et al., 2022). DeepLabCut, a markerless pose estimation toolbox which utilises deep learning, has the potential to allow non-invasive tracking of multiple animals, and their behaviours, simultaneously. However, this work lies outside of the scope of this thesis.

6.2.4.1 Behavioural paradigm

In order to provide a direct comparison between data recorded in the homecage and in conditions matching those in previous studies (Tan et al., 2015; Bassett et al., 2018), the following protocol was employed: Rat pups (Cohort 1) were recorded in the homecage (Homecage-A; mother and littermates present), followed by a standard open-field recording (Open-Field; laboratory). The behavioural protocol is illustrated in Figure 6.3A. Homecage recordings occurred in the independent animal unit where the animals were housed (Figure 6.2A), and open-field recordings were conducted in an electrophysiology-dedicated laboratory (Figure 6.2C). The pup was transported alone from one room to the other inside a carrier box (Stanley; box dimensions 32 x 18.8 x 13.2cm). The trolley housing the recording equipment (Figure 6.2B) was also moved from the animal unit to the electrophysiology laboratory while the pup remained in the carrier box. The equipment was then set-up in preparation for the following trial (preparation time approximately 5 minutes). The inter-trial interval was 15 minutes total, during which time the pup was kept in the transfer box and remained plugged into the neural data logger.

Proximal cues in the homecage were available to the pup in the form of the dam, littermates, and bedding during homecage trials. Cage enrichment such as tunnels, tissue paper and wooden blocks were removed for homecage recordings so as not to constrain the animal's movements. A salient distal visual cue was present in the form of a white cue-card to the west of the homecage. Dimensions of the recording environments were 42 x 32 x 21cm. The homecage was made of transparent acrylic plastic (Techniplast). All homecage recordings were conducted with a transparent acrylic plastic panel (Cut My Plastic, UK; length 68 cm, width 50 cm, thickness 2mm) placed over the homecage to prevent the dam from jumping out of the cage. The open-field environment was placed in the laboratory, in a context replicating that in previous studies (i.e. on a raised platform in the middle of a black-curtained arena, with a distal visual cue available in the form of a white cue card; Figure 6.2C). The only difference in this experiment to previous studies (for instance, Bassett et al.,

2018) was that the open-field environment was custom made to be the same dimensions as the homecage, in order to avoid the environment size being a potential confound. The open-field environment was constructed with medium-density fibreboard painted with mauve-coloured, vinyl matt paint (Leyland Trade, UK) and assembled with superglue (Gorilla Glue, USA).

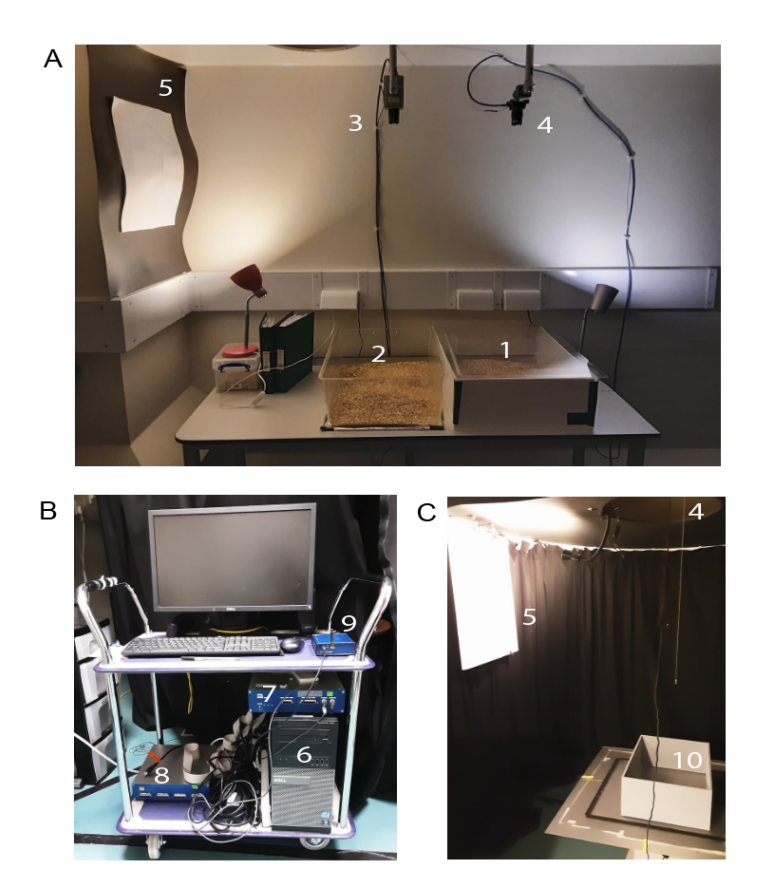


Figure 6.2: Experimental set-up for homecage experiments and the corresponding open field laboratory recordings. (A) Animal unit arrangement. The litter homecage was moved from the main animal unit which housed the entire rodent colony to a separate animal unit. The homecage was placed on a bench with an opaque screen around the outside to reduce exposure of the animals. The litter remained in this separate unit from the week preceding surgeries to the end of the experimental period. Above the homecage was the camera set-up for logger recordings. Adjacent to the homecage was another cage which was used for pre-experimental screening for single-unit activity. Screening was conducted using the DACQ data acquisition system (camera overhead, Axona Ltd., UK). A white cue card was placed to the west of the homecage which acted as a distal visual cue after eye-opening in pups (median age P15). (B) A mobile recording set-up was established for recordings in both the animal unit and laboratory. A trolley housed the host computer, Axona set-up (system unit and preamplifier, from which the headstage tether was attached) and logger set-up (transceiver and Arduino). (C) During experiments, an open field trial was conducted in the laboratory in accordance with traditional developmental studies of head direction cells. In this case a walled enclosure of the same dimensions of the homecage was used. As in the animal unit, a distal visual cue was erected to the west of the recording environment. Key: 1: Homecage recording environment; 2: Screening cage; 3: Recording camera for animal tracking during screening trials (using the Axona system); 4: Recording camera for animal tracking during homecage trials; 5: Polarising distal visual cue; 6: PC on mobile recording set-up; 7: Axona system unit for screening trials; 8: Axona pre-amplifier for screening trials; 9:Transceiver for neural data logger; 10: Open-field recording arena (laboratory).

6.2.4.2 Second behavioural paradigm: Introduction of small box

An extended behavioural paradigm was introduced in a subset of animals (Cohort 2). This protocol was the same as for Cohort 1 (described above), with two additional trials (Figure 6.3B): a return-to-baseline trial in the homecage (Homecage-B; mother and littermates present), and a subsequent small box trial (Small Box; mother and littermates present).

Homecage-B was used as a control to ensure that any changes observed between Homecage-A and Open Field were not caused by tetrode drift or plasticity. The introduction of Homecage-B also served as an additional check that the cells return to their previous state upon return of the pup to the homecage (i.e. the cells don't permanently alter their activity by exposure to the Open Field).

The Small Box trial was conducted in order to provide a direct comparison with the reported findings that from P13 HD cells may be stabilised in a small environment (Bassett et al., 2018). Small Box trials involved the placing of a transparent, rectangular box of smaller dimensions to the Homecage and Open Field environments which was placed into the pup's homecage. The dimensions of the Small Box environment were length 31.5cm, width 20.5 cm, height 27 cm, and the material was transparent polypropylene plastic (Really Useful Products Ltd., UK). The choice of Small Box dimension was motivated by the similarity in size to the small box environment employed in the Bassett et al., 2018 study (20cm x 20cm) but maintaining the same rectangular shape (i.e. aspect ratio) as the Homecage and Open Field environments in this paradigm. In this way, the only variable being changed is the size. Bedding was present at the bottom of this box, and the trial was conducted with the dam and littermates also being placed in the box.

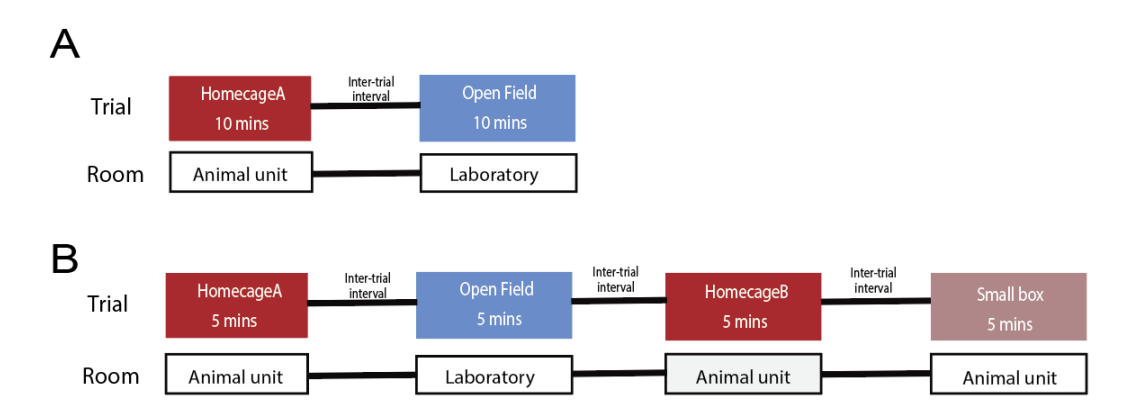


Figure 6.3: Behavioural paradigm for investigation of the postnatal development of head direction cells in a naturalistic environment. (A) An initial trial was conducted in the animal's homecage in the animal unit in the presence of its mother and littermates (Homecage-A; 5 minute trial duration). During a 15 minute inter-trial interval the animal is transported via a carrier box from the homecage in the animal unit to the laboratory for the open field trial (Open Field; 5 minute trial duration). (B) An extended protocol was implemented in a subset of animals (Cohort 2), which involved the pup being transported back to the animal unit, where a subsequent homecage trial is conducted (Homecage-B; 5 minutes) and a Small Box trial (Small Box; 5 minutes).

6.2.5 Classification of head direction cells

Cells were classified as HD cells if they surpassed the 95th percentile threshold Rayleigh vector (RV) length for spatially shuffled data (1000 shuffles) from the same cell for each trial. Within-cell shuffling is an effective way of ensuring that any HD cell correlates observed are not artefactual. This was performed as follows: Shuffled data was computed by shifting the cell's spike times relative to position by a random amount (ranging between 20 seconds after trial onset and 20 seconds before trial end; Wills et al., 2010). In this way, both the temporal structure of the cell's spike train as well as the positional data is preserved but are offset from each other. The HD cell directional map for the shuffled data was computed, and the RV length was computed.

Given that a confounding factor of the within-cell shuffling method is that for cells with high firing rates (such as fast-spiking interneurons), the shuffled threshold is very low and so any small deviation from perfect uniformity will result in cells being classified as HD cells. Given that we only want to assess cells with clear directional tuning, a secondary minimum threshold for RV length of 0.15 was implemented to ensure only cells with spatial tuning were included.

To ensure a single unit from the ADN was included in analysis only if it fired more than 75 spikes per recording trial, a minimum mean firing rate threshold of 0.25 Hz was defined. This served to mitigate false-positive classification of head direction cells due to artefact spatial-tuning from under sampling. Additionally, cells were only classified if the animal had rotated its head fully more than 10 times in the corresponding trial, to ensure all directional bins were well sampled. To maintain equivalence between cohorts, cells were classified as a HD cell in all trials if they met the above conditions in at least one of the Homecage-A, or Open Field trials (not Homecage-B or Small Box trials).

6.2.6 Analysis of directional and spatial sampling

During recordings, periods during which the LEDs on the animal were occluded for more than 1 second were ignored. Periods during which the experimenter moved the animal, denoted by logged string events on the logger, were also removed from the analysis.

Directional path length (number of full head turns) was calculated as the cumulative sum of absolute angular movements, computed as the sum of the absolute difference between the unwrapped radian phase angles of the trial.

Cumulative directional sampling was used as a measure of the bias of the animal for either CW or CCW head turns. This was computed as the difference between the first and last element of the vector of unwrapped radian phase angles of the trial.

Uniformity of directional sampling in trials was inferred by the mean resultant vector (RV) length of all momentary directional heading samples for a given trial, wherein a high RV length indicated a non-uniformity of directional sampling of the animal. The Kullback-Leibler divergence of all

momentary directional heading samples for a given trial was calculated as an additional measure for the uniformity of head direction sampling. This measured the divergence of the actual directional sampling of the animal from a fully uniform distribution of directional sampling (where all heading directions are sampled equally). This was calculated by the following equation:

$$KL(P||Q) = \operatorname{sum of} x \operatorname{in} P(x) * log(P(x)/Q(x))$$
(6.1)

Where P is a vector of probabilities representing the distribution of actual heading direction of the animal, and Q is a vector of probabilities representing a uniform distribution of heading direction.

6.2.7 Analysis of epochs between passive movement

Epochs of active movement of the animal were extracted as follows: During the experiment, immediately before the experimenter moved the pup (passive movement epoch), an event string was manually input and sent to the logger to log a timestamp of the beginning of the event. Once the pup had been passively moved, another event string was sent to the logger to log a timestamp of the end of the event. At the time of data analysis, the timestamps for all periods of passive movement by the experimenter were extracted. Epochs of active movement of the animal were classified as periods of time between these passive movement events, when the experimenter had not touched the pup. Within-epoch stability was calculated as the Pearson's correlation (r) of directional rate map in the first half of the epoch compared to the second half of the epoch. Across-epoch stability was calculated as the Pearson's correlation (r) of directional rate map in a given epoch compared to the subsequent epoch, ignoring the period of passive movement between these two periods of active movement. Within-epoch directional information and within-epoch directional tuning (the mean RV length) were computed as described in Section 4.6.5.2.

6.2.8 Random resampling of active movement epochs in open field trials

In order to control for the disparity in active movement epoch durations between Open Field trials and Homecage trials, Open Field data was resampled at random, with a distribution of resampled epoch durations that matched the distribution of actual epoch durations in the Homecage. Probability distributions were fit to the data of epoch duration from Homecage trials at each recorded age (P12 to P16). The following probability distributions were fit to the data: normal distribution, Weibull distribution, logistic distribution, kernel distribution, and gamma distribution. The probability density function and log likelihood was then computed for each distribution. The distribution which most closely modelled the sample data was chosen on the basis of the highest log-likelihood. The mean and standard deviation of the chosen sample was then calculated and 200 samples were generated using a random number generator using these distribution parameters. n samples were then randomly selected from this array of generated epoch durations, where n was the median number of epochs for the corresponding age bin in Homecage trials. Epochs were included in analysis if they passed the following criteria: minimum of one complete head turn, minimum duration of 30 seconds, and a minimum mean firing rate of 0.25 Hz.

6.2.9 Quantification of temporal and spatial coupling of cell pairs on short-timescales

Temporal cross-correlograms were generated from the cross-correlation of the spike train (constructed using the MATLAB *xcorr* function), bin size 0.2 seconds with a maximum time lag of 0.5 seconds. The raw temporal cross-correlograms were normalised by the mean of a spike-shuffled population of cell pair cross-correlograms (100 shuffles per cell pair) in order to compare the temporal cross-correlograms of all cell pairs. Temporally-

shuffled data was computed by shifting the cell's spike times relative to the other cell's spike times by a random amount (ranging between 20 seconds after trial onset and 20 seconds before trial end; Bassett et al., 2018). Cell pairs were analysed only if they met the criteria for HD cell classification in both Open Field and Homecage trials.

Time-windowed spatial cross-correlograms (TWCs) were computed with respect to head direction as follows. Spike times of one neuron was used as a 'reference' to define an array of 10 second time-windows (5 seconds before and after the reference spike), beginning at the time of each reference spike. If the time-window fell at the end of the trial, the timewindow was clipped to the end of the trial. For each reference spike, the heading direction of the animal at that moment was assigned to zero degrees ('reference heading'). Within each time-window, a histogram of the heading directions of the animal associated with spikes times of a second ('test') neuron were defined relative to the reference heading. The histogram was then summed and smoothed with a 30° boxcar filter, to produce a time-windowed directional map of test neuron spike times associated with reference neuron spike times. The time-windowed directional map was then normalised to the TWC of a population of spike-shuffled (100 shuffles per cell pair) reference cells (Bassett et al., 2018). Positionshuffled data was computed by shifting the cell's spike times relative to position by a random amount (ranging between 20 seconds after trial onset and 20 seconds before trial end; Wills et al., 2010).

To assess the spatially-coupled firing and angle of directional offset between cell pairs, the spatial cross-correlogram was limited to turns of $\pm 180^\circ$, such that the final correlogram could be treated as a circular map, and hence directionality assessed using the RV length. A large RV length indicates strong directional coupling between the test and reference cells within the time-window. The association between angular offsets in the Open Field and Homecage was compared using circular-circular correla-

tion (computed using the Matlab *circ_corrcc* function).

As the small numbers of spikes included in the short time-window may give rise to an artefactually, directionally-biased correlogram, we also assessed what the probability was of observing any given correlate by chance (under the null hypothesis of there being no cell pairing), by comparing the actual correlogram with a population derived from shuffled data. Deviation from the shuffled mean was computed as the absolute maximum of the TWC following normalisation of the TWC to the shuffle. In this way, the maximum value is a Z-score calculation indicating the number of standard deviations of the shuffle data that the peak firing rate of the TWC is above the mean of the shuffled data. Normalisation here refers to TWCs being converted to percentiles of a shuffled population (100 shuffles). To quantify the number of TWCs which were statistically significant, a Sidak correction was implemented according to the following formula:

$$\alpha_{SID} = 1 - (1 - \alpha)^{\frac{1}{m}} \tag{6.2}$$

where α = 0.05 and m = 61 independent multiple comparisons (corresponding to the 61 directional bins of the TWC). This resulted in a corrected significance threshold of z=3.1415 (equivalent to p=0.05, assuming a normal z-distribution).

6.2.10 Statistics

Statistics were conducted as described in Section 4.6.6. For statistical analysis of both cohorts, a 2-way mixed ANOVA was conducted, with environment being the within-subjects factor and age being the across-subjects factor (postnatal day P12 to P16; as neurons were assumed to be different populations across days, even in rats that contributed data on more than one day).

6.3 Results

6.3.1 Behavioural profile of animals in different environmental contexts

6.3.1.1 Directional sampling

Animal behaviour was analysed to compare whether there were any key differences in the behavioural profile of pups in different environmental contexts. The directional sampling of animals was inferred in a number of ways. Firstly, the number of head turns of the animals was computed as a measure of directional path length (Figure 6.4A). There was a significant main effect of both environment (2-way mixed ANOVA: F(3,102)=20.915, p<0.001, η_p^2 =0.381) and age (2-way mixed ANOVA: F(4,34)=9.012, p<0.001, η_p^2 =0.515) on directional path length. There was also a significant interaction between environment and age on the resultant number of head turns (2-way mixed ANOVA: F(12,102)=1.856, p=0.049, η_p^2 =0.179). Pairwise comparison shows that the directional sampling in the Small Box was significantly less than in the other environments (Homecage-A vs Small Box: p<0.001; Open Field vs Small Box: p<0.001; Homecage-B vs Small Box: p<0.001). This is to be expected considering the movement constraints imposed on the animal by the dimensions of the Small Box in conjunction with the presence of the pup's mother and littermates. It is interesting to note that at the youngest recorded ages, the path length of animals was highest in the Homecage environment (Homecage-A and Homecage-B trials). The difference between Open Field and Homecage environments in terms of the directional path length then decreased with an increase in age.

In tandem with directional path length, the RV length of all directional sampling measured in a recording trial was computed as a proxy measure for the uniformity of directional sampling (Figure 6.4B). An RV length close to zero is ideal as it infers uniform sampling of all directional bins, whereas

an RV length close to one implies that the animal has spent the majority of the trial pointing its head in one direction only. A 2-way mixed ANOVA concluded that there was no significant main effect of age (2-way mixed ANOVA: F(4,47)=0.941, p=0.449, $\eta_p^2=0.074$) on the uniformity of directional sampling overall, nor was there a significant interaction between environment and age in terms of equality of directional sampling (2-way mixed ANOVA: F(8,94)=0.393, p=0.922, $\eta_p^2=0.032$). However, the recording environment that the animal was in had a statistically significant impact on the uniformity of directional sampling (2-way mixed ANOVA: F(2,94)=7.698, p<0.001, $\eta_p^2=0.141$). The Open Field condition had the most uniform directional sampling, which was significantly different to both Homecage-A (p=0.012) and Homecage-B (p<0.001).

The Kullback-Leibler (KL) divergence was used as a secondary measure of directional sampling uniformity (Figure 6.4C). This calculated the extent to which the distribution of the animal's actual directional heading throughout a given trial strayed from a perfectly uniform sampling of all directional headings. Using this measure, like the positional RV length measure, there was only an effect of environment on the KL divergence (2-way mixed ANOVA: F(2,94)=5.407, p=0.006, $\eta_p^2=0.103$). The Open Field environment had a significant impact on KL divergence (i.e. Open field trials here have the lowest divergence from a uniform distribution of heading direction; Homecage-A vs Open Field: p=0.032; Open Field vs Homecage-B: p<0.001).

Finally, the cumulative sum of directional sampling was used to infer whether the animal had any potential bias toward head rotations in either the CW or CCW direction (Figure 6.4D). This was of interest due to previous reports that anterior thalamic head direction cells may shift their directional preference in line with corresponding rotations of the head (Blair and Sharp, 1995). A 2-way mixed ANOVA found no statistically significant main effect of environment (F(3,57) = 0.074, p=0.974, η_p^2 =0.004) or

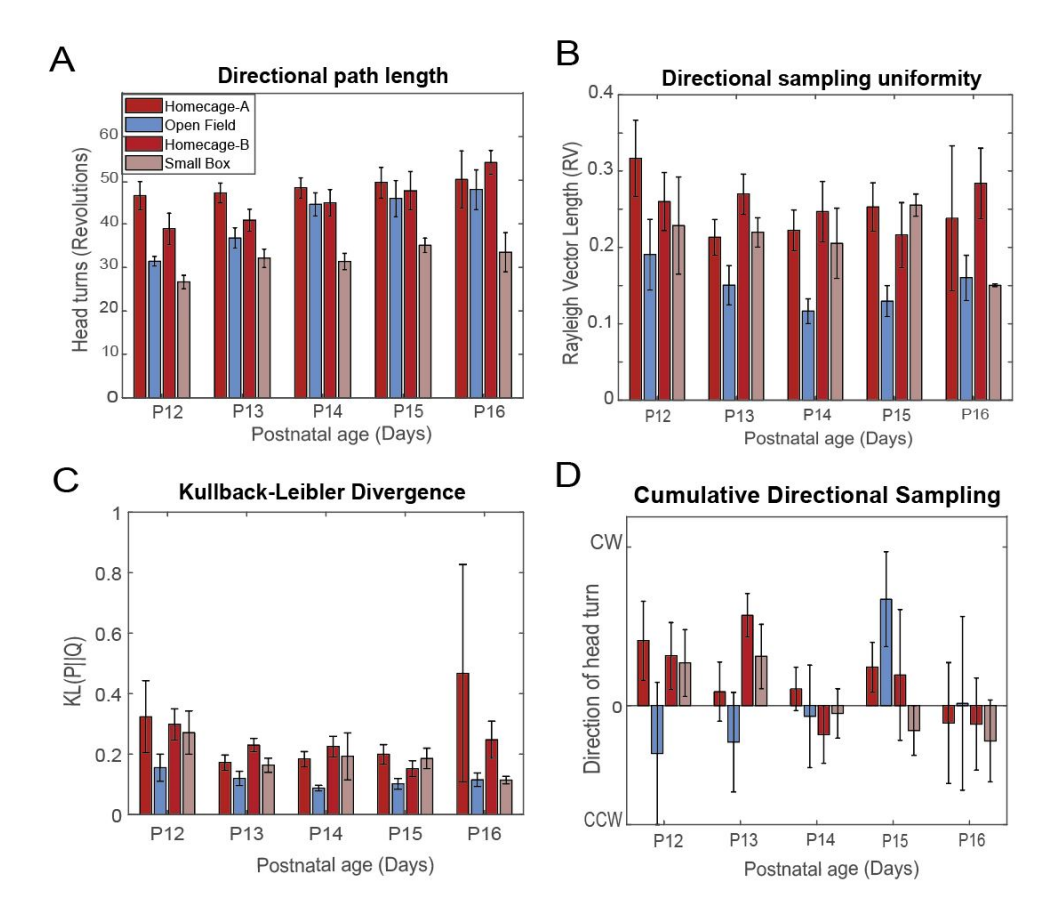


Figure 6.4: Directional sampling of animals in the Homecage-A, Open Field, Homecage-B and Small box trials respectively, across all recorded ages (postnatal day **12 to 16).** Trials per age group: P12: n=12; P13: n=20; P14: n=23; P15: n=16; P16: n=10. (A) Directional path length. There was a significant main effect of the environment on directional sampling (2-way mixed ANOVA: F(3,102)=20.915, p<0.001, $\eta_p^2=0.381$) There was a significant interaction between environment and age in terms of directional sampling (2-way mixed ANOVA: F(12,102)=1.856,p=0.049, η_p^2 =0.179). There was a significant main effect of age on directional sampling overall (2-way mixed ANOVA: F(4,34)=9.012, $p<0.001,\eta_p^2=0.515$).(B) Uniformity of directional sampling. There was a significant main effect of environment on directional sampling RV length overall (2-way mixed ANOVA: F(2,94)=7.698, p<0.001, η_p^2 =0.141). There was no significant interaction between environment and age in terms of directional sampling RV length (2-way mixed ANOVA: $F(8,94)=0.393,p=0.922,\eta_p^2=0.032)$. There was no significant main effect of age on directional RV overall (2-way mixed ANOVA: $F(4,47)=0.941, p=0.449, \eta_p^2=0.074$). (C) Kullback-Leibler divergence of directional sampling from a uniform distribution of directional sampling. There was a significant main effect of the environment on KL divergence (2way mixed ANOVA: F(2,94)=5.407, p=0.006, η_p^2 =0.103). There was no significant interaction between environment and age in terms of KL divergence (2-way mixed ANOVA: $F(8,94)=0.115,p=0.217, \eta_p^2=0.105)$. There was no significant main effect of age on KL divergence overall (2-way mixed ANOVA: F(4,47)=2.006, p=0.109, $\eta_p^2=0.146$).(**D**) **Cumulative** directional sampling of animals in either the clockwise or counterclockwise rotation of head turns. There was no significant main effect of environment on cumulative direction sampling (2-way mixed ANOVA: F(3,57)=0.074, p=0.974, η_p^2 =0.004). There was no significant interaction between environment and age in terms of cumulative direction sampling (2-way mixed ANOVA: $F(12,57)=0.986, p=0.474, \eta_p^2=0.172$). There was no significant main effect of age on cumulative direction sampling (2-way mixed ANOVA: F(4,19)=0.621, p=0.653, $\eta_p^2=0.116$).

age (F(4,19)=0.621, p=0.653, η_p^2 =0.116) on the cumulative directional sampling of animals. This means that the animals did not have any reliable difference in the direction of head rotations in the different conditions, nor with a change in age. There was furthermore no significant interaction between age and environment (2-way mixed ANOVA: F(12,57)=0.986, p=0.474, η_p^2 =0.172). Therefore, there was no apparent preference of the animal for head turns in either direction which may bias the skew of firing in the range of the cell's preferred heading direction.

In summary, while at the youngest recorded ages (P12 and P13) the directional path length of animals was higher during Homecage trials than the Open Field, this effect decreased with age such that from P14 onwards there was a comparable path length observed in both environments. By contrast, the path length of animals in the Small Box was consistently lower than both Homecage and Open Field trials. This is unsurprising considering the small area of the environment in tandem with the presence of conspecifics limiting the range of movement of the animal. The uniformity of directional sampling was much improved in the Open Field compared to both Homecage and Small Box trials at every age, suggesting a wider range of motion of the animal's head during these trials. Whilst a certain level of directional bias was also observed, this was not significant.

6.3.1.2 Spatial sampling

Next, the spatial sampling of the animal in each environment was assessed in two-dimensional space. The trial environment had a significant effect on the path length of animals overall (Figure 6.5A; 2-way mixed ANOVA: F(3,102)=22.54, p<0.001, $\eta_p^2=0.399$). Animals consistently travelled further in the Open Field condition than in the Homecage or Small Box trials (Tukey's HSD: Homecage-A vs Open Field: p<0.001; Open Field vs Homecage-B: p<0.001; Open Field vs Small Box: p=0.003). There was a concurrent increase in the distance travelled with an increase in age, which was statistically significant (2-way mixed ANOVA: F(4,24)=5.278,

p=0.002, η_p^2 =0.383) and was particularly apparent in the Small Box condition (Pairwise comparison of Small Box trials: P12 vs P15: p=0.006; P12 vs P16: p=0.029; P13 vs P15: p=0.054). One reason for the apparent improvement in spatial sampling observed in the Open Field may be the wider range of movement and increased thigmotactic response (Martinez and Morato, 2004). This is supported by the finding that animals spent a significantly higher proportion of time within the wall zone (see Section 4.6.3.1) of the environment in the Open Field trials than either Homecage-A or Small Box trials (Figure 6.5B; 2-way mixed ANOVA: F(3,108)= 4.047, p<0.001. Pairwise comparisons: Homecage-A vs Open Field: p=0.002; Open Field vs Small Box: p<0.001). The inclination of the animal to remain close to the environmental boundaries in the Open Field is also evidenced in the paths of the animal shown in representative trials in Figure 6.5C-G.

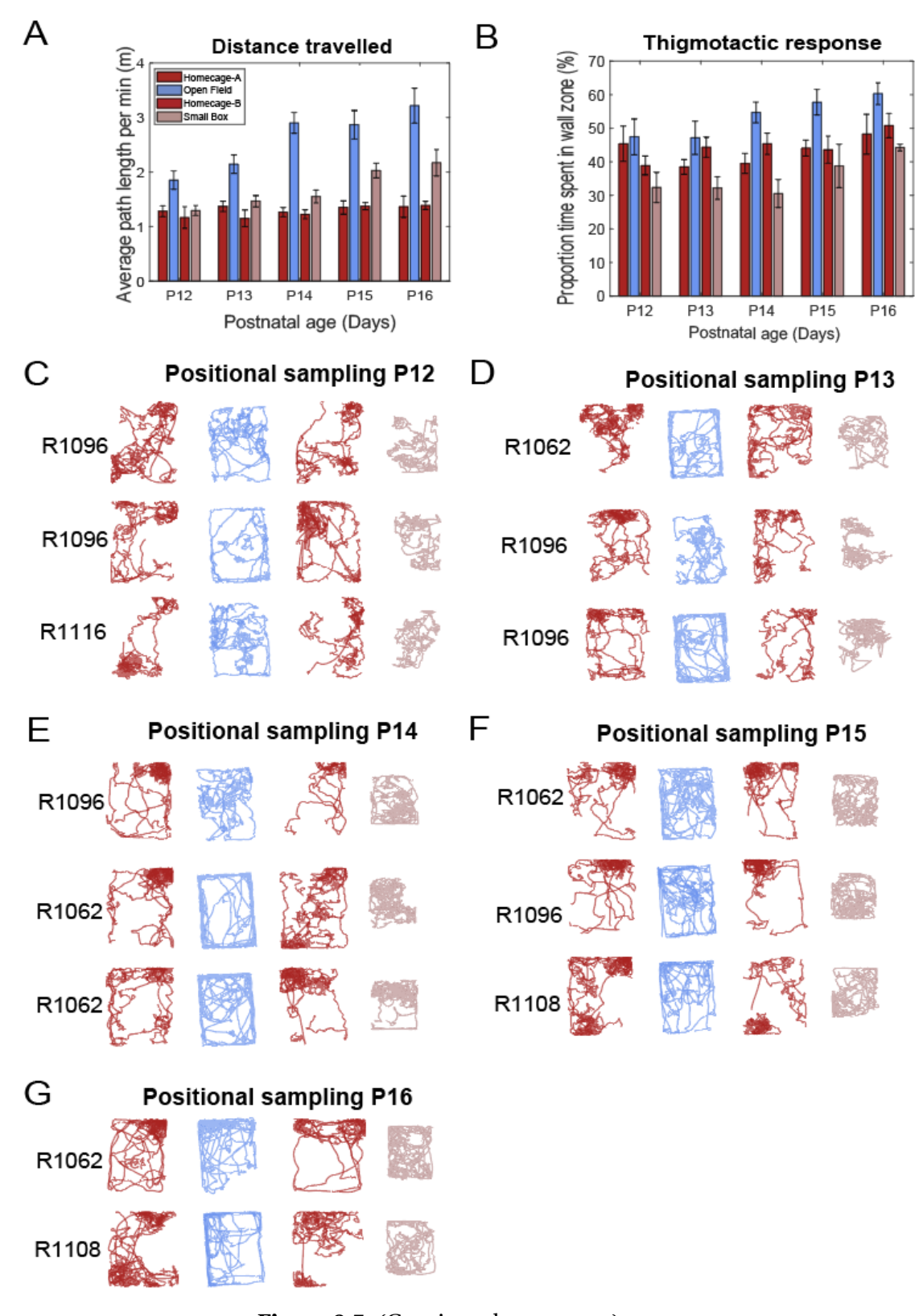


Figure 6.5: (Continued over page.)

Figure 6.5: Spatial sampling of animals in the Homecage-A, Open Field, Homecage-B and Small box trials respectively, across all recorded ages (post**natal day 12 to 16).** Trials per age group: P12: n=12; P13: n=20; P14: n=23; P15: n=16; P16: n=10. (A) Distance travelled by pups per minute of recording trial. There was a significant main effect of the recording environment on path length overall (2-way mixed ANOVA: F(3,102)=22.54, p<0.001, η_p^2 =0.399). There was no significant interaction between environment and age in terms of linear path length (2-way mixed ANOVA: F(12,102)=1.401, p=0.178, η_p^2 =0.141). There was a significant main effect of age on path length overall (2-way mixed ANOVA: F(4,24)=5.278, p=0.002, $\eta_p^2=0.383$). (B) Thigmotactic response of pups. There was a significant main effect of the environment on thigmotactic behaviour (2-way mixed ANOVA: F(3,108)=4.047, p<0.001, η_p^2 =0.224). There was no significant interaction between environment and age in terms on the thigmotactic response (2-way mixed ANOVA: F(12,108)=0.997, p=0.457, η_p^2 =0.1). There was a significant main effect of age on thigmotaxis (2-way mixed ANOVA: F(4,36)=3.464, p=0.017, η_p^2 =0.278). (C-G) Example paths taken by animals during the duration of the recording trial across each age. Each row corresponds to one trial, each column corresponds to the recording environment (Homecage-A, Open Field, Homecage-B, and Small Box, respectively).

6.3.1.3 Movement velocity

Finally, the linear and angular velocity of the animals was compared across environments (Figure 6.6). The recording environment had a statistically significant influence on both linear velocity (Figure 6.6A-B; 2-way mixed ANOVA: F(3,102)=63.98, p<0.001, η_p^2 =0.653) and AHV (Figure 6.6C-D; 2way mixed ANOVA: F(3,102)=2.765, p=0.046, η_p^2 =0.075), but the effect size was much larger with respect to linear velocity (η_p^2 =0.653 versus η_p^2 =0.075). Pairwise comparison indicated that running speed in the Open Field was significantly higher than the other environments (Homecage-A vs Open Field: p<0.001; Open Field vs Homecage: p<0.001; Open Field vs Small Box p<0.001), and this effect is statistically significant from P14 onwards (P14: Homecage-A vs Open Field: p<0.001, Open Field vs Homecage-B: p<0.001, Open Field vs Small Box: p<0.001; P15: Homecage-A vs Open Field: p=0.001, Open Field vs Homecage-B: p=0.007, Open Field vs Small Box: p=0.029; P16: Homecage-A vs Open Field: p<0.001, Open Field vs Homecage-B: p<0.001, Open Field vs Small Box: p=0.004). Evidence of this is also seen from the overall distribution of linear velocity between recording environment and age (Figure 6.6B), where running speed is skewed towards higher values in the Open Field, particularly around P14 to P16 (in agreement with there being a significant effect of age on the linear velocity of animals, 2-way mixed ANOVA: F(4,34)=3.462, p=0.03, η_p^2 =0.264). This contrasts somewhat with median AHV values (Figure 6.6C), wherein there is no significant main effect of age on angular velocity (2-way mixed ANOVA: F(4,34)=0.449, p=0.773, η_p^2 =0.05), nor a significant interaction between recording environment and age on angular velocity (2-way mixed ANOVA: F(12,102)=1.308, p=0.226, η_p^2 =0.133). Pairwise comparison shows a significant difference in median angular velocity values in the Small Box condition compared to the Open Field (Open Field vs Small Box: p=0.018). These results are also presented in Figure 6.6D, where the distributions of median angular head velocity values do not significantly change with age but do change as a result of the recording environment (2-way mixed ANOVA F(3,102)=2.765, p=0.046, η_p^2 =0.075).

Broadly, these results show that there is a clear improvement in the distance travelled by animals during Open Field trials. This may be expected due to both the absence of conspecifics as well as floor bedding rendering the Open Field easier to manoeuvre around when compared to the other environments. The animal likely tires more slowly and as such is able to sample the environment to a greater extent. There is furthermore an age-dependent increase in the linear velocity of animals in the Open Field compared to Homecage and Small Box trials (from P14). The linear velocity of animals in the Homecage and Small Box environments remain similar to each other across age bins. By comparison, the AHV profile of animals does not change in an age-dependent manner. The AHV of animals differs only by environment, wherein the AHV of animals is lowest in the Small Box. This is likely interlinked with the data discussed in Section 6.3.1.1, given the directional sampling of the animal in the Small Box environment was significantly poorer than the preceding trials.

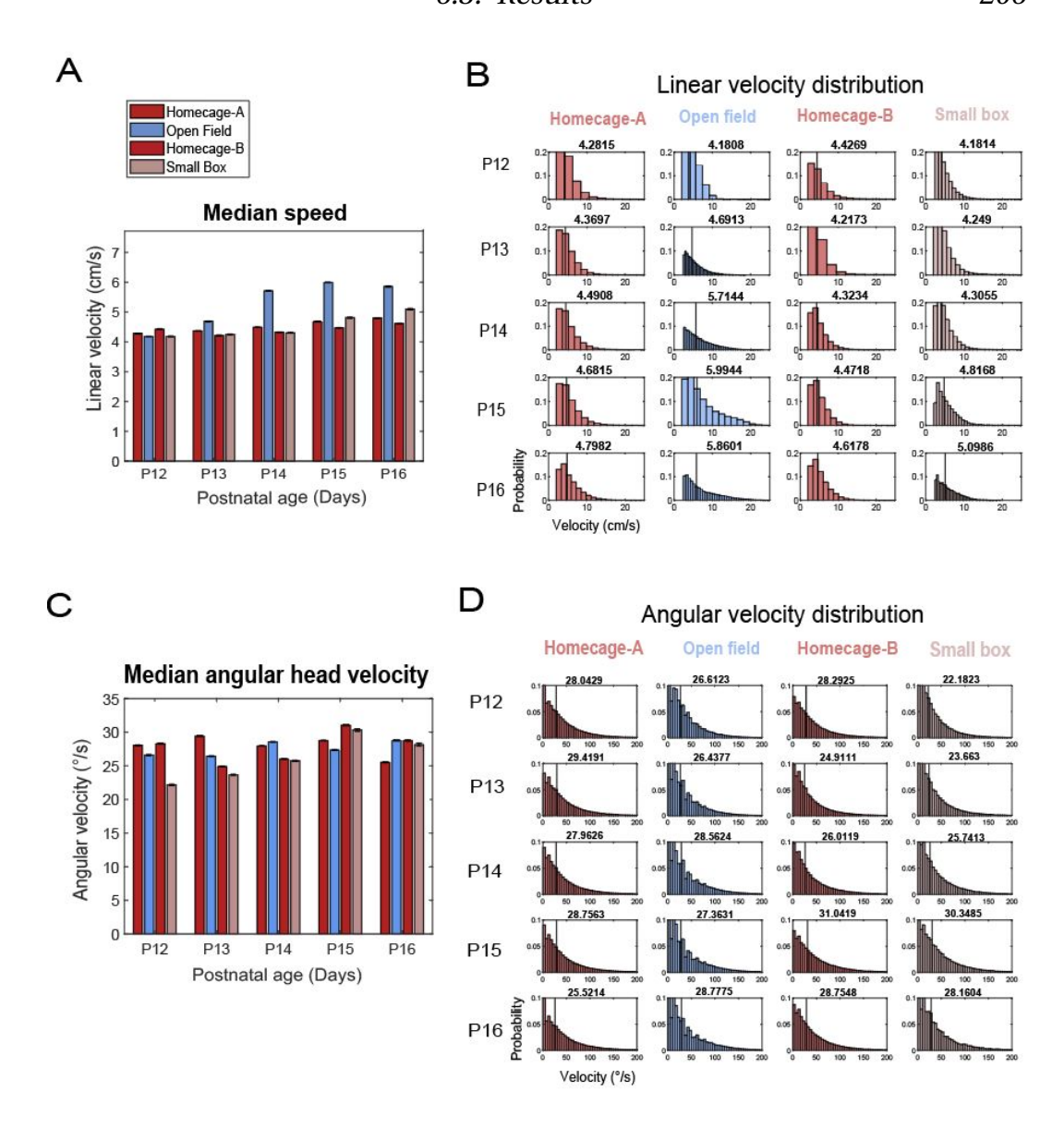


Figure 6.6: Linear and angular velocity profiles of animals in the Homecage-A, Open Field, Homecage-B and Small box trials respectively, across all recorded ages (postnatal day 12 to 16). Trials per age group: P12: n=12; P13: n=20; P14: n=23; P15: n=16; P16: n=10. (A) Median speed of animals. There was a significant main effect of the recording environment on linear velocity overall (2-way mixed ANOVA: F(3,102)=63.98, p<0.001, η_p^2 =0.653). There was a significant interaction between environment and age in terms of linear velocity (2-way mixed ANOVA: F(12,102)=3.516, p<0.001, η_p^2 =0.293). There was a significant main effect of age on linear velocity overall (2-way mixed ANOVA: $F(4,34)=3.462, p=0.03, \eta_p^2=0.264)$. (B) Distribution of linear velocity samples of all animals. The black vertical line corresponds to the median speed value as depicted in (A). The number above the plot depicts the median speed value for each age and trial. (C) Median angular head velocity of animals. There was a significant main effect of environment on angular velocity overall (2-way mixed ANOVA: F(3,102)=2.765, p=0.046, η_p^2 =0.075). There was no significant interaction between environment and age in terms of angular velocity (2-way mixed ANOVA: F(12,102)=1.308, p=0.226, η_p^2 =0.133). There was no significant main effect of age on angular velocity overall (2-way mixed ANOVA: F(4,34)=0.449, p=0.773, $\eta_p^2=0.05$). (D) Distribution of angular head velocity samples of all animals. The black vertical line corresponds to the median speed value as depicted in (C). The number above the plot depicts the median speed value.

6.3.2 Head direction cell firing differs between the homecage and open field

6.3.2.1 General properties of recorded cells

The general properties of HD cells recorded in the ADN during this experiment are presented in Figure 6.7. As mentioned in Section 6.2.5, HD cells in this case were classified on the basis of a number of criteria. A cell was included in analysis if it met the criteria for HD cell classification in either the Homecage-A or Open Field trials. One prerequisite for inclusion in analysis was the calculation of RV lengths, computed from position data shuffled with respect to spike trains for each cell in each condition. The 95th percentile value of the shuffled RV length scores were then used as a preliminary minimum threshold for directional tuning. A summary of the 95th percentile shuffled scores for all cells are presented in Figure 6.7A. There was a difference in the distribution of RV length scores across environment conditions (Friedman test: $\chi^2(3) = 33.467$, p=0.001), however this was only apparent at older ages (at which point lower RV thresholds are observed during Open Field trials). The total number of HD cells recorded from the ADN markedly increased with age (Figure 6.7B), reaching its peak at the oldest recorded age (P16), consistent with previous reports of ADN HD cells in the developing rat (Tan et al., 2015; Bassett et al., 2018).

The mean and peak firing rates of HD cells were computed across age and environment, with differences quantified by means of a 2-way mixed ANOVA. There was a gradual overall increase in both the mean (Figure 6.7C) and peak (Figure 6.7D) firing rates of cells with age (consistent with other reports; Tan et al., 2015). There was no significant main effect of the trial environment on the mean firing rate overall (2-way mixed ANOVA: F(3,78)=0.7, p=0.555, $\eta_p^2=0.026$), nor an interaction between environment and age in terms of mean firing rate (F(12,78)=1.735, p=0.075, $\eta_p^2=0.211$). There was a significant main effect of age on mean firing rate overall, for

which the effect size was large (F(4,26)=4.175, p=0.01, η_p^2 =0.391). Specifically, there was a significant difference in mean firing rate of cells at P16 and all other recorded ages except P15 (Tukey's HSD: P12 versus P16: p=0.042; P13 versus P16: p=0.022; P14 versus P16: p=0.01). This is expected in line with a maturation of the HD cell circuit. Interestingly, the recording environment had a significant effect on the peak firing rate of cells (2-way mixed ANOVA: F(2,92)=4.184, p=0.018, η_p^2 =0.083). There was furthermore a significant interaction between environment and age on peak firing rates (2-way mixed ANOVA: F(8,92)=2.287, p=0.028, $\eta_p^2=0.166$) such that at the oldest ages, there was a pronounced increase in the firing rates of cells recorded in the Open Field compared to the Homecage and Small Box trials (Pairwise comparison P16: Homecage-A vs Open Field: p<0.001, Homecage-B vs Open Field: p<0.001, Open Field vs Small Box: p<0.001). The peak firing rates of cells were also significantly impacted by age (2way mixed ANOVA: F(4,26)=6.251, p=0.001, $\eta_p^2=0.49$). As with the mean firing rate, there was a significant difference in mean firing rate between the earliest recorded ages and P16, indicating an expected maturation of cell firing with respect to age (Tukey's HSD: P12 versus P16: p=0.006; P13 versus P16: p=0.004; P14 versus P16: p<0.001; P15 versus P16: p=0.043).

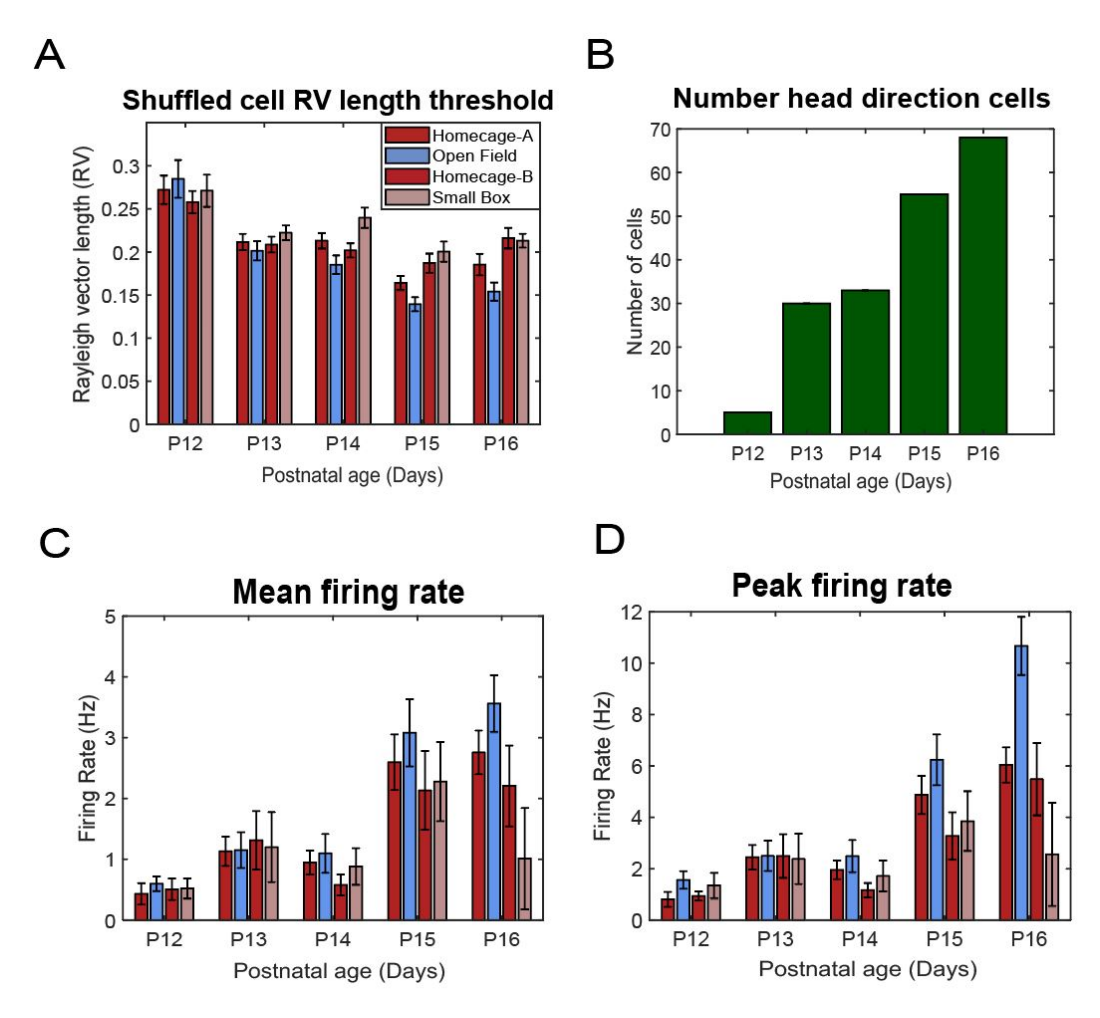
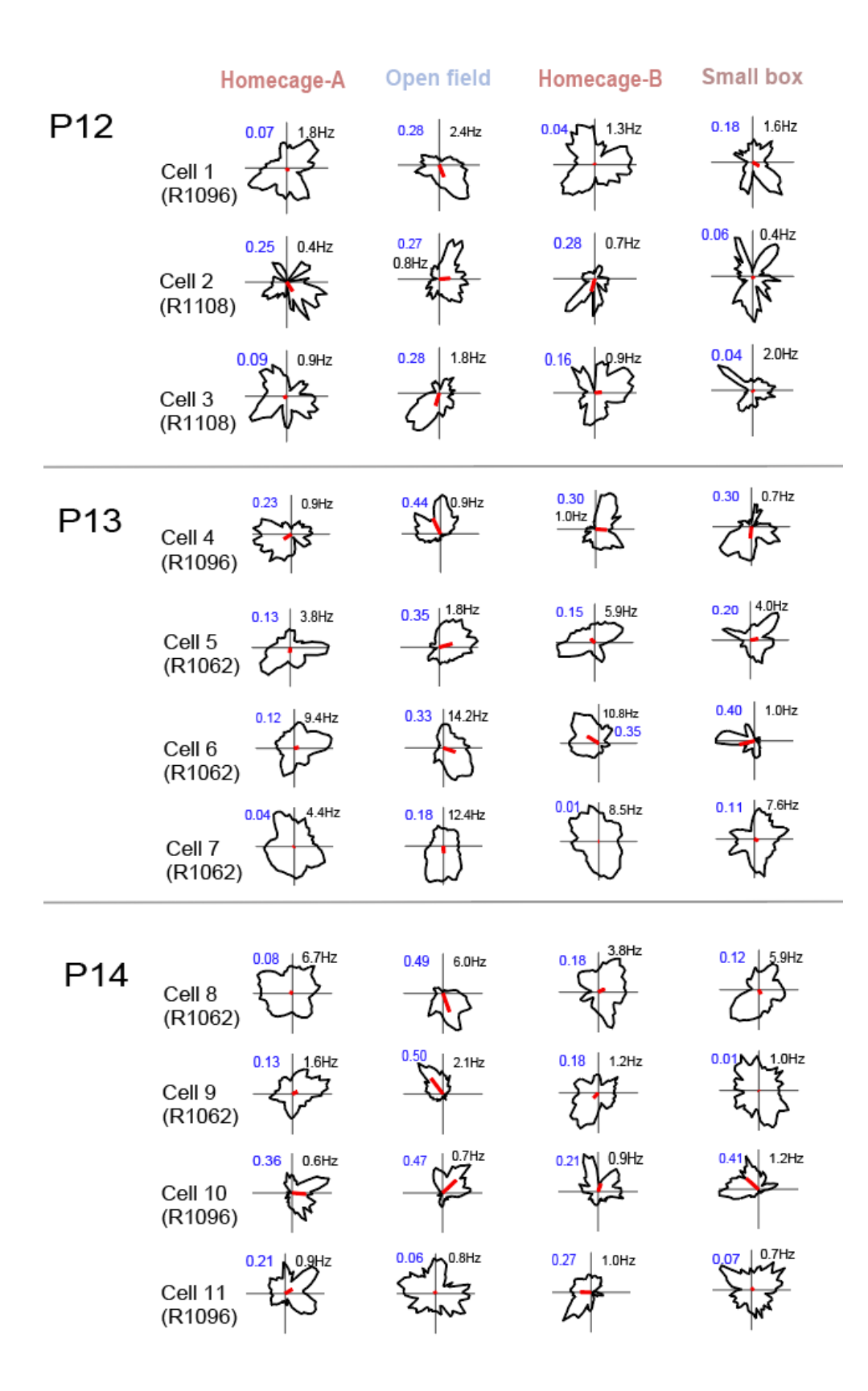


Figure 6.7: General properties of cells across ages. Cells per age group: P12: n=5; P13: n=30; P14: n=33; P15: n=55; P16: n=68. (A) Rayleigh vector length thresholds computed for each cell for each trial. The 95th percentile value of a shuffled population of RV scores for each cell was used to define a minimum threshold for HD cell inclusion. There was a significant difference between environments; Friedman test: $\chi^2(3) = 33.467$, p=0.001. (B) The number of single-units classified as head direction cells for each age bin. Cells were considered head direction cells in all trials for that recording session if they met the criteria for head direction selection in at least one of the Homecage-A or Open Field trials. (C) Mean firing rate of cells. There was a significant increase in mean firing rate of head direction cells with age (2-way mixed ANOVA: F(4,26)=4.175, p=0.01, η_p^2 =0.391). There was no significant effect of environment on mean firing rate (2-way mixed ANOVA: F(3,78) = 0.7, p = 0.555, η_p^2 = 0.026), and no significant interaction between environment and age in terms of mean firing rate (2-way mixed ANOVA: F(12,78)=1.735, p =0.075, $\eta_p^2 = 0.211$). (D) Peak firing rate of cells. There was a significant main effect of environment on peak firing rate overall (2-way mixed ANOVA: F(2,92)=4.184, p=0.018, η_p^2 =0.083), and a significant interaction between environment and age (2-way mixed ANOVA: F(8,92)=2.287, p=0.028, $\eta_p^2=0.166$). There was also an overall significant increase in the peak firing rate of cells across age (2-way mixed ANOVA: F(4,26)=6.251, p=0.001, $\eta_p^2=0.49$).

6.3.2.2 Directional modulation of recorded cells



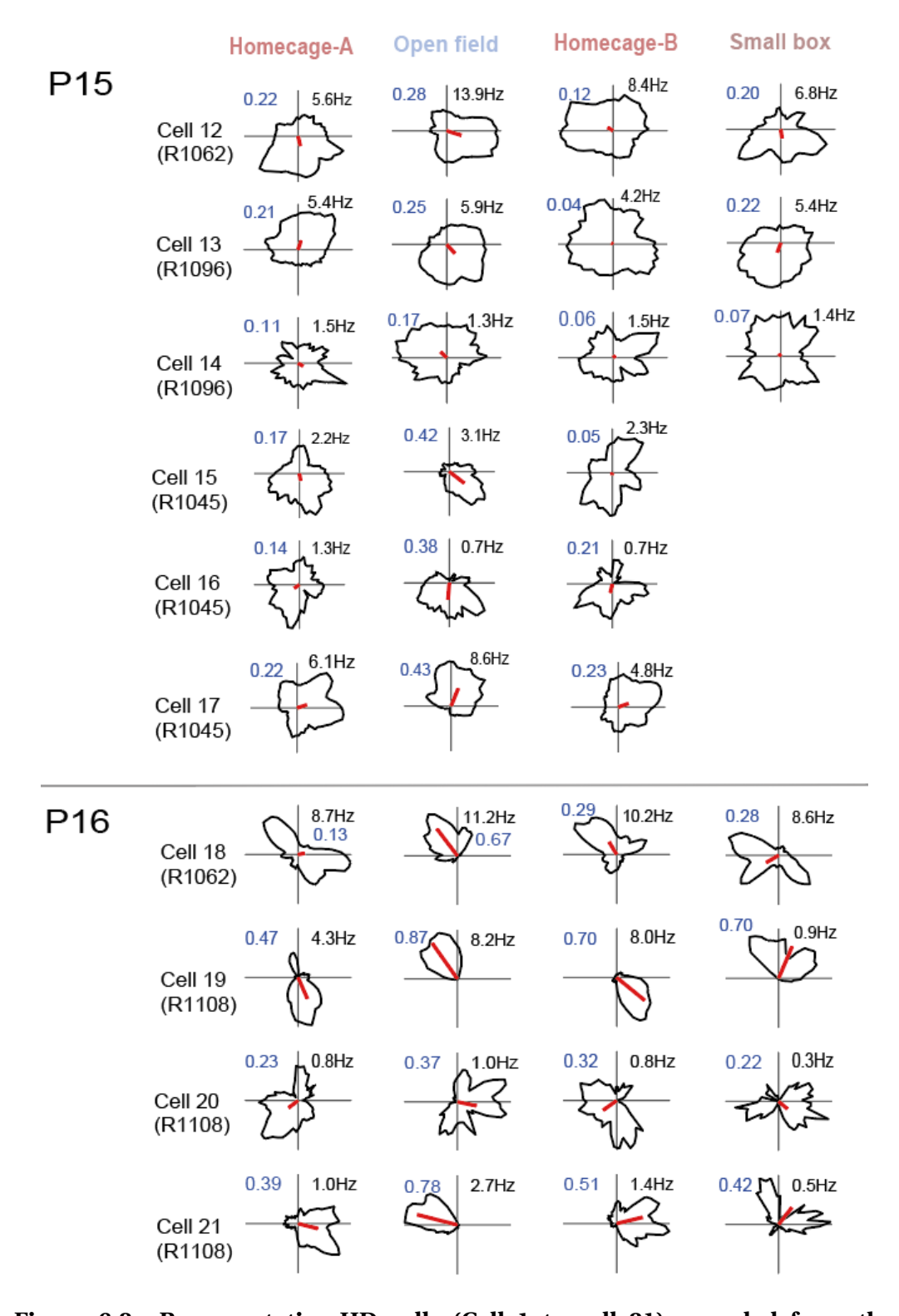


Figure 6.8: Representative HD cells (Cell 1 to cell 21) recorded from the Homecage, Open Field and Small Box environments across all recorded ages (postnatal day 12 to 16). Shown here are polar plots of cell firing rate versus head direction. The number in blue indicates the Rayleigh vector (RV) length, and the number in black indicates the peak firing rate (Hz). There is more precise unidirectional tuning of head direction cells in the Open Field compared to the Homecage at all ages, indicated by higher RV lengths of cells in the Open Field.

Representative single neurons from cells in each condition are shown in Figure 6.8. A qualitative difference in the directional tuning of cells in the Open Field and the Homecage is apparent: HD cells recorded in the Open Field condition have a directional correlate even from P12, indicated by the defined (albeit broad) tuning curve of cell polar plots and higher respective RV lengths compared to the other conditions. The same cells recorded in the Homecage and Small Box environments do not retain this unidirectional tuning in many cases. Instead, many cells appear directional but multi-lobed, corresponding to heightened rates of firing in more than one heading direction.

In order to quantify this observation, the mean resultant vector length (RV length) and directional information of cells was computed. A key distinction between RV length and directional information is that RV length indicates the unidirectional tuning preference of a given HD cell, whilst directional information quantifies any directional modulation of cells either unidirectional or multidirectional in nature. There is a clear difference in results pertaining to these two measures (Figure 6.9).

In line with the recording environment having a significant main effect on HD cell RV length (2-way mixed ANOVA: F(1,175)=33.59, p<0.001, η_p^2 =0.161), RV length was consistently higher in the Open Field compared to the Homecage (Simple main effects: p<0.001). There was also a significant interaction between environment and age on the average RV length of cells in the Homecage-A and Open Field trials (2-way mixed ANOVA: F(4,176)=4.366, p=0.002, η_p^2 =0.091). From P14, there was a significant difference between RV in the Open Field condition compared to the Homecage (Pairwise comparison; P14: Homecage-A vs Open Field: p=0.002; P15: Homecage-A vs Open Field: p<0.001; P16: Homecage-A vs Open Field: p<0.001).

When subsidiary hypotheses were tested with the addition of the Homecage-B and Small Box environments, a statistically significant main

effect of the environment on unidirectional tuning was again observed (Figure 6.9A, 2-way mixed ANOVA: F(3,69)=15.575, p<0.001, η_p^2 =0.404), wherein the RV length of cells was consistently higher in the Open Field compared to all other recording environments (Homecage-A vs Open Field: p<0.001; Open Field vs Homecage-B: p=0.001; Open Field vs Small Box: p<0.001). Furthermore, there was again a significant interaction between age and environment for RV length (2-way mixed ANOVA: F(12,69)=2.139, p=0.025, $\eta_p^2=0.271$), such that the Open Field RV length was significantly different to all other recording environments from P14 (P14: Homecage-A vs Open Field p=0.008; Open Field vs Homecage-B: p<0.001; Open Field vs Small Box: p<0.001; P15: Homecage-A vs Open Field p<0.001; Open Field vs Homecage-B: p<0.001; Open Field vs Small Box: p<0.001; P16: Homecage-A vs Open Field p<0.001; Open Field vs Homecage-B: p=0.039; Open Field vs Small Box: p=0.002). A clear result here is that RV length in the return-to-baseline trial, Homecage-B, is lower than Homecage-A. The likely explanation for this is instability of cell firing, or a regression to the mean effect as a result of the smaller sample size in Homecage-B recordings and the fact that HD cells are classified on the basis of Homecage-A or Open field trials, not Homecage-B trials.

RV values of cells in the Open Field are consistent with previous reports of RV length and directional information in age- and brain areamatched animals (increasing gradually from approximately 0.2 to 0.6 between ages P12 and P16; Bassett et al., 2018). The largest increase in RV length occurred between P15 to P16, concurrent with the period of eye-opening in this cohort of animals (modal eye-opening age: P15). For all ages P12 to P15, the pairwise comparison with P16 was statistically significant (Tukey HSD: P12-P16: p=0.042; P13-P16: p<0.001; P14-P16: p<0.001; P15-P16: p<0.001). In summary, these findings pertaining to RV length suggest that not only are there increases in the unidirectional tuning of cells in the Open Field compared to the animal's Homecage, but this dif-

ference is compounded by an increase in age and therefore integration of a wider array of sensorimotor capabilities (primarily vision). Contrary to the hypothesis that HD cells may have higher directional tuning in a naturalistic environment than in an open field environment, the opposite appears to be the case.

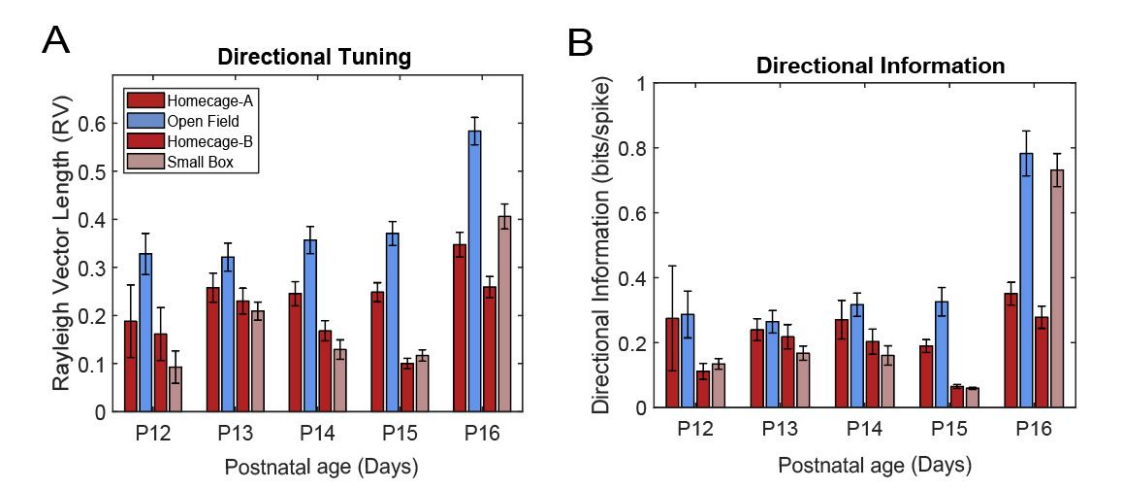


Figure 6.9: Directional modulation metrics of recorded cells. Cells per age group: P12: n=5; P13: n=30; P14: n=33; P15: n=55; P16: n=68. **(A) Directional tuning of head direction cells.** There was a significant main effect of the environment on RV length $(F(3,69)=15.575, p<0.001, \eta_p^2=0.404)$. There was a significant interaction between environment and age in terms of RV length $(F(12,69)=2.139, p=0.025, \eta_p^2=0.271)$. There was a significant main effect of age on RV length overall $(F(4,23)=7.85, p<0.001, \eta_p^2=0.577)$. **(B) Directional information of head direction cells.** There was a significant main effect of the environment on cell directional information $(F(3,69)=11.519, p<0.001, \eta_p^2=0.334)$. There was a significant interaction between environment and age in terms of cell directional information $(F(12,69)=4.415, p<0.001, \eta_p^2=0.434)$. There was a significant main effect of age on cell directional information overall $(F(4,23)=10.59, p<0.001, \eta_p^2=0.648)$.

Interestingly, the mean RV length of cells recorded in the Small Box environment tended to vary widely but appeared to substantially improve at P16, coinciding with eye-opening. One may surmise that the directional tuning in the Small Box is poor compared to the Homecage and Open Field trials at the youngest ages because the pup is coming in contact with mobile cues in the form of its conspecifics to a much greater degree than in the larger Homecage and Open Field enclosures, and the extent to which this may disorient the animal is not mitigated by an increase in spatial sampling of the environment until the animal is older or its eyes have opened.

When the directional information of cells was compared, the recording environment again had a significant effect on the directional information of cells (2-way mixed ANOVA: F(1,176)=11.441, p<0.001, $\eta_p^2=0.061$) in Homecage-A and Open Field recordings, as well as a significant interaction between environment and age (2-way mixed ANOVA: F(4,176)=10.568, p<0.001, $\eta_p^2=0.194$). Specifically, directional information of cells in the Open Field and Homecage are not significantly different except at P16 (Tukey's HSD: p<0.001). This is an interesting distinction from the results of RV length: while directional information is only different in older animals, RV is significantly different on the majority of recording days except at the youngest ages. This is indicative of the multi-peaked firing of cells in the Homecage, especially at younger ages, and unidirectional firing observed in the Open Field.

When the subset of trials was also considered (Homecage-B and Small Box trials), a similar trend was observed with respect to the encoded directional information of these cells (Figure 6.9B). There was a statistically significant main effect of environment (2-way mixed ANOVA: F(3,69)=11.519, p<0.001, η_p^2 =0.334), as well as an interaction between environment and age (2-way mixed ANOVA: F(12,69)=4.415, p<0.001, η_p^2 =0.434), on directional information. The interesting pairwise comparison is Homecage versus Open Field, at each age: there was again no significant difference in environments regarding directional information until P16. At this age, directional information in the Open Field and Small Box environments were significantly increased compared to the Homecage environments (Homecage-A vs Open Field: p<0.001; Homecage-A vs Small Box: p<0.001; Open Field vs Homecage-B: p<0.001; Homecage-B vs Small Box: p<0.001). Directional information of cells in the Small Box and Open Field were also significantly different to each other at P16 (p=0.011). Homecage-A and Homecage-B are both largely differing from the Open Field overall (p<0.001 in both cases), as well as from the Small Box environment overall (Homecage-A vs Small Box: p<0.001; Homecage-B vs Small Box: p=0.007). Directional information in the Small Box, however, is not statistically different from cells recorded in the Open Field trial (p=0.086), in accordance with the findings of Bassett et al. (2018), that cells demonstrate increased directional information in a smaller environment.

In summary, there is a clear improvement in the unidirectional signalling of HD cells in animals at all ages in the Open Field compared to the Homecage. However, this effect is not reflected in the directional information of recorded cells. The directional information of cells is instead the same (in some cases higher, such as at P12) in the Homecage compared to the Open Field and Small Box until eye-opening. This is reflected in the tuning curves of cells, in that HD cells in the Homecage exhibit multipeaked firing corresponding to multiple preferred firing directions within a given recording trial.

6.3.2.3 Stability of recorded cells

The stability of HD cells is measured as the correlation of directional firing either between the first and second half of a given trial (within-trial stability), or between two recording trials (across-trial stability). The within-trial stability is another useful measure for assessing directional firing of cells, in addition to the RV length and directional information discussed above.

In this experiment, recording environment had a significant effect on the within-trial stability of cell firing in the Open Field and Homecage-A trials (Figure 6.10A; 2-way mixed ANOVA: F(1,174)=26.997, p<0.001, $\eta_p^2=0.134$). Specifically, stability of cell firing between the first and second half of Open Field trials was significantly higher than the corresponding Homecage-A trials (Pairwise comparison: p<0.001). As anticipated, there was a significant increase in cell stability concurrent with an increase in age (2-way mixed ANOVA: F(4,174)=29.359, p<0.001, $\eta_p^2=0.403$) on the within-trial stability of HD cells. There was furthermore a significant interaction between environment and age on the within-trial firing stabil-

ity, such that there are larger differences in cell stability between Open Field and Homecage-A trials at the oldest age points recorded (Pairwise of comparison of Open Field and Homecage-A trials at P15 and P16, both p<0.001).

When Homecage-B and Small Box trials were also considered in the statistical tests, there was again a significant effect of both environment (2-way mixed ANOVA: F(3,54)=14.295, p<0.001, $\eta_p^2=0.443$) and age (2-way mixed ANOVA: F(4,38)=4.166, p=0.007, $\eta_p^2=0.305$) on the within-trial stability of HD cells (Figure 6.10A). The was a significant improvement in the within-trial stability of cells during Open Field trials when compared to all other trials (Pairwise comparison: Homecage-A vs Open Field: p<0.001; Homecage-B vs Open Field: p<0.001; Small Box vs Open Field: p<0.001). In line with maturation of the HD cell circuit, there was also a significant effect of age on cell stability (2-way mixed ANOVA: F(4,108)=17.87, p<0.001, $\eta_p^2=0.398$).

One reason for the imbalance in stability and directional firing of cells between Homecage and Small Box recordings and the Open Field may be the relative dependence on proximal cues in the Homecage that are not present in the Open Field. More specifically, the presence of conspecifics in the Homecage may be serving as mobile, proximal cues which the pup dynamically uses to orient itself, in combination with tactile cues present in the Homecage such as cage bedding which may serve to transiently anchor the HD cells of the rat as it moves past (however, given the movement statistics of these animals being relatively difficult to discern without tracking all animals in the Homecage, this analysis is beyond the scope of this thesis). The Open Field is comparatively cue-deprived before eye-opening, with the geometric boundaries of the environment likely being the primary anchoring cue for the head direction cells (Bassett et al., 2018). Another reason for instability may be the resetting of HD cells brought on by the picking up and moving of pups throughout recording trials, which

will be discussed further in Section 6.3.3.

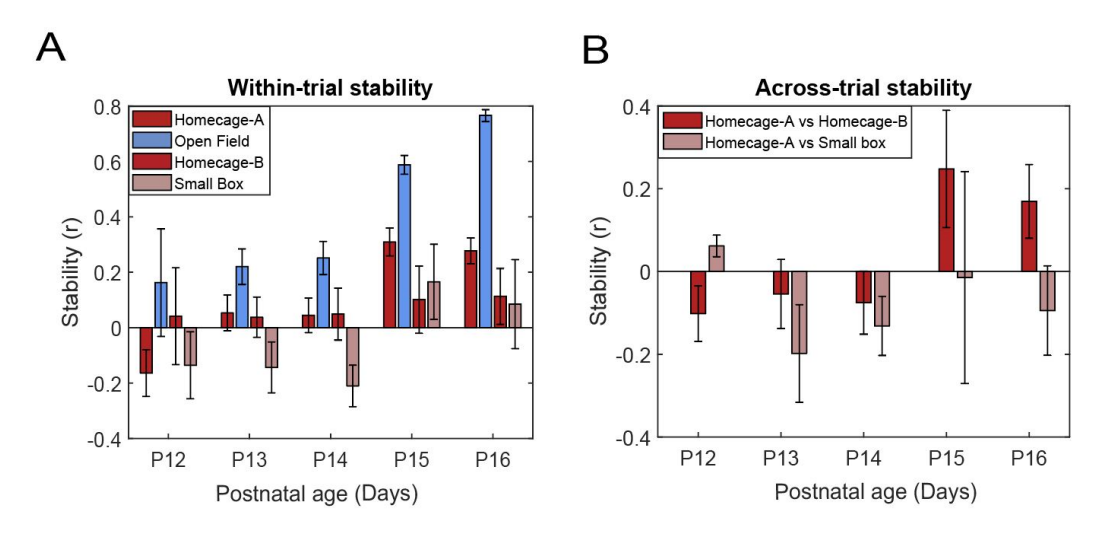


Figure 6.10: Stability of cell firing within and between recording trials. Cells per age group: P12: n=5; P13: n=30; P14: n=33; P15: n=55; P16: n=68. **(A) Within-trial stability of head direction cells.** There was a significant main effect of the environment on within-trial cell stability (F(3,54)=14.295, p<0.001, η_p^2 =0.443). There was no significant interaction between environment and age in terms of within-trial cell stability (F(12,54)=1.505, p=0.151, η_p^2 =0.251). There was a significant main effect of age on within-trial cell stability overall (F(4,108)=17.87, p<0.001, η_p^2 =0.398). **(B)** Across-trial stability of head direction cells. There was no significant main effect of the environment on across-trial cell stability (F(1,41)=1.742,p=0.194, η_p^2 =0.041). There was no significant interaction between environment and age in terms of across-trial cell stability (F(4,41)=0.73,p=0.577, η_p^2 =0.066). There was no significant main effect of age on across-trial cell stability overall (F(4,41)=1.079, p=0.379, η_p^2 =0.095).

The across-trial stability of HD cells between homecage trials and Open Field trials was ignored in statistical analysis of Homecage-A and Open Field trials, given that rats were transported to another room for Open Field recordings. Instead, the across-trial stability of cells between Homecage-A, Homecage-B and Small Box trials were considered as these trials were conducted in the same room (Figure 6.10B). The recording environment did not have a statistically significant impact on the correlation of directional firing between trials (2-way mixed ANOVA: F(1,41)=1.742, p=0.194, $\eta_p^2=0.041$), nor did age (2-way mixed ANOVA: F(4,41)=1.079, p=0.379, $\eta_p^2=0.095$). Nonetheless, the across-trial stability of recorded cells before eye-opening was consistently low (r<=0.2). Qualitatively, there is an apparent improvement in the stability of cells between Homecage-A

and Homecage-B trials on P15 and P16, coinciding with the period of eyeopening in these animals. This is to be expected based on the trials occurring in the same recording environment and with the same proximal and distal cues. It appears that at younger ages there is less likelihood of HD cells returning to baseline (Homecage-A) upon return to the homecage (Homecage-B) trial. The ability of the cells to return to baseline appears to increase concurrently with integration of allothetic inputs, including vision. One possibility is that visual inputs aid the animal in performing pattern completion for memory of the Homecage. Additionally, HD cells in pups younger than P15 cannot recall a preferred firing direction from memory, which is seen here likely as a consequence of the long inter-trial intervals and movement between separate rooms.

Overall, the within-trial stability presents a striking pattern of spatial firing being better in Open Field than the Homecage. When taken together with the multi-peaked nature of the cell rate maps in the Homecage, and differences between RV and SI, it suggests that HD cells are unstable and may frequently reset their PFD within the homecage environment. There is furthermore an improvement in the across-trial stability of cells parallel to the period of eye-opening in these animals, suggesting that the stability of cell firing between recording trials is assisted by the integration of allothetic (visual) inputs.

6.3.3 Investigation of head direction cell activity during active movement epochs

One possibility for the apparent disruption to directional tuning observed in the Homecage and Small Box trials are the relatively frequent passive movement events of the pup, either by the experimenter (to encourage spatial sampling of the animal's Homecage) or the mother (who frequently moves the animals around throughout the recording trial, either to nest or to migrate the huddle to another section of the cage). In comparison, conspecifics were absent during the Open Field and there were significantly

fewer occasions involving the experimenter touching the pup during the course of the recording trial given less encouragement was needed by the experimenter for the animal to sample the environment. This raises the possibility that at each point the pup is passively moved by either the experimenter or the mother, the pup undergoes a period of reorientation which resets the cells and therefore results in drift of the cell's PFD.

While movements made by the mother were not registered on the neural data logger, event strings were transmitted to the logger at every instance of the experimenter touching the pup and this was marked with a timestamp. An initial step in investigating the directional firing of HD cells before and after passive movement events was to break up each trial into epochs of active movement during which time the animal was not moved by the experimenter. The number of passive movements of the pup was significantly affected by the recording environment (Figure 6.11A; 2-way mixed ANOVA: F(3,102)=28.262, p<0.001, η_p^2 =0.454), with trials in the Homecage (Homecage-A and Homecage-B) having a much higher incidence of these events compared to the corresponding Open Field and Small Box trials (Pairwise comparison: Homecage-A vs Open Field: p<0.001; Homecage-A vs Small Box: p<0.001; Homecage-B vs Open Field: p<0.001). Pups were moved more frequently by the experimenter during Homecage recordings, but the amount of times that they were moved did not change with age (2-way mixed ANOVA: F(4,22)=0.813, p=0.53, η_p^2 =0.129). Correspondingly, there was a significant impact of recording environment on the average duration of active movement epochs (2-way mixed ANOVA: F(3,66)=13.419, p<0.001, η_p^2 =0.379). As expected, the average duration of active movement epoch was significantly higher in the Open Field compared to Homecage and Small Box trials (Figure 6.11B; Pairwise comparison: Homecage-A vs Open Field: p=0.003; Open Field vs Homecage-B: p<0.001; Open Field vs Small Box: p=0.001).

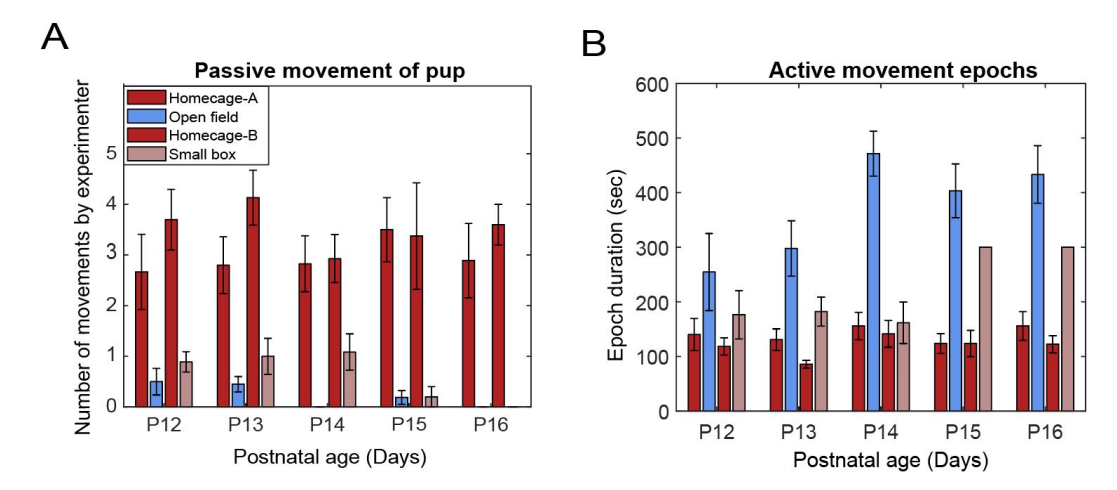


Figure 6.11: Passive movement of animals during recording trials. Trials per age group: P12: n=12; P13: n=20; P14: n=23; P15: n=16; P16: n=10. **(A) Number of passive movements of the pup by experimenter.** There was a significant main effect of the environment on the number of passive movement events $(F(3,102)=28.262, p<0.001, \eta_p^2=0.454)$. There was no significant interaction between environment and age on the number of passive movements $(F(12,102)=0.827, p=0.623, \eta_p^2=0.089)$. There was no significant main effect of age on the number of movement events $(F(4,34)=1.376, p=0.263, \eta_p^2=0.139)$. **(B) Active movement epoch duration.** There was a significant main effect of the environment on epoch duration $(F(3,66)=13.419, p<0.001, \eta_p^2=0.379)$. There was a significant interaction between environment and age on epoch duration $(F(12,66)=2.111, p=0.001, \eta_p^2=0.277)$. There was no significant main effect of age on epoch duration $(F(4,22)=0.813, p=0.53, \eta_p^2=0.129)$.

Due to the difference in epoch duration, it is not possible to directly compare epochs of active movement in the Homecage to epochs in the Open Field. In order to ascertain whether the effect observed in prior analyses was due to the passive movement of the pup by the experimenter, the next step was to resample epochs from both Open Field and Small Box trials of duration comparable to those of the Homecage trials. In order to resample the Open Field data, we first parameterised the population of active movement epoch distributions in the Homecage, so as to allow the random resampling of a matched population in the Open Field. To do this, all active movement epoch durations from Homecage-A and Homecage-B trials were merged for each age bin, P12-P16. A number of probability distributions were then fit to the data (Figure 6.12) and the log likelihood computed for each. The distribution which best fit the actual data was

Probability distribution of active movement epoch duration in homecage

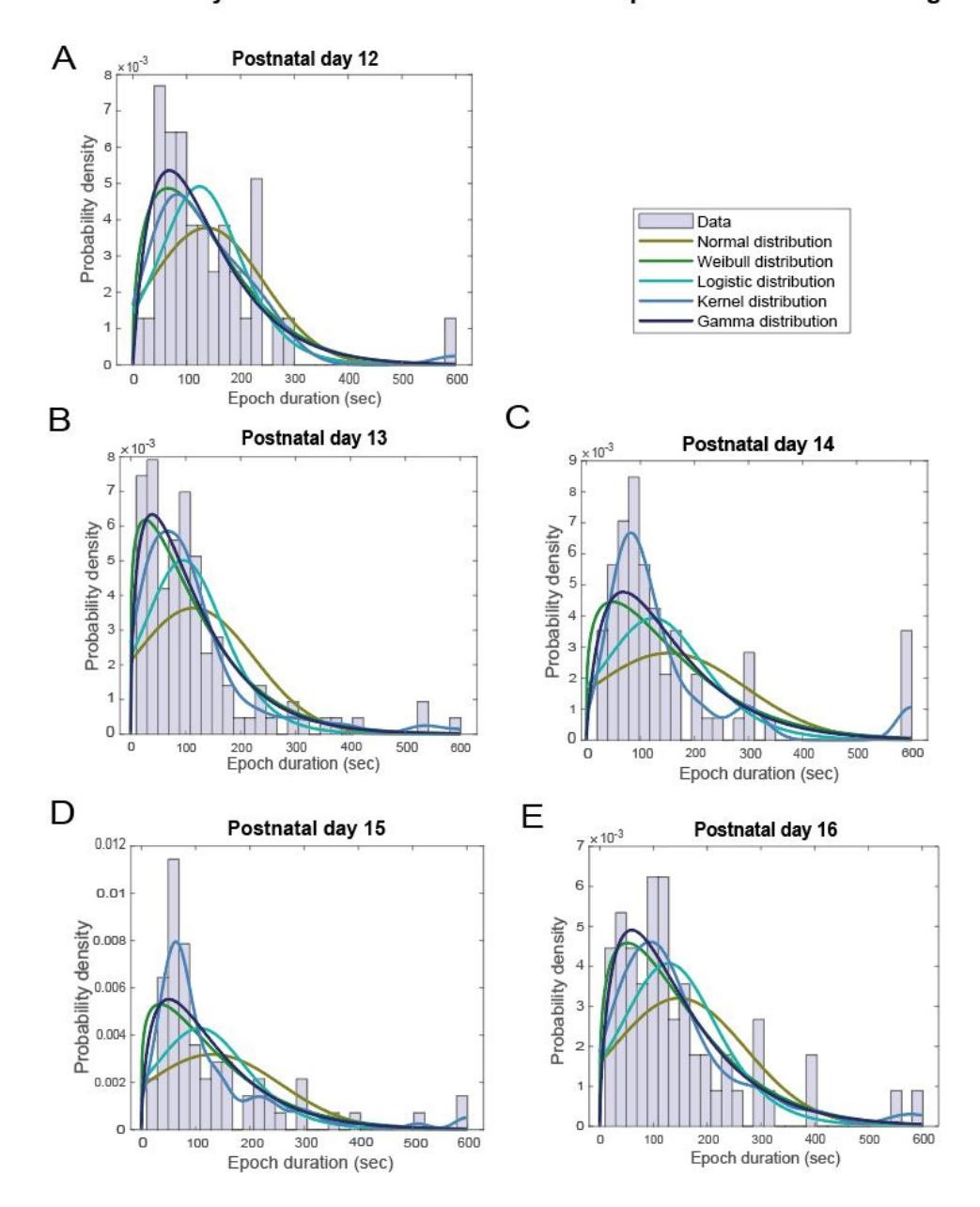


Figure 6.12: Probability distribution of active movement epoch duration in the homecage. Epoch durations were sampled from each distribution corresponding to the recorded ages P12-P16, given the distribution of best fit (chosen on the basis of highest log likelihood). Open Field and Small Box trials were then randomly sampled for active movement epochs of the sampled durations. **(A) P12.** Best fit distribution: Normal, log likelihood 236.56; mean: 137.07 seconds; standard deviation: 105.58 seconds. **(B) P13.** Best fit distribution: Normal, log likelihood 666.22; mean: 114.47 seconds; standard deviation 109.7. **(C) P14.** Best fit distribution: Normal, log likelihood 464.95; mean: 152.25 seconds; standard deviation: 142.18 seconds. **(D) P15.** Best fit distribution: Normal, log likelihood 443.21; mean: 131.12 seconds; standard deviation: 125.27 seconds. **(E) P16.** Best fit distribution: Normal, log likelihood 355.37; mean: 147.43 seconds; standard deviation: 124.5 seconds.

chosen on the basis of the maximum log likelihood. For each age bin presented here, a normal (Gaussian) distribution represented the data best. Using the distribution information including the mean and standard deviation, a new distribution of epoch durations were modelled and resampled for each age bin. The number of resampled epochs corresponded to the median number of epochs observed for that age bin in the Homecage. Epochs were then resampled as described in Section 6.2.8, ensuring that epochs were only included in this analysis if they met a number of predefined criteria. A caveat of this method is that the resampling procedure is incapable of mitigating the cumulative drift in the directional signal of HD cells induced by passive movement periods made by the experimenter nor the mother, however it remains a useful analysis to discern whether passive movement contributes to the low unidirectional tuning of homecage-recorded cells across an entire trial.

As seen in Figure 6.13, following resampling of active movement epochs from Open Field trials there was no significant effect of environment on either the epoch duration (Figure 6.13A; Homecage-A and Homecage-B were combined for this statistical test; 2-way mixed ANOVA: F(2,492) = 2.42, p=0.09) or the number of active movement epochs (Figure 6.13B; 2-way mixed ANOVA: F(3,126)= 1.65, p=0.181). With respect to the within-epoch stability subsequent to resampling (Figure 6.13C), there remained a significant main effect of the recording environment on the stability of cells (2-way mixed ANOVA: F(3,60) = 3.892, p=0.013). Overall, cells recorded in the Small Box were significantly less stable within active movement epochs than in corresponding Homecage and Open Field trials (Pairwise comparison: Homecage-A vs Open Field: p=0.026; Open Field vs Small Box: p=0.031; Homecage-B vs Small Box: p=0.057). The finding that the within-epoch stability of cells remains low in the Homecage and Open Field is striking. The reason for low within-epoch stability is unclear, but is most likely a consequence of the small amount of data within these short

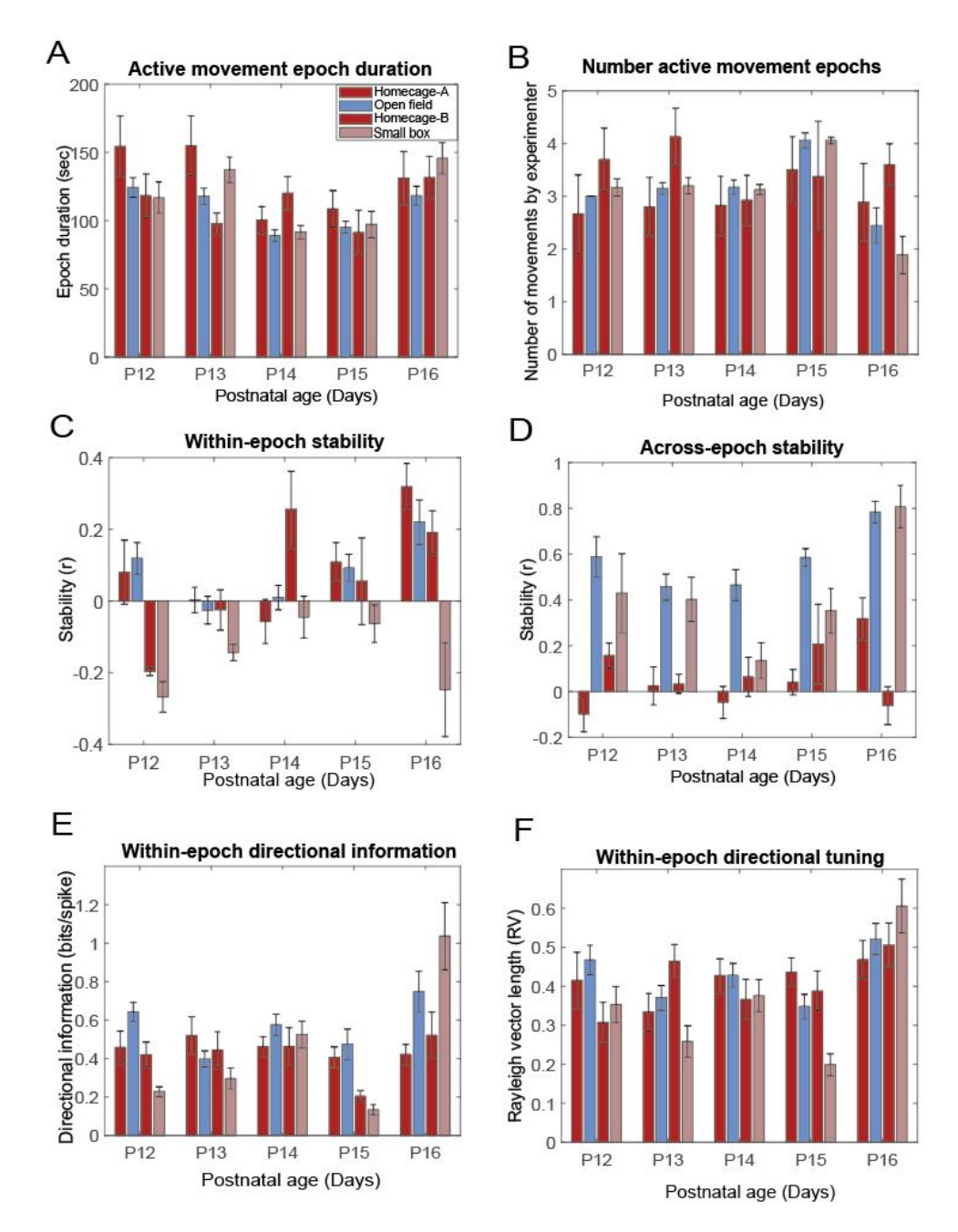


Figure 6.13: Analysis of HD cell activity during active movement epochs after resampling from Open Field and Small Box trials. Trials per age group: P12: n=12; P13: n=20; P14: n=23; P15: n=16; P16: n=10. Cells per age group: P12: n=5; P13: n=30; P14: n=33; P15: n=55; P16: n=68. (A) Epoch duration. Duration of active movement epochs across recording trials was the same following resampling (2-way mixed ANOVA: F(2,492) = 2.42, p=0.09, η_p^2 =0.305 = 0.01). (B) Number of active movement epochs. After resampling, there were an equal number of active movement epochs across trials (2-way mixed ANOVA: F(3,126) = 1.65, p=0.181, $\eta_p^2 = 0.305 = 0.038$). (C) Within-epoch stability. Recording environment had a significant effect on the within-epoch stability of cells (2-way mixed ANOVA: F(3,60) = 3.892, p=0.013). (D) Across-epoch stability. Recording environment had a significant effect on the across-epoch stability of cells (2-way mixed ANOVA: $F(3,144)=21.084, p<0.001, \eta_p^2=0.305)$. (E) Within-epoch directional information. There was a significant main effect of the environment on within-epoch directional information $(F(3,192)=5.288,p=0.002, \eta_p^2=0.076)$. (F) Within-epoch directional tuning. There was a significant main effect of the environment on within-epoch RV (F(3,192)=6.710,p<0.001, $\eta_p^2 = 0.095$).

epochs (during both Homecage and Open Field trials) or due to the mother passively moving the pup (during Homecage trials).

Parallel with the stability of cells during the entire recording trial, the across-epoch stability was significantly different between recording environments (Figure 6.13D; 2-way mixed ANOVA: F(3,144)=21.084, p<0.001, η_p^2 =0.305). Specifically, stability between active movement epochs in the Open Field was significantly higher than in the corresponding homecage (but not Small Box) trials (Pairwise comparison: Homecage-A vs Open Field: p<0.001; Homecage-B vs Open Field: p<0.001). One reason for this improvement of across-epoch stability in Open Field epochs is likely due to the overall stability of cells in the Open Field for an entire recording trial. Given the cell firing is stable over longer time periods (five minutes), it follows that cell firing will remain stable also over shorter time periods dictated by epoch duration. The low across-epoch stability in the Homecage, by comparison, is consistent with the PFD of HD cells resetting when animals are passively moved.

Furthermore, the recording environment had a significant effect on the directional information of cells during active movement epochs (Figure 6.13E; F(3,192)=5.288, p=0.002, η_p^2 =0.076). There was also a significant interaction between age and environment on the directional information of cells during active movement epochs (2-way mixed ANOVA: F(12,654) = 7.455, p<0.001). While the within-epoch directional information of cells in the Homecage stays relatively stable with age, there is a vast increase in the Small Box condition and to a lesser degree the Open Field. Most strikingly, the directional information of cells in the Open Field did not significantly differ from Homecage-A after resampling (p=0.075).

Interestingly, the unidirectional tuning of HD cells recorded in Homecage-A trials was vastly improved in comparison to analysis of the entire trial. As a consequence, there was no significant difference between Homecage-A and the Open Field in terms of cell RV length during these epochs (p=0.378). Nevertheless, the unidirectional tuning of cells during active epochs was also significantly affected by environment (Figure 6.13F; 2-way mixed ANOVA: F(3,684)=5.110, p=0.02, η_p^2 =0.022), such that RV length of cells during Small Box trials was significantly different to Open Field trials (Pairwise comparison: p<0.001). The effect observed in Homecage-A during epochs seems to best capture the main effect observed in homecage trials, particularly considering that Homecage-A is the primary probe condition and best sampled trial of the homecage trials.

Representative HD cell polar plots before and after a period of passive movement are presented in Figure 6.14, for a cell during a Homecage-A trial (Figure 6.14A; P13), a Homecage-B trial (Figure 6.14B; P15), and an Open Field trial (Figure 6.14C; P15). What is apparent is that during a given active movement epoch, the amount of drift in the PFD of a given neuron is small. This is observed by comparing the polar plots of cells during the first and second half of that epoch. Some drift is still observed, particularly in the P13 example (Figure 6.14A), reflective of the low within-epoch stability observed at this age. Differences in recording trials become apparent across epochs (i.e. after a period of passive movement), whereby there are large changes observed in the PFD of cells during Homecage trials, but not Open Field trials. No large changes in PFD are observed in the Open Field trial as no real passive movement occurs in these trials.

Evidence of this is further seen in Figure 6.15. Significant changes in the directional correlate of cells are observed across successive active movement epochs during Homecage trials. In contrast, no discernible changes are observed in the directional correlate of cells in the Open Field across consecutive epochs as there is no interval of passive movement accounted for with the resampling procedure. This trend persists across all ages at which recordings were made (P12-P16; Figure 6.15A-E).

What these findings suggest is that within Homecage-A trials, resetting of HD cells is frequent and specifically happens after periods of pas-

sive movement. Thus directional correlation of cell firing within trials may be poor. However, on short timescales of active movement, these cells successfully integrate any number of proximal cues (conspecifics, olfactory or tactile cues) which are available in addition to those which are also present in the Open Field (walls and corners), therein conferring additional directional selectivity. It is intriguing that the same measures computed for cells recorded in Homecage-B trials was substantially lower than the corresponding Homecage-A trials (although not statistically significant between the two). One possibility is that few active movement epochs in Homecage-B trials passed the criteria for inclusion in this analysis. Interestingly, across both measures the Small Box active movement epochs are diminished in comparison to both Homecage and Open Field conditions until post eye-opening (P16).

As outlined in Section 6.2.4, the mother rat had a proclivity for reorganising the pups into a huddled configuration within the cage, typically relocating them two to three times during a given trial. This maternal behaviour inadvertently prompted additional passive movement of the recorded pup. While video recordings were captured for each trial, offering the potential to analyse the frequency and duration of these passive movements by the mother, the complexity of tracking multiple animals and distinguishing the mother from the litter posed significant challenges. Consequently, this specific analysis was beyond the scope of this thesis. Nevertheless, it's important to acknowledge that comprehending the impact of the dam's passive movements on the results remains challenging. Subsequent investigations should aim to disentangle these two events within the context of the finding presented here.

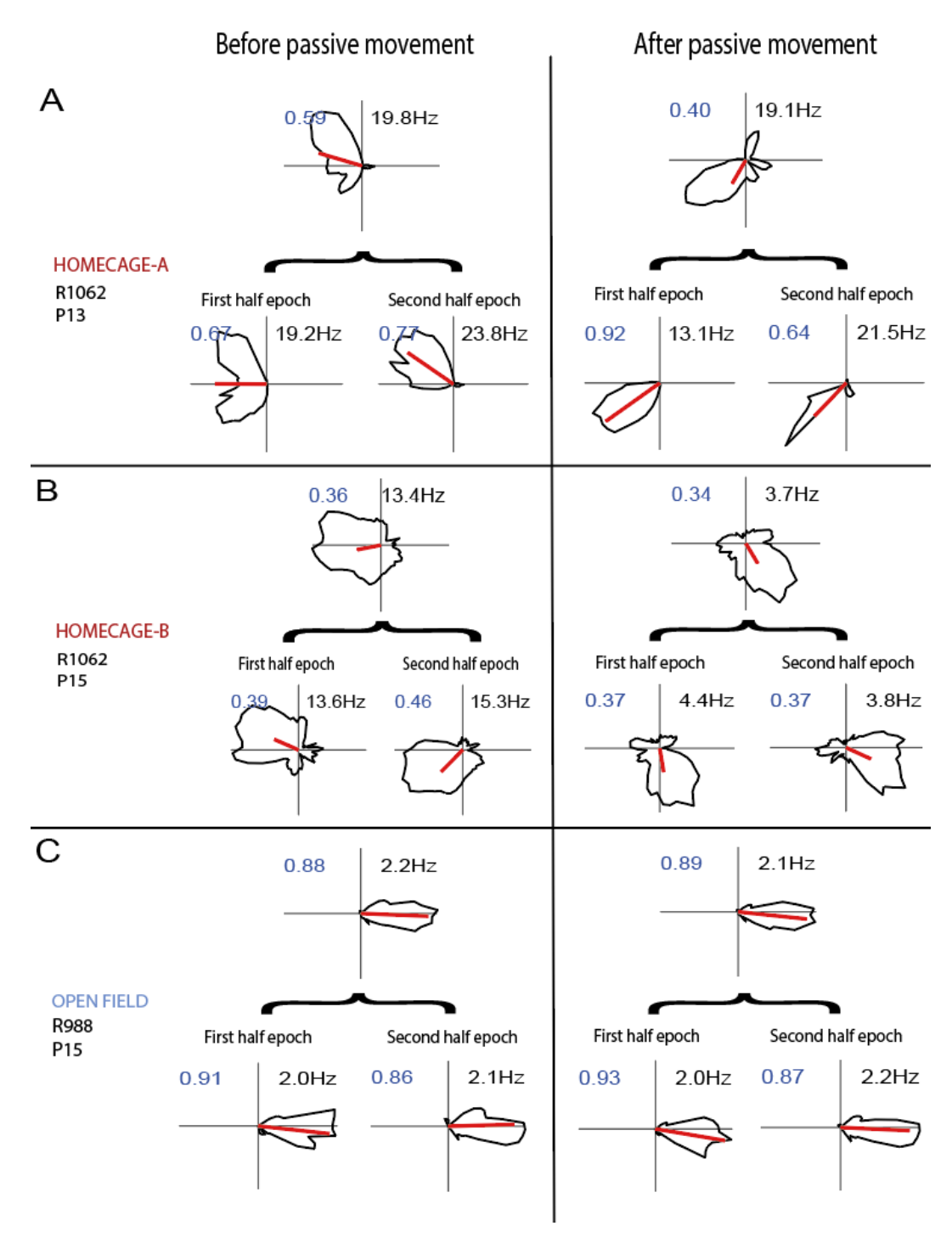


Figure 6.14: Representative HD cells before (left panel) and after (right panel) a period of passive movement recorded during a (A) Homecage-A trial, (B) Homecage-B trial, or (C) Open Field trial. Shown here are polar plots of cell firing rate versus head direction. The number in blue indicates the Rayleigh vector (RV) length, and the number in black indicates the peak firing rate (Hz). Within an active movement epoch, there are minimal changes in cell PFD ('First half epoch' versus 'Second half epoch'). Conversely, following passive movement, we observe substantial shifts in cell PFD in Homecage trials (A-B). No significant changes are observed in Open Field trials (C) following resampling as there is no real period of passive movement.

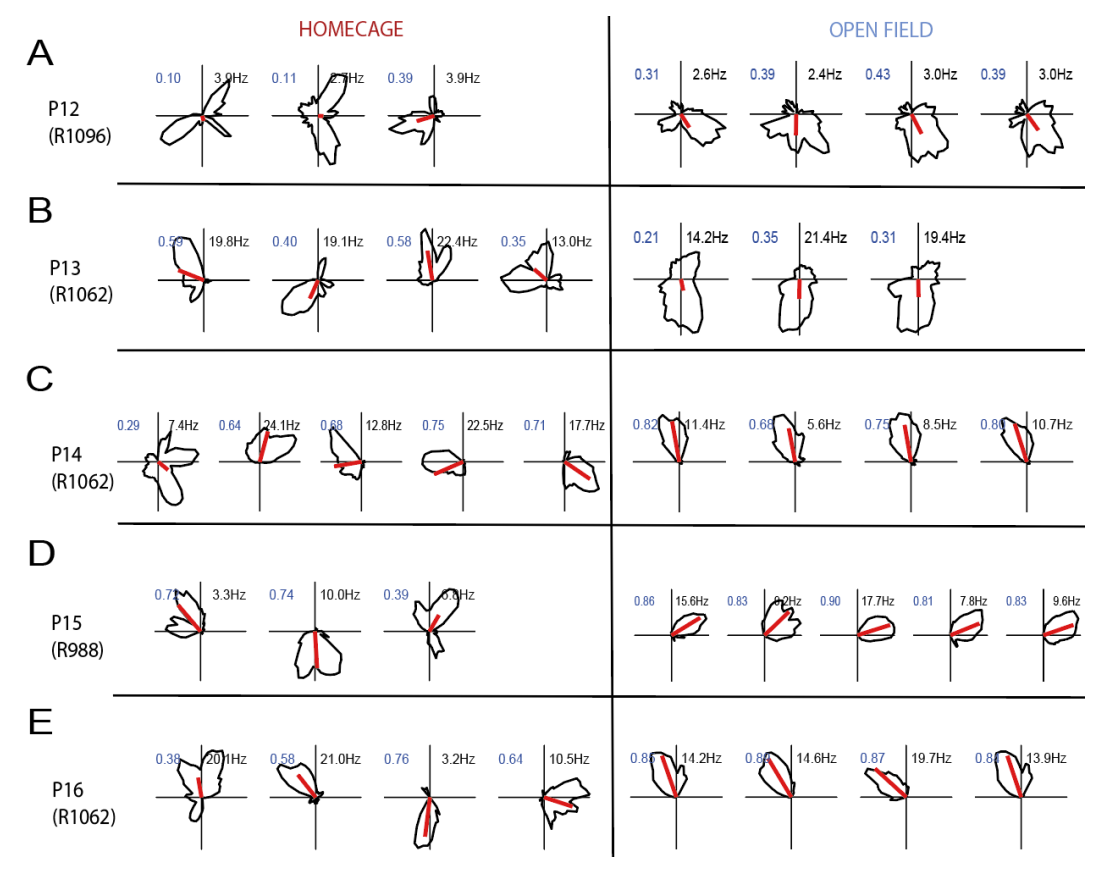


Figure 6.15: Representative HD cells across consecutive epochs within a Homecage trial (left panel) or Open Field trial (right panel). Examples are given for each recorded age, from (A) P12 to (E) P16. Shown here are polar plots of cell firing rate versus head direction. The number in blue indicates the Rayleigh vector (RV) length, and the number in black indicates the peak firing rate (Hz). Each polar plot within a given row shows the directional correlate of the cell during consecutive active movement epochs (interspersed with intervals of passive movement). There are significant changes in the directional correlate of cells across consecutive epochs in the Homecage which is not seen in Open Field trials.

6.3.4 Temporal and spatial coupling of recorded cells on short-timescales

One important attribute of the attractor network properties of the HD network in rodents is that cells with similar PFDs will fire in close temporal proximity, whilst cells with highly different PFDs will fire with a temporal delay, in line with movement of the 'hill of activity' (i.e. the rat's heading direction) around a one-dimensional ring attractor network. The cells within the HD ring attractor rotate coherently during drift or landmark control, such that the relative offset in mean direction between cells remains stable.

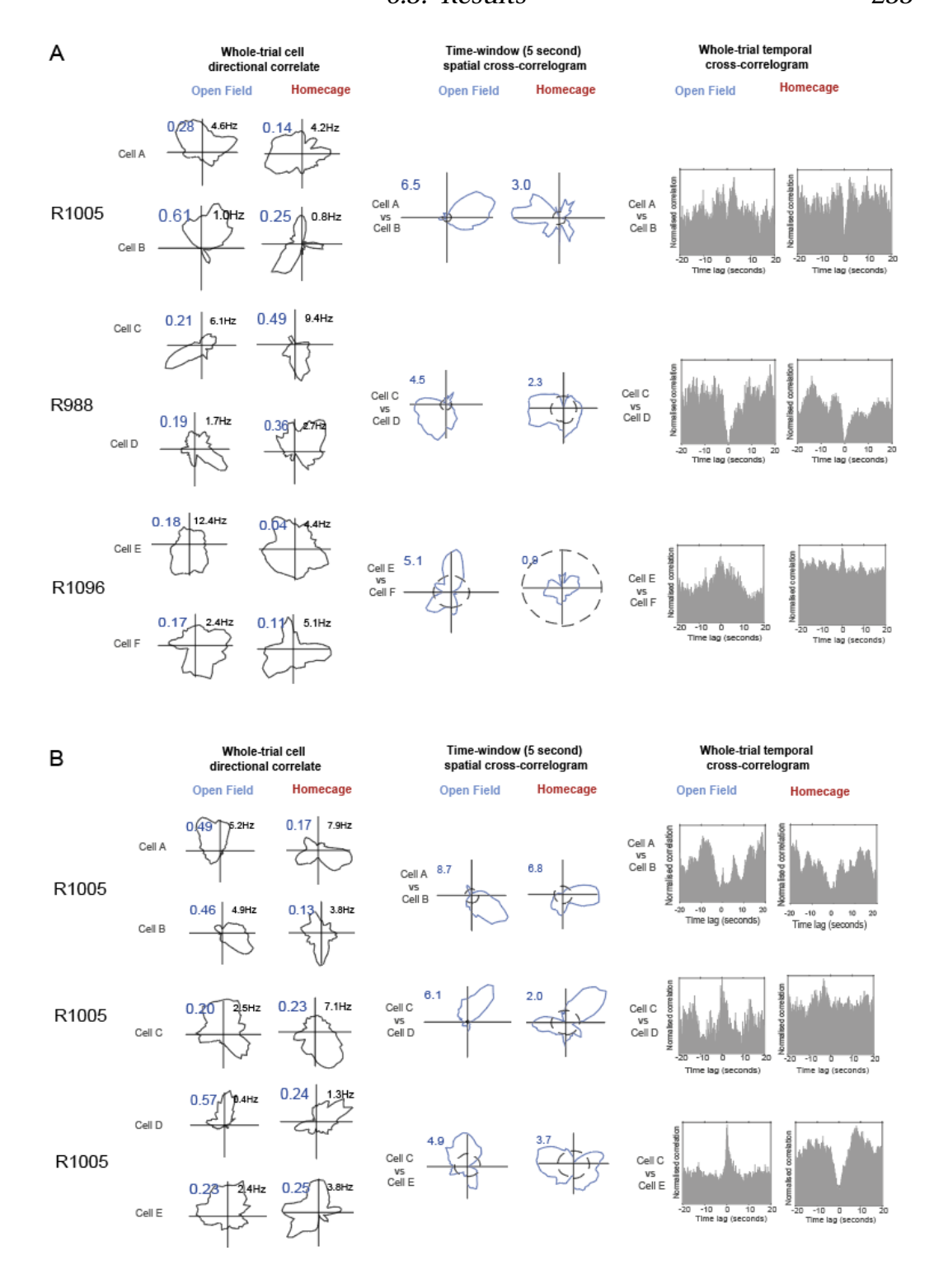
As discussed in Section 6.1.1, prior work has demonstrated the existence of these temporal and spatial couplings between co-recorded HD cells in line with the continuous attractor network properties described, preceding stability of the cells' PFD over long timescales (on the order of minutes; Bassett et al., 2018). Given that the described experiment probed the attractor dynamics of HD cells pre eye-opening in just one environmental 'context' (an open field, of both large and small dimensions), it remains to be shown whether the effect observed in Bassett et al. (2018) was applicable to all environmental contexts.

Therefore, the attractor network properties of cell ensembles were calculated on short timescales in the Homecage and Open Field. Temporal cross-correlograms and time-windowed spatial cross-correlograms (TWCs) were computed on short-timescales (5 seconds) for all cells which passed the criteria for HD cell inclusion. Given the results thus far suggesting that HD cells are significantly more stable and exhibit higher directional tuning in the Open Field, for all subsequent analyses the Open Field trial was treated as the canonical trial from which the ordering of cells was dictated whilst the Homecage trial was considered the probe trial. Note that as there were no co-recorded cell pairs during P12 recordings, P12 has been excluded from this analysis.

It is important to highlight that this analysis allows for a direct assessment of the inherent connectivity among HD cells in both homecage and open field trials, as it remains unaffected by the cumulative drift observed in HD cells recorded within homecage trials due to passive movement periods. We selected five-second windows for cross-correlation analysis, as no passive movement episodes occurred within intervals shorter than 10 seconds. Consequently, the cross-correlation analysis was exclusively conducted during timeframes when the animal was not subjected to passive movement by the experimenter. Nevertheless, it is difficult to rule out the possibility of the mother passively moving the pup during these timewindows.

Representative examples of TWCs are seen in Figure 6.16. As expected, the whole-trial directional correlate of cells have stronger unidirectional tuning in the Open Field than in the Homecage. This is reflected in the TWC: Whilst there is a clear directional correlate in the TWC of cells during Open Field trials, the corresponding spatial correlate in the Homecage TWC is present but with less pronounced directional tuning. This suggests that either there is drifting on the short-timescales of the TWCs (in this case, 5 second windows), or that the attractor is less tightly coupled in the Homecage. The increased unidirectional tuning of the TWC in the Open Field suggests a more coherent internal network structure than the Homecage. The TWC tuning curve in the Open Field also deviates further from the shuffled mean (black dotted line) than in the Homecage. This indicates that the level of spatial coupling in the Open Field is unlikely to be experienced by chance, whereas the same may not be said for cell pairs in the Homecage. The temporal cross-correlogram for cells with similar PFDs display a characteristic peak in line with the cell pairs both firing in quick succession. Conversely, the temporal cross-correlogram of cells with largely differing PFDs show a clear trough in line with a delay in the time between one cell and then the other firing. Given the level of drift of cell PFD in the Homecage, this effect is less pronounced in the whole-trial cross-correlogram of the Homecage than the Open Field.

The population-level effect of the TWCs, separated by age, are shown in the left and middle panels of Figure 6.17. Each heatmap represents all co-recorded cell pairs for each respective age bin, sorted by the difference in the PFD of the Open Field TWC. Cell pairs closest to the top and bottom have the largest difference in PFD, while cells towards the middle of the heat map have the smallest difference in PFD. Adult-like coherence between cell pairs is seen at P16 (Figure 6.17D), where there is a distinct yellow, diagonal band corresponding to the preservation of PFD offset between cell pairs. This effect is consistent in both Open Field and Homecage conditions. This effect slowly degrades at progressively younger ages, particularly at P13 (Figure 6.17A). While in the Open Field, there appears to be some preservation of the fixed spatial offsets between cells (as predicted by an attractor network), this effect appears to deteriorate in the Homecage (there is no trend to the peak firing rate of cell pairs, in line with a lack of spatial coupling). A caveat of this observation is that the number of co-recorded cell pairs is much larger at P15 and P16, compared to at P13 and P14. When this effect is quantified by a circular-circular correlation of the mean direction in the TWC (Figure 6.17, right panel), the correlation between Open Field and Homecage TWCs is lacking at P13 and P14 (r^2 =0.03), which rapidly increases in quick succession from r^2 = 0.29 at P15, to $r^2 = 0.43$ at P16.



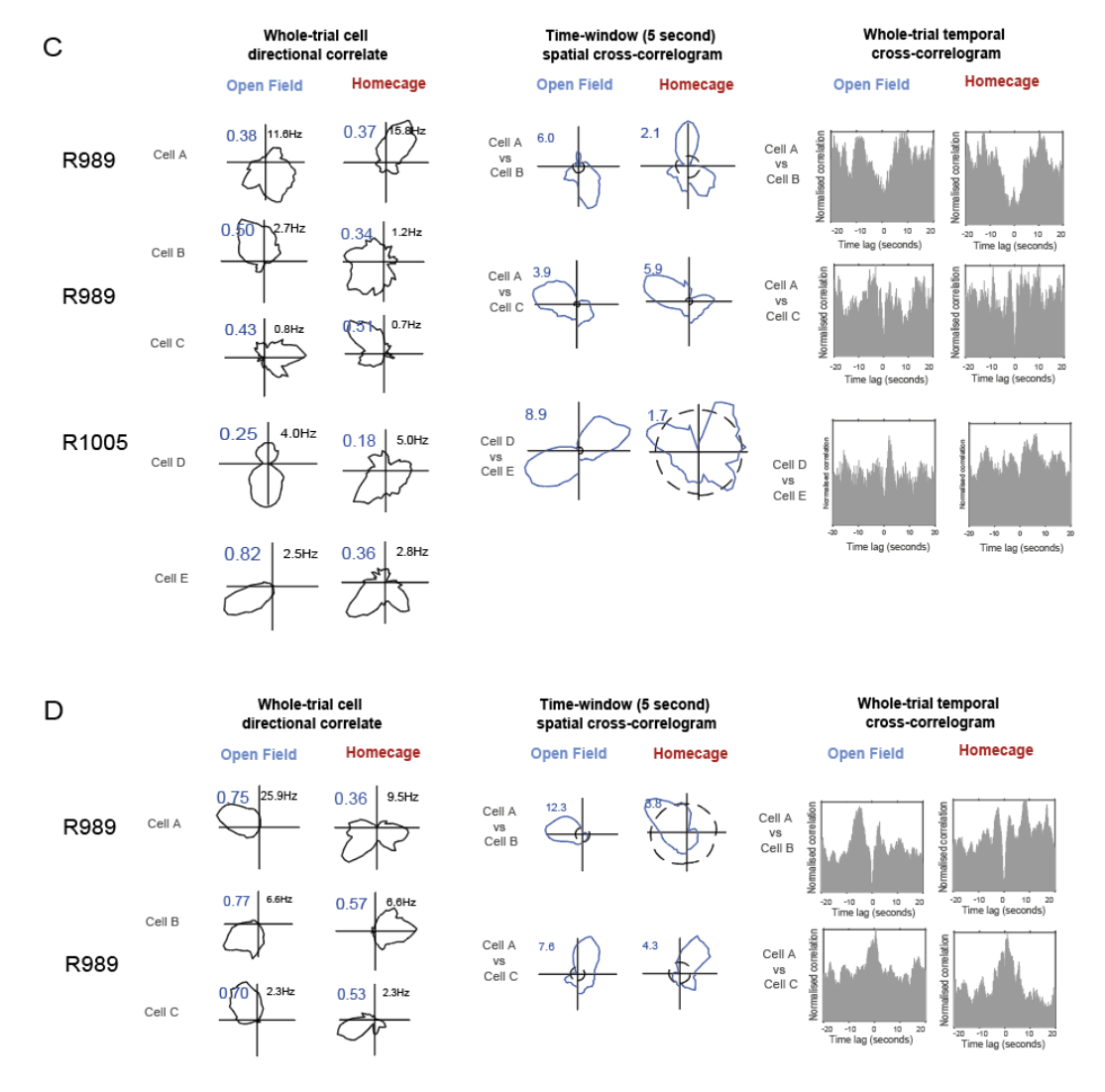


Figure 6.16: Spatial and temporal coupling between representative head direction cells, at each recorded age: (A) P13, (B) P14, (C) P15 and (D) P16. From left to right; Left: Whole-trial directional correlate of simultaneously recorded HD cells in the Open Field and Homecage trials. Middle: Time-windowed (5 second window) spatial cross-correlograms of cells in the Homecage and Open Field trials (blue tuning curve). The black dotted line represents the tuning curve for the mean of the shuffled population of TWCs. The number in the top left corner of the polar plot indicates the maximum value of the TWC. Right: Whole-trial, normalised temporal cross-correlogram of cell pairs, in the Homecage and Open Field trials.

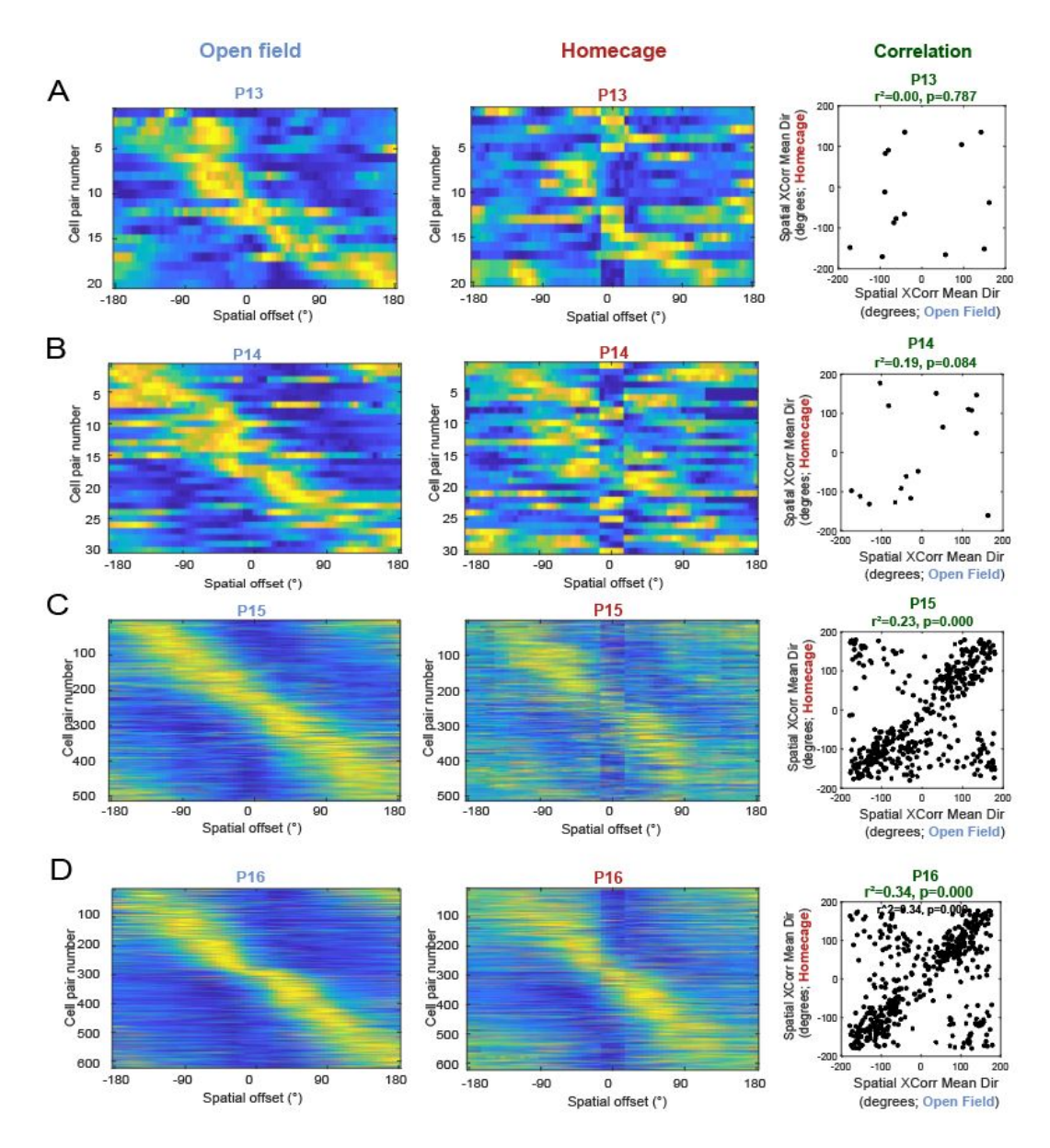


Figure 6.17: Spatial cross-correlogram of head direction cells in age bins P13 (A) to P16 (D), sorted by the magnitude of difference in preferred firing direction in the Open Field, in the Open Field (left panel) and Homecage (middle panel). The heat map shows the firing rate (Hz) of the spatial cross-correlogram. Minimum values are shown in blue, maximum values are shown in yellow. Cell identity order is the same in both conditions, for each respective age bin. **Right panel:** Circular-circular correlation of the spatial cross-correlogram mean direction in the Open Field (x-axis) and Homecage (y-axis), where r^2 is the circular-circular correlation coefficient, and p is the test statistic for a null hypothesis of no correlation.

Figure 6.18 highlights a similar effect with respect to the temporal coupling of cell pairs. At P13 (Figure 6.18A) and P14 (Figure 6.18B), the strength of temporal coupling between cell pairs is relatively poor (indi-

cated by the lack of a strong symmetrical bell curve, left and middle panels). At these ages, the temporal coupling appears strongest for cells with a minimal difference in mean firing direction (with time lag close to zero, the 'peak'), and for those with large differences in PFD (in both heading directions, CW and CCW, the 'trough'). This effect is also more clearly evident between cell pairs during Open Field trials compared to Homecage trials. At P15 (Figure 6.18C) and P16 (Figure 6.18D), the differences between environments is diminished and there is overall a consistent effect of temporal coupling between cell pairs. This effect is reflected in the far right panel of Figure 6.18, wherein the correlation between recording environments is quantified by the mean normalised spike count of the central one second of the temporal cross-correlogram. Linear regression analysis showed a significant association between the temporal cross-correlogram of Open Field and Homecage cell pairs ($r^2 = 0.2$ at P13, p=0.007), which steadily increases with age until there is a significantly higher similarity at P15 ($r^2 = 0.77$, p = 0.000) and P16 ($r^2 = 0.76$, p = 0.000). The presence of temporal coupling at younger ages, but not spatial coupling, may indicate discrepancies in the sampling of animals in the homecage trial impacting the relative spatial offsets of cells.

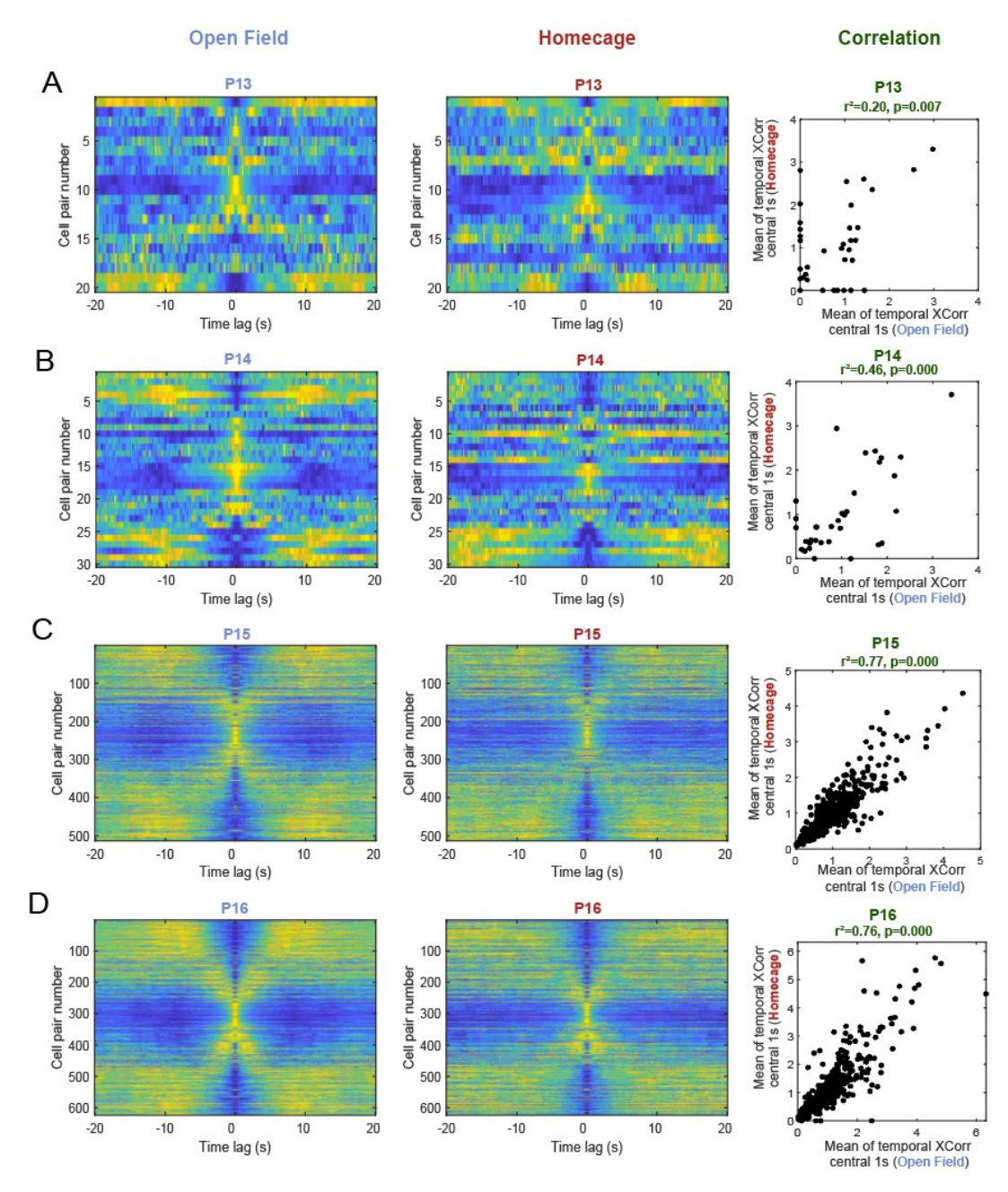


Figure 6.18: Temporal cross-correlogram of head direction cells in age bins P13 (A) to P16 (D), sorted by the magnitude of difference in preferred firing direction in the Open Field, in the Open Field (left panel) and Homecage (middle panel). The heat map shows the correlation of the temporal cross-correlogram, normalised between minimum values (blue) and maximum values (yellow). The top of the heat map corresponds to clockwise heading direction, while the bottom of the heat map corresponds to counter-clockwise heading direction. Cell identity order is the same in both conditions, for each respective age bin. **Right panel:** Correlation of the spatial cross-correlogram of cells in the Open Field (x-axis) and Homecage (y-axis), where r^2 is the linear regression correlation coefficient, and p is the test statistic for a null hypothesis of no correlation.

Pairwise correlation of the TWC directional maps between the Open Field and the Homecage was then quantified. The correlation between directional firing increased with age, with an abrupt increase in correlation between P16 and the preceding age bins (Figure 6.19A; 1-way ANOVA F(3,2532) = 50.837, p<0.001). The maximum of the TWCs (how far the TWC deviates from a shuffled population, or the Z-score), remains significantly higher across age bins in the Open Field compared to the Homecage (Figure 6.19B). Whilst the Z-score of TWCs in the Homecage remains relatively stable across age bins, there is a gradual increase in the Z-score in the Open Field, reaching a maximum, as expected, at P16 (A Friedman test was conducted, showing there was a statistically significant difference in Z-score depending on which environment, $\chi^2(2) = 4083.811$, p<0.001). This indicates the extent to which the TWC is likely to be seen by chance, with higher Z-scores indicating a higher probability of the TWC being observed as a consequence of real effect rather than by chance (given it deviates further from the shuffle). In order to assess the proportion of these TWCs which were significant, a Sidak correction was implemented in order to account for the independent multiple comparisons corresponding to the 61-bin directional maps of the TWC, resulting in a new significance threshold of 3.1415. There was a significant impact of the environment on the number of TWCs exceeding the significance threshold (Figure 6.19C; 2-way mixed ANOVA: F(1,30)=24.952, p<0.001), for which the effect size was large (η_p^2 =0.454). Specifically, the proportion of statistically significant TWCs was reliably higher in the Open Field than in the Homecage, at all ages. A 2-way mixed ANOVA also showed no significant effect of age (F(3,30)=1.321, p=0.286), nor interaction of environment and age (F(3,30)=2.357, p=0.092) on the number of TWCs exceeding the Sidak-corrected significance threshold. The unidirectional tuning of the normalised TWCs was also compared (Figure 6.19D). While the RV length of TWCs in the Open Field was consistently higher than in the Homecage,

there was a gradual increase in the RV length of Homecage TWCs corresponding to an increase in the tuning and stability of whole-trial HD cell firing. The disparity in RV length of TWCs at all ages likely reflects the increased spatial coupling in the Open Field, even on short-timescales. This was confirmed with a Friedman test, showing there was a statistically significant difference in RV length by environment ($\chi^2(2) = 3936.437$, p<0.001). Nonetheless, at all ages the RV length of TWCs remained low (between 0.2 and 0.3), which is likely a consequence of the very small timewindow (5 seconds) resulting in a high degree of noise in cell firing.

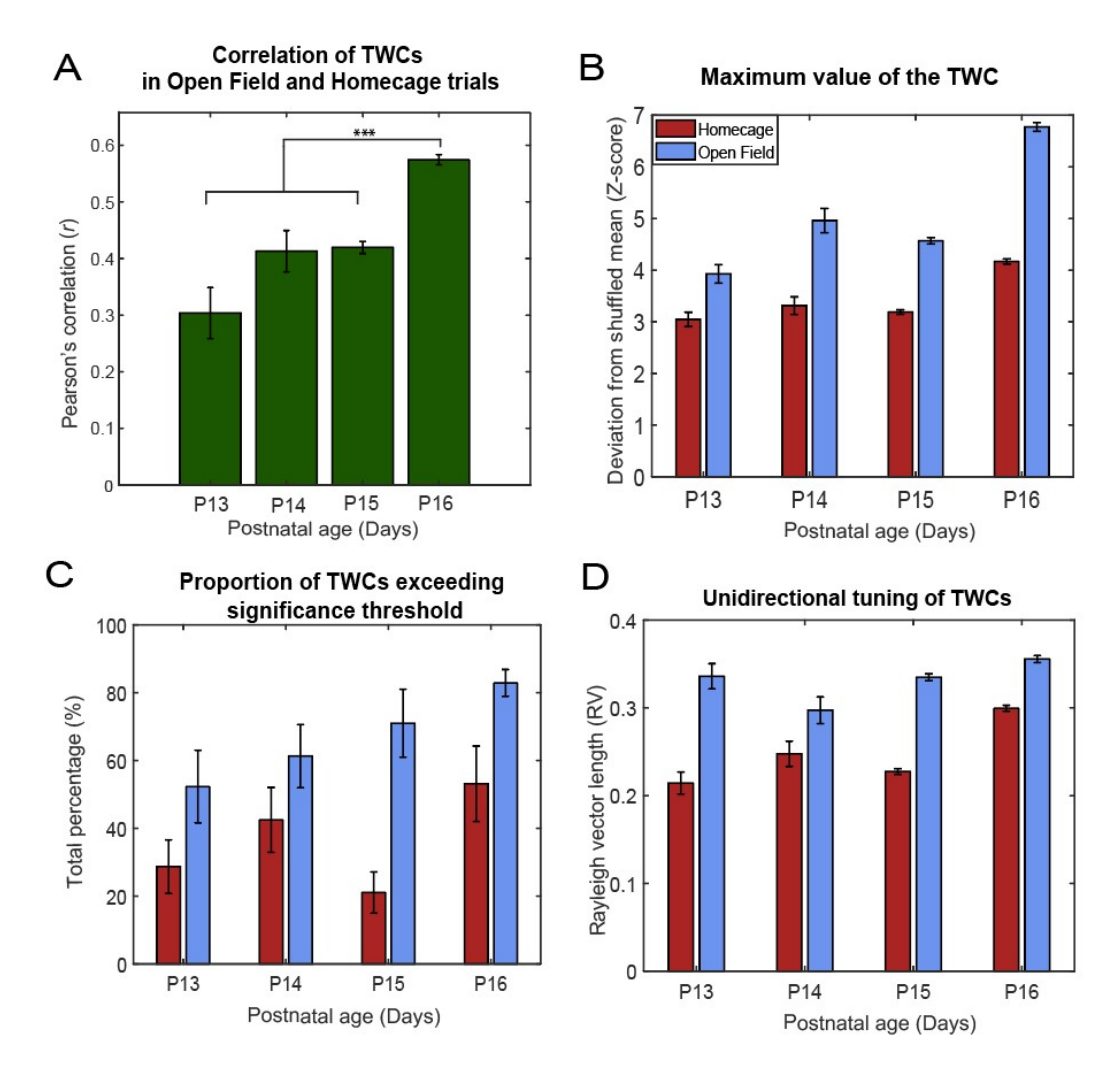
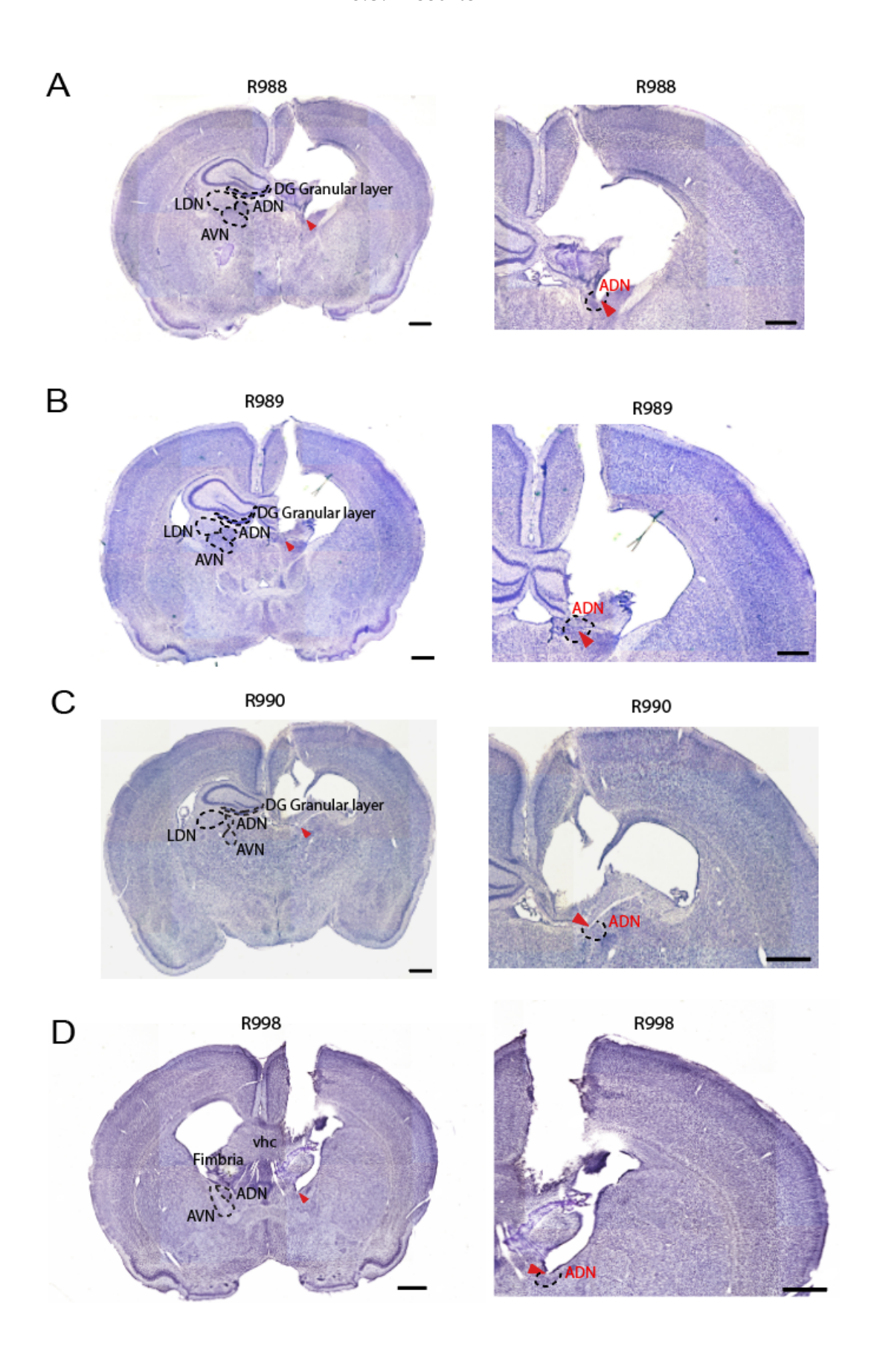


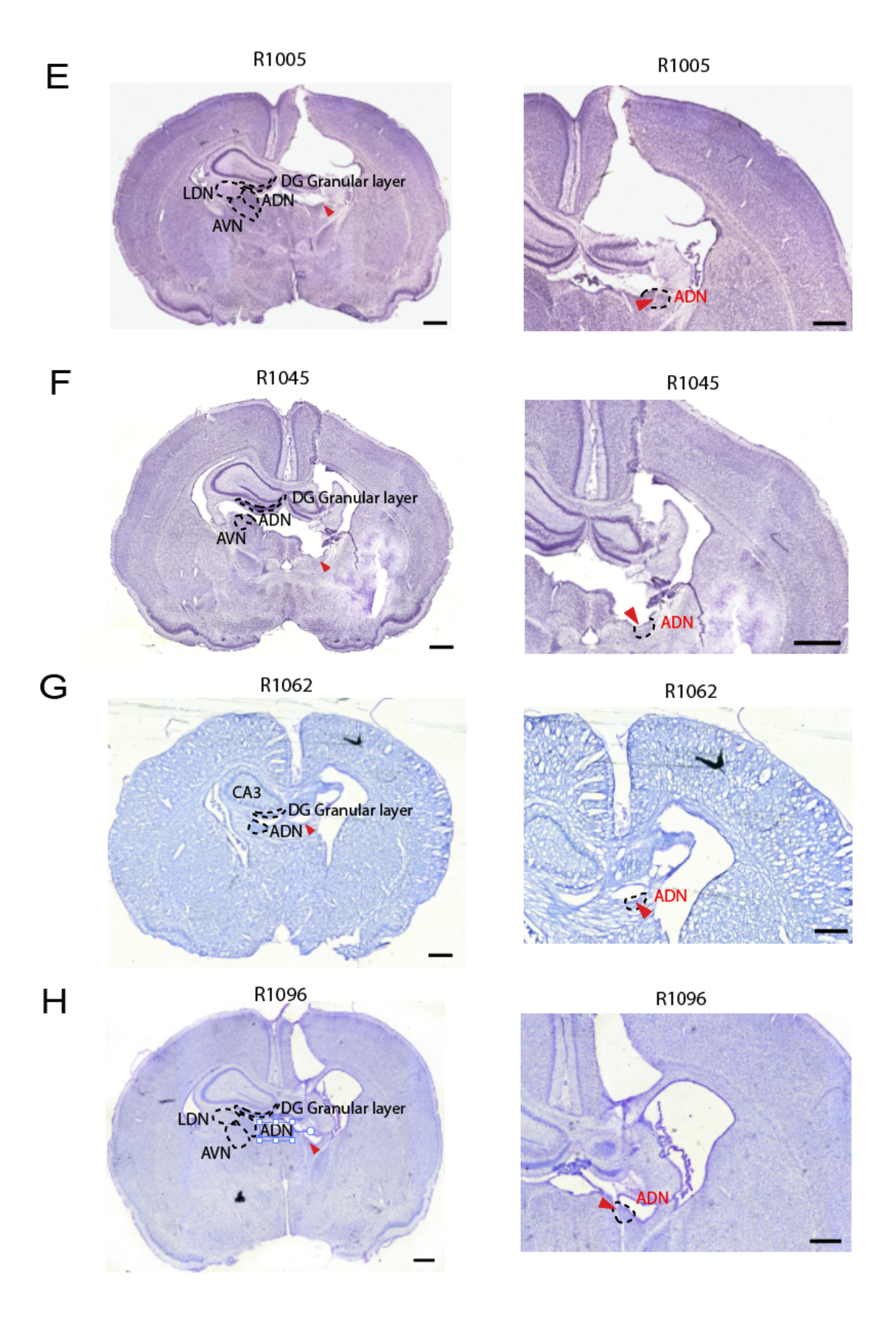
Figure 6.19: Summary properties of time-windowed spatial cross-correlograms of head direction cells in the Open Field and Homecage. Number of TWCs per age group: P13: n=98; P14: n=99; P15: n=1077; P16: n=1323. (A) Pearson's correlation of time-windowed (5 second) spatial cross-correlogram in the Homecage and Open Field. 1-way ANOVA F(3,2532) = 50.837, p<0.001. A Tukey post hoc test revealed that there was a statistically significant increase in correlation of TWCs at P16 compared to all earlier ages (P13-P16: p<0.001; P14-P16: p<0.001; P15-P16: p<0.001). Also between P15 and P13 (p=0.038). **(B) Deviation of time-windowed** spatial cross-correlograms (TWC) from a population of 100 shuffled TWCs. A Friedman test was conducted, showing there was a statistically significant difference in Z-score depending on which environment, $\chi^2(2) = 4083.811$, p<0.001. Post hoc analysis with a Wilcoxon signed-rank test: p<0.001. (C) Proportion of TWCs in the Open Field and the Homecage exceeding a Sidak-corrected significance threshold. There was a significant main effect of the environment on the number of TWCs exceeding the significance threshold (2-way mixed ANOVA: F(1,30)=24.952, p<0.001, $\eta_p^2=0.454$). There was no significant interaction between environment and age in terms of TWCs exceeding the threshold (2-way mixed ANOVA: F(3,30)=1.321, p=0.286, η_p^2 =0.117). There was no significant main effect of age on the number of significant TWCs (2-way mixed ANOVA: F(3,30)=2.357, p=0.092, η_p^2 =0.191). (D) Unidirectional tuning of TWCs in the Open Field and Homecage. A Friedman test was conducted, showing there was a statistically significant difference in RV length by environment, $\chi^2(2) = 3936.437$, p<0.001.

6.3.5 Histology

Confirmation of tetrode placement was confirmed after experiment end, with histological results presented here (Figure 6.20). Note that animals with tetrode implants confirmed not to be in the ADN were excluded from electrophysiological analysis and so are not shown here. All implanted animals, whether tetrode placement was confirmed in the ADN or not, were included in behavioural analysis (summarised in Table 6.1).

Placement of tetrode tracks in the ADN of rats was confirmed with reference to the Rat Brain Atlas (Paxinos and Watson, 2006). In some cases it appears that as a result of the deep implantation of a steel cannula in the brain, there is a certain level of neuronal tissue compression in the hemisphere containing the implanted microdrive. To a certain extent this is unavoidable, but may make precise histological interpretation difficult to determine in some instances. In one particular instance (r1062; Figure 6.20G) there was predominant cryodamage as a consequence of faulty refrigerator settings, but best efforts have been made to ascertain the anatomical localisation of electrodes tracks based on both the histological examination as well as experimenter tetrode-lowering notes from recording trials.





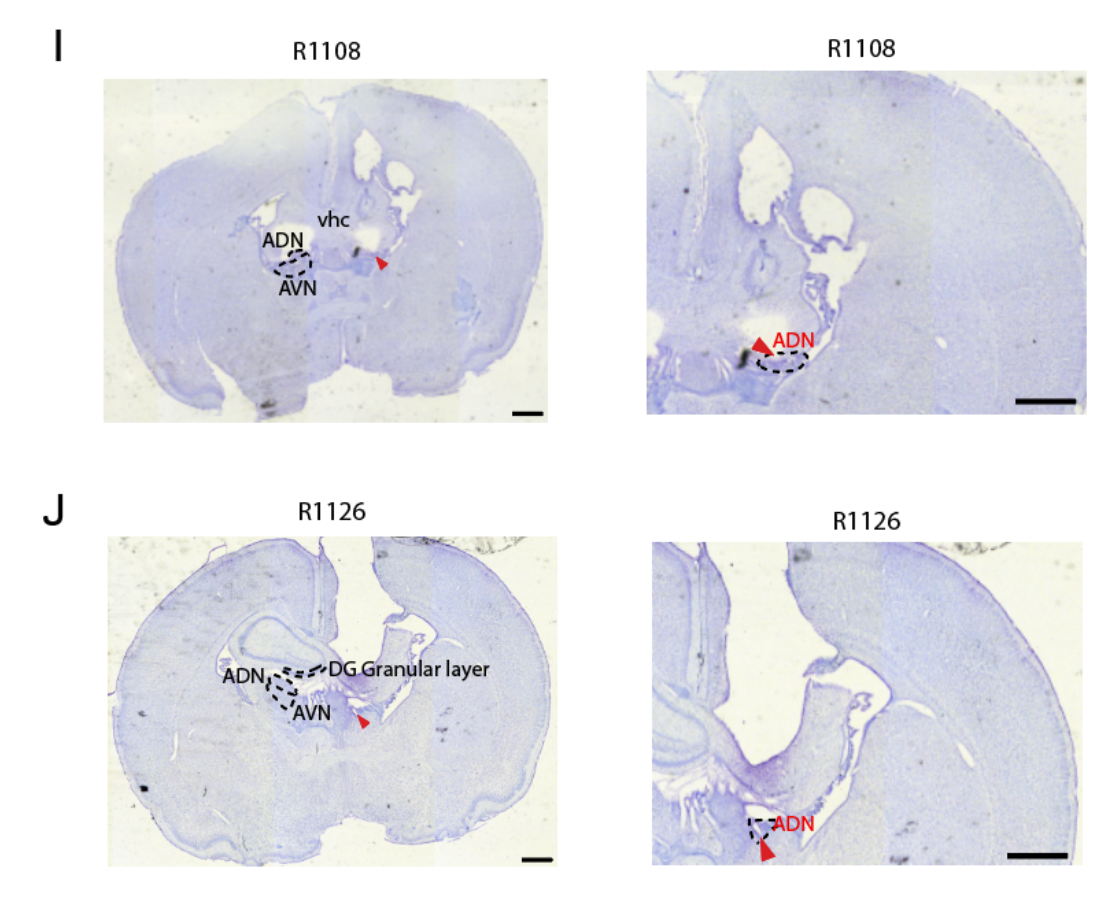


Figure 6.20: Histology of electrophysiology animal subjects. Each row A-J corresponds to a different animal. Note that rat 1062 brain was subject to cryodamage due to electrical fault fridge temperature storing this brain. Red arrows point to electrode tracks in the ADN. Black scale bars represent 1mm. ADN: Anterodorsal thalamic nucleus; AVN: Anteroventral thalamic nucleus; DG: Dentate gyrus; LDN: Laterdorsal thalamic nucleus; vhn: ventral hippocampal commissure.

6.4 Chapter discussion

Making use of the wireless technology presented in Chapter 5, this experiment sought to assess the postnatal development of head direction cells in a relatively naturalistic environment compared to exploration in a standard open field enclosure of the same dimension. It is important to note that rearing with enrichment was not being tested here, so a classic environmental enrichment experiment was not being conducted. Instead, the purpose was to ascertain whether the manifestation of hard-wired neural circuits for spatial navigation in early development is dependent on the context within which the animal is situated. We explored whether the stabilisation of the HD network emerges earlier in environments having increased familiarity and cue complexity (more 'naturalistic' environments) compared to the open field, to assess whether HD neurons reach adult-like stability at the same time that attractor connectivity emerges. The possibility that attractor connectivity precedes stable HD firing in all contexts was an outstanding caveat to the conclusion of Bassett et al., 2018, and was a hypothesis which was investigated in this study. The results indicate that whilst temporal coupling is present at all ages, spatial coupling was absent at the youngest recorded ages in the homecage.

Some important caveats must be noted in this regard, which make it difficult to make direct postulations that the age of the animal and the homecage setting disrupting the HD cell attractor as shown. Variations in the frequency of passive movements introduced by the experimenter during homecage experiments have likely contributed to cumulative drift in the directional correlation of cells, posing challenges for precise control in our analyses. Five-second time windows for cross-correlation analysis was used to mitigate this issue, as no period of passive movement occurred over a timespan less than 10 seconds, ensuring the analysis was not conducted across intervals when the animal was passively moved by the experimenter. However, it remains challenging to completely account for

the potential influence of passive movement made by the mother, which may have similar effects. The mother's tendency to move the pups occurred typically between two to three times per trial, but our scope did not allow for precise pinpointing of these occurrences. Consequently, the cross-correlation analysis may not represent an entirely unbiased measure for quantifying the temporal and spatial coupling of cells comprising the HD attractor across homecage and open field trials. Additional variables may have also contributed to the observed findings, such as the low firing rates of some cells, the number of recorded cells at each age or the animal's movement statistics. Notably, the increase in the number of recorded HD cells with age results in fewer cell pairs at younger ages, limiting the inferences that can be drawn from our analysis. Additionally, variations in angular velocity and spatial sampling among animals could further impact the results. Therefore, future work may seek to investigate this research question by controlling for such variables.

The main differences of note between the Homecage and Open Field trials were the presence of conspecifics, bedding, and the litter 'nest' where the huddle spends the majority of the time outside of recording trials. It is likely that the presence of other moving animals with which the pup frequently encounters may be serving as proximal, highly mobile orienting cues. Given that these cues are absent in the Open Field, which is a novel environment to the animal upon first exposure, pups tended to evoke more thigmotactic behaviour which resulted in a higher number of encounters with the boundaries of the enclosure. In addition to this, or indeed as a consequence of this, the directional sampling of animals was improved in the Open Field to the Homecage and Small Box trials. When the animal is in the Homecage, instead of demonstrating thigmotactic behaviour, the animal instead has a tendency to return to the huddle where the littermates are situated. Before the trial onset, the pups were dispersed throughout the Homecage in order to encourage exploration of

the Homecage. Nonetheless, there were fundamental differences in the movement statistics of animals in one environment and the other. This may have had a discernible impact on analysis of the directional tuning of classified HD cells during Homecage trials, particularly if the directional sampling of the rats during homecage trials was poorer than in the Open Field.

To investigate the research question, a number of spatial modulation metrics were computed. The directional modulation of cells with respect to unidirectional tuning was increased at all ages in the Open Field compared to the Homecage. However, this effect was not reflected in the directional information of recorded cells. Instead, the directional information of cells was equal between environments until P16. This suggests that in this context information regarding heading direction is encoded via multiple preferred firing directions within a given recording trial (corresponding to frequent resetting of HD cells in the Homecage). This was reflected by the poor within-trial stability of cells during Homecage and Small Box trials, which in concert suggests that HD cells are unstable and may frequently reset their PFD within this environment.

In line with maturation of the HD cell circuit, there was a gradual improvement in both Open Field and Homecage HD cell firing properties until P16, at which time HD cells exhibited adult-like firing properties. The modal age of eye opening in this study was 15, with a minimum eye-opening age of P14 and maximum eye-opening age of P16. The findings presented here are thus consistent with previous reports that patterned vision in rats brings about a rapid switch in the stability of HD cell firing (Tan et al., 2015). Interestingly, even after eye-opening in this cohort of animals, the increase in directional tuning and stability of cells did not appear to reach adult-like maturity in the Homecage environment. A possibility worth considering is that, although a distal polarising visual cue is available to the animal in the form of a white cue card, the rats may still be

utilising proximal cues contained within the boundaries of the Homecage to which the HD cells become affixed. This contrasts with previous studies suggesting that when proximal and distal visual cues are both available to an animal, it is the distal landmarks which are preferentially utilised (Zugaro et al., 2001a). This suggests that there are age-specific strategies for cue selection in developing animals. Another study has shown that distinct environmental boundaries (such as a trapezoid environment) are preferentially recruited as a reference for directional firing unless a sufficient number of salient distal landmarks are available (Clark et al., 2012b). It would be interesting to assess whether the inclusion of additional, highly salient visual cues in addition to the single white cue visible to the animal from the Homecage in this experiment may render additional directional tuning on recorded HD cells in the ADN in the period following eyeopening.

Given that there was a discernible difference in directional tuning and stability of cells in the Homecage compared to the Open Field, we sought to probe whether it was a diminished incidence of encounters of the animal with the boundaries of the environment which was the source of this instability. We know from other studies that HD cells can stabilise to boundaries (corners, in particular) of an environment when integration of landmark cues is not yet possible (Bassett et al., 2018). This occurs to the extent that when HD cells are recorded in a small box HD cells exhibit adult-like stability, several days before the onset of patterned vision when this stability is typically observed in a standard-sized open field (Bassett et al., 2018). Given that directional firing and stability of cells in the Small Box was particularly poor in comparison to the larger-dimension Open Field enclosure, as well as the Homecage, the contrast in results presents a strong case that it is the presence of conspecifics that disrupts stable HD tuning before eye-opening. The presence of the conspecifics conceivably results in a greater incidence of disorientation in the animal which the environmental boundaries did not succeed in rectifying. Upon eye-opening, the integration of visual landmark cues appeared to offset this effect and subsequently the directional firing of cells was comparable to that of the Open Field. Nevertheless, the uniformity of directional sampling in the Open Field compared to the Homecage and Small Box conditions offer one potential reason for the improved directional tuning of HD cells in the Open Field, compared to conditions in the Homecage and Small Box: all directional headings are sampled significantly more and with greater uniformity.

In the early stages of development, rats tend to remain huddled together until they begin active exploration around postnatal day 15 (P15; Gerrish and Alberts, 1996). To ensure meaningful data on head direction encoding, it was crucial to gather sufficient data from various directions. Therefore, before each trial recording, the experimenter scattered the huddled pups and placed them randomly around the cage, encouraging them to explore their environment. If an implanted pup, equipped with a neural data logger, remained motionless for over two minutes, the experimenter repositioned it within the cage. This served a dual purpose by altering the animal's orientation, increasing the sampling of different directional bins and the path length during the trial.

Additionally, the mother rat had a tendency to rearrange the pups into a huddle configuration within the cage, relocating them two to three times during each trial. She accomplished this by picking up each pup individually (by the scruff) and moving them within the cage. Subsequently, the pups would either naturally return to a huddle formation or explore away from where the mother had placed them. Video recordings were made of these behaviours, however the task of simultaneously monitoring multiple animals and differentiating the mother from the litter presented considerable difficulties. Therefore, this analysis fell outside the scope of this thesis. Future potential analysis will be possible using tools such as DeepLabCut

(Mathis et al., 2018; Lauer et al., 2022), which allows non-invasive tracking of multiple animals and their behaviours simultaneously.

Experimenter intervention was therefore used as a means to offset the natural tendency for the animal to return immediately to the huddle and to encourage excursive movement throughout the Homecage. The consequence of the passive movement events by the experimenter was that there were significantly shorter periods, or epochs, uninterrupted by passive movement of the animal in the Homecage compared to the Open Field. To assess whether the spatial correlate of HD cells was higher during epochs between passive movement, homecage trials were first segregated into active movement epochs within which the pup moved of its own volition without involvement of the experimenter. Next, Open Field and Small Box trials were randomly resampled to establish active movement epochs of comparable length to homecage epochs at the population level. When assessing the activity of HD cells during these epochs, the across-epoch stability remained high in the Open Field and Small Box trials (in line with the within-trial stability of these cells), the across-epoch stability of cells in Homecage-A and Homecage-B trials remained low (consistent with passive movement of the animal causing a resetting of HD cell preferred directions). This suggests that during Open Field and Small Box trials the animal is using a stable anchoring cue as a directional frame of reference, likely the corners and walls of the enclosure. After eye-opening, the animal was able to use the distal, polarising visual cue as an additional frame of reference which conferred additional stability on the recorded cells.

Most notably, the relative directional tuning and directional information encoded by cells during active movement epochs in the Homecage did not significantly differ from the Open Field. That is, the difference in directional modulation of HD cells between the Homecage and Open Field was much reduced, or no longer present. Furthermore, the within-epoch stability of cell firing did not differ between environments. If our hypoth-

esis was correct, then we should also expect to see higher within-epoch stability for active movements. Unfortunately, within-epoch stability was uniformly low, most likely due to insufficient sampling of directional position or the short duration of epochs. We cannot therefore make strong conclusions regarding the stability of cell firing during active movement epochs. This may suggest that on short timescales in the Homecage, HD cells exert directional firing in line with orientation to a stable frame of reference, such as the location of the huddle, or other tactile cues such as nest bedding. The pup may be transiently utilising these cues as a directional anchor as it encounters them, then switching to another, more proximal cue depending on the saliency. Potential bearing of HD cells towards the location of the nest was not assessed in this study, due primarily to the fact that the mother would attempt to move the location of the huddle to various points in the Homecage throughout the duration of the experiment. Furthermore, the improved directional signalling in the days preceding eye-opening during active movement epochs in the Homecage compared to the Small Box, despite fewer encounters with the geometry of the environment, suggests that the animal is effectively integrating local cues, or idiothetic cues in the Homecage which confer high directional signalling, that are distinct from the less familiar Small Box or Open Field enclosures.

Finally, the temporal and spatial relationships of cell ensembles were quantified over short time-windows, to assess whether the presence of attractor connectivity typical of HD cell networks was present in both Open Field and Homecage environments. The results presented here demonstrate that while the attractor network properties of HD cells are present in the Open Field environment, the extent to which cell ensembles are coupled on short time-scales is diminished in the context of the Homecage, particularly with respect to spatial coupling. The relative coupling is weak in the Homecage compared to the Open Field, before the HD cells

are able to be stabilised by anchoring to external landmarks upon eyeopening (between P15 and P16). This suggests that the attractor connectivity which has previously been shown to precede landmark integration of HD cells (Bassett et al., 2018) may not be resilient to all environmental contexts. One reason for this may be that the rate of drift in HD cells in the Homecage is not stable across the ensemble of recorded cells before the ability of cells to anchor to a visual cue, in such a way that the coherent shifting of the cells is not preserved even on very short timescales. However, as mentioned, there are a number of confounding variables which should be accounted for in future analyses.

In summary, we can conclude that pup HD cells recorded in a familiar, cue-rich environment did not stabilise at earlier age points than previously reported in open field enclosures. This experiment therefore did not disprove the notion that attractor network properties of head direction cells precede the adult-like stability of HD cell firing. Despite this, the directional firing of cells between environments was striking. While HD cells in the open field exhibited unidirectional firing typical of canonical HD cells, these same cells in the homecage trials exhibited poorer unidirectional tuning but comparable directional information. The directional information of cells in the homecage was indicative of the multi-peaked firing corresponding to multiple preferred firing directions. When quantified on short timescales corresponding to periods of uninterrupted active movement epochs, directional modulation of cells was the same across environments. In the context of this thesis, only periods of passive movement of the pup by the experimenter were considered. However, it raises the possibility that HD cells in the homecage also reset in response to episodes of passive movement by the mother. These movements were not explicitly recorded during these experiments. Given the relative frequency at which the mother moves the pups throughout the course of their early development, it is feasible that the observed instability of HD cells at younger ages

is not only a function of their ability to integrate visual inputs, but also the extent to which pups become independent from their mother. Given the dependence of pups on their mother for food and protection, it may be argued that the mother is the most salient cue to a pup up till the point of weaning. It is therefore an intriguing possibility that the relative interaction of pups with their mother has a quantifiable influence on the developmental trajectory of HD cell dynamics to adult-like stability.

Chapter 7

General Discussion

7.1 Summary of findings

The work presented in this thesis sought to exploit the advantages of wireless technologies in the study of developing neural circuits for navigation in rats. A method for implementation of wireless recordings in developing animals has not previously been reported. The first experiment presented in this thesis was therefore a feasibility study demonstrating that wireless recordings of spatial cells in rat pups are comparable to standard techniques, focusing on HD cells and place cells as these have been extensively studied in conventional developmental studies. Following implementation of a commercially available neural data logger, these spatiallymodulated cell types were recorded and fundamental spatial modulation metrics were reproduced to a similar standard as a well-established tethered data acquisition system. For a given cell recorded across both systems, the logger reproduced several key spatial coding metrics including directional (HD cells) and spatial (place cells) information. Cell stability within trials was not significantly different between the systems, and cell stability across trials was similar to previous reports of age-matched data (Tan et al., 2015; Muessig et al., 2015). A clear improvement in animal behaviour in terms of AHV and path length was observed, suggesting that wireless recordings may elicit more naturalistic and ethologically relevant behaviours to tethered recordings.

The second experiment took advantage of this new method to investigate whether the maturation of HD cells follows a different trajectory in a naturalistic environment to that previously observed in traditional openfield recordings. To address this, ensembles of HD cells were wirelessly recorded in the homecage from P12 to P16. Results suggested that HD cells in the homecage exhibit poorer unidirectional tuning than in the open field environment, but comparable directional information reflecting the multi-peaked firing of HD cells in the homecage. When this result was probed by partitioning recording trials into shorter epochs of active movement, HD cells recorded in the homecage had comparable unidirectional tuning, directional information and within-epoch firing stability as the respective open field trials. This suggests that in the homecage, where the animal frequently encounters mobile, highly salient cues (namely, conspecifics), the HD cells reset often such that over the duration of a full recording trial the rate maps exhibit multiple peaks corresponding to multiple heading directions of heightened firing. Finally, the short timescale temporal and spatial coupling of recorded HD ensembles was investigated to assess whether the attractor network properties typical of the canonical ADN HD network is preserved in all contexts before the onset of adultlike firing. Most strikingly, unlike in previous reports (Bassett et al., 2018), the spatial coupling of HD cell ensemble firing did not precede the presence of stable unidirectional tuning in the Homecage nor was the internal organisation structure of the network preserved between Open Field and Homecage trials. Instead, the strength of the attractor network appeared to be reflective of the level of drift of HD cells. At P13 and P14, the temporal and spatial coupling of cells was weak, but this rapidly improved to adult-like coupling at P15 and P16, parallel to the onset of patterned vision when cells may anchor to external landmarks. The level of spatial and temporal coupling of cell pairs in the Open Field was consistent with the

result observed by Bassett et al. (2018), indicative of attractor connectivity from the youngest age in this analysis (P13) and before the onset of stable HD cell responses. This means that the conclusion of Bassett et al. (2018), where we assumed that the attractor connectivity is present in all contexts, is not necessarily true, also that this connectivity is dependent on exact behavioural and environmental context. Future analyses will be useful to investigate this further by controlling for potentially confounding variables such as passive movements made by the mother, low cell and spike count at younger ages, and differing movement statistics of the animals in the Homecage versus Open Field environments.

7.2 Discussion and future work

A well established characteristic of the mature rodent HD network is that the relative offset of cell firing remains constant despite changes of the cells' preferred direction in response to changes in the external environment (most often, visual cues). This property leads the HD cell network to often be described as a continuous attractor neural network (Skaggs et al., 1995; Redish et al., 1996; Zhang, 1996), which for any given heading direction will have a localised hill of activity corresponding to a subset of HD cell firing. Many computational models have attempted to explain how this network connectivity may self-organise, with most models requiring visual input to entrain the cell ensembles into a coherent network structure. By a combination of idiothetic (usually AHV information) and allothetic (visual information) inputs, the networks are generally trained by a process of Hebbian-like associative or competitive learning rules with variable levels of biologically plausible parameters (Stringer et al., 2002; Hahnloser, 2003; Stringer and Rolls, 2006; Stratton et al., 2010).

However, a striking experimental finding in recent years was that when a pre eye-opening rat is placed in a small environment conducive to short-term stability of HD cell firing, temporal and spatial coupling was present and this intrinsic connectivity remained even when the animal was transferred to a larger environment and the cells were no longer stable nor had significant unidirectional firing properties (Bassett et al., 2018). This result appeared to disprove modelling work suggesting that the onset of adult-like firing stability and persistent temporal and spatial coupling of cell ensembles would arise concurrently.

To this end, the work presented in this thesis shows that the effect observed in Bassett et al. (2018) is context-dependent, and rather supports prior computational models which posit that the strength of HD cell coupling is contingent on the stability of cell firing and the rate of drift. Does this mean that the HD system actually only starts to 'develop' in its adult form when the pup leaves the nest? This conclusion is drawn from the finding that the strength of temporal and spatial coupling in recorded ensembles was weaker in the Homecage than the Open Field. Furthermore, the lack of correlation between the spatial offsets of co-recorded cells in the Homecage and Open Field suggests that the internal organisation of the HD network collapses across environments. Considering the likely attentional effect of the animal moving through a cue-rich space such as the Homecage, and the frequent encounters with mobile cues, it seems likely that the reliance on idiothetic inputs (as opposed to tactile, auditory, or olfactory) inputs is lower than in the Open Field. In the Open Field, given the relative sparsity of this environment, the animal is likely more dependent on idiothetic inputs. We know from both experimental (Bassett et al., 2018) and computational (Skaggs et al., 1995; Redish et al., 1996) work the importance of idiothetic inputs in the entraining of the attractor network before visual inputs are available. Consequently, this may therefore be one reason for the relative collapse of the intrinsic network structure in the Homecage compared to the Open Field. Upon reaching P15, the intrinsic structure appears to be preserved across environments, suggesting that this response is both context- and age-dependent.

In this respect, the overarching finding that the directional signal of HD cells in the homecage is unstable and contains less information in some respects is not surprising. A significant factor which may be interfering with a stable directional signal in the homecage, as mentioned, is the presence of the pups' littermates and mother. The dynamics of HD cells in the presence of numerous, non-static cues to the animal has not previously been studied but raises intriguing questions about how a developing animal orients itself in such environments. A recent computational model attempted to extrapolate the dynamics of retrosplenial HD cells in terms of landmark coding in complex environments (Yan et al., 2021). In this model, a population of cells downstream from visual neurons are defined as 'abstract landmark-bearing' cells. These cells encode a unimodal directional representation based on an abstract accumulation of the global cues in a scene, rather than one specific cue. The model does not dictate where in the HD or visual circuit these cells reside, but the authors postulate that they may be present in the retrosplenial cortex in line with this area's role in landmark processing for directional orientation. These cells are able to maintain a robust directional encoding of a complex scene (i.e. an environment where cues are either multimodal or have poor directional specificity) despite the presence of cues that are considered unreliable, such as a constantly moving landmark or a landmark that intermittently appears and disappears. These cells are modelled such that they are independent of vestibular input and rely wholly on allothetic inputs. These findings have yet to be supported with empirical evidence, but the theoretical model of a subset of cells which provide a unimodal, compressed representation of landmark bearing is compelling. In terms of developing animals, an analogous population of cells which integrate a diverse set of non-visual cues in complex environments is worth considering. Such cells may provide a moment-to-moment directional orientation sense to pre eye-opening animals in tandem with idiothetic feedback mechanisms.

Other studies have illuminated further the malleability of the cognitive map of space with respect to the movement constraints and complexity of the recording environment (reviewed in Jeffery, 2021). This is not just restricted to the boundaries of a given environment, but also the dimensionality of the rat's exploration (two-dimensional versus threedimensional space). Therefore, the opportunity to expand the research question to larger scales of navigation is also possible. Whilst the ecological approach to studying the ontogeny of spatial navigation is to observe animals in natural, complex scenes over multiple scales, the systems neuroscience approach has been to study the neuronal activity underlying spatial navigation and spatial learning behaviours (Gega-Sagiv et al., 2015) on a small scale in laboratory environments. Given that there is some evidence to support the idea that the repertoire of sensory information available at any given time to an animal dictates the resolution of the spatial mapping cells, it is something to consider moving forward within the context of utilising wireless technology across multiple scales. For example, one study has shown that the place field size of hippocampal place cells are smaller when visual landmarks are visible, and larger when they are absent (Zhang et al., 2014). In a similar vein, place fields have been shown to expand when rats run along a featureless track versus a cue-enriched track (Battaglia et al., 2004). Given the aforementioned studies it is possible that large scale navigation such as in the wild, or in humans, is not just a scaled version of what is observed in rodents in confined laboratory enclosures (Gega-Sagiv et al., 2015). Is the way the cells behave in these controlled situations relevant to real-life navigation? For example, wild rats are known to travel distances of up to several kilometres away from their burrow (Taylor, 1978), which suggests they possess spatial navigation abilities outside of the currently studied range in laboratory contexts. In this regard, it is possible that laboratory-reared rats do not possess the same large scale neural representations of space, unlike their wild-reared

counterparts. Therefore, comparing the ontogeny of spatially-modulated cell types in the context of rearing environments and multiscale spatial representations may shed further light on the importance of environmental context and experience in the ontogeny of neural representations of space. For HD cells, directional modulation of cells is likely independent of the scale of space experienced, given their encoding of direction in azimuth space. However, one aspect of directional encoding which remains unclear is how this is reflected in three-dimensional space. A number of studies have attempted to ascertain the dynamics at play in such situations in rodents (Shinder and Taube, 2019; Angelaki et al., 2020).

With this in mind, a complementary avenue to the work presented in this thesis which is worth mentioning is the ethological study of natural behaviours of rodents during early postnatal development. Focusing on the emergence of exploration and foraging, even the interaction between littermates, may enable us to ascertain which cues are most salient to an animal before eye-opening, and therefore which feature cues are utilised by the animal when they are navigating. Previous studies employing computational methods for investigating rat pup behaviour have used video recordings of litters over a period of days. In one such study, 'digitised measurements of the location of each individual [were] captured every 5 seconds' (Alberts, 2006). They observed whether the respective pups were in contact with walls, corners, other pups, or not in contact with anything. They also measured the circumference of the huddle as a metric for regulatory huddling. The motivation for this is that the ontogeny of certain behaviours in rats which live in caged environments need to be characterised such that the modulation of behaviours in experimental settings is understood. However, studies such as these tend to lack corresponding neuronal data of spatial mapping cells. It may be possible to successfully study meaningful behaviours of rodents in early postnatal development using recent advances in deep learning tools in conjunction with wireless

technology such as the neural data logger implemented in this thesis. For example, DeepLabCut (Mathis et al., 2018) is a markerless pose estimation toolbox which utilises deep learning and enables non-invasive tracking of multiple animals and their behaviours, simultaneously (Lauer et al., 2022). There is also potential for more detailed analytical procedures to assess underlying neural correlates for these behaviours outside of the scope of this thesis. For instance, an unsupervised learning method has been employed recently using a Hidden Markov model in an attempt to unearth behaviourally relevant brain states with no *a priori* notions, in this case while rats are playing hide-and-seek (Bagi et al., 2022). Neural manifold analysis has been employed for similar reasons given the low-dimensionality of the head direction structure (Chaudhuri et al., 2019). There are furthermore a number of possible methods which permit meaningful analysis on yields of cells larger than those achieved in this thesis, including Bayesian decoding, a method of studying attractor dynamics which has been previously used in this lab (Bassett et al., 2018) and others (Peyrache et al., 2015).

As we have seen, naturalistic behaviours are highly complex and multi-modal by comparison to the nature of standard open-field experiments, in which animals tend to exhibit simplified, constrained behaviours. This thesis has made initial attempts to probe the activity of the cognitive map within the context of the complexity of an animal's rearing environment. Wireless recordings offered the opportunity to explore this question in a new way, permitting the study of HD cell development with minimal disturbance to the natural nesting, nursing and exploratory behaviour of the animal. It should be mentioned that inferences about the activity of the spatial mapping cells are only reliable if there is sufficient uniformity and quantity of spatial sampling in a given environment (McNaughton et al., 1983b). This poses limits to the extent to which these spatial cells may be studied in the homecage, given there may initially be

poorer spatial sampling due to young rats typically spending the majority of their early development huddling (Alberts, 1978). Similarly, nest egression is not typically seen in rats until around P16 (Altman and Sudarashan, 1975). In this respect, HD cells were an ideal spatial cell for early homecage recordings, as minimal spatial sampling is required for meaningful analysis compared to other spatial cells. There are further possibilities worth mentioning with regards to uses for wireless technology in developing animals. A rat's natural habitat is a burrow: a series of subterranean, interconnected tunnels within which the rats reside (Pisano and Storer, 1948; Calhoun, 1963). In a laboratory environment, enrichment in the form of short tunnels, or small plastic structures are provided in an attempt to provide substance for play for the animals. However, there remains a distinction between the rearing environment of animals found in the lab and those found in the wild.

There are also critical periods of plasticity in sensorimotor development, which may be impacted by differential experimental protocols. In broad terms, critical developmental periods refer to short periods of time when sensory experience is necessary for the development of a structure to its full functional capabilities. Certain brain regions require a particular amount of external sensory information to effectively tune the functional organisation of constituent neurons when the encoded information cannot be predicted and is not genetically preconfigured. For example, dark rearing can delay the onset of the critical period for development of visual capabilities (Hensch and Fagiolini, 2005) which in turn can have a deleterious effect on performance in spatial learning tasks (Tees et al., 1990). In fact, the rearing environment in early development can have long standing impacts on spatial cognition. While those rats reared in either complex rearing environments tend to have superior performance in maze-based tasks such as the radial arm maze task than their counterparts who are reared in standard cages (in this particular experiment they looked at the

effect of rearing environment on post-weaning animals; Seymoure et al., 2013). Future work may therefore investigate these findings further within the context of understanding which sensory cues affect directional signalling before eye-opening. The rearing environment may be manipulated to include the standard homecage, a circular homecage and a burrow-like homecage. Recordings may then be conducted to assess the relative impact of geometric cues on HD cell stability. This will indicate whether a geometric cue-deprived environment (circular homecage) hinders the early stabilisation of HD cells compared to a geometrically-polarised (standard homecage) or geometric cue-enriched (burrow homecage) rearing environment. Feature cues may also be manipulated wherein odour and texture-varied enrichment are added to the homecage. By altering the rearing environment we may investigate further if the development of HD networks includes periods of heightened plasticity.

Further capabilities of wireless devices are the ability to make simultaneous recordings from multiple devices using the MouseLog16 (Deuteron Technologies Ltd., Israel). This is a major asset in the ontogenetic study of social behaviours and spatial learning in natural group settings. For instance, it may be used in studying the acquisition of social rank (Dwortz et al., 2022) in development, mother-pup interactions, and other social group behaviours. There is also growing evidence to suggest that the allocentric spatial representations of the cognitive map may have more abstract implications than spatial navigation, such as allocentric coding for social cognition (reviewed in Arzy and Kaplan, 2022). An application for this in the context of spatial learning and memory is to investigate how the position of others is represented in the brain. Studies such as this have begun to be conducted in adult rats (Danjo et al., 2018) and bats (Omer et al., 2018). Findings from these studies suggest that in addition to spatial cell types encoding self-location within an environment, there are a subset of place cells which become modulated by the presence of another individual within the same environment. In these experiments, the paradigm involved one animal (the 'observer') watching another animal (the 'demonstrator') perform a specific spatial task. This raises an intriguing question around how the developing rat begins to recognise the presence of its mother and littermates in the critical first weeks of life. Is this encoding innate or learned with time spent in the huddle, and time spent feeding? Conversely, from the point of view of the mother is it possible that there is a population of neurons which fire in response to the presence of her pups. The implementation of wireless technology presented in this thesis paves the way for such experiments.

7.3 Concluding Remarks

Previous work investigating the postnatal development of spatial cells are limited to the extent to which naturalistic and ethologically relevant behaviours were studied. The use of wireless technology for the *in vivo* recording of spatial cells set forth in this thesis expands on current techniques in the challenging domain of ontogenetic studies in awake, behaving animals. This thesis presented the first application of wireless neural recordings in rat pups, studying the postnatal development of spatial cells with a particular focus on head direction cells.

These results lay the basis for a number of experimental pipelines which can engage further with the natural rearing of animals in the context of spatial cognition, tracking the emergence of spatial signals without interfering with the natural spatial exploratory drive of the animals. The question remains unanswered regarding the extent to which preconfigured networks versus sensory experience contribute to the development of spatial neural networks. In light of this, the importance of studying spatial cells in naturalistic and complex scenes in development is compelling, as it may permit a more comprehensive understanding of the neural basis of spatial learning and memory and its emergence in the rodent

model.

Chapter 8

References

Acharya, L., Aghajan, Z.M., Vuong, C., Moore, J.J., Mehta, M.R. (2016) Causal influence of visual cues on hippocampal directional selectivity. *Cell* 164: 197-207.

Aggleton, J.P., Neave, N., Nagle, S., Hunt, P.R. (1995) A comparison of the effects of anterior thalamic, mammillary body and fornix lesions on reinforced spatial alternation. *Behavioral Brain Research* 68: 91-101.

Aggleton, J.P., Hunt, P.R., Nagle, S., Neave, N. (1996) The effects of selective lesions within the anterior thalamic nuclei on spatial memory in the rat. *Behavioral Brain Research* 81: 189-198.

Akers, K.G., Candelaria, F.T., Hamilton, D.A. (2007) Preweanling rats solve the Morris water task via directional navigation. *Behavioral Neuroscience* 121: 1426-1430.

Alberini, C.M., Travaglia, A. (2017) Infantile amnesia: A critical period of learning to learn and remember. *Journal of Neuroscience* 37: 5783-5795.

Alberts, J.R. (1978a) Huddling by rat pups: Group behavioral mechanisms of temperature regulation and energy conservation. *Journal of Comparative and Physiological Psychology* 92(2): 231-245.

Alberts, J.R. (1978b) Huddling by rat pups: multisensory control of contact behavior. *Journal of Comparative and Physiological Psychology* 92(2): 220.

Alberts, J.R., and Leimbach, M.P. (1980) The first foray: Maternal influ-

ences in nest egression in the weanling rat. *Developmental Psychobiology:* The Journal of the International Society for Developmental Psychobiology 13(4): 417-429.

Alberts, J.R. (2007) Huddling by rat pups: ontogeny of individual and group behavior. *Developmental Psychobiology: The Journal of the International Society for Developmental Psychobiology* 49(1): 22-32.

Allen, G.V., and Hopkins, D.A. (1989) Mammillary body in the rat: to-pography and synaptology of projections from the subicular complex, prefrontal cortex, and midbrain tegmentum. *Journal of Comparative Neurology* 286: 311-336.

Allen, K., Gil, M., Resnik, E., Toader, O., Seeburg, P., Monyer, H. (2014) Impaired path integration and grid cell spatial periodicity in mice lacking GluA1-containing AMPA receptors. *Journal of Neuroscience* 34(18): 6245-6259.

Alme, C.B., Miao, C., Jezek, K., Treves, A., Moser, E.I., Moser, M.B. (2014) Place cells in the hippocampus: eleven maps for eleven rooms. *Proceedings of the National Academy of Sciences* 111(52): 18428-18435.

Altman, J., and Sudarshan, K. (1975) Postnatal development of locomotion in the laboratory rat. *Animal Behavior* 23(4): 896-920.

Altman, J. (1982) Morphological development of the rat cerebellum and some of its mechanisms. *The Cerebellum- New Vistas*: 8-49.

Amaral, D.G., and Witter, M.P. (1995) Hippocampal formation. Amaral DG, Witter MP (1995) *Hippocampal formation. In G Paxinos, ed., The Rat Nervous System.* Second Edition. San Diego, CA: Academic Press: 443–493.

Anderson, M.I., and Jeffery, K.J. (2003) Heterogeneous modulation of place cell firing by changes in context. *Journal of Neuroscience* 23(26): 8827-8835.

Angelaki, D.E., Ng, J., Abrego, A.M., Cham, H.X., Asprodini, E.K., Dickman, J.D., Laurens, J. (2020) A gravity-based three-dimensional compass in the mouse brain. *Nature Communications* 11: 1-13.

Aronov, D., Nevers, R., Tank, D.W. (2017) Mapping of a non-spatial dimension by the hippocampal-entorhinal circuit. *Nature* 543: 719-722.

Arzy, S., and Kaplan, R. (2022) Transforming social perspectives with cognitive maps. *Social Cognitive and Affective Neuroscience* 17: 939-955.

Asumbisa, K., Peyrache, A., Trenholm, S. (2022) Flexible cue anchoring strategies enable stable head direction coding in both sighted and blind animals. *Nature Communications* 13(5483).

Bagi, B., Brecht, M., Sanguinetti-Scheck, J.I. (2022) Unsupervised discovery of behaviorally relevant brain states in rats playing hide-and-seek. *Current Biology* 32(12): 2640-2653.

Barnett, S.A. (1957) An analysis of social behaviour in wild rats. *Proceedings of the Zoological Society of London* 130(1): 107-152. Oxford, UK: Blackwell Publishing Ltd.

Barry, C., Lever, C., Hayman, R., Hartley, T., Burton, S., O'Keefe, J., Jeffery, K., Burgess, N. (2006) The boundary vector cell model of place cell firing and spatial memory. *Reviews in the Neurosciences* 17(1-2): 71-98.

Barry, C., Hayman, R., Burgess, N., Jeffery, K. (2007) Experience-dependent rescaling of entorhinal grids. *Nature Neuroscience* 10: 682-684.

Barry, C., Ginzberg, L.L., O'Keefe, J., Burgess, N. (2012) Grid cell firing patterns signal environmental novelty by expansion. *Proceedings of the National Academy of Sciences* 109(43): 17687-17692.

Bassett, J.P., and Taube, J.S. (2001) Neural correlates for angular head velocity in the rat dorsal tegmental nucleus. *Journal of Neuroscience* 21: 5740-5751.

Bassett, J.P., and Taube, J.S. (2003) Persistent neural activity in head direction cells. *Cerebral Cortex* 13(11): 1162-1172.

Bassett, J.P., Zugaro, M.B., Muir, G.M. Golob, E.J., Muller, R.U., Taube, J.S. (2005) Passive movements of the head do not abolish anticipatory firing properties of head direction cells. *Journal of Neurophysiology* 93: 1304-1316.

Bassett, J.P., Tullman, M.L., Taube, J.S. (2007) Lesions of the tegmentomammillary circuit in the head direction system disrupt the head direction signal in the anterior thalamus. *Journal of Neuroscience* 27(28): 7654-7577.

Bassett, J.P., Wills, T.J., Cacucci, F. (2018) Self-organized attractor dynamics in the developing head direction circuit. *Current Biology* 28(4): 609-615.

Battaglia, F.P., Sutherland, G.R., McNaughton, B.L. (2004) Local sensory cues and place cell directionality: additional evidence of prospective coding in the hippocampus. *Journal of Neuroscience* 24(19): 4541-4550.

Ben-Yishay, E., Krivoruchko, K., Ron, S., Ulanovsky, N., Derdikman, D., Gutfreund, Y. (2021) Directional tuning in the hippocampal formation of birds. *Current Biology* 31(12): 2592-2602.

Beracochea, D.J., Jaffard, R., Jarrard, L.E. (1989) Effects of anterior or dorsomedial thalamic ibotenic lesions on learning and memory in rats. *Behavioral and Neural Biology* 51(3): 364-376.

Berdoy, M. (2002) The laboratory rat: a natural history. Oxford University, 2002.

Biazoli, C.E., Goto, M., Campos, A.M., Canteras, N.S. (2006) The supragenual nucleus: a putative relay station for ascending vestibular signs to head direction cells. *Brain Research* 1094: 138-148.

Bilkey, D.K., Cheyne, K.R., Eckert, M.J., Lu, X., Chowdury, S., Worley, P.F., Crandall, J.E., Abraham, W.C. (2017) Exposure to complex environments results in more sparse representations of space in the hippocampus. *Hippocampus* 27(11): 1178-1191.

Blair, H.T., and Sharp, P.E. (1995) Anticipatory head direction signals in anterior thalamus: evidence for a thalamocortical circuit that integrates angular head motion to compute head direction. *Journal of Neuroscience* 15(9): 6260-6270.

Blair, H.T., and Sharp, P.E. (1996) Visual and vestibular influences on

head-direction cells in the anterior thalamus of the rat. *Behavioral Neuro- science* 110(4): 643.

Blair, H.T., Cho, J., Sharp, P.E. (1998) Role of the lateral mammillary nucleus in the rat head direction circuit: a combined single-unit recording and lesion study. *Neuron* 21: 1387-1397.

Blair, H.T., and Sharp, P.E. (1999) The anterior thalamic head-direction signal is abolished by bilateral but not unilateral lesions of the lateral mammillary nucleus. *Journal of Neuroscience* 19(15): 6673-6683.

Blodgett, H.C. (1929) The effect of the introduction of reward upon the maze performance of rats. *University of California Publications in Psychology* 4: 113-134.

Bjerknes, T.L., Moser, E.I., Moser, M.B. (2014) Representation of geometric borders in the developing rat. *Neuron* 82: 71-78.

Bjerknes, T.L., Langston, R.F., Kruge, I.U., Moser, E.I., Moser, M.B. (2015) Coherence among head direction cells before eye opening in rat pups. *Current Biology* 25(1): 103-108.

Boice, R. (1977) Burrows of wild and albino rats: effects of domestication, outdoor raising, age, experience, and maternal state. *Journal of Comparative and Physiological Psychology* 91(3): 649-661.

Boccara, C.N., Sargolini, F., Thoresen, V.H., Solstad, T., Witter, M.P., Moser, E.I., Moser, M.B. (2010) Grid cells in pre- and parasubiculum. *Nature Neuroscience* 13(8): 987-994.

Boccara, C.N., Nardin, M., Stella, F., O'Neill, J., Csicsvari, J. (2019) The entorhinal cognitive map is attracted to goals. *Science* 363(6434): 1443-1447.

Bonnevie, T., Dunn, B., Fhyn, M., Hafting, T., Derdikman, Kubie, J.L., Roudi, Y., Moser, E.I., Moser, M.B. (2013) Grid cells require excitatory drive from the hippocampus. *Nature Neuroscience* 16(3): 309-317.

Bostock, E., Muller, R.U., Kubie, J.L. (1991) Experience-dependent modifications of hippocampal place cell firing. *Hippocampus* 1: 193-205.

Brandon, M.P., Bogaard, A.R., Libby, C.P., Connerney, M.A., Gupta, K., Hasselmo, M.E. (2011) Reduction of theta rhythm dissociates grid cell spatial periodicity from directional tuning. *Science* 332(6029): 595-599.

Brandon, M.P., Koenig, J., Leutgeb, J.K., Leutgeb, S. (2014) New and distinct hippocampal place codes are generated in a new environment during septal inactivation. *Neuron* 82(4): 789-796.

Bronstein, P.M., and Spear, N.E. (1972) Acquisition of a spatial discrimination by rats as a function of age. *Journal of Comparative and Physiological Psychology* 78(2): 208-212.

Brown, R.W., and Whishaw, I.Q. (2000) Similarities in the development of place and cue navigation by rats in a swimming pool. *Developmental Psychobiology* 37(4): 238-245.

Brun, V.H. Otness, M.K., Molden, S., Steffenach, H.A., Twitter, M.P., Moser, M.B., Moser, E.I. (2002) Place cells and place recognition maintained by direction entorhinal-hippocampal circuitry. *Science* 296(5576): 2243-2246.

Brun, V.H., Leutgeb, S., Wu, H.Q, Schwartz, R., Twitter, M.P., Moser, E.I., Moser, M.B. (2008) Impaired spatial representation in CA1 after lesion of direct input from entorhinal cortex. *Neuron* 57(2): 290-302.

Brunjes, P.C., and Alberts, J.R. (1981) Early auditory and visual function in normal and hyperthyroid rats. *Behavioral and Neural Biology* 31(4): 393-412.

Bulut, F., and Altman, J. (1974) Spatial and tactile discrimination learning in infant rats motivated by homing. *Developmental Psychobiology* 7: 465-473.

Burak, Y., Fiete, I.R. (2009) Accurate path integration in continuous attractor network models of grid cells. *PLOS Computational Biology* 5(2):e1000291.

Burgalossi, A., Herfst, L., von Heimendahl, M., Forste, H., Haskic, K., Schmidt, M., Brecht, M. (2011) Microcircuits of functionally identified

neurons in the rat medial entorhinal cortex. Neuron 70(4): 773-786.

Burgess, N., and O'Keefe, J. (1996) Neuronal computations underlying the firing of place cells and their role in navigation. *Hippocampus* 6: 749-762.

Burgess, N., Donnett, J.G., Jeffery, K.J., O'Keefe, J. (1997) Robotic and neuronal simulation of the hippocampus and rat navigation. *Philosophical Transactions of the Royal Society B.* 352: 1535-1543.

Burgess, N. (2002) The hippocampus space and viewpoints in episodic memory. *Quarterly Journal of Experimental Psychology* 55A: 1057-1080.

Burgess, N., Barry, C., O'Keefe, J. (2007) An oscillatory interference model of grid cell firing. *Hippocampus* 17: 801-812.

Burwell, R. D. (2000) The parahippocampal region: corticocortical connectivity. *Annals of the New York Academy of Sciences* 911(1): 25-42.

Bush, D., Barry, C., Manson, D., Burgess, N. (2015) Using grid cells for navigation. *Neuron* 87(3): 507-520.

Butler, W.N., and Taube, J.S. (2015) The nucleus prepositus hypoglossi contributes to head direction cell stability in rats. *Journal of Neuroscience* 35(6): 2547-2558.

Butler, W.N., Hardcastle, K., Giacomo, L.M. (2019) Remembered reward locations restructure entorhinal spatial maps. *Science* 363(6434): 1447-1452.

Buzsaki, G., Stark, E., Berenyi, A., Khodagholy, D., Kipke, D.R., Yoon, E., Wise, K.D. (2015) Tools for probing local circuitsL high-density silicon probes combined with optogenetics. *Neuron* 86: 92-105.

Caballero-Bleda, M., and Witter, M.P. (1993) Regional and laminar organization of projections from the presubiculum and parasubiculum to the entorhinal cortex: an anterograde tracing study. *Journal of Comparative Neurology* 328: 115-129.

Cacucci, F., Lever, C., Wills, T.J., Burgess, N., O'Keefe, J.O. (2004) Theta-modulated place-by-direction cells in the hippocampal formation in the

rat. Journal of Neuroscience 24(38): 8265-8277.

Cacucci, F., Muessig, L., Hauser, J., Wills, T.J. (2013) The role of environmental boundaries in the ontogeny of the hippocampal neural code for space. *Society for Neuroscience Abstracts*. 485.16.

Cahusac, P.M.B, Miyashita, Y., Rolls, E.T. (1989) Responses of hip-pocampal formation neurons in the monkey related to delayed spatial response and object-place memory tasks. *Behavioural Brain Research* 33(3).

Calhoun, J.B. (1963) The ecology and sociology of the Norway rat. US Department of Health, Education and Welfare, Public Health Service.

Calton, J.L., Stackman, R.W., Goodridge, J.P., Archey, W.B., Dudchenko, P.A, Taube, J.S. (2003) Hippocampal place cell instability after lesions of the head direction cell network. *Journal of Neuroscience* 29(30): 9719-9731.

Calton, J.L., and Taube, J.S. (2005) Degradation of head direction cell activity during inverted locomotion. *Journal of Neuroscience* 25(9): 2420-2428.

Carpenter, F., Manson, D., Jeffery, K., Burgess, N., Barry, C. (2015) Grid cells form a global representation of connected environments. *Current Biology* 25(9): 1176-1182.

Castelhano-Carlos, M.J., and Baumans, V. (2009) The impact of light, noise, cage cleaning and in-house transport on welfare and stress of laboratory rats. *Laboratory Animals* 43(4): 311-327.

Champagne, F.A., and Curley, J.P. (2009) Epigenetic mechanisms mediating the long-term effects of maternal care on development. *Neuroscience / Biobehavioral Reviews* 33(4): 593-600.

Chaudhuri, R., Gercek, B., Pandey, B., Peyrache, A., Fiete, I. (2019) The intrinsic attractor manifold and population dynamics of a canonical cognitive circuit across waking and sleep. *Nature Neuroscience* 22(9): 1512-1520.

Cheng, K. (1986) A purely geometric module in the rat's spatial representation. *Cognition* 23: 149-178.

Chen, L.L., Hin, L.H., Green, E.J., Barnes, C.A., McNaughton, B.L. (1994a) Head-direction cells in the rat posterior cortex. I. Anatomical distribution and behavioral modulation. *Experimental Brain Research* 101(1): 8-23.

Chen, L.L., Lin, L.H., Barnes, C.A., McNaughton, B.L. (1994b) Head-direction cells in the rat posterior cortex II. Contributions of visual and idiothetic information to the directional firing. *Experimental Brain Research* 101: 24-34.

Chen, G., Manson, D., Cacucci, F., Wills, T.J. (2016) Absence of visual input results in the disruption of grid cell firing in the mouse. *Current Biology* 26(17): 2335-2342.

Cheslock, S.J., Varlinskaya, E.I., Petrov, E.S., Spear, N.E. (2000) Rapid and robust olfactory conditioning with milk before suckling experience: promotion of nipple attachment in the newborn rat. *Behavioral Neuroscience* 114(3): 484-495.

Cho, J., and Sharp, P.E. (2001) Head direction, place and movement correlates for cells in the rat retrosplenial cortex. *Behavioral Neuroscience* 115: 3-25.

Clark, B.J., Bassett, J.P., Wang, S.S., Taube, J.S. (2010) Impaired head direction cell representation in the anterodorsal thalamus after lesions of the retrosplenial cortex. *Journal of Neuroscience* 30(15): 5289-5302.

Clark, B.J., and Taube, J.S. (2012a) Vestibular and attractor network basis of the head direction cell signal in subcortical circuits. *Frontiers in Neural Circuits* 6: 7.

Clark, B.J., Harris, M.K., Taube, J.S. (2012b) Control of anterodorsal thalamic head direction cells by environmental boundaries: Comparison with conflicting distal landmarks. *Hippocampus* 22: 172-187.

Clark, B.J., Brown, J.E., Taube, J.S. (2012b) Head direction cell activity in the anterodorsal thalamus requires intact supragenual nuclei. *Journal of Neurophysiology* 108: 2767-2784.

Clowry, G.J., and Flecknell, P.A. (2000) The successful use of fentanyl–fluanisone ('Hypnorm') as an anaesthetic for intracranial surgery in neonatal rats. *Lab Anim* 34: 260–264.

Cohen, J. (1988) Statistical power analysis for the Social Sciences (2nd Edition). Hillsdale, New Jersey, Lawrence Erlbaum Associates.

Colonnese, M.T., Kaminska, A., Minlebaev, M., Milh, M., Bloem, B., Lescure, S., Moriette, G., Chiron, C., Ben-Ari, Y., Khazipov, R. (2010) A conserved switch in sensory processing prepares developing neocortex for vision. *Neuron* 67(3): 480-498.

Cooper, B.G., and Mizumori, S.J. (2001) Temporary inactivation of the retrosplenial cortex causes a transient reorganization of spatial coding in the hippocampus. *Journal of Neuroscience* 21: 3986-4001.

Cornwell-Jones, C., and Sobrian, S.K. (1977) Development of odorguided behavior in Wistar and Sprague-Dawley rat pups. *Physiology & Behavior* 19(5): 685-688.

Couzen, I.D. (2009) Collective cognition in animal groups. *Trends in Cognitive Sciences* 13(1): 36-43.

Csicsvari, J., Hirase, H., Czurko, A., Mamiya, A., Buzsaki, G. (1999) Oscillatory coupling of hippocampal pyramidal cells and interneurons in the behaving rat. *Journal of Neuroscience* 19(1): 274-287.

Curthoys, I.S. (1979a) The development of function of horizontal semicircular canal primary neurons in the rat. *Brain Research* 167(1): 41-52.

Curthoys, I.S. (1979b) The vestibulo-ocular reflex in newborn rats. *Acta Otolaryngol* 87: 484-489.

Czajkowski, R., Sugar, J., Zhang, S.J., Couey, J.J., Ye, J., Witter, M.P. (2013) Superficially projecting principal neurons in layer V of medial entorhinal cortex in the rat receive excitatory retrosplenial input. *Journal of Neuroscience* 33(40): 15779-15792.

Danjo, T., Toyoizumi, T., Fujisawa, S. (2018) Spatial representations of

self and other in the hippocampus. Science 359(6372): 213-218.

Dannenberg, H., Lazaro, H., Nambiar, P., Hoyland, A., Hasselmo, M.E. (2020) Effects of visual inputs on neural dynamics for coding of location and running speed in medial entorhinal cortex. *Elife* 9: e62500.

Davis, D.E. (1953) The characteristics of rat populations. *The Quarterly Review of Biology* 28: 373-401.

Dechesne, C., Mbiene, J.P., Sans, A. (1986) Postnatal development of vestibular receptor surfaces in the rat. *Acta Otolaryngol* 101: 11-18.

Derdikman, D., Whitlock, J.R., Tsao, A., Fyhn, M., Hafting, T., Moser, M.B., Moser, E.I. (2009) Fragmentation of grid cell maps in a multicompartment environment. *Nature Neuroscience* 12(10): 1325-1332.

Diba, K., and Buzsaki, G. (2007) Forward and reverse hippocampal place-cell sequences during ripples. *Nature Neuroscience* 10: 1241-1242.

Douglas, R.J. (1967) The hippocampus and behavior. *Psychological Bulletin* 67(6): 416.

Dragoi, G. and Buzsaki, G. (2006) Temporal encoding of place sequences by hippocampal cell assemblies. *Neuron* 50: 145-157.

Dragoi, G. (2013) Internal operations in the hippocampus: Single cell and ensemble temporal coding. *Frontiers in Systems Neuroscience* 7: 46.

Dudai, Y., and Morris, R. G. (2000) To consolidate or not to consolidate: what are the questions? *Brain, perception, memory: Advances in cognitive neuroscience*: 149-162.

Dudchenko, P.A., Goodridge, J.P., Taube, J.S. (1997) The effects of disorientation on visual landmark control of head direction cell orientation. *Experimental Brain Research* 115(2): 375-380.

Dupret, D., O'Neill, J., Pleydell-Bouverie, B., Csicsvari, J. (2010) The reorganization and reactivation of hippocampal maps predict spatial memory performance. *Nature Neuroscience* 13: 995-1002.

Dwortz, M.F., Curley, J.P., Tye, K.M., Padilla-Coreano, N. (2022) Neural systems that facilitate the representation of social rank. *Philosophical*

Transactions of the Royal Society B 377(1845): 20200444.

Eilam, D., and Smotherman, W.P. (1998) How the neonatal rat gets to the nipple: common motor modules and their involvement in the expression of early motor behavior. *Developmental Psychobiology* 32(1): 57-66.

Ekstrom, A.D., Kahana, M.J., Caplan, J.B., Fields, T.A., Isham, E.A., Newman, E.I., Fried, I. (2003) Cellular networks underlying human spatial navigation. *Nature* 425: 184-188.

Erdem, U.M., and Hasselmo, M. (2012) A goal-directed spatial navigation model using forward trajectory planning based on grid cells. *Journal of Neuroscience* 35(6): 916-931.

Fagiolini, M., Pizzorusso, T., Berardi, N., Domenici, L., Maffei, L. (1994) Functional postnatal development of the rat primary visual cortex and the role of visual experience: dark rearing and monocular deprivation. *Vision Research* 34(6): 709-720.

Fan, D., Rich, D., Holtzman, T., Ruther, P., Dalley, J.W., Lopez, A., Rossi, M.A., Barter, J.W., Salas-Meza, D., Herwik, S., Holzhammer, T., Morizo, J., Yin, H.H. (2011) A wireless multi-channel recording system for freely behaving mice and rats. *PLoS One* 6(7): e22033.

Farooq, U., Dragoi, G. (2019) Emergence of preconfigured and plastic time-compressed sequences in early postnatal development. *Science* 363: 168-173.

Feng, A.Y., and Himsworth, C.G. (2014) The secret life of the city rat: a review of the ecology of urban Norway and black rats (Rattus norvegicus and Rattus rattus). *Urban Ecosystems* 17(1): 149-162.

Feng, T., Silva, D., Foster, D.J. (2015) Dissociation between the experience-dependent development of hippocampal theta sequences and single-trial phase precession. *Journal of Neuroscience* 35: 4890-4902.

Ferguson, J.E., Boldt, C., Redish, A.D. (2009) Creating low-impedance tetrodes by electroplating with additives. *Sensors and Actuators A: Physical* 156(2): 388-393.

Finkelstein, A., Derdikman, D., Rubin, A., Foerster, J.N., Las, L., Ulanovsky, N. (2015) Three-dimensional head-direction coding in the bat brain. *Nature* 517(7533): 159-164.

Flannelly, K., and Lore, R. (1977) Observations of the subterranean activity of domesticated and wild rats (Rattus norvegicus): A descriptive study. *The Psychological Record* 27(1): 315-329.

Flecknell, P.A., Richardson, C.A., Popovic, A. (2007) Laboratory animals. p 983–988. In: Tranquilli WJ, Thurmon JC, Grimm KA. *Lumb and Jones' veterinary anesthesia*. Ames (IA): Blackwell Publishing.

Flick, R.P., Katusic, S.K., Colligan, R.C., Wilder, R.T., Voigt, R.G., Olson, M.D., Sprung, J., Weaver, A.L., Schroeder, D.R., Warner, D.O. (2011) Cognitive and behavioral outcomes after early exposure to anesthesia and surgery. *Pediatrics* 128(5):1053–1061.

Foreman, N., and Altaha, M. (1991). The development of exploration and spontaneous alternation in hooded rat pups: Effects of unusually early eyelid opening. *Developmental Psychobiology* 24(7): 521–537.

Foster, D.J., and Wilson, M.A. (2006) Reverse replay of behavioural sequences in hippocampal place cells during the awake state. *Nature* 440: 680-683.

Foster, D.J. (2017) Replay comes of age. *Annual Review of Neuroscience* 25(40): 581-602.

Fox, K. (1992) A critical period for experience-dependent synaptic plasticity in rat barrel cortex. *Journal of Neuroscience* 12(5): 1826-1838.

Frohardt, R.J., Bassett, J.P., Taube, J.S. (2006) Path integration and lesions within the head direction cell circuit: comparison between the roles of the anterodorsal thalamus and dorsal tegmental nucleus. *Behavioral Neuroscience* 120(1): 135.

Frost, B.E., Martin, S.K., Cafalchio, M., Islam, M.N., Aggleton, J.P., O'Mara, S. (2021) Anterior thalamic inputs are required for subiculum spatial coding, with associated consequences for hippocampal spatial mem-

ory. Journal of Neuroscience 41(30): 6511-6525.

Fuhs, M.C., Vanrhoads, S.R., Casale, A.E., McNaughton, B., Touretzky, D.S. (2005) Influence of path integration versus environmental orientation on place cell remapping between visually identical environments. *Journal of Neurophysiology* 94(4): 2603-2616.

Fuhs, M.C., Touretzky, D.S. (2006) A spin glass model of path integration in rat medial entorhinal cortex. *Journal of Neuroscience* 26(16): 4266-4276.

Fyhn, M., Hafting, T., Treves, A., Moser, M.B., Moser, E.I. (2007) Hip-pocampal remapping and grid realignment in entorhinal cortex. *Nature* 446(7132): 190-194.

Fyhn, M., Hafting, T., Witter, M.P., Moser, E.I., Moser, M.B. (2008) Grid cells in mice. *Hippocampus* 18(12): 1230-1238.

Gerrish, C.J., Alberts, J.R. (1996) Environmental temperature modulates onset of independent feeding: Warmer is sooner. *Developmental Psychobiology* 29(6): 483-495.

Gandhi, S.P., Cang, J., Stryker, M.P. (2005) An eye-opening experience. *Nature Neuroscience* 8(1): 9-10.

Geisler, H.C., Westerga, J., Gramsbergen, A. (1993) Development of posture in the rat. *Acta Neurobiologiae Experimentalis* 53(4): 517-523.

Gener, T., Perez-Mendez, L., Sanchez-Vives, M.V. (2013) Tactile modulation of hippocampal place fields. *Hippocampus* 23: 1453-1462.

Gerlei, K., Passlack, J., Hawes, I., Vandrey, B., Stevens, H., Papastathopoulos, I., Nolan, M.F. (2020) Grid cells are modulated by local head direction. *Nature Communications* 11(4228).

Geva-Sagiv, M., Las, L., Yovel, Y, Ulanovsky, N. (2015) Spatial cognition in bats and rats: from sensory acquisition to multiscale maps and navigation. *Nature Reviews Neuroscience* 16(2): 94-108.

Gil, M., Ancau, M., Schlesiger, M.I., Neitz, A., Allen, K., De Marco, R.J., Monyer, H. (2018) Impaired path integration in mice with disrupted grid

cell firing. Nature Neuroscience 21: 81-91.

Ginosar, G., Aljadeff, J., Burak, Y., Sompolinsky, H., Las, L., Ulanovsky, N. (2021) Locally ordered representation of 3D space in the entorhinal cortex. *Nature* 596(7872): 404-409.

Giocomo, L.M., Stensola, T., Bonnevie, T., Van Cauter, T., Moser, M.B., Moser, E.I. (2014) Topography of head direction cells in medial entorhinal cortex. *Current Biology* 24(3): 252-262.

Girardeau, G., Benchenane, K., Wiener, S.L., Buzsaki, G., Zugaro, M.B. (2009) Selective suppression of hippocampal ripples impairs spatial memory. *Nature Neuroscience* 12: 1222-1223.

Golob, E.J., and Taube, J.S. (1997) Head direction cells and episodic spatial information in rats without a hippocampus. *Proceedings of the National Academy of Sciences* 94(14): 7645-7650.

Golob, E.J., Wolk, D.A., Taube, J.S. (1998) Recordings of postsubiculum head direction cells following lesions of the laterodorsal thalamic nucleus. *Brain Research* 780: 9-19.

Golob, E.J., Stackman, R.W., Wong, A.C., Taube, J.S. (2001) On the behavioral significance of head direction cells: neural and behavioral dynamics during spatial memory tasks. *Behavioral Neuroscience* 115: 285-304.

Gonzalo-Ruiz, A., Sanz-Anquela, J.M., Spencer, R.F. (1993) Immuno-histological localization of GABA in the mammillary complex of the rat. *Neuroscience* 54(1): 143-156.

Gonzalo-Ruiz, A., Morte, L., Lieberman, A.R. (1997) Evidence for collateral projections to the retrosplenial granular cortex and thalamic reticular nucleus from glutamate and/or aspartate-containing neurons of the anterior thalamic nuclei in the rat. *Experimental Brain Research* 116(1): 63-72.

Goodridge, J.P., and Taube, J.S. (1995) Preferential use of the landmark navigation system by head direction cells in rats. *Behavioral Neuroscience*

109(1): 49.

Goodridge, J.P, and Taube, J.S. (1997) Interaction between postsubiculum and anterior thalamus in the generation of head direction cell activity. *Journal of Neuroscience* 17: 9315-9330.

Goodridge, J.P., Dudchenko, P.A., Worboys, K.A., Golob, E.J., Taube, J.S. (1998) Cue control and head direction cells. *Behavioural Neuroscience* 112(4): 749-761.

Gothard, K.M., Skaggs, W.E., McNaughton, B.L. (1996) Dynamics of mismatch correction in the hippocampal ensemble code for space: interaction between path integration and environmental cues. *Journal of Neuroscience* 16(24): 8027-8040.

Grant, R.A., Mitchinson, B., Prescott, T.J. (2012) The development of whisker control in rats in relation to locomotion. *Developmental Psychobiology* 54(2): 151-168.

Green, J.D. and Arduini, A.A. (1954) Hippocampal electrical activity in arousal. *Journal of Neurophysiology* 17: 533-57.

Green, R.J., and Stanton, M.E. (1989) Differential ontogeny of working memory and reference memory in the rat. *Behavioural Neuroscience* 103(1): 98-105.

Gregory, E.H., and Pfaff, D.W. (1971) Development of olfactory-guided behavior in infant rats. *Physiology & Behavior* 6(5): 573-576.

Grieves, R.M., Jenkins, B.W., Harland, B.C., Wood, E.R., Dudchenko, P.A. (2016) Place field repetition and spatial learning in a multicompartment environment. *Hippocampus* 26(1): 118-134.

Grieves, R.M. and Jeffery, K.J. (2017) The representation of space in the brain. *Behavioural Processes* 135: 113-131.

Grieves, R.M., Jedidi-Ayoub, S., Mishchanchuk, K., Liu, A., Renaudineau, S., E., Jeffery, K.J. (2020) The place-cell representation of volumetric space in rats. *Nature Communications* 7(11): 1-3.

Grieves, R.M., Jedidi-Ayoub, S., Mishchanchuk, K., Liu, A., Re-

naudineau, S., Duvelle, E., Jeffery, K.J. (2021) Irregular distribution of grid cell firing fields in rats exploring a 3D volumetric space. *Nature Neuro-science* 24(11): 1567-1573.

Groenewegen, H.J., and van Dijk, C.A. (1984) Efferent connection of the dorsal tegmental region in the rat, studied by means of anterograde transport of the lectin phaseolus vulgari-leucoagglutinin (PHA-L). *Brain Research* 304: 367-371.

Grota, L.J., and Ader, R. (1969) Continuous recording of maternal behaviour in Rattus norvegicus. *Animal Behaviour* 17(4): 722-729.

Guillery, R.W. (1955) A quantitative study of the mammillary bodies and their connexions. *Journal of Anatomy* 89: 19-32.

Hall, C.S., and Ballachey, E.L. (1932) A study of the rat's behavior in a field: a contribution to methods in comparative psychology. *University of California Publications in Psychology* 6: 1-12.

Guzowski, J.F., Miyashita, T., Chawla, M.K, Sanderson, J., Maes, L.I., Houston, F.P., Lipa, P., McNaughton, B.L., Worley, P.F., Barnes, C.A. (2006) Recent behavioral history modifies coupling between cell activity and Arc gene transcription in hippocampal CA1 neurons. *Proceedings of the National Academy of Sciences* 103(4): 1077-1082.

Hall, F.S. (1998) Social deprivation of neonatal, adolescent, and adult rats has distinct neurochemical and behavioral consequences. *Critical Reviews in Neurobiology* 12(1-2).

Hafting, T., Fhyn, M., Molden, S., Moser, M.B., Moser, E.I. (2005) Microstructure of a spatial map in the entorhinal cortex. *Nature* 436(7052): 801-806.

Hafting, T., Fhyn, M., Bonnevie, T., Moser, M.B., Moser, E.I. (2008) Hippocampus-independent phase precession in entorhinal grid cells. *Nature* 453: 1248-1252.

Hahnloser, R.H.R. (2003) Emergence of neural integration in the head-direction system by visual supervision. *Neuroscience* 120(3): 877-891.

Hardcastle, K., Maheswaranathan, N., Ganguli, S., Giacomo, L.M. (2017) A multiplexed, heterogeneous, and adaptive code for navigation in medial entorhinal cortex. *Neuron* 94(2): 375-387.

Harding, A., Halliday, G., Caine, D., Kril, J. (2000) Degeneration of anterior thalamic nuclei differentiates alcoholics with amnesia. *Brain* 123: 141-154.

Hargreaves, E.L., Yoganarasimha, D., Knierim, J.J. (2007) Cohesiveness of spatial and directional representations recorded from neural ensembles in the anterior thalamus, parasubiculum, medial entorhinal cortex, and hippocampus. *Hippocampus* 17(9): 826-841.

Harland, B., Wood, E.R., Dudchenko, P.A. (2015) The head direction cell system and behavior: the effects of lesions to the lateral mammillary bodies on spatial memory in a novel landmark task and in the water maze. *Behavioral Neuroscience* 129: 709-719.

Harland, B., Grieves, R.M., Bett, D., Stentiford, R., Wood, E.R., Dudchenko, P.A. (2017) Lesions of the head direction cell system increase hippocampal place field repetition. *Current Biology* 27: 2706-2712.

Harris, K.D., Henze, D.A., Csicsvari, J., Hirase, H., Buzsaki, G. (2000) Accuracy of tetrode spike separation as determined by simultaneous intracellular and extracellular measurements. *Journal of Neurophysiology* 84: 401-414.

Hartley, T., Tom, H., Burgess, N., Lever, C., Cacucci, F., O'Keefe, J. (2000) Modeling place fields in terms of the cortical inputs to the hippocampus. *Hippocampus* 10: 369-379.

Hartman, M.J. (2011) A night in the life of a rat: vibrissal mechanics and tactile exploration. *Annals of the New York Academy of Sciences* 1225(1): 110-118.

Hasegawa, T., Fujimoto, H., Tashiro, K., Nonomura, M., Tsuchiya, A., Watanabe, D. (2015) A wireless neural recording system with a precision motorized microdrive for freely behaving animals. *Scientific Reports*

5(7853): doi 10.1038/srep0785.

Hasselmo, M. E., Schnell, E., Barkai, E. (1995) Dynamics of learning and recall at excitatory recurrent synapses and cholinergic modulation in rat hippocampal region CA3. *Journal of Neuroscience* 15(7): 5249-5262.

Hayakawa, T., and Zyo, K. (1989) Retrograde double-labeling study of the mammillothalamic and the mammillotegmental projections in the rat. *Journal of Comparative Neurology* 298: 1-11.

Hayakawa, T., and Zyo, K. (1990) Fine structure of the lateral mammillary projection to the dorsal tegmental nucleus of Gudden. *Journal of Comparative Neurology* 298(2): 224-236.

Hensch, T.K., and Fagiolini, M. (2005) Excitatory-inhibitory balance and critical period plasticity in developing visual cortex. *Progress in Brain Research* 147: 115-124.

Hermer, L., and Spelke, E.S. (1994) A geometric process for spatial reorientation in young children. *Nature* 370: 57-59.

Hicks, S.P., and D'Amato, C.J. (1975) Motor-sensory cortex-cortico-spinal system and developing locomotion and placing in rats. *American Journal of Anatomy* 143: 1-42.

Hinman, J.R., Brandon, M.P., Climer, J.R., Chapman, G.W., Hasselmo, M.E. (2016) Multiple running speed signals in medial entorhinal cortex. *Neuron* 3(3): 666-679.

Hok, V., Lenck-Santini, P.P., Roux, S., Save, E., Muller, R.U., Poucet, B. (2007) Goal-related activity in hippocampal place cells. *Journal of Neuro-science* 27(3): 472-482.

Hollup, S.A., Molden, S., Donnett, J.G., Moser, M.B., Moser, E.I. (2001) Accumulation of hippocampal place fields at the goal location in an annular watermaze task. *Journal of Neuroscience* 21(5): 1635-1644.

Hoydal, O.A., Skytoen, E.R., Andersson, S.O., Moser, M.B., Moser, E.I. (2019) Object-vector coding in the medial entorhinal cortex. *Nature* 568(7752): 400-404.

Hyson, R.L., and Rudy, J.W. (1984) Ontogenesis of learning: II. Variation in the rat's reflexive and learned responses to acoustic stimulation. *Developmental Psychobiology* 17(3): 263-283.

Hubel, D.H. (1957) Tungsten microelectrode for recording from single units. *Science* 125: 549-550.

Huxter, J., Burgess, N., O'Keefe, J. (2003) Independent rate and temporal coding in hippocampal pyramidal cells. *Nature* 425: 828-832.

Hull, C.L. (1950) Behavior postulates and corollaries. *Psychological Review* 57: 173-180.

Huss, M. K., Chum, H. H., Chang, A. G., Jampachairsi, K., Pacharinsak, C. (2016) The physiologic effects of isoflurane, sevoflurane, and hypothermia used for anesthesia in neonatal rats (*Rattus norvegicus*). *Journal of the American Association for Laboratory Animal Science* 55(1): 83-88.

Inglis, I.R., Shepherd, D.S., Smith, P., Haynes, P.J., Bull, D.S., Cowan, D.P., Whitehead, D. (1996) Foraging behaviour of wild rats (Rattus norvegicus) towards new foods and bait containers. *Applied Animal Behaviour Science* 47(3-4): 175-190.

Ishizuka, N., Weber, J., Amaral, D. G. (1990) Organization of intrahip-pocampal projections originating from CA3 pyramidal cells in the rat. *Journal of Comparative Neurology* 295:580–623.

Jacob, P.Y., Casali, G., Spieser, L., Page, H., Overington, D., Jeffery, K. (2017) An independent, landmark-dominated head-direction signal in dysgranular retrosplenial cortex. *Nature Neuroscience* 20(2): 173-175.

Jacob, P.Y., Capitano, F., Poucet, S., Save, E., Sargolini, F. (2019) Path integration maintains spatial periodicity of grid cell firing in a 1D circular track. *Nature Communications* 10(1): 1-13.

Jeewajee, A., Barry, C., Douchamps, V., Manson, D., Lever, C., Burgess, N. (2014) Theta phase precession of grid and place cell firing in open environments. *Philosophical Transactions of the Royal Society B* 369: 20120532.

Jeffery, K.J., Grieves, R., Donnett, J. (2018) Chapter 5- Recording the

spatial mapping cells: Place, head direction and grid cells. *Handbook of Behavioural Neuroscience* 28: 95-121.

Jeffery, K.J. (2021) How environmental movement constraints shape the neural code for space. *Cognitive Processing* 22: 97-104.

Jercog, P.E., Ahmadian, Y., Woodruff, C., Deb-Sen, R., Abbott, L.F., Kandel, E.R. (2019) Heading direction with respect to a reference point modulates place-cell activity. *Nature Communications* 10: 2333.

Jevtovic-Todorovic, V., Hartman, R.E., Izumi, Y., Benshoff, N.D., Dikranian, K., Zorumski, C.F., Olney, J.W., Wozniak, D.F. (2003) Early exposure to common anesthetic agents causes widespread neurodegeneration in the developing rat brain and persistent learning deficits. *Journal of Neuroscience* 23:876–82.

Kant, I. (1781) Kritik Der Reinen Vernunft.

Karlsson, M.P., and Frank, L.M. (2009) Awake replay of remote experiences in the hippocampus. *Nature Neuroscience* 12(7): 913-918.

Keinath, A.T., Julian, J.B., Epstein, R.A., Muzzio, I.A. (2017) Environmental geometry aligns the hippocampal spatial reorientation. *Current Biology* 27: 309-317.

Kempter, R., Leibold, C., Buzsaki, G., Diba, K., Schmidt, R. (2012) Quantifying circular-linear associations: Hippocampal phase precession. *Journal of Neuroscience Methods* 207: 113-124.

Keshavarzi, S., Bracey, E.F., Faville, R.A., Campagner, D., Tyson, A.L., Lenzi, S.C., Branco, T., Margrie, T.W. (2021) The retrosplenial cortex combines internal and external cues to encode head velocity during navigation. *BioRxiv*.

Kim, S.S., Rouault, H., Druckmann, S., Jayaraman, V. (2017) Ring attractor dynamics in the *Drosophila* central brain. *Science* 356(6340): 849-853.

Knierim, J.J., Kudrimoti, H.S., McNaughton, B.L. (1995) Place cells, head direction cells, and the learning of landmark stability. *Journal of Neu-*

roscience 15(3): 1648-1659.

Knierim, J.J., Kudrimoti, H.S., McNaughton, B.L. (1998) Interactions between idiothetic cues and external landmarks in the control of place cells and head direction cells. *Journal of Neurophysiology* 80(1): 425-446.

Knight, R., Hayman, R., Ginzberg, L.L., Jeffery, K. (2011) Geometric cues influence head direction cells only weakly in non disorientated rats. *Journal of Neuroscience* 31(44): 15681-15692.

Kocsis, B., and Vertes, R.P. (1994) Characterization of neurons of the supramammillary nucleus and mammillary body that discharge rhythmically with the hippocampal theta rhythm in the rat. *Journal of Neuroscience* 14(11): 7040-7052.

Koenig, J., Linder, A.N., Leutgeb, J.K., Leutgeb, S. (2011) The spatial periodicity of grid cells is not sustained during reduced theta oscillations. *Science* 332(6029): 592-595.

Koganezawa, N., Gisetstad, R., Husby, E., Doan, T.P., Witter, M.P. (2015) Excitatory postrhinal projections to principal cells in the medial entorhinal cortex. *Journal of Neuroscience* 35:15860-15874.

Koolhaas, J.M. (2000) The laboratory rat. The UFAW handbook on the care and management of laboratory and other research animals 8: 311-326.

Kornienko, O., Latuske, P., Bassler, M., Kohler, L., Allen, K. (2018) Non-rhythmic head-direction cells in the parahippocampal region are not constrained by attractor network dynamics. *Elife* 7: e35949.

Kraus, B.J., Robinson, R.J., White, J.A., Eichenbaum, H., Hasselmo, M.E. (2013) Hippocampal 'time cells': time versus path integration. *Neuron* 78: 1090-1101.

Kropff, E., Carmichael, J.E., Moser, MB., Moser, E.I. (2015) Speed cells in the medial entorhinal cortex. *Nature* 523: 419-424.

Krupic, J., Bauza, M., Burton, S., Barry, C., O'Keefe, J. (2015) Grid cell symmetry is shaped by environmental geometry. *Nature* 518: 232-235.

Kubie, J.L., and Fenton, A.A. (2012) Linear look-ahead in conjunctive cells: an entorhinal mechanism for vector-based navigation. *Frontiers in Neural Circuits* 6: 20.

Landers, M., and Zeigler, H.P. (2006) Development of rodent whisking: trigeminal input and central pattern generation. *Somatosensory & Motor Research* 23(1-2): 1-10.

Lannou, J., Precht, W., Cazin, L. (1979) The postnatal development of functional properties of central vestibular neurons in the rat. *Brain Research* 175(2): 219-232.

Langston, R.F., Ainge, J.A., Couey, J.J., Canto, C.B., Bjerknes, T.L., Witter, M.P., Moser, E.I., Moser, M.B. (2010) Development of the spatial representation system in the rat. *Science* 328(5985): 1576-1580.

Lauer, J., Zhou, M., Shaokai, Y., Menegas, W., Schneider, S. Nath, T., Rahman, M.M., Di Santo, V., Soberanes, D., Feng, G., Murthy, V.N., Lauder, G., Dulac, C., Mathis, M.W., Mathis, A. (2022) Multi-animal pose estimation, identification and tracking with DeepLabCut. *Nature* 19: 496-504.

Laurens, J., Kim, B., Dickman, J.D., Angelaki, D.E. (2016) Gravity orientation tuning in macaque anterior thalamus. *Nature Neuroscience* 19: 1566-1568.

Leblanc, M.O., Bland, B.H. (1979) Developmental aspects of hip-pocampal electrical activity and motor behavior in the rat. *Experimental Neurology* 66(2): 220-237.

Lee, B. H., Chan, J. T., Kraeva, E., Peterson, K., Sall, J. W. (2014) Isoflurane exposure in newborn rats induces long-term cognitive dysfunction in males but not females. *Neuropharmacology* 83: 9-17.

Lee, I., Yoganarasimha, D., Rao, G., Knierim, J. J. (2004) Comparison of population coherence of place cells in hippocampal subfields CA1 and CA3. *Nature* 430(6998): 456-459.

Leon, M., Croskerry, P.G., Smith, G.K. (1978) Thermal control of mother-young contact in rats. *Physiology Behavior* 21(5): 793-811.

- Lever, C., Burton, S., Jeewajee, A., O'Keefe, J., Burgess, N. (2009) Boundary vector cells in the subiculum of the hippocampal formation. *Journal of Neuroscience* 29(31): 9771-9777.
- Leutgeb, S., Ragozzino, K.E., Mizumori, S.J. (2000) Convergence of head direction and place information in the CA1 region of the hippocampus. *Neuroscience* 100:11-19.
- Leutgeb, S., Leutgeb, J.K., Barnes, C.A., Moser, E.I., McNaughton, B.L., Moser, M.B. (2005) Independent codes for spatial and episodic memory in hippocampal neuronal ensembles. *Science* 309(5734): 619-623.
- Lever, C., Wills, T.J., Cacucci, F., Burgess, N., O'Keefe, J. (2002) Long-term plasticity in hippocampal place-cell representation of environmental geometry. *Nature* 416(6876): 90-94.
- Liu, R., Chang, L., Wickern, G. (1984) The dorsal tegmental nucleus: an axoplasmic transport study. *Brain Research* 310(1:) 123-132.
- Liu, D., Diorio, J., Day, J.C., Francis, D.D., Meaney, M.J. (2000) Maternal care, hippocampal synaptogenesis and cognitive development in rats. *Nature Neuroscience* 3(8): 799-806.
- Loewen, I., Wallace, D.G., Whishaw, I.Q. (2005) The development of spatial capacity in piloting and dead reckoning by infant rats: use of the huddle as a home base for spatial navigation. *Developmental Psychobiology* 46(4): 350-361.
- Lomi, E., Mathiasen, M.L., Cheng, H.Y., Zhang, N., Aggleton, J.P., Mitchell, A.S., Jeffery, K.J. (2021) Evidence for two distinct thalamocortical circuits in retrosplenial cortex. *Neurobiology of Learning and Memory* 185: 107525.
- Lopes, G., Bonacchi, N., Frazao, J., Neto, J.P., Atallah, B.V., Soares, S., Moreira, L., Matias, S., Itskov, P.M., Correia, P.A., Medina, R.E., Calcaterra, L., Dreosti, E., Paton, J.J., Kampff, A.R. (2015) Bonsai: An event-based framework for processing and controlling data streams. *Frontiers in Neuroinformatics* 9(7).

Lopez, J., Gamache, K., Milo, C., Nader, K. (2017) Differential role of the anterior and intralaminar/lateral thalamic nuclei in systems consolidation and reconsolidation. *Brain Structure and Function* 223(1): 63-76.

Lorente de Nó, R. (1934) Studies on the structure of the cerebral cortex. II. Continuation of the study of the ammonic system. *Journal für Psychologie und Neurologie* 46: 113–177.

Maguire, E.A. (2001) The retrosplenial contribution to human navigation: a review of lesion and imaging findings. *Scandinavian Journal of Psychology* 42: 225-238.

Markus, E.J., Qin, Y.L., Leonard, B., Skaggs, W.E., McNaughton, B.L., Barnes, C.A. (1995) Interactions between location and task affect the spatial and directional firing of hippocampal neurons. *Journal of Neuroscience* 15(11): 7079-7094.

Marr, D. (1971) A theory of archicortical function. *Proceedings of the Royal Society B: Biological Sciences* 262: 23-81.

Martin, P.D., and Berthoz, A. (2002) Development of spatial firing in the hippocampus of young rats. *Hippocampus* 12(4): 465-480.

Martinez, R., and Morato, S. (2004) Thigmotaxis and exploration in adult and pup rats. *Revista de Etologia* 6(1): 49-54.

Marx, V. (2021) Neuroscientists go wireless. *Nature Methods* 18(10): 1150-1154.

Mathis, A., Mamidanna, P., Cury, K.M., Abe, T., Murthy, V.N., Mathis, M.W., Bethge, M. (2018) DeepLabCut: Markerless pose estimation of user-defined body parts with deep learning. *Nature Neuroscience* 21(9): 1281-1289.

McNaughton, B.L., O'Keefe, J., Barnes, C.A. (1983a) The stereotrode: a new technique for simultaneous isolation of several single unit in the central nervous system from multiple unit records. *Journal of Neuroscience Methods* 8(4): 391-397.

McNaughton, B.L., Barnes, C.A., O'Keefe, J. (1983b) The contributions

of position, direction, and velocity to single unit activity in the hippocampus of freely-moving rats. *Experimental Brain Research* 52: 41-49.

McNaughton, B. L., and Morris, R. G. (1987) Hippocampal synaptic enhancement and information storage within a distributed memory system. Trends in neurosciences 10(10): 408-415.

McNaughton, B.L., Chen, L., Markus, E. (1991) 'Dead reckoning', land-mark learning, and the sense of direction: a neurophysiological and computational hypothesis. *Journal of Cognitive Neuroscience* 3: 190-202.

McNaughton, B.L., Barnes, C.A., Gerrard, J.L., Gothard, K., Jung, M.W., Knierim, J.J., Kudrimoti, H., Qin, Y., Skaggs, W.E., Suster, M., Weaver, K.L. (1996) Deciphering the hippocampal polyglot: the hippocampus as a path integration system. *Journal of Experimental Biology* 199: 173-185.

McNaughton, B.L., Battaglia, F.P., Jensen, O., Moser, E.I., Moser, M.B. (2006) Path integration and the neural basis of the 'cognitive map'. *Nature Reviews Neuroscience* 7(8): 663-678.

Mehlman, M.L., and Taube, J.S. (2018) Chapter 9 - In vivo electrophysiological approaches for studying head direction cells. *Handbook of Behavioural Neuroscience Academic Press*, Volume 28: 169-187.

Melamed, O., Gerstner, W., Maass, W., Tsodyks, M., Markram, H. (2004) Coding and learning of behavioral sequences. *Trends in Neurosciences* 27(1): 11-14.

Miao, C., Cao, Q., Moser, M.B., Moser, E.I. (2017) Parvalbumin and somatostatin interneurons control different space-coding networks in the medial entorhinal cortex. *Cell* 171: 507-521.

Middleton, S.J. and McHugh, T.J. (2016) Silencing CA3 disrupts temporal coding in the CA1 ensemble. *Nature Neuroscience* 19(7): 945-951.

Mitchinson, B., Martin, C.J., Grant, R.A., Prescott, T.J. (2007) Feedback control in active sensing: rat exploratory whisking is modulated by environmental contact. *Proceedings of the Royal Society B: Biological Sciences* 274(1613): 1035-1041.

Mittelstaedt, M.L., Mittelstaedt, H. (1980) Homing by path integration in a mammal. *Naturwissenschaften* 67: 566-567.

Mizumori, S.J., and Williams, J.D. (1993) Directionally selective mnemonic properties of neurons in the lateral dorsal nucleus of the thalamus of rats. *Journal of Neuroscience* 13: 4015-4028.

Mizumori, S.J., Miya, D.Y., Ward, K.E. (1994) Reversible inactivation of the lateral dorsal thalamus disrupts hippocampal place representation and impairs spatial learning. *Brain Research* 644: 168-174.

Mogil, J.S. (2019) Mice are people too: Increasing evidence for cognitive, emotional and social capabilities in laboratory rodents. *Canadian Psychology/ Psychologie Canadienne* 60(1): 14.

Morris, R.G. (1981) Spatial localization does not require the presence of local cues. *Learning and Motivation* 12(2): 239-260.

Morris, R.G.M., Garrud, P., Rawlins, J.N.P., O'Keefe, J. (1982) Place navigation impaired in rats with hippocampal lesions. *Nature* 297: 681-683.

Moser, E.I., and Moser, M.B. (2008) A metric for space. *Hippocampus* 18(12): 1142-1156.

Moye, T. B., and Rudy, J. W. (1985). Ontogenesis of learning: VI. Learned and unlearned responses to visual stimulation in the infant hooded rat. *Developmental Psychobiology: The Journal of the International Society for Developmental Psychobiology* 18(5): 395-409.

Muessig, L., Hauser, J., Wills, T.J., Cacucci, F. (2015) A developmental switch in place cell accuracy coincides with grid cell maturation. *Neuron* 86(5): 1167-1173.

Muessig, L., Hauser, J., Wills, T.J., Cacucci, F. (2016) Place cell networks in pre-weanling rats show associative memory properties from the onset of exploratory behavior. *Cerebral Cortex* 26(8): 3627-3636.

Muessig, L., Lasek, M., Varsavsky, I., Cacucci, F., Wills, T.J. (2019) Coordinated emergence of hippocampal replay and theta sequences during post-natal development. *Current Biology* 29(5): 834-840.

Muir, G.M., Brown, J.E., Carey, J.P., Hirvonen, T.P., Della Santina, C.C., Minor, L.B., Taube, J.S. (2009) Disruption of the head direction cell signal after occlusion of the semicircular canals in the freely moving chinchilla. *Journal of Neuroscience* 29: 14521-14533.

Muller, R.U., and Kubie, J.L. (1987) The effects of changes in the environment on the spatial firing of hippocampal complex-spike cells. *Journal of Neuroscience* 7: 1951-1968.

Muller, R.U., Kubie, J.L., Ranck Jr., J.B. (1987) Spatial firing patterns of hippocampal complex-spike cells in a fixed environment. *Journal of Neuroscience* 7: 1935-1950.

Muller, R.U., Bostock, E., Taube, J.S., Kubie, J.L. (1994) On the directional firing properties of hippocampal place cells. *Journal of Neuroscience* 14: 7235-7251.

Murphy, K. L., and Baxter, M. G. (2013) Long-term effects of neonatal single or multiple isoflurane exposures on spatial memory in rats. *Frontiers in neurology* 4: 87.

Nadel, L., Wilson, L., Kurz, E.M. (1992) Hippocampus: Effects of alterations in timing of development. *Developmental Time and Timing. Psychology Press*: 253-272.

Naninck, E.F., Hoejimakers, L., Kakava-Georgiadou, N., Meesters, A., Lazic, S.E., Lucassen, P.J., Korosi, A. (2015) Chronic early life stress alters developmental and adult neurogenesis and impairs cognitive function in mice. *Hippocampus* 25(3): 309-328.

Nemati, F., Kolb, B., Metz, G.A. (2013) Stress and risk avoidance by exploring rats: implications for stress management in fear-related behaviours. *Behavioural Processes* 94: 89-98.

Nissl, F. (1894). Ueber eine neue Untersuchungsmethode des Centralorgans zur Feststellung der Localisation der Nervenzellen. *Neurologisches Centralblatt* 13: 507-508.

Oitzl, M.S., Workel, J.O., Fluttert, M., Frosch, F., De Kloet, E.R. (2000)

Maternal deprivation affects behaviour from youth to senescence: amplification of individual differences in spatial learning and memory in senescent Brown Norway rats. *European Journal of Neuroscience* 12(10): 3771-3780.

O'Keefe, J. and Dostrovsky, J. (1971) The hippocampus as a spatial map. Preliminary evidence from unit activity in the freely moving rat. *Brain Research* 34: 171-175.

O'Keefe, J. and Nadel, L. (1978) The Hippocampus as a Cognitive Map. Oxford University Press, New York.

O'Keefe, J., and Speakman, A. (1987) Single unit activity in the rat hip-pocampus during a spatial memory task. *Experimental Brain Research* 68(1): 1-27.

O'Keefe, J. and Recce, M.L. (1993) Phase relationship between hip-pocampal place units and the EEG theta rhythm. *Hippocampus* 3: 317-330.

O'Keefe, J., and Burgess, N. (1996) Geometric determinants of the place fields of hippocampal neurons. *Nature* 381: 425-428.

Olton, D.S., Branch, M., Best, P.J. (1978) Spatial correlates of hip-pocampal unit activity. *Experimental Neurology* 58: 387-409.

Omer, D.B., Maimon, S.R., Las, L., Ulanovsky, N. (2018) Social placecells in the bat hippocampus. *Science* 359(6372): 218-224.

Oomen, C.A., Soeters, H., Audureau, N., Vermunt, L., Van Hasselt, F.N., Manders, E.M., Joels, M., Lucassen, P.J., Krugers, H. (2010) Severe early life stress hampers spatial learning and neurogenesis, but improves hippocampal synaptic plasticity and emotional learning under high-stress conditions in adulthood. *Journal of Neuroscience* 30(19): 6635-6645.

Packard, M.G., Hirsh, R., White, N.M. (1989) Differential effects of fornix and caudate nucleus lesions on two radial maze tasks: Evidence for multiple memory systems. *Journal of Neuroscience* 9: 1465-1472.

Packard, M.G., and White, N.M. (1991) Dissociation of hippocampus

and caudate nucleus memory systems by posttraining intracerebral injection of dopamine agonists. *Behavioral Neuroscience* 105: 295-306.

Packard, M.G., and McGaugh, J.L. (1992) Double dissociation of fornix and caudate nucleus lesions on acquisition of two water maze tasks: Further evidence for multiple memory systems. *Behavioral Neuroscience* 106: 439-446.

Packard, M.G., Cahill, L., McGaugh, J.L. (1994) Amygdala modulation of hippocampal-dependent and caudate nucleus-dependent memory processes. *Proceedings of the National Academy of Sciences* 91: 8477-8481.

Packard, M.G., and McGaugh, J.L. (1996) Inactivation of hippocampus or caudate nucleus with lidocaine differentially affects expression of place and response learning. *Neurobiology of Learning and Memory* 65: 65-72.

Packard, M.G., and Teather, L.A. (1997) Double dissociation of hip-pocampal and dorsal-striatal memory systems by posttraining intracerebral injections of 2-amino-5-phosphonopentanoic acid. *Behavioral Neuroscience* 111(3): 543-551.

Page, H.J., Walters, D., Stringer, S.M. (2018a) A speed-accurate self-sustaining head direction cell path integration model without recurrent excitation. *Network: Computation in Neural Systems* 29(1-4): 37-69.

Page, H.J., Wilson, J.J., Jeffery, K.J. (2018b) A dual-axis rotation rule for updating the head direction cell reference frame during movement in three dimensions. *Journal of Neurophysiology* 119(1): 192-208.

Papez, J.W. (1937) A proposed mechanism of emotion. *Archives of Neurology Psychiatry* 28: 725-743.

Park, S., Holzman, P.S. (1992) Schizophrenics show spatial working memory deficits. *Archives of General Psychiatry* 49: 975-982.

Paxinos, G., and Watson, C. (2006) The rat brain in stereotaxic coordinates sixth edition. *Academic Press* 170(547612): 10-1016.

Pecchia, T., Vallortigara, G. (2010) View-based strategy for reorientation by geometry. *Journal of Experimental Biology* 213: 2987-2996.

Peckford, G., Dwyer, J.A., Snow, A.C., Thorpe, C.M., Martin, G.M., Skinner, D.M. (2014) The effects of lesions to the postsubiculum or the anterior dorsal nucleus of the thalamus on spatial learning in rats. *Hippocampus* 128: 654-665.

Pellis, S.M., and Pellis, V.C. (1998) Play fighting of rats in comparative perspective: a schema for neurobehavioral analyses. *Neuroscience Biobehavioral Reviews* 23(1): 87-101.

Perez-Escobar, J.A., Kornienko, O., Latuske, P., Kohler, L., Allen, K. (2016) Visual landmarks sharpen grid cell metric and confer context specificity to neurons of the medial entorhinal cortex. *eLife* 5: e16937.

Petsche, H., Stumpf, C., Gogolak, G. (1962) The significance of the rabbit's septum as a relay station between the midbrain and the hippocampus. I. The control of hippocampus arousal activity by the septum cell. *Electroencephalography and Clinical Neurophysiology* 14: 202-211.

Peyrache, A., Lacroix, M.M., Peterson, P.C., Buzsaki, G. (2015) Internally organized mechanisms of the head direction sense. *Nature Neuroscience* 18(4): 569-575.

Peyrache, A., Schieferstein, N., Buzsaki, G. (2017) Transformation of the head-direction signal into a spatial code. *Nature Communications* 8(1): 1-9.

Pisano, R.G., and Storer, T.I. (1948) Burrows and feeding of the Norway rat. *Journal of Mammalogy* 29(4): 374-383.

Polan, H.J., and Hofer, M.A. (1998) Olfactory preference for mother over home nest shavings by newborn rats. *Developmental Psychobiology* 33(1): 5-20.

Pothuizen, H.J., Aggleton, J.P., Vann, S.D. (2008) Do rats with retrosplenial cortex lesions lack direction? *European Journal of Neuroscience* 28(12): 2486-2498.

Pothuizen, H.J., Davies, M., Albasser, M.M., Aggleton, J.P., Vann, S.D. (2009) Granular and dysgranular retrosplenial cortices provide qualita-

tively different contributions to spatial working memory: evidence from immediate-early gene imaging in rats. *European Journal of Neuroscience* 30(5): 877-888.

Poulter, S., Lee, S.A., Dachtler, J., Wills, T.J., Lever, C. (2021) Vector trace cells in the subiculum of the hippocampal formation. *Nature Neuroscience* 24(2): 266-275.

Prevost, F., Lepore, F., Guillemot, J.P. (2010) Cortical development of the visual system of the rat. *Neuroreport* 21(1): 50-54.

Quirk, G.J., Muller, R.U., Kubie, J.L. (1990) The firing of hippocampal place cells in the dark depends on the rat's recent experience. *Journal of Neuroscience* 10: 2008-2017.

Quirk, G.J., Muller, R.U., Kubie, J.L., Ranck, J.R. (1992) The positional firing properties of medial entorhinal neurons: description and comparison with hippocampal place cells. *Journal of Neuroscience* 12(5): 1945-1963.

Ramon y Cajal, S. (1902) Sobre un ganglio especial de la corteza esfeno occipital. *Trab. del Lab. de Invest. Biol. Univ. Madrid* 1: 189–206.

Ranck, J.B.J. (1984) Head-direction cells in the deep layer of dorsal presubiculum in freely moving rats. *Society for Neuroscience Abstract*.

Rauch, S.L., and Raskin, L.A. (1984) Cholinergic mediation of spatial memory in the preweanling rat: Application of the radial arm maze paradigm. *Behavioral Neuroscience* 98(1): 35-43.

Redish, A.D., Elga, A.N., Touretzky, D.S. (1996) A coupled attractor model of the rodent head direction system. *Network: Computation in Neural Systems* 7: 671-685.

Robertson, R.G., Rolls, E.T., Georges-Francois, P., Panzeri, S. (1999) Head direction cells in the primate pre-subiculum. *Hippocampus* 9(3): 206-219.

Rondi-Reig, L., Le Marec, N., Caston, J., Mariani, J. (2002) The role of climbing and parallel fibers input to cerebellar cortex in navigation. *Be*-

havioral Brain Research 132(1): 11-18.

Rosenblatt, J.S. (1976) Stages in the early behavioural development of altricial young of selected species of non primate mammals. *Growing points in ethology.*

Routtenberg, A., Strop, M., Jerdan, J. (1978) Response of the infant rat to light prior to eyelid opening: mediation by the superior colliculus. *Developmental Psychobiology* 11(5): 469-78.

Rubin, A., Yartsev, M.M., Ulanovsky, N. (2014) Encoding of head direction by hippocampal place cells in bats. *Journal of Neuroscience* 34: 1067-1080.

Rudy, J.W., and Cheatle, M.D. (1977) Odor-aversion learning in neonatal rats. *Science* 198(4319): 845-846.

Rudy, J.W., and Hyson, R.L. (1984) Ontogenesis of learning. III. Variation in the rat's differential reflexive and learned responses to sound frequencies. *Developmental Psychobiology: The Journal of the International Society for Psychobiology* 17(3): 285-300.

Rudy, J.W., Stadler-Morris, S., Albert, P. (1987) Ontogeny of spatial navigation behaviors in the rat: dissociation of 'proximal'- and 'distal'-cuebased behaviors. *Behavioral Neuroscience* 101(1): 62-73.

Ruppert, P.H., Dean, K.F., Reiter, L.W. (1985) Development of locomotor activity of rat pups in figure-eight mazes. *Developmental Psychobiology* 18: 247-260.

Salgado-Pineda, P., Landin-Romero, R., Portillo, F., Bosque, C., Pomes, A., Spanlang, B., Franquelo, J.C., Teixido, C., Sarro, S., Salvador, R., Slater, M., Pomarol-Clotet, E., McKenna, P.J. (2016) Examining hippocampal function in schizophrenia using a virtual reality spatial navigation task. *Schizophrenia Research* 172: 86-93.

Salmon, D.P., and Bondi, M.W. (2009) Neuropsychological assessment of dementia. *Annual Review of Psychology* 60: 257-282.

Sanguinetti-Scheck, J.I., Brecht, M. (2020) Home, head direction sta-

bility, and grid cell distortion. *Journal of Neurophysiology* 123(4): 1392-1406.

Sarel, A., Finkelstein, A., Las, L., Ulanovsky, N. (2017) Vectorial representation of spatial goals in the hippocampus of bats. *Science* 355(6321): 176-180.

Sargolini, F., Fyhn, M., Hafting, T., McNaughton, B.L., Witter, M.P., Moser, M.B., Moser, E.I. (2006) Conjunctive representation of position, direction, and velocity in entorhinal cortex. *Science* 312(5774): 758-762.

Save, E., Cressant, A., Thinus-Blanc, C., Poucet, B. (1998) Spatial firing of hippocampal place cells in blind rats. *Journal of Neuroscience* 28: 1841-1853.

Schenk, F. (1985) Development of place navigation in rats from weaning to puberty. *Behavioural and Neural Biology* 43: 69-85.

Schlesiger, M.I., Cannova, C.C., Boubil, B.L., Hales, J.B., Mankin, E.A., Brandon, M.P., Leutgeb, J.K., Leibold, C., Leutgeb, S. (2015) The medial entorhinal cortex is necessary for temporal organization of hippocampal neuronal activity. *Nature Neuroscience* 18(8): 1123-1132.

Schmitzer-Torbert, N., Jackson, J., Henze, D., Harris, K., Redish, A.D. (2005) Quantitative measures of cluster quality for use in extracellular recordings. *Neuroscience* 131(1): 1-11.

Schrijver, N.C.A., Pallier, P.N., Brown, V.J., Wurbel, H. (2004) Double dissociation of social environmental stimulation on spatial learning and reversal learning in rats. *Behavioral Brain Research* 152(2): 307-314.

Schweinfurth, M.K., Neuenschwander, J., Engqvist, L., Schneeberger, K., Rentsch, A.K., Gygax, M., Taborsky, M. (2017) Do female Norway rats form social bonds? *Behavioral Ecology and Sociobiology* 71(6): 1-9.

Scott, R.C., Richard, G.R., Holmes, G.L., Lenck-Santini, P.P. (2011) Maturational dynamics of hippocampal place cells in immature rats. *Hippocampus* 21(4): 347-353.

Scoville, W.B., and Milner, B. (1957) Loss of recent memory after bilat-

eral hippocampal lesions. *Journal of Neurology, Neurosurgery, and Psychiatry* 20(1): 11.

Seelig, J.D., and Jayaraman, V. (2015) Neural dynamics for landmark orientation and angular path integration. *Nature* 521(7551): 186-191.

Sestakova, N., Puzserova, A., Kluknavsky, M., Bernatova, I. (2013) Determination of motor activity and anxiety-related behaviour in rodents: methodological aspects and role of nitric oxide. *Interdisciplinary Toxicology* 6(3): 126-135.

Seymoure, P., Dou, H., Juraska, J.M. (2013) Sex differences in radial arm maze performance: Influence of rearing environment and room cues. *Psychobiology* 24: 33-37.

Sharp, P.E. (1996) Multiple spatial/behavioral correlates for cells in the rat postsubiculum: multiple regression analysis and comparison to other hippocampal areas. *Cerebral cortex* 6(2): 238-259.

Sharp, P.E., Tinkelman, A., Cho, J. (2001a) Angular velocity and head direction signals recorded from the dorsal tegmental nucleus of Gudden in the rat: Implications for path integration in the head direction cell circuit. *Behavioural Neuroscience* 115(3): 571-588.

Sharp, P.E., Blair, H.T., Cho, J. (2001b) The anatomical and computational basis of the rat head-direction cell signal. *Trends in Neurosciences* 24(5): 289-294.

Sharp, P.E., Turner-Williams, S., Tuttle, S. (2006) Movement-related correlates of single-cell activity in the interpeduncular nucleus and habenula of the rat during a pellet-chasing task. *Behavioral Brain Research* 166: 55-70.

Sharp, P.E., and Koester, K. (2008) Lesions of the mammillary body region severely disrupt the cortical head direction, but not place cell signal. *Hippocampus* 18(8): 766-784.

Shibata, H. (1987) Ascending projections to the mammillary nuclei in the rat: a study using retrograde and anterograde transport of wheat germ agglutinin conjugated to horseradish peroxidase. *Journal of Comparative Neurology* 264: 205-215.

Shibata, H. (1989) Descending projections to the mammillary nuclei in the rat, as studied by retrograde and anterograde transport of wheat germ agglutinin-horseradish peroxidase. *Journal of Comparative Neurology* 285: 436-452.

Shibata, H. (1992) Topographic organization of subcortical projections to the anterior thalamic nuclei in the rat. *Journal of Comparative Neurology* 323: 117-127.

Shibata, H. (1993) Direct projections from the anterior thalamic nuclei to the retrohippocampal region in the rat. *Journal of Comparative Neurology* 337: 431-445.

Shibata, H. (1998) Organization of projections of rat retrosplenial cortex to the anterior thalamic nuclei. *European Journal of Neuroscience* 10: 3210-3219.

Shibata, H. (2000) Organization of retrosplenial cortical projections to the laterodorsal thalamic nucleus in the rat. *Neuroscience Research* 38: 303-311.

Shinder, M.E., and Taube, J.S. (2019) Three-dimensional tuning of head direction cells in rats. *Journal of Neurophysiology* 121(1): 4-37.

Shine, J.P., Valdes-Herrera, J.P., Hegarty, M., Wolbers, T. (2016) The human retrosplenial cortex and thalamus code head direction in a global reference frame. *Journal of Neuroscience* 36: 6371-6381.

Skaggs, W.E., McNaughton, B.L., Gothard, K.M., Markus, E.J. (1993) An information-theoretic approach to deciphering the hippocampal code. *Advances in Neural Information Processing Systems* 5: 1030-1037.

Skaggs, W.E., Knierim, J.J., Kudrimoti, H.S., McNaughton, B.L. (1995) A model of the neural basis for a rat's sense of direction. *Advances in Neural Information Processing Systems* 7: 173-180.

Skaggs, W.E., and McNaughton, B.L. (1996) Replay of neuronal firing

sequences in rat hippocampus during sleep following spatial experience. *Science* 271: 1870-1873.

Skaggs, W.E., McNaughton, B.L., Wilson, M.A., Barnes, C.A. (1996) Theta phase precession in hippocampal neuronal populations and the compression of temporal sequences. *Hippocampus* 6: 149-172.

Smith, A.E., Cheek, O.A., Sweet, E.L., Dudchenko, P.A., Wood, E.R. (2019) Lesions of the head direction cell system impair direction discrimination. *Behavioral Neuroscience* 133(6): 602.

Smithe, T.S.C., and Stringer, S.M. (2022) The role of idiothetic signals, landmarks, and conjunctive representations in the development of place and head-direction cells: A self-organizing neural network model. *Cerebral Cortex Communications* 3(1): 1-22.

Sokoloff, G., and Blumberg, M.S. (2001) Competition and cooperation among huddling infant rats. *Developmental Psychobiology: The Journal of the International Society for Developmental Psychobiology* 39(2): 65-75.

Solstad, T., Boccara, C.N., Kropff, E., Moser, M.B., Moser, E.I. (2008) Representation of geometric borders in the entorhinal cortex. *Science* 322(5909): 1865-1868.

Spiers, H.J., Hayman, R.M., Jovalekic, A., Marozzi, E., Jeffery, K.J. (2015) Place field repetition and purely local remapping in a multicompartment environment. *Cerebral Cortex* 25: 10-25.

Squire, L. R., Cohen, N. J., Nadel, L. (1984) The medial temporal region and memory consolidation: A new hypothesis. *Memory consolidation: Psychobiology of cognition*: 185-210.

Squire, L.R. (1992) Memory and the hippocampus: a synthesis from findings with rats, monkeys, and humans. *Psychological Review* 99: 195-231.

Squire, L. R., and Alvarez, P. (1995) Retrograde amnesia and memory consolidation: a neurobiological perspective. *Current opinion in neurobiology* 5(2): 169-177.

Squire, L. R., Genzel, L., Wixted, J. T., Morris, R. G. (2015) Memory consolidation. *Cold Spring Harbor perspectives in biology* 7(8): a021766.

Stacho, M., and Manahan-Vaughan, D. (2022) Mechanistic flexibility of the retrosplenial cortex enables its contribution to spatial cognition. *Trends in Neurosciences* 45(4): 284-296.

Stackman, R.W., Taube, J.S. (1997) Firing properties of head direction cells in the rat anterior thalamic nucleus: Dependence on vestibular input. *Journal of Neuroscience* 17(11): 4349-4358.

Stackman, R.W., and Taube, J.S. (1998) Firing properties of rat lateral mammillary single units: head direction, head pitch and angular head velocity. *Journal of Neuroscience* 18(21): 9020-9037.

Stackman, R.W., Tullman, M.L., Taube, J.S. (2000) Maintenance of rat head direction cell firing during locomotion in the vertical plane. *Journal of Neurophysiology* 83: 393-405.

Stackman, R.W., Clark, A.S., Taube, J.S. (2002) Hippocampal spatial representations require vestibular input. *Hippocampus* 12: 291-303.

Stackman, R.W., Golob, E.J., Bassett, J.P., Taube, J.S. (2003) Passive transport disrupts directional path integration by rat head direction cells. *Journal of Neurophysiology* 90: 2862-2874.

Steiniger, F. (1950) Beiträge zur Soziologie und sonstigen Biologie der Wanderratte. *Zeitschrift für Tierpsychologie* 7(3): 356-379.

Stensola, H., Stensola, T., Solstad, T., Froland, K., Moser, M.B., Moser, E.I. (2012) The entorhinal grid map is discretized. *Nature* 492(7427): 72-78.

Stewart, S., Jeewajee, A., Wills, T.J., Burgess, N., Lever, C. (2013) Boundary coding in the rat subiculum. *Philosophical Transactions of the Royal Society B* 369(1635): 20120514.

Stratmann, G., May, L.D., Sall, J.W., Alvi, R.S., Bell, J.S., Ormerod, B.K., Rau, V., Hilton, J.F., Dai, R., Lee, M.T., Visrodia, K.H., Ku, B., Zusmer, E.J., Guggenheim, J., Firouzian, A. (2009a) Effect of hypercarbia and isoflurane on brain cell death and neurocognitive dysfunction in 7-day-old rats.

Anesthesiology 110:849-861.

Stratmann, G., Sall, J.W., May, L.D., Bell, J.S., Magnusson, K.R., Rau, V., Visrodia, K.H., Alvi, R.S., Ku, B., Lee, M.T., Dai, R. (2009b) Isoflurane differentially affects neurogenesis and long-term neurocognitive function in 60-day-old and 7-day-old rats. *Anesthesiology* 110:834–848.

Stratton, P., Wyeth, G., Wiles, J. (2010) Calibration of the head direction network: a role for symmetric angular head velocity cells. *Journal of Computational Neuroscience* 28: 527-538.

Stringer, S.M., Trappenberg, T.P., Rolls, E.T., Araujo, I. (2002) Self-organizing continuous attractor networks and path integration: one-dimensional models of head direction cells. *Network: Computation in Neural Systems* 13(2): 217-242.

Stringer, S.M., and Rolls, E.T. (2006) Self-organizing path integration using a linked continuous attractor and competitive network: path integration of head direction. *Network: Computation in Neural Systems* 17(4): 419-445.

Sullivan, R.M., Landers, M.S., Fleming, J., Vaught, C., Young, T.A., Polan, H.J. (2003) Characterizing the functional significance of the neonatal rat vibrissae prior to the onset of whisking. *Somatosensory & Motor Research* 20(2): 157-162.

Takahashi, N., Kawamura, M., Shiota, J., Kasahata, N., Hirayama, K. (1997) Pure topographic disorientation due to a right retrosplenial lesion. *Neurology* 49: 464-469.

Tan, H.M., Bassett, J.P., O'Keefe, J., Cacucci, F., Wills, T.J. (2015) The development of the head direction system before eye opening in the rat. *Current Biology* 25(4): 479-483.

Tan, H.M., Wills, T.J., Cacucci, F. (2017) The development of spatial and memory circuits in the rat. Wiley Interdisciplinary Reviews: Cognitive *Science* 8(3): e1424.

Taube, J.S., Muller, R.U., Ranck, J.B. (1990a) Head-direction cells

recorded from the postsubiculum in freely moving rats I. Description and Quantitative Analysis. *Journal of Neuroscience* 10(2): 420-435.

Taube, J.S., Muller, R.U., Ranck, J.B. (1990b) Head-direction cells recorded from the postsubiculum in freely moving rats II. Effects of Environmental Manipulations. *Journal of Neuroscience* 10(2): 436-447.

Taube, J.S., Kesslak, J.P., Cotman, C.W. (1992) Lesions of the rat post-subiculum impair performance on spatial tasks. *Behavioral and Neural Biology* 57: 131-143.

Taube, J.S. (1995) Head direction cells recorded in the anterior thalamic nuclei of freely moving rats. *Journal of Neuroscience* 15: 70-86.

Taube, J.S., and Burton, H.L. (1995) Head direction cell activity monitored in a novel environment and during a cue conflict situation. *Journal of Neurophysiology* 74(5): 1953-1971.

Taube, J.S., and Muller, R.U. (1998) Comparisons of head direction cell activity in the postsubiculum and anterior thalamus of freely moving rats. *Hippocampus* 8: 87-108.

Taube, J.S., Wang, S.S., Kim, S.Y., Frohardt, R.J. (2013) Updating of the spatial reference frame of head direction cells in response to locomotion in the vertical plane. *Journal of Neurophysiology* 109(3): 873-888.

Taylor, K.D. (1978) Range of movement and activity of common rats (Rattus norvegicus) on agricultural land. *Journal of Applied Ecology*: 663-677.

Tees, R.C., Buhrmann, K., Hanley, J. (1990) The effect of early experience on water maze spatial learning and memory in rats. *Developmental Psychobiology* 23(5): 427-439.

Tees, R.C. (1999) The influences of rearing environment and neonatal choline dietary supplementation on spatial learning and memory in adult rats. *Behavioral Brain Research* 105(2): 173-188.

Teicher, M.H., and Blass, E.M. (1977) First suckling response of the newborn albino rat: the roles of olfaction and amniotic fluid. *Science*

198(4317): 635-636.

Thiels, E., Alberts, J.R., Cramer, C.P. (1990) Weaning in rats: II. Pup behavior patterns. *Developmental Psychobiology: The Journal of the International Society for Developmental Psychobiology* 23(6): 495-510.

Thistlethwaite, D. (1951) A critical review of latent learning and related experiments. *Psychological Bulletin* 48(2): 97-129.

Thompson, S.M., and Robertson, R.T. (1987) Organization of subcortical pathways for sensory projections to the limbic cortex I. Subcortical projections to the medial limbic cortex in the rat. *Journal of Comparative Neurology* 265: 175-188.

Tolman, E.C., and Honzik, C.H. (1930) Introduction and removal of reward, and maze performance in rats. *University of California Publications in Psychology* 4: 257-275.

Tolman, E.C., Ritchie, E.F., Kalish, D. (1946) Studies in spatial learning. I. Orientation and the short-cut. *Journal of Experimental Psychology* 36(1): 13-24.

Tolman,E.C. (1948). Cognitive maps in rats and men. *Psychological review* 55(4): 189.

Touretzky, D.S., and Redish, A.D. (1996) Theory of rodent navigation based on interacting representations of space. *Hippocampus* 6: 247-270.

Treves, A., and Rolls, E. T. (1994) Computational analysis of the role of the hippocampus in memory. *Hippocampus* 4(3): 374-391.

Tsanov, M., Chah, E., Vann, S.D., Reilly, R.B., Erichsen, J.T., Aggleton, J.P., O'Mara, S. (2011) Theta-modulated head direction cells in the rat anterior thalamus. *Journal of Neuroscience* 31: 9489-9502.

Twyman, A.D., Newcombe, N.S., Gould, T.J. (2013) Malleability in the development of spatial reorientation. *Developmental Psychobiology* 55(3): 243-255.

Ulanovsky, N., Moss, C.F. (2007) Hippocampal cellular and network activity in freely moving echolocating bats. *Nature Neuroscience* 10: 224-

Uziel, A., Romand, R., Marot, M. (1981) Development of cochlear potentials in rats. *Audiology* 20: 89-100.

Valerio, S., and Taube, J.S. (2012) Path integration: how the head direction signal maintains and corrects spatial information. *Nature Neuroscience* 10: 1445-1453.

Van der Meer, M., Richmond, Z., Braga, R.M., Wood, E.R., Dudchenko, P.A. (2010) Evidence for the use of an internal sense of direction in homing. *Behavioral Neuroscience* 124: 164-169.

Vanderwolf, C.H. (1969) Hippocampal electrical activity and voluntary movement in the rat. *Electroencephalography and Clinical Neurophysiology* 26: 407-418.

Van Groen, T., and Wyss, J.M. (1990) The postsubicular cortex in the rat: characterization of the fourth region of the subicular cortex and its connections. *Brain Research* 529: 165-177.

Van Groen, T., and Wyss, J.M. (1992) Connections of the retrosplenial dysgranular cortex in the rat. *Journal of Comparative Neurology* 315: 200-216.

Van Groen, T., Kadish, I., Wyss, J.M. (2002a) The role of the laterodorsal nucleus of the thalamus in spatial learning and memory in the rat. *Behavioral Brain Research* 136: 329-337.

Van Groen, T., Kadish, I., Wyss, J.M. (2002b) Role of the anterodorsal and anteroventral nuclei of the thalamus in spatial memory in the rat. *Behavioral Brain Research* 132: 19-28.

Van Groen, T., and Wyss, J.M. (2003) Connections of the retrosplenial granular b cortex in the rat. *Journal of Comparative Neurology* 463: 249-263.

Vann, S.D., and Aggleton, J.P. (2004) Testing the importance of the retrosplenial guidance system: effects of different sized retrosplenial cortex lesions on heading direction and spatial working memory. *Behavioral*

Brain Research 155(1): 97-108.

Vann, S.D., and Aggleton, J.P. (2005) Selective dysgranular retrosplenial cortex lesions in rats disrupt allocentric performance of the radial-arm maze task. *Behavioral Neuroscience* 119(6): 1682-1686.

Vann, S.D. (2005) Transient spatial deficit associated with bilateral lesions of the lateral mammillary nuclei. *European Journal of Neuroscience* 21: 820-824.

Vann, S.D., Saunders, R.C., Aggleton, J.P. (2007) Distinct, parallel pathways link the medial mammillary bodies to the anterior thalamus in macaque monkeys. *European Journal of Neuroscience* 26(6): 1575-1586.

Vann, S.D. (2011) A role for the head-direction system in geometric learning. *Behavioral Brain Research* 224: 201-206.

Vertes, R.P., Albo, Z., Di Prisco, G.V. (2001) Theta-rhythmically firing neurons in the anterior thalamus: implications for mnemonic functions of Papez's circuit. *Neuroscience* 104(3): 619-625.

Vetere, G., Xia, F., Ramsaran, A.I., Tran, L.M., Josselyn, S.A., Frankland, P.W. (2021) An inhibitory hippocampal-thalamic pathway modulates remote memory retrieval. *Nature Neuroscience* 24(5): 685-693.

Vinepinsky, E., Donchin, O., Segev, R. (2017) Wireless electrophysiology of the brain of freely swimming goldfish. *Journal of Neuroscience Methods* 278: 76-86.

Vinepinsky, E., Cohen, L., Perchik, S., Ben-Shahar, O., Donchin, O., Segev, R. (2020) Representation of edges, head direction, and swimming kinematics in the brain of freely-navigating fish. *Scientific Reports* 10(1): 1-6.

Vrolyk, V., Haruna, J., Benoit-Biancamano, M.O. (2018) Neonatal and juvenile ocular development in Sprague-Dawley rats: a histomorphological and immunohistochemical study. *Veterinary Pathology* 55(2): 310-330.

Wang, Y., Romani, S., Lustig, B., Leonardo, A., Pastalkova, E. (2015) Theta sequences are essential for internally generated hippocampal firing fields. Nature Neuroscience 18(2): 282-288.

Watson, J.B. (1919) Psychology: From the standpoint of a behaviorist. JB Lippincott.

Weaver, I.C., Cervoni, N., Champagne, F.A., D'Alessio, A.C., Sharma, S., Seckl, J.R., Dymov, S., Szyf, M., Meaney, M.J. (2004) Epigenetic programming by maternal behavior. *Nature Neuroscience* 7(8): 847-854.

Weiss, S., Talhami, G., Gofman-Regev, X., Rapoport, S., Eilam, D., Derdikman, D. (2017) Consistency of spatial representations in rat entorhinal cortex predicts performance in a reorientation task. *Current Biology* 27(23): 3658-3665.

Weiss, S. and Derdikman, D. (2018) Role of the head-direction signal in spatial tasks: when and how does it guide behavior? *Journal of Neuro-physiology* 120(1): 78-87.

Welker, W.I. (1964) Analysis of sniffing of the albino rat 1. *Behaviour* 22(3-4): 223-244.

Whishaw, I.Q., and Brooks, B.L. (1999) Calibrating space: exploration is important for allothetic and idiothetic navigation. *Hippocampus* 9(6): 659-667.

Whishaw, I.Q., Gharbawie, O.A., Clark, B.J., Lehmann, H. (2006) The exploratory behavior of rats in an open environment optimizes security. *Behavioral Brain Research* 171(2): 230-239.

Wiener, S.I. (1993) Spatial and behavioral correlates of striatal neurons in rats performing a self-initiated navigation task. *Journal of Neuroscience* 13: 3802-3817.

Wilkenheiser, A.M., Redish, A.D. (2015) Hippocampal theta sequences reflect current goals. *Nature Neuroscience* 18(2): 289-294.

Wills, T.J., Cacucci, F., Burgess, N., O'Keefe, J. (2010) Development of the hippocampal cognitive map in preweanling rats. *Science* 328(5985): 1573-1576.

Wills, T.J., Barry, C., Cacucci, F. (2012) The abrupt development of

adult-like grid cell firing in the medial entorhinal cortex. *Frontiers in Neu- ral Circuits* 6: 21.

Wills, T.J., Muessig, L., Cacucci, F. (2014) The development of spatial behaviour and the hippocampal neural representation of space. *Philosophical Transactions of the Royal Society B* 369: 20130409.

Wilson, M.A., and McNaughton, B.L. (1993) Dynamics of the hip-pocampal ensemble code for space. *Science* 261(5124): 1055-1058.

Wilson, M.A., and McNaughton, B.L. (1994) Reactivation of hippocampal ensemble memories during sleep. *Science* 265(5172): 676-679.

Wilton, L.A.K., Baird, A.L., Muir, J.L., Honey, R.C., Aggleton, J.P. (2001) Loss of the thalamic nuclei for 'head direction' impairs performance on spatial memory tasks in rats. *Behavioral Neuroscience* 115: 861-869.

Winson, J. (1972) Interspecies differences in the occurrence of theta. *Behavioural Biology* 7:479-487.

Winter, S.S., Clark, B.J., Taube, J.S. (2015) Disruption of the head direction cell network impairs the parahippocampal grid cell signal. *Science* 347(6224): 870-874.

Wirtshafter, D., and Stratford, T.R. (1993) Evidence for GABAergic projections from the tegmental nuclei of Gudden to the mammillary body in the rat. *Brain Research* 630: 188-194.

Witter, M. P., Groenewegen, H. J., Da Silva, F. L., Lohman, A. H. M. (1989) Functional organization of the extrinsic and intrinsic circuitry of the parahippocampal region. *Progress in neurobiology* 33(3): 161-253.

Wolbers, T., Dudchenko, P.A., Wood, E.R. (2014) Spatial memory- a unique window into healthy and pathological aging. *Frontiers in aging neuroscience*. 35.

Wood, E.R., Dudchenko, P.A., Eichenbaum, H. (1999) The global record of memory in hippocampal neuronal activity. *Nature* 397: 613-616.

Wyss, J.M., Swanson, L.W., Cowan, W.M. (1979) A study of subcortical afferents to the hippocampal formation in the rat. *Neuroscience* 4: 463-

Wyss, J.M., and Sripanidkulchai, K. (1984) The topography of the mesencephalic and pontine projections from the cingulate cortex of the rat. *Brain Research* 293: 1-15.

Wyss, J.M, and van Groen, T. (1992) Connections between the retrosplenial cortex and the hippocampal formation in the rat: a review. *Hippocampus* 2(1): 1-11.

Xu, H., Baracskay, P., O'Neill, J., Csicsvari, J. (2019) Assembly responses of hippocampal CA1 place cells predict learned behavior in goal-directed spatial tasks on the radial eight-arm maze. *Neuron* 101(1): 119-132.

Yan, Y., Burgess, N., Bicanski, A. (2021) A model of head direction and landmark coding in complex environments. *PLoS Computational Biology* 17(9): e1009434.

Yoder, R.M., and Taube, J.S. (2009) Head direction cell activity in mice: robust directional signal depends on intact otolith organs. *Journal of Neuroscience* 29: 1061-1076.

Yoder, R.M., Clark, B.J., Brown, J.E., Lamia, M.V., Valerio, S., Shinder, M.E., Taube, J.S. (2011) Both visual and idiothetic cues contribute to head direction cell stability during navigation along complex routes. *Journal of Neurophysiology* 105: 2989-3001.

Yoder, R.M., and Taube, J.S. (2014) The vestibular contribution to the head direction signal and navigation. *Frontiers in Integrative Neuroscience* 8(32): 1-13.

Yoder, R.M., Peck, J.R., Taube, J.S. (2015) Visual landmark information gains control of the head direction signal at the lateral mammillary nuclei. *Journal of Neuroscience* 35(4): 1354-1367.

Yoder, R.M., Valerio, S., Crego, A.C., Clark, B.J., Taube, J.S. (2019) Bilateral postsubiculum lesions impair visual and nonvisual homing performance in rats. *Behavioral Neuroscience* 133(5): 496.

Yoganarasimha, D., Yu, X., Knierim, J.J. (2006) Head direction cell rep-

resentations maintain internal coherence during conflicting proximal and distal cue rotations: comparison with hippocampal place cells. *Journal of Neuroscience* 26: 622-631.

Zar, J.H. (2010) Biostatistical analysis. *Prentice Hall, Upper Saddle River, New Jersey.*

Zhang, K. (1996) Representation of spatial orientation by the intrinsic dynamics of the head-direction cell ensemble: A theory. *Journal of Neuroscience* 30: 13850-1360.

Zhang, L.I., Bao, S., Merzenich, M.M. (2001) Persistent and specific influences of early acoustic environments on primary auditory cortex. *Nature Neuroscience* 4: 1123-1130.

Zhang, T.Y., Hellstrom, I.C., Bagot, R.C., Wen, X., Diorio, J., Meaney, M.J. (2010) Maternal care and DNA methylation of a glutamic acid decarboxylase 1 promoter in rat hippocampus. *Journal of Neuroscience* 30(39): 13130-13137.

Zhang, S.J., Ye, J., Miao, C., Tsao, A., Cerniauskas, I., Ledergerber, D., Moser, M.B., Moser, E.I. (2013) Optogenetic dissection of entorhinal-hippocampal functional connectivity. *Science* 340(6148): 1232627.

Zhang, S., Schonfeld, F., Wiskott, L., Manahan-Vaughan, D. (2014) Spatial representations of place cells in darkness are supported by path integration and border information. *Frontiers in behavioral neuroscience* 8: 222.

Ziv, Y., Burns, L.D., Cocker, E.D., Hamel, E.O., Ghosh, K.K., Kitsch, L.J., Gamal, A.E., Schnitzer, M.J. (2013) Long-term dynamics of CA1 hippocampal place codes. *Nature Neuroscience* 16: 264-266.

Zugaro, M.B., Berthoz, A., Wiener, S.I. (2001a) Background, but not foreground, spatial cues are taken as references for head direction responses by rat anterodorsal thalamus neurons. *Journal of Neuroscience* 21(14): RC154.

Zugaro, M.B., Berthoz, A., Wiener, S.I. (2002) Peak firing rates of rat

anterodorsal thalamic head direction cells are higher during faster passive rotations. *Hippocampus* 12: 481-486.

Zugaro, M.B., Arleo, A., Berthoz, A., Wiener, S.I. (2003) Rapid spatial reorientation and head direction cells. *Journal of Neuroscience* 23(8): 3478-3482.

Zutshi, I., Fu, M.L., Lilascharoen, V., Leutgeb, J.K., Lim, B.K., Leutgeb, S. (2018) Recurrent circuits within medial entorhinal cortex superficial layers support grid cell firing. *Nature Communications* 9: 3701.